THE UNIVERSITY
of EDINBURGH

Design and testing of *ex vivo* vascularization methods for kidney explants in order to overcome the diffusion limit of oxygen and nutrients in 3D-culture-systems

Julia Tarnick

A thesis submitted in fulfilment of the requirements for the degree of Doctor of Philosophy at the University of Edinburgh

2021

Abstract

The best way of treating end-stage renal disease is the transplantation of a donor organ. However, the number of patients requiring a transplant exceeds the number of available kidneys. Growing kidneys from induced pluripotent stem cells could help to close the gap between organ demand and supply and could omit the need to take immunosuppressants if the engineered kidneys were to be generated from the patient's own cells.

Kidney organoids from murine kidney cells are similar to embryonic kidneys but, with traditional culture methods, the organoids, as well as the kidneys themselves, grow rather flat and spread out, which does not represent the overall shape of a kidney grown *in vivo.* Embedding kidney explants in type 1 collagen resulted in a more spherical shape, but also in central necrosis, most likely caused by hypoxia.

Staining of the explants for endothelial markers revealed the presence of capillaries, which remained immature. In some tissues, arterial differentiation is induced by neurons. To analyse whether the renal arterial maturation is controlled by neurons, developing kidneys were isolated and co-stained for vascular and neuronal markers. The co-staining revealed that innervation occurs after formation of the smooth muscle cell lining and during upregulation of calponin 1, which is involved in smooth muscle cell contraction.

Several studies link vascular differentiation to mechanical stimuli caused by the onset of blood flow. To detect whether connecting the kidneys to the vasculature of a host would enhance vascular maturity, the explants were grafted onto the chick chorioallantoic membrane. Injection of the chick vessels following isolation and staining of the explant confirmed blood flow through the graft vessels. However, vascular maturity was not improved as indicated by the lack of vascular smooth muscle cells.

The use of fertilized eggs makes it difficult to influence the growth environment of the explants. Isolating blood vessels and co-culturing them under perfusion with

embryonic kidneys *in vitro* would allow more control over available growth factors and mechanical cues by adjusting the stiffness of the surrounding matrix as well the flow rate through the blood vessels. For this purpose, I have designed a culture device that allows the long-term perfusion of arteries and veins. Using this device, I have demonstrated that isolated blood vessels respond to proangiogenic treatment by forming sprouts. In co-cultures of the blood vessels with embryonic kidneys, endothelial sprouts were seen between both tissues and appeared to form a connection between the vessel and the explant, which sets the basis for the *in vitro* vascularisation of kidney explants.

Vascularizing kidney explants can aid identifying methods to vascularize kidney organoids *in vitro*. This is a critical step in renal tissue engineering as it would improve organoid growth and enable testing their functionality in terms of blood filtration. A functional vasculature will also be essential in generation transplantable renal tissue, which could on day help to treat kidney disease.

Lay abstract

Kidneys are vital organs. They remove toxins from the blood, help to maintain bone health and regulate the production of red blood cells which supply the body with oxygen. Consequently, kidney disease can have huge implications for an individual's health. In the UK, one in 25 people will experience some sort of persistent kidney problem. In severe cases, a kidney transplant from a donor is usually the best form of treatment. However, there are not enough donor organs available. Recreating kidneys from human cells could increase the amount of donor organs and drastically reduce the waiting time for a transplant.

To date, scientists can create something like a miniature kidney. These "mini-kidneys" show a lot of the features of an early embryonic kidney, but instead of a kidney bean-like shape, they grow in a more disk-like shape. This growth form is shared with embryonic kidneys when these are taken out of the embryo and grown in culture.

I attempted to recreate a more natural environment for embryonic kidneys to help them to maintain their natural shape. To do this I have embedded the kidney in type-1 collagen, a protein which is found in all organs and helps to hold cells of different types together. When surrounded by collagen, the kidneys grew with a more spherical shape. However, the cells in the centre of the sphere started to die, because they were not supplied with enough oxygen.

In the body, oxygen is transported to cells via the blood stream. In culture, kidneys do have blood vessels, but there is no blood flow, because they are not connected to the heart. One way of getting blood flow into the kidneys is putting them inside a fertilized chicken egg. During its development, the chicken embryo is covered with a thin membrane that contains many blood vessels. Kidneys can be put on this membrane, called "chorioallantoic membrane", to connect them with the blood stream of the chicken embryo. The kidneys that connected were kept alive, while those that did not connect stopped growing. However, after looking at the blood vessels of kidneys that connected to the chick embryo, I noticed that they looked very

abnormal compared to the ones that would normally develop if the kidney was left inside the embryo, showing that the growth environment in the egg was not optimal.

A better way of controlling the growth environment would be to take a single or pair of blood vessels and connect them to a pump system to keep a flow through the vessels. The blood vessels could then connect with kidneys and supply them with nutrients. To do so, I have developed an apparatus that can be used to let blood vessels grow outside the body.

In the future, this might help to improve the growth of natural and artificially created kidneys to a size suitable for transplantation and thereby reduce the waiting time for a kidney transplant.

Declaration

I declare that this thesis has been composed solely by myself and that it has not been submitted, in whole or in part, in any previous application for a degree. Except where states otherwise by reference or acknowledgment, the work presented is entirely my own.

Julia Tarnick

8/3/2021

Acknowledgements

Firstly, I would like to thank Kidney Research UK for funding my work.

Further, I would like to express my gratitude to Jamie for the freedom to pursue my own research interests and his extensive and immensely helpful feedback.

Many thanks to Paddy for the help in conference preparations and his advice on the blood vessels cultures as well as the very helpful comments on my thesis draft.

I would also like to thank Jennifer and Naomi for their support and guidance.

Vielen Dank an Papa, für die Bioreaktoren, das Druckmessgerät, den Funktionsgenerator und für die vielen hilfreichen Hinweise und an Mama dafür dass du immer ein offenes Ohr für mich hattest.

I am very grateful to Melanie and Chris for teaching the kidney dissection and how to generate the organoids and to Patricia for her help in optimizing the grafting experiments. Many thanks to Ian for his feedback on the introduction. I would also like to thank Junxi, Mona, David and Anwar for the helpful discussions and advice as well as to Lorna for showing me how to suture blood vessels.

Many thanks to Vrushali for lab and life advice and all the fun adventures around Scotland.

Lastly, much appreciation to HRB and BVS support staff for their immense help in finding all required resources.

Contents

List of figures

List of tables

Chapter 1 - Introduction

1.1 Project Aim and Outline

Kidney cell-derived renal organoids display a high degree of anatomical similarity to cultured embryonic kidneys (Mills *et al.*, 2017). However, like kidney explants, they grow rather flat and spread out, which does not represent the natural shape of a kidney (Ganeva *et al.*, 2011; Mills *et al.*, 2017; Sebinger *et al.*, 2010).

In this thesis, I aim to induce a more three-dimensional growth of kidney explants by embedding them in an extracellular matrix. In the first results chapter, I analyse whether embedding the explants in type 1 collagen can induce three-dimensional growth and whether it affects the morphology of kidney explants (**Chapter 3**).

Three-dimensional culture systems often result in the formation of a gradient of oxygen and nutrients from the periphery to the centre (Glicklis *et al.*, 2004; McMurtrey, 2016; Sakaguchi *et al.*, 2013). *In situ*, oxygen and nutrients are supplied via the circulatory system. Therefore, I further aim to confirm the presence of blood vessels within kidney explants as described previously (Munro *et al.*, 2017) and determine the maturity of forming blood vessels (**Chapter 3**).

Subsequently, I examine different factors that potentially contribute to vascular maturation. At first, I test the hypothesis that neuron-derived signals are necessary for renal vascular maturation *in situ* (**Chapter 4**). Subsequently, I graft kidney explants onto the chick chorioallantoic membrane, to investigate whether the connection to the circulatory system of a host would affect their vascular maturity (**Chapter 5**).

Lastly, I aimed to construct a device for the *ex vivo* culture of adult and embryonic blood vessels and determined its potential use in vascularizing kidney explants *in vitro* (**Chapter 6**).

1.2 Kidney anatomy and function

1.2.1 Anatomy of the kidney

Human kidneys weigh about 115-175 g and are located on either side of the midline, between the levels of vertebra T12 and vertebra L3, the right kidney lying slightly lower than the left one. They are covered by a fibrous capsule consisting of extracellular matrix components. In a frontally sectioned kidney (**Figure 1-1**), two main regions are visible; the outer cortex, and inner medullary region (Saxén, 1987).

The medullary region contains 10 to 18 triangular renal pyramids separated by renal columns (Saxén, 1987). These pyramids are connected to the minor calyces, which fuse to the major calyx. The major calyx connects via the renal pelvis to the ureter (Saxén, 1987).

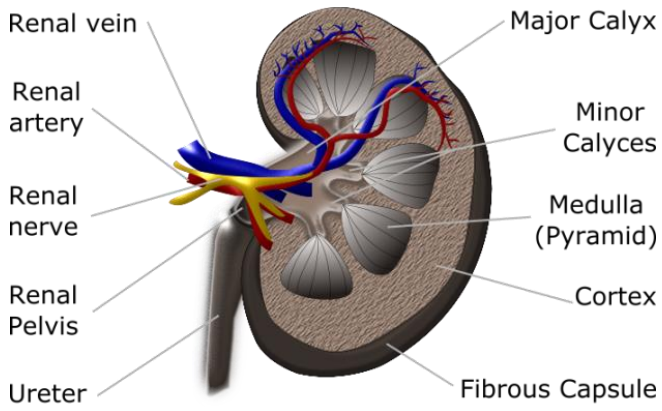

Figure 1-1: Illustration of renal gross anatomy (reproduced with modifications from OpenStax, 2016)

The kidneys are vascularized by the renal artery and vein (Bowman, 1842; Saxén, 1987). The renal artery ramifies into segmental arteries (Bowman, 1842; Saxén, 1987). The segmental arteries branch into the interlobular arteries which run between the pyramids of the medulla (Bowman, 1842; Saxén, 1987). From the interlobular arteries branch the arcuate arteries, which in turn branch into cortical radiate arteries and afferent arterioles (Bowman, 1842; Saxén, 1987). The afferent arterioles enter the glomeruli of the nephrons, which lie in the cortical region of the kidney (Bowman, 1842; Saxén, 1987). Blood vessels leaving the glomeruli are named efferent arterioles and branch into the peritubular capillaries (Bowman, 1842; Saxén, 1987). From there, the blood exits the kidney via the interlobular vein then the arcuate vein, segmental vein and renal vein (Bowman, 1842; Saxén, 1987).

The blood flow is, in part, controlled by the renal nerves which run alongside the renal artery and vein (Saxén, 1987).

1.2.2 Renal blood filtration

The main function of the kidney is to remove toxins and metabolic waste products from the blood (Bowman, 1842). This occurs within the Bowman's capsule, a cup-like structure connected to the proximal tubules of the nephron (Bowman, 1842). Blood enters the Bowman's capsule via the afferent arteriole which ramifies to form the glomerulus, a dense capillary network that is structurally supported by a stalk-like aggregate of mesangial cells (Bowman, 1842; Sakai and Kriz, 1987). The glomerular capillaries are structurally adapted to support the removal of toxins while maintaining important nutrients within the blood. A coating of the heavily fenestrated capillaries with negatively charged glycoproteins helps to retain certain molecules, such as albumin, within the blood vessels (Dane *et al.*, 2013; Hjalmarsson *et al.*, 2004). This is further supported by the adsorption of plasma molecules in the glycocalyx leading to the formation of a 200 nm thick endothelial surface layer, which is essential for the filtration of the blood (Hjalmarsson *et al.*, 2004).

The endothelium is basally surrounded by the glomerular basement membrane (GBM), which separates it from a layer of podocytes. Consisting of a network of highly organized fibrils that form pores of about 10 nm size, the GBM represents the second layer of the glomerular filtration system (Hironaka *et al.*, 1993). Defects of the GBM formation result in proteinuria and haematuria underlining its importance in retaining essential blood components (Alport, 1927; Yoshikawa *et al.*, 1981). *In vitro* experiments with isolated GBM preparations indicate that it acts as a size- rather than charge-specific filtration barrier (Bolton *et al.*, 1998).

Podocytes are specialized cells which form interdigiting foot-like processes around the glomerular capillaries. They are connected via specialized adherens junctions, the slit diaphragms (Farquhar *et al.*, 1961; Reiser *et al.*, 2000). Slit diaphragms form pores by self-repulsion of the negatively charged sialoprotein, podocalyxin (Kerjaschki *et al.*, 1984; Takeda *et al.*, 2000). They play a crucial role in the size and charge permselectivity of the glomerular filtration barrier as defects of one of the core structural proteins such as nephrin, podocin and Neph1 result in glomerular filtration impairment (Boute *et al.*, 2000; Donoviel *et al.*, 2001; Kestilä *et al.*, 1998).

Small uncharged molecules can pass through the glomerular filtration barrier and are collected as primary urine in the Bowman's space, a lumen between the podocytes and the parietal epithelial cells that form the outer layer of the glomerulus (Chang *et al.*, 1975; Rennke and Venkatachalam, 1977).

The Bowman's capsule is connected to the proximal convoluted tubule of the nephron where most of the water and nutrients are reabsorbed (reviewed by Curthoys and Moe, 2014). The proximal tubule connects to the loop of Henle that descends in the medullary region which displays a gradient of increasing tissue osmolarity from cortex to core (Henle, 1862; Knepper, 1982).

The salinity of the medulla plays an important role in concentrating the primary urine via a countercurrent system (**Figure 1-2**) (Dantzler *et al.*, 2011; Kuhn, 1959). While upper proportion of the descending Loop of Henle expresses Aquaporin 1 and is

highly permeable to water, the lower part as well as the ascending Loop of Henle are impermeable to water and expresses the chloride channel C1C-K1 (CLCKNA) (Dantzler *et al.*, 2011; Rocha and Kokko, 1973). According to the urine concentration model of Dantzler *et al.*, water is withdrawn from the proximal part of the descending loop of Henle due to the salinity of the surrounding system (Dantzler *et al.*, 2011; Kuhn, 1959). This leads to an increased salt concentration in the distal descending loop of Henle (Dantzler *et al.*, 2011; Kuhn, 1959). A subset of Loops of Henle display a wide bend region which is closely wrapped around the collecting duct in the inner medulla (Dantzler *et al.*, 2011). Between the bend region of the Loops of Henle and the collecting ducts a microdomain, called the 'interstitial nodal space' (INS), is formed. The loops of Henle secrete NaCl into the INS which causes water to be drawn from the collecting duct resulting in an increase of the osmolarity in the collecting duct (Dantzler *et al.*, 2011). The water permeability of the collecting duct is regulated by arginine-vasopressin (Sands *et al.*, 1987). The concentrated solute from the INS is partially absorbed by ascending blood vessels (Dantzler *et al.*, 2011). The ascending blood vessels run in parallel to the collecting duct making contact via microvilli and thereby establish a countercurrent system in which water is withdrawn from the collecting duct and absorbed by the ascending blood vessels resulting in the osmolarity decreasing in the collecting duct and increasing in the ascending blood vessel (Dantzler *et al.*, 2011). While still needing experimental validation, Dantzler's model computes a urine osmolarity similar to the one observed *in vivo* and highlights the importance of the special arrangement of nephrons, collecting ducts and blood vessels.

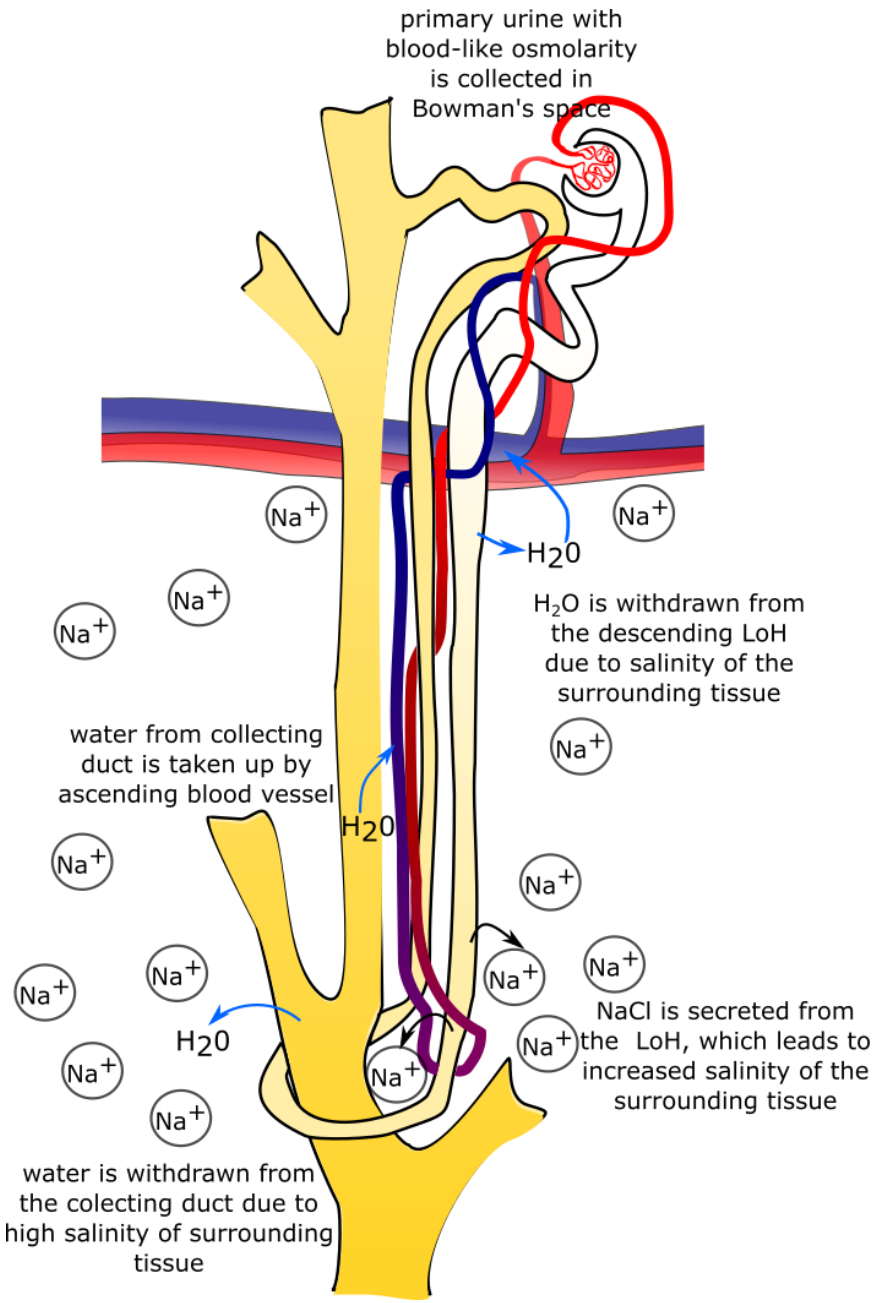

Figure 1-2: Illustration of urine concentration mechanism. The primary urine is collected in the Bowman's space. Water is withdrawn from the proximal part of the descending loop of Henle (LoH) due to salinity of the surrounding tissue. Sodium chloride is pumped out the distal part of the descending loop of Henle as well as from the ascending loop of Henle, which leads to increased salinity of the surrounding tissue. The high osmolarity of the stroma leads to water absorption from the collecting duct which further concentrated the urine. The water is taken up by the ascending vasa recta.

1.2.3 Other functions of the kidney

Kidneys fulfil several other functions, in addition to filtering blood. One of them is the control of local and systemic blood pressure. The glomerular filtration rate is affected by blood pressure changes within the renal circulation (Tobian *et al.*, 1964). To maintain an optimal filtration rate, it is therefore critical that the blood flow can be regulated within the kidney independently of the systemic blood pressure. This is achieved by two main mechanisms; the myogenic response and the tubuloglomerular feedback (reviewed by Burke *et al.*, 2014). The myogenic response describes the intrinsic ability of blood vessels to influence the blood pressure by constricting or dilating (Burke *et al.*, 2014). The tubuloglomerular feedback is based on an increase of sodium uptake by the distal tubule (Burke *et al.*, 2014). In response to elevated blood pressure and therefore accelerated urine flow the sodium uptake in the predistal segments of the nephron is reduced which leads to higher salinity of the urine in the distal tubule (Burke *et al.*, 2014). This increase leads to elevated levels of intracellular calcium which stimulates the release of ATP. The extracellular ATP is converted to adenosine which activates the adenosine 1A receptor leading to constriction of the afferent arteriole and thereby reduction the blood flow through the nephron (Burke *et al.*, 2014).

The kidneys can also influence the systemic blood pressure (Goldblatt *et al.*, 1934). The systemic blood pressure is regulated via the renin-angiotensin system which is reviewed in detail elsewhere (Te Riet *et al.*, 2015). Briefly summarized, low blood pressure or high blood osmolarity stimulate the juxtaglomerular cells on the afferent arteriole to secrete renin into the blood system (Kohlstaedt and Page, 1940; Taugner *et al.*, 1979; Young and Rostorfer, 1973). The circulating renin then cleaves angiotensinogen, which is released mainly by the liver, to angiotensin I (Braun-Menendez *et al.*, 1940; Page and Helmer, 1940). Angiotensin I can be converted to angiotensin II by the angiotensin converting enzyme (ACE) which is abundantly expressed on the vascular endothelial cells (Dorer *et al.*, 1975; Skeggs *et al.*, 1954).

Angiotensin II then stimulates the constriction of the vascular smooth muscle cells, enhances the cardiac contractibility and increases thirst to promote water uptake resulting in an increase of blood pressure (Baker *et al.*, 1984; Johnson *et al.*, 1981; Skeggs *et al.*, 1954).

Additionally, the kidneys sense the oxygen level of the blood and release erythropoietin in response to reduced levels of oxygen (Jacobson *et al.*, 1957; Pan *et al.*, 2011). Erythropoietin then stimulates the formation of red blood cells in the bone marrow to improve oxygenation of the blood (Jacobson *et al.*, 1956).

The kidneys also play an important role in the vitamin D3 synthesis by the conversion of 25-hydroxyvitamin D3 to 1,25-dihydroxyvitamin D3 (Fraser and Kodicek, 1970; Gray *et al.*, 1971; Shultz *et al.*, 1983). Additionally, the kidneys are involved in regulating the calcium, magnesium and phosphate concentration in the blood (Levin *et al.*, 2007). An impairment of kidney function can therefore lead to osteodystrophy, hyperparathyroidism, arterial or urinary calcification (Almquist *et al.*, 2020; Moe *et al.*, 2006; Palit and Kendrick, 2014).

Given the variety of functions the kidneys fulfil, it is not surprising that patients with impairment or complete loss of renal function require intensive monitoring and treatment (Eknoyan *et al.*, 2013). A kidney transplant is generally the best treatment for patients with end stage renal disease (Wolfe *et al.*, 1999). However, the number of patients requiring a transplant (4745 at the end of the financial year 2017/2018 in the UK) exceeds the number of available donor organs (3596 at the end of the financial year 2017/2018, 28 % were living donors), which results in a median waiting time of 2.1 years (Pankhurst *et al.*, 2019).

Engineered kidneys from induced pluripotent stem cells could bridge the gap between organ demand and supply. The generation of a protocol to generate renal tissue requires an understanding of the developmental processes during kidney morphogenesis.

1.3 Overview of kidney development

1.3.2 Ureteric bud (UB) induction and branching

In mice, metanephric kidney development starts around embryonic day (E) 10 by clustering of Ret-positive cells within the Wolffian duct (WD) (Chi *et al.*, 2009). The cells in the metanephric mesenchyme (MM) secrete Glial cell-derived neurotrophic factor (GDNF), a Ret ligand, which induces budding of the WD (Moore *et al.*, 1996; Pichel *et al.*, 1996; Sainio *et al.*, 1997). During budding, the Ret positive cells form a tip region while Ret negative cells form the trunk of the ureteric bud (UB) (Chi *et al.*, 2009; Costantini and Shakya, 2006). Ectopic budding of the WD is prevented by bone morphogenic protein 4 (BMP4) (Michos *et al.*, 2007). Ectopic budding is further prevented by separation of the MM from the WD in a SLIT2/ROBO2 dependent matter (Wainwright *et al.*, 2015). The tailbud-derived periwolffian mesenchyme (PWM) occupies the space between the MM and WD and prevents branching by secretion of BMP4 (Brenner-Anantharam *et al.*, 2007).

Stimulated by GDNF and Gremlin1, the UB elongates and bifurcates to form a T-shaped structure at E11.5 (**Figure 1-3**) (Michos *et al.*, 2004; Sainio *et al.*, 1997). The UB undergoes several rounds of branching to form a dense network of collecting ducts reaching about 1300 tips after 11 generations of branching at E16.5 (Short *et al.*, 2014). The collision of the collecting ducts is prevented by secretion and sensing of BMP7 (Davies *et al.*, 2014).

The branching rate decreases with formation of the renal pelvis (Short *et al.*, 2014). With the onset of pelvic development, the collecting duct tree undergoes extensive remodelling. While newly formed branches have an angle of about 100° , the angle of the earlier branch generations decreases over time (Short *et al.*, 2014). The change of the branch angle is caused by shortening of early branch generations via node retraction (Lindstrom *et al.*, 2015a).

Ectopic branching of the trunk is prevented by BMP4 (Cain *et al.*, 2005; Michos *et al.*, 2007; Miyazaki *et al.*, 2000). BMP4 also regulates the elongation of the ureteric trunk and induces the differentiation of the ureter (Cain *et al.*, 2005; Mamo *et al.*, 2017; Mills *et al.*, 2017; Miyazaki *et al.*, 2000; Miyazaki *et al.*, 2003).

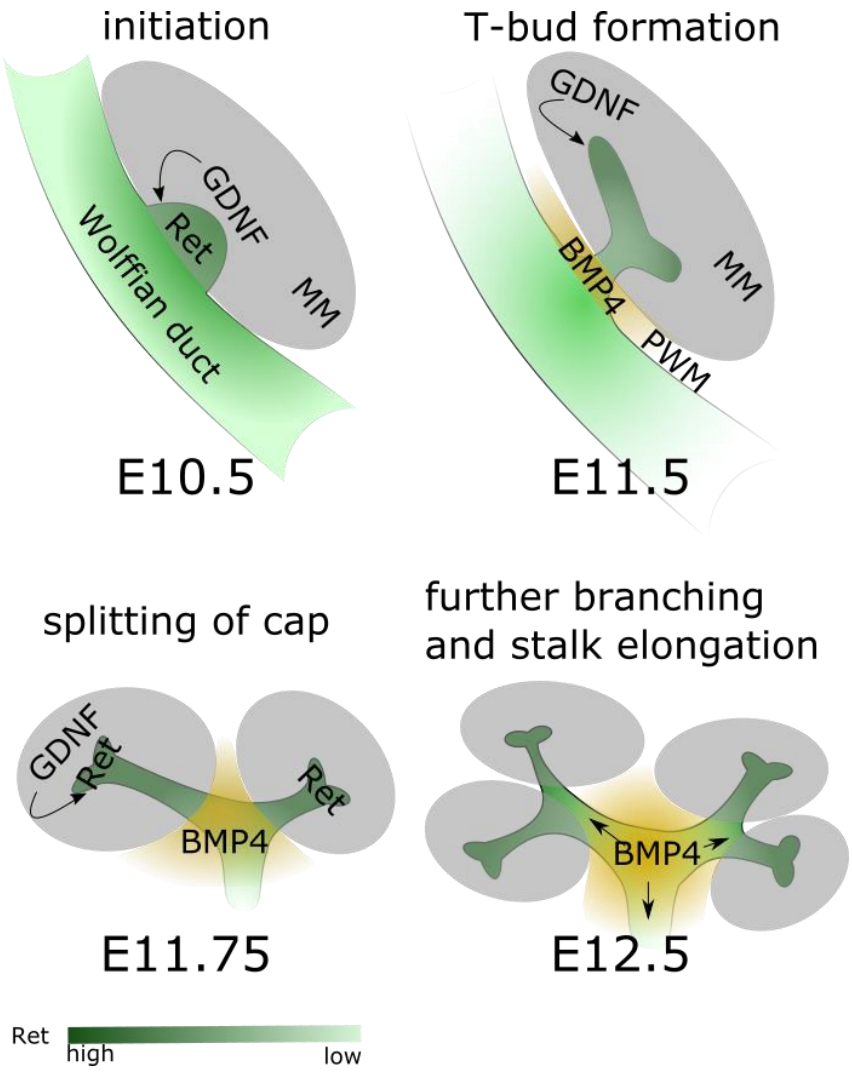

Figure 1-3: Ureteric bud induction and initial branch cycles. At E10.5 Ret positive cells of the ureteric bud form a cluster and proliferate in response to Glial cell-derived neurotrophic factor (GDNF), resulting in the formation of a bud. Around E11.5 the metanephric mesenchyme (MM) is separated from the Wolffian duct via the periwolffian mesenchyme (PWM). The ureteric bud has elongated and branched into a T-shaped structure. Ret positive cells cluster at the tips of the ureteric bud. GDNF induces the tip cells to proliferate and thereby forming additional branches. Branching of the stalk is prevented by BMP4 signalling.

1.3.3 Nephron development

The metanephric mesenchyme contains two main populations of cells – Six2+ nephron progenitors and FoxD1+ stromal progenitors which originate from a common progenitor population (Naiman *et al.*, 2017). The nephron progenitor cells (NPCs) arrange in characteristic cap-like structures around the collecting duct tips. The formation of these NPC-caps is controlled by the FoxD1 positive stromal cells (Hum *et al.*, 2014). This process is likely mediated by the Hippo pathway members Fat4 and Dch1, which are expressed in the stroma and cap mesenchyme respectively (Mao *et al.*, 2015). The survival of NPCs is regulated by BMP7, and members of the fibroblast growth factor (FGF) family (Brown *et al.*, 2011; Dudley *et al.*, 1999).

Nephrons are induced by ureteric bud derived Wnt9b, which leads to condensation of the NPCs (Carroll *et al.*, 2005). The peritubular aggregate then forms the polarized renal vesicle (Carroll *et al.*, 2005). The renal vesicles transition into a S-shaped stage (Potter, 1972). The distal region of the S-shaped body fuses with the collecting duct, while the proximal region forms the glomerulus (Cho *et al.*, 1998; Georgas *et al.*, 2009). The medial proportion of the nephron extends into the medullary region of the kidney to form the loop of Henle (**Figure 1-4**) (Cho *et al.*, 1998). The pattering of the developing nephron in proximal, medial and distal region is achieved by a gradient of canonical Wnt signalling (**Figure 1-4**B) (Lindstrom *et al.*, 2015b).

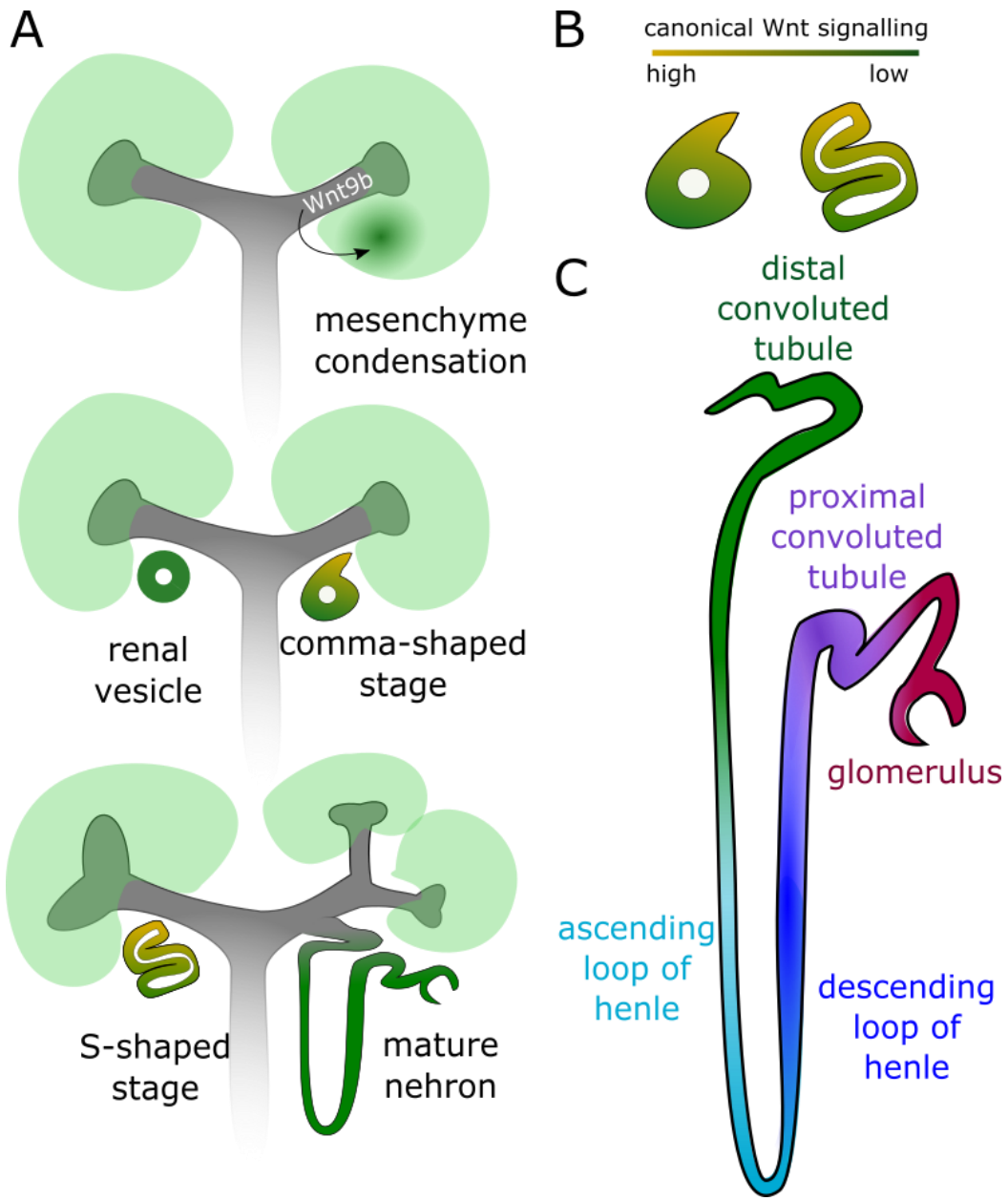

Figure 1-4: Nephron development. A: stages of nephron development. The nephron development begins with the condensation of nephron progenitor cells in response to Wnt9b. The condensated cells undergo MET and form the renal vesicle, which then forms the comma-shaped body. The comma-shaped nephron develops into the s-shaped nephron which fuses with the stalk of the collecting ducts. Subsequently the medial segment of the s-shaped nephrons extents into medullary region of the kidney to form the Loop of Henle. The distal region of the nephrons matures into the glomerulus. B: patterning of the nephron is induced by a gradient of canonical Wnt signalling. C: segments of the mature nephron.

1.5.2 Renal vascular development

The vasculature is critical for the growth and function of the kidneys. This paragraph is intended to give a brief overview on vascular development in general and about the vascularization of the kidney. A more detailed review on vascular development in general has been published by Udan *et al.*(2013).

In the embryo, the first blood vessels form via a process called vasculogenesis (Drake and Fleming, 2000). Vasculogenesis describes the *de novo* formation of blood vessels from vascular progenitors called angioblasts (His, 1900). In mice, clusters of TAL1+/Flk1+ angioblasts can be observed at E6.5 in the extraembryonic region and around E7.0 within the embryo (Drake and Fleming, 2000). At E7.3, two angioblast populations extend bilaterally along the midline (Drake and Fleming, 2000). The angioblasts arrange in cords connected by junctions (**Figure 1-5A**) (Strilic *et al.*, 2009). Then the endothelial cords polarize to form an apical surface at the interface between two cells (Strilic *et al.*, 2009). CD34-Sialomucins are transferred to the apical membrane where they cause the repulsion of the apical membranes of the two endothelial cells creating a small space between both cells (Strilic *et al.*, 2009). The lumen is then extended by non-muscular-Myosin II, resulting in the formation of luminized aortae (Strilic *et al.*, 2009). The two aortae fuse to form the dorsal aorta (Coffin and Poole, 1988). Subsequently, the lateral vascular networks are formed and anastomose with the dorsal aorta (Drake and Fleming, 2000).

The vascular network extends via sprouting and splitting of the initial vessels, a process called angiogenesis (Burri and Djonov, 2002). Splitting, or “intussusceptive”, angiogenesis describes the longitudinal fission of a vessel by involution of the contra-lateral endothelia to create an intra-luminal tissue pillar resulting in the formation of a second lumen within the vessel (**Figure 1-5B**) (Burri and Djonov, 2002). Splitting angiogenesis is mainly regulated by haemodynamic forces (Clark and Clark, 1940; Djonov *et al.*, 2002). Studies in chick kidneys suggest that splitting angiogenesis is the predominant form of angiogenesis in later stages of development, while sprouting

angiogenesis (**Figure 1-5C**) (hereafter referred to as angiogenesis) dominates earlier stages of development (Makanya *et al.*, 2005).

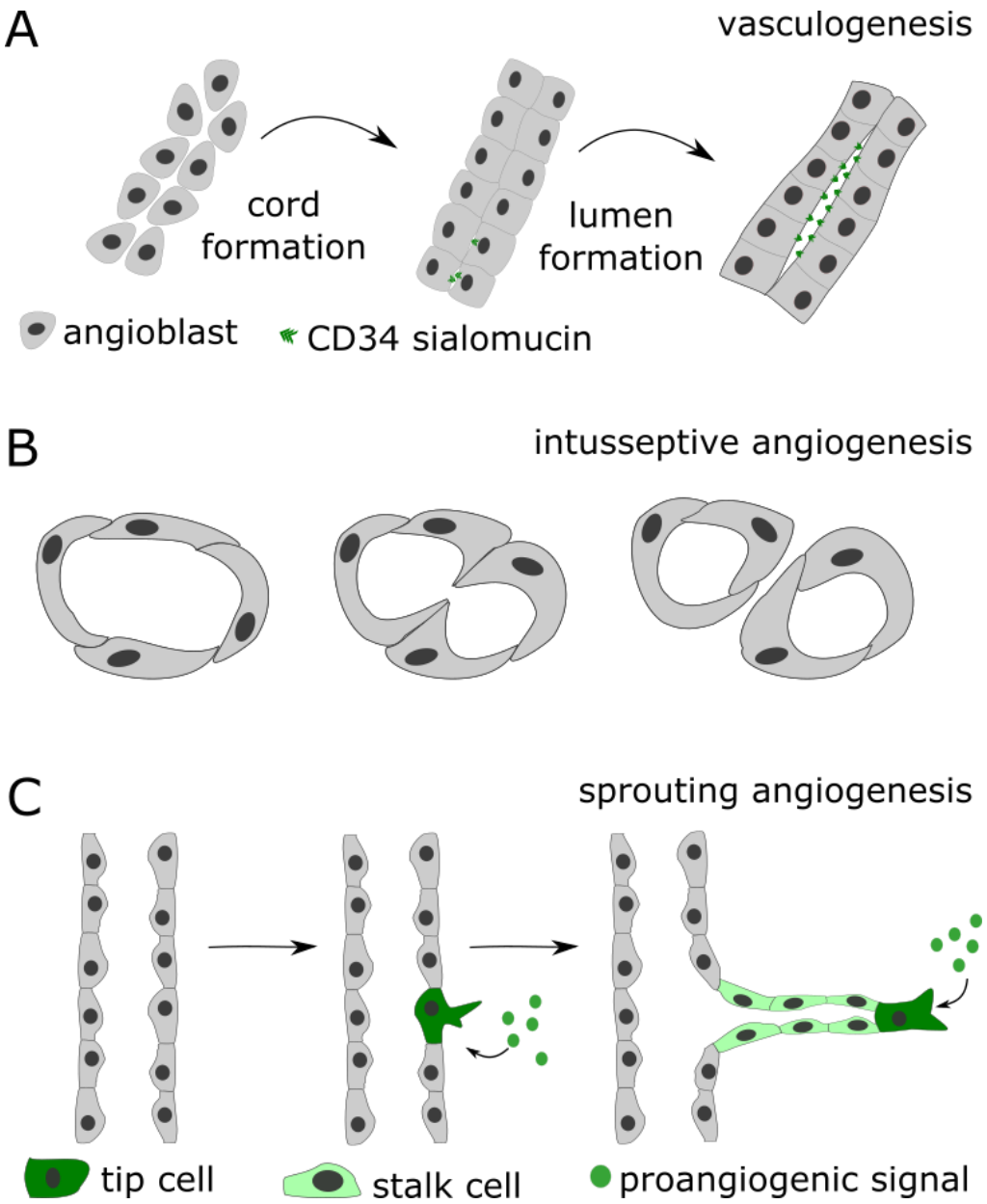

Figure 1-5: blood vessel development. A: Process of vasculogenesis: Endothelial precursor cells arrange in cords. Subsequently a lumen is formed by apical deposition of repulsive CD34 sialomucins. B: intussusceptive angiogenesis: The apical membrane of a blood vessel extends into the lumen towards the contralateral side. Once both sides meet the vessel separates longitudinal into two vessels. C: sprouting angiogenesis. One cell of the endothelial cell wall specifies into a tip cell. The tip cell senses pro-angiogenic signals and induces the adjacent stalk cells to proliferate which leads to formation of a blood vessel sprout.

Angiogenesis occurs in response to a proangiogenic stimulus such as vascular endothelial growth factor (VEGF)-A. It is initiated by detachment of the pericytes from the vessel wall (Benjamin *et al.*, 1998). The endothelial basal membrane is proteolytically degraded resulting in exposure of the endothelial cell layer to the surrounding tissue (Ausprunk and Folkman, 1977; Chang *et al.*, 2009; Schoefl, 1963). One of the endothelial cells differentiates into a tip cell which senses VEGF-A (Gerhardt *et al.*, 2003). VEGF-A induces the expression of Dll4 in the tip cells which turns the neighbouring cells into stalk cells that proliferate in order to elongate the sprouting vessel (Gerhardt *et al.*, 2003; Hellstrom *et al.*, 2007). During maturation of the nascent vessels the pericytes are recruited followed by smooth muscle cells (Benjamin *et al.*, 1998).

Angiogenesis is the dominant process during the vascularization of the kidney (Munro *et al.*, 2017). During branching of the ureteric bud into a T-shape, blood vessels sprouting from the common iliac arteries form a ring structure around the ureteric stalk (Munro *et al.*, 2017) (**Figure 1-6A**). While the kidneys migrate cranially, new vascular connections with the dorsal aorta are formed and previous ones degenerate (Isogai *et al.*, 2010). After splitting of the cap mesenchyme around day 12 of development, the vessels migrate within the forming metanephric interstitium while avoiding cap mesenchyme and staying in close proximity to the collecting duct (Munro *et al.*, 2017) (**Figure 1-6B**). With the onset of nephron development, the endothelia form a plexus around the newly formed renal vesicles (Daniel *et al.*, 2018) . During the transition into the S-shaped stage, the endothelia migrate into the cleft and form a dense network around the distal end of the nephron (Daniel *et al.*, 2018) (**Figure 1-6C**).

The migration of endothelia into the nephron is induced by expression of VEGF-A from podocytes which form a layer of cuboidal cells within the vascular cleft (Eremina *et al.*, 2003; Vaughan and Quaggin, 2008). During vascularization the podocyte layer

segregates from the proximal tubules to form the glomerulus (Vaughan and Quaggin, 2008). The endothelia within the glomerulus proliferate to form a dense capillary network and form lumen under control of Transforming growth factor β (TGFβ) which induces apoptosis of the lumen-occupying endothelial cells (Fierlbeck *et al.*, 2003).

The early renal blood vessels at E11.5 were found to carry erythrocytes which could indicate that they are connected to the circulatory system, though they may also be formed by haemovasculogenesis (Munro *et al.*, 2017). Prior studies, using fluorescent dyes to visualize the blood flow, confirmed perfusion of the major renal blood vessels at E13.5 but not in earlier kidneys (Rymer *et al.*, 2014; Rymer and Sims-Lucas, 2015).

Around day E13.5, a tree of large-diameter blood vessels becomes visible, which express the arterial marker connexin-40 (Daniel *et al.*, 2018) (**Figure 1-6D**). Daniel *et al* detected venous blood vessels aligning with arteries in "artery-vein doublets" based on their morphology starting from E14.5. Within the next day of development, a smooth muscular lining forms around the renal arteries (Hurtado *et al.*, 2015). Smooth muscle cells differentiate from Foxd1+ stromal progenitors, by decreased expression of Pbx1 and subsequently migrate towards the blood vessel to form the smooth muscle cell lining of the renal arteries (Hurtado *et al.*, 2015).

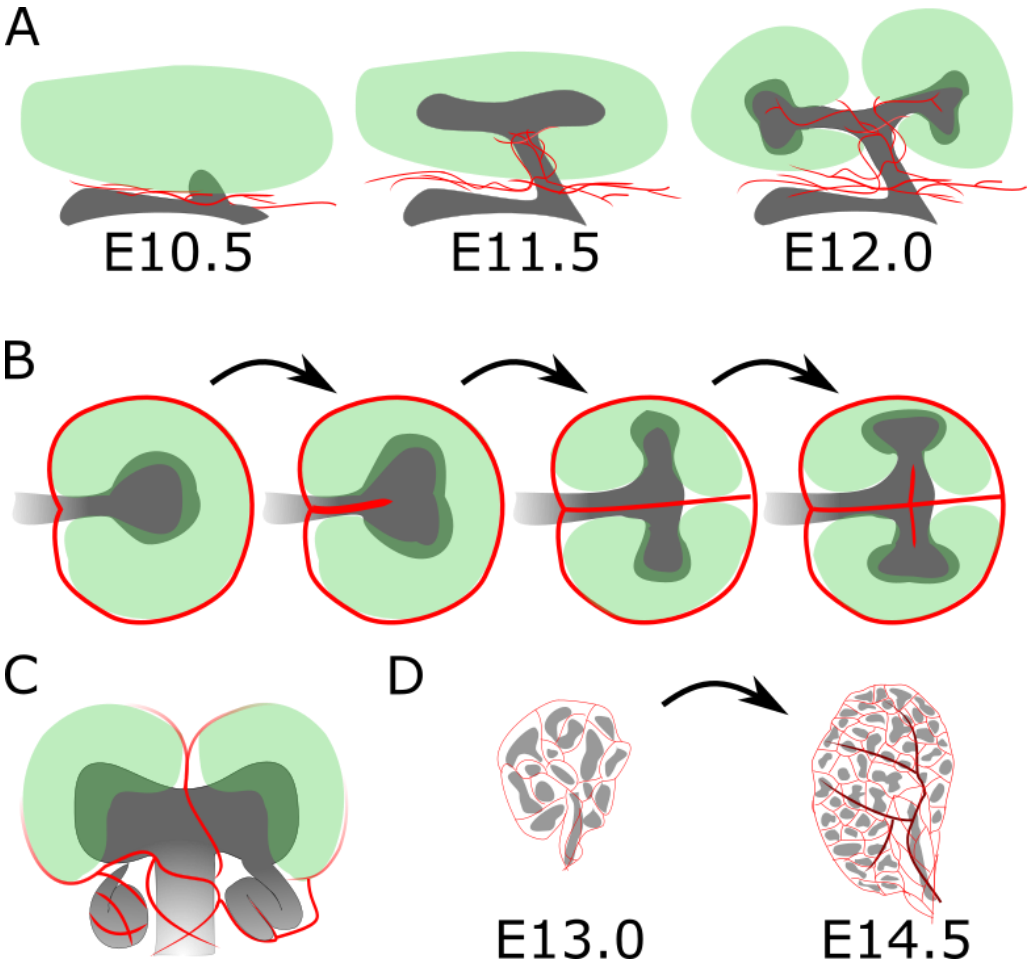

Figure 1-6: renal vascular development. A: Blood vessels enter the kidney along the collecting duct. B: Formation of the vascular plexus during ureteric branching and splitting of the cap mesenchyme. C: The blood vessels grow around a comma-shaped nephron. After transition to the s-shaped stage, the blood vessels grow in the vascular cleft. D: A hierarchical vascular network forms between E13.0 and E14.5. The arteries contain a smooth muscle cell lining at E14.5. Illustration inspired by works of Munro *et al.*, (2017) and Daniel *et al.*, (2018)

1.4 Kidney organoids

1.4.1 Kidney cultures and generation of kidney organoids from renal progenitors

Embryonic kidney explants can mature to a certain degree in culture. Early kidney explant cultures were performed by using a matrix from clotted fowl serum as growth

substrate (Bentley, 1936). Later on, it was found that kidneys develop well when cultured on a permeable filter placed on a metal grid (Grobstein, 1956; Saxén, 1987; Trowell, 1954). This culture method, also referred to as Trowel culture (**Figure 1-7**), allows the kidney to branch and for early stage nephrons to form (Saxén, 1987). However more mature nephrons containing Loops of Henle are rarely observed in this method (Sebinger *et al.*, 2010). A higher degree of maturity can be achieved by culturing the kidney explants on glass with a thin coat of medium, a method called low-volume culture (Sebinger *et al.*, 2010).

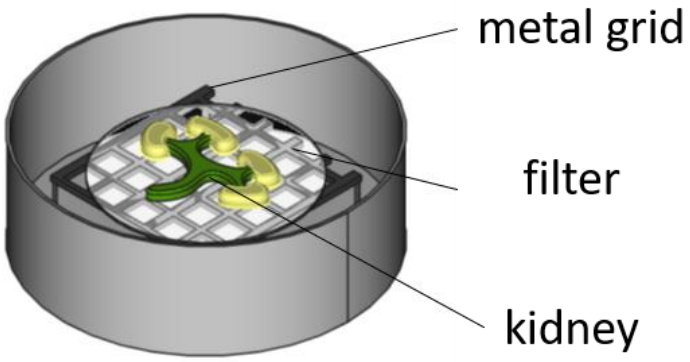

Figure 1-7: Trowel culture method. The kidney explant is cultured on a filter which is placed on a metal grid to keep it at the air liquid interface.

Embryonic kidneys were used to create the first kidney organoids (**Figure 1-8**). By dissociation and reaggregation of the explants it was shown that kidney cells can self-organize into kidney-like structures, such as short collecting duct fragments, surrounded by nephron progenitors and nephrons (**Figure 1-8A**) (Unbekandt and Davies, 2010). The isolation of one of the collecting duct fragments from either an embryonic kidney or a reaggregated kidney organoid following recombination with isolated metanephric mesenchyme leads to the formation of a kidney organoid containing a single collecting duct network (**Figure 1-8B and C**) (Ganeva *et al.*, 2011). The realism of these kidney organoids can be further improved by providing a local stimulus using BMP4 (Mills *et al.*, 2017). BMP4 inhibits branching and induces the differentiation into a urothelium (Michos *et al.*, 2007). Therefore a local stimulus of BMP4 supresses branching and results in the formation of an asymmetric kidney

organoid containing a branched collecting duct network on one side and a uroplakin-positive unbranched structure on the other side, very similar to an embryonic kidney explant (**Figure 1-8D**) (Mills *et al.*, 2017).

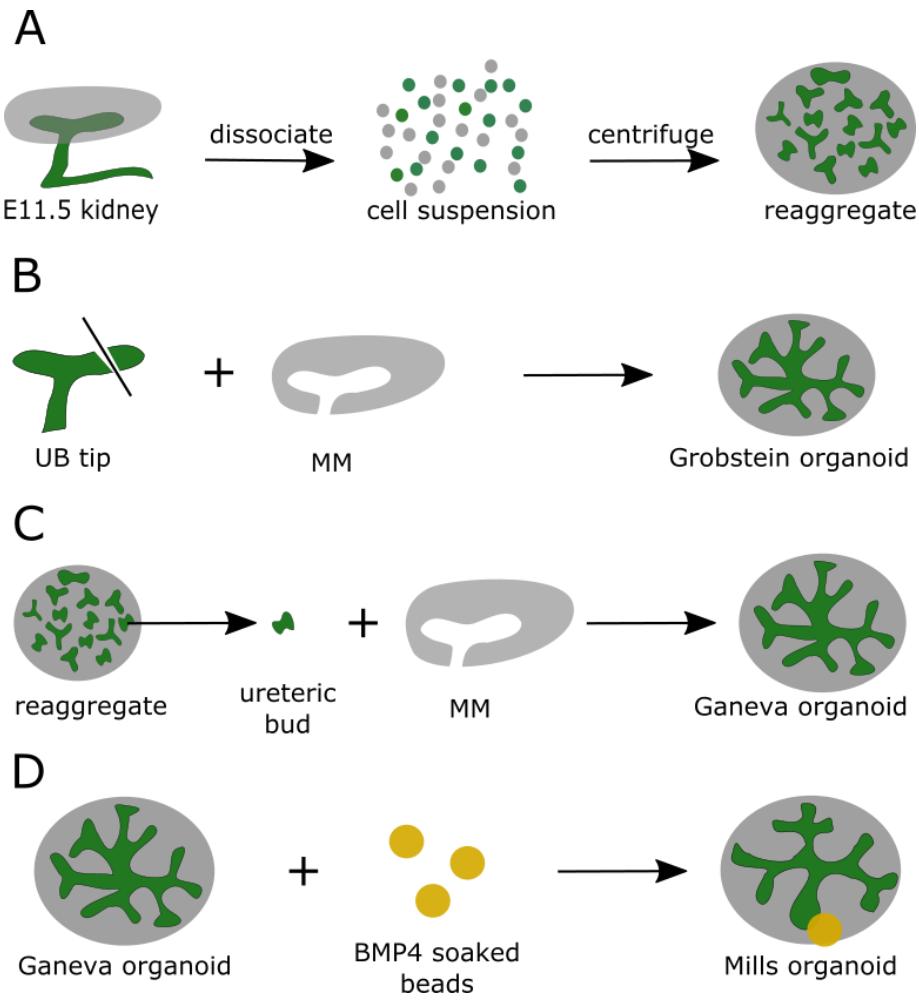

Figure 1-8: types of embryonic kidney derived organoids. A: Dissociation and reaggregation of an embryonic kidney produces an organoid that contains disconnected branches of ureteric buds (green) surrounded by metanephric mesenchyme (grey). B: combining the tip of the ureteric bud (UB) from a kidney with metanephric mesenchyme (MM) results in an organoid containing a continues collecting duct network (green) surrounded by MM (grey). C: An organoid with a continues collecting duct network may also be generate by isolating a ureteric bud (UB) fragment from a reaggregated organoid, as described in A, and combining it with metanephric mesenchyme (MM). D: The realism of the organoid produced as illustrated in B and C can be improved by placing a bead soaked in bone morphogenic protein 4 (BMP4) near one of the branches of the collecting duct (green). The targeted branch will stop branching and express uroplakin, mimicking the ureter of a kidney. Illustration inspired by Mills *et al.* 2017

1.4.2 Kidney organoids from ES and iPS cell lines

Kidney organoids from murine renal progenitors display a great degree of similarity to early embryonic kidneys, which makes them a valuable model to study kidney development and disease. However, their use for regenerative medicine and drug testing is limited due to potential species differences between mouse and human. The use of human embryonic kidneys would circumvent problems occurring through species differences but is limited by availability of human fetal material. An alternative could be the generation of kidney organoids from reprogrammed induced pluripotent stem cells (iPSCs).

While adult kidneys are complex organs that comprise of over 20 cell types, the majority of these cells originate from three progenitor populations present in early embryonic kidneys: Gata3+ ureteric bud cells, Six2+ nephron progenitors and Meis1+ stromal progenitors (Park *et al.*, 2018). There are several protocols that can generate kidney organoids containing cells from all three compartments in varying proportions including protocols for large scale production of organoids (Kumar *et al.*, 2019; Takasato *et al.*, 2016; Takasato *et al.*, 2015). While these organoids display some microscale structural realism such as pattered nephron segments, they lack the macroscale anatomy of a kidney consisting of a single, asymmetric collecting duct network (Kumar *et al.*, 2019; Takasato *et al.*, 2016; Takasato *et al.*, 2015).

One way of introducing a macroscale anatomic realism would be to separately generate ureteric buds, stromal progenitor and nephron progenitors following recombination of these cellular compartments. Ureteric buds have been previously generated from mouse embryonic stem cells and human iPSCs (Taguchi and Nishinakamura, 2017). Recombination of these ureteric buds with sorted nephron progenitors and stromal progenitors resulted in the formation of a single branched collecting duct network similar to Ganeva-type organoids (**Figure 1-8D**) (Taguchi and Nishinakamura, 2017). There are also protocols that generate nephron progenitors from human iPSCs with 80 to 90 % specificity or to selectively propagate and thereby

enrich nephron progenitors in culture (Brown *et al.*, 2015; Li *et al.*, 2016; Morizane and Bonventre, 2017; Tanigawa *et al.*, 2016). However, there is currently no protocol to selectively induce or propagate stromal progenitor cells. Additional limitations for the generation of organoids from iPS cells are currently the abundance of non-renal off-target cells, commonly referred to as "off-target cells" and the variability of differentiation efficiency between runs (Phipson *et al.*, 2019; Wu *et al.*, 2018). These challenges will need to be addressed in order to generate organotypic iPSC-derived kidney organoids.

A major limitation for the medical use of kidney organoids is the lack of a perfusable vasculature as main function of the kidney is to filter blood. Without proper vascularization it would be difficult to tell how efficient the kidney organoids filter blood, and therefore it would be challenging to estimate whether they would be suitable for transplantation. There would also be practical concerns, since without blood vessels the organoid cannot be connected to the patient's vasculature. While a transplanted non-vascularized organoid may be able to connect to the patient's vasculature after implantation (van den Berg *et al.*, 2018), there would be little control over where it connects and how the vasculature develops. Additionally, it is unlikely that non-vascularized organoids could grow to a sufficient size for transplantation, as the diffusion of oxygen and nutrients within 3D tissues is limited (McMurtrey, 2016).

The presence of a functional vasculature could also aid in using renal organoids for drug testing as using perfused, vascularized kidney organoids for nephrotoxicity tests has potential advantages compared to non-vascularized organoids. Firstly, perfusion of drugs rather than adding them to the medium, could give a more realistic readout about nephrotoxicity, because only the cells that would naturally be in contact with the drug would be exposed to it. In contrast, when adding a drug to the medium all peripheral cells, including the ones that would normally not be exposed, for example the stromal cells, would be in contact with the drug, which could lead to false positive nephrotoxicity results. Additionally, perfusing the drug could give a better indication

how effectively it is filtered out by the organoid, since it would be primarily in contact with the glomerular cells, where the filtration occurs.

To date, the generation of anatomically realistic iPSC derived organoids is limited by above factors. Murine embryonic kidney-derived organoids (**Figure 1-8**), do not share all limitations of iPSC derived organoids, but they do lack a functional vascular system and do not represent the natural shape of their tissue of origin, as they grow rather flat. These limitations also apply to embryonic kidneys cultured *in vitro*. Using kidney explants as a model, I aim to induce a more natural three-dimensional growth by embedding the explants in type I collagen and to enhance the maturity of their vascular system.

Chapter 2 – Methods

2.1 Chapter 3 and 4 methods

2.1.1 Animals

Tissue and embryos were obtained from pregnant CD-1 females which were culled by a staff member of the Bioresearch & Veterinary Service (University of Edinburgh) using a method listed under the Schedule 1 of the UK Animals Scientific Procedures Act 1986.

2.1.2 Kidney dissection and culture

Embryos were removed from the uterine using two scalpel blades. All further steps were performed using 25G needles (Fisher Scientific). The embryos were decapitated and cut between dorsal superior limb buds and ventral inferior limb buds. Subsequently, the dorsal part was cut sagittally along the spine. The embryo was arranged with the ventral side facing the bottom. The dorsal tissue was flipped over the limb bud exposing the kidney on the medial side. The kidney was removed from the embryo by cutting along the sagittal axis. The dissected kidneys were cultured at 37 °C and 5 % CO_2 on Transwell plates (0.4 µm pore polyester, Scientific Laboratory Supplies, 3450) with 1.5 ml kidney culture medium (KCM, Minimum essential Eagle Medium (MEM, Merck M5650) supplemented with 10 % foetal bovine serum (FBS, Biosera) and 1 % Penicillin/Streptomycin (Thermo Fisher) or embedded in 1 mg/ml type 1 collagen (Corning).

For the three-dimensional culture of kidneys, type 1 rat tail collagen (Corning) was diluted in MEM (Merck, M5650) to a final concentration 1 mg/ml in a volume of 300 µl/well of a 24 well plate. The pH of the collagen dilution was adjusted by addition of 100 µl 0.1 N NaOH for each ml of collagen. After polymerization for a minimum of 15 min at 37 °C the kidney explants were added on top of the collagen and unless otherwise specified overlaid with additional 300 µl collagen solution (1 mg/ml). If necessary, kidney explants were dispersed immediately using dissection needles. After polymerization for 15 - 30 min, the collagen was overlaid with 600 µl of KCM.

2.1.3 3D plasticity assay

E11.5 kidney explants were isolated and cultured on a Transwell. After 3 or 6 days of culture the explants were gently scraped from the Transwell using a 25G dissection needle. Then the explants were embedded into type 1 collagen and cultured for additional 3 days. Subsequently the explants were removed from the collagen using dissection needles and fixed with paraformaldehyde (PFA, Merck).

1.2.4 Generation of reaggregated and organotypic organoids

Reaggregated kidney organoids were produced as described previously (Unbekandt and Davies, 2010). In brief, eight to ten E11.5 kidneys were incubated for 3 min in 1x trypsin-EDTA (Merck, T4174). Then the trypsinised kidneys were transferred into KCM and dissociated with a pipette. The single cell suspension was passed through a cell strainer (40 µm pore size, VWR, 734-0002) and aggregated by centrifugation for 3 min at 3000 rounds per minute (rpm) (equivalent to 800 times relative centrifugal force (rcf)). The aggregate was transferred onto a polycarbonate membrane (Millipore, TMTP02500) and cultured for one to seven days in KCM at 37 °C and 5 % CO_2.

Organotypic kidney organoids were generated by recombination of a single ureteric bud from a one-day cultured reaggregated organoid with the mesenchyme of eight to ten E11.5 kidneys as described previously (Ganeva *et al.*, 2011). After culture overnight at 37 °C and 5 % CO_2 on polycarbonate filters, the organotypic organoids were transferred onto 1 mg/ml type I collagen. To prevent detachment of the organotypic organoids, they were overlaid with 1 mg/ml type 1 collagen prior to addition of KCM.

2.1.5 Standard immunofluorescent staining

Embedded kidneys were removed from the collagen using 25G dissection needles. Transwell-cultured kidneys were fixed on the Transwell membrane. The kidneys were fixed in 100 % prechilled methanol (Fisher Scientific) for a minimum of 30 min at -20 °C. The methanol was removed and the samples were washed three times with phosphate-buffered saline (PBS) at room temperature (RT). Non-specific binding was prevented by 30 min incubation in blocking buffer (3 % donkey serum, 10 % dimethyl sulfoxide (DMSO), 0.2 % Triton-X-100 in PBS, prepared from tablets, Merck, P4417). The primary antibodies (see Appendix **Table A 1**) were diluted 1:200 in blocking buffer and incubated over night at 4 °C. Unbound primary antibodies were removed by three washes with PBS. The secondary antibodies (see Appendix **Table A 2**) were diluted 1:200 in blocking buffer and incubated 2 h at RT or overnight at 4 °C If indicated Topro-3 (Thermo Fisher) was diluted 1:4000 and incubated with the secondary antibodies. After three washes with PBS Transwell-cultured kidneys were mounted on glass slides using VectaShield (Vector Laboratories). Collagen-cultured kidneys were transferred to an 18 well µSlide (ibidi) for imaging.

To evaluate specificity of the secondary antibodies in isolated E13.5 kidneys, Transwell-cultured kidneys and collagen-cultured kidneys were stained with the secondary antibody only (Appendix, **Figure A 1** to **Figure A 6**).

2.1.6 Immunofluorescence staining with PFA prefixation

Kidneys were fixed with 4 % PFA (in PBS, pH adjusted to 7.2 using NaOH) for 30 min to 4 h (depending on the tissue volume) and permeabilized by dehydration in steps (20%, 40%, 60%, 80% and 100% methanol). Subsequently, autofluorescence was bleached by 15 min incubation in 5 % hydrogen peroxide. The kidneys were rehydrated in steps and washed three times with PBS. Subsequently, the samples were incubated for 30 min to 4 h in permeabilization buffer (20 % DMSO, 300 mM glycine and 0.2 % Triton-x-100 in PBS). After permeabilization the kidneys were blocked and stained as described above.

2.1.7 Ethyl cinnamate clearing

Stained samples were dehydrated through graded alcohols (20%, 40%, 60%, 80%, 100% methanol). Subsequently the samples were transferred into 100 % ethyl cinnamate and incubated until transparency (adapted from Klingberg *et al.*, 2017). Samples may be stored in ethyl cinnamate in a tightly sealed polypropylene or glass tube for up to a week at RT. During storage, care was taken to avoid exposing the samples to light. Samples should not be stored in polystyrene containers, as those are dissolved by ethyl cinnamate. Prior to imaging, the cleared samples were transferred to an 18-well µSlide (ibidi) and imaged in 20 µl ethyl cinnamate.

2.1.8 Detection of Hypoxia

E11.5 kidney explants were cultured for 30 h either on a Transwell or embedded in 1 mg/ml type 1 collagen as described in section **2.1.2 Kidney dissection and culture**. Subsequently half of the Transwell-cultured kidneys were used as a positive control and treated with KCM containing 400 µM $CoCl_2$ to mimic hypoxia by induction of hypoxia-inducible factor 1α (Hif1α) (Chachami *et al.*, 2004). In collagen-cultured

kidneys the volume of culture medium was equal to the volume of collagen. Under the assumption of the collagen as 100 % liquid, the explants were treated with KCM containing 800 µM $CoCl_2$, yielding in a final concentration of 400 µM. After 16 h of treatment kidney explants were fixed and stained for Hif1α as described in section **2.1.6 Immunofluorescence staining with PFA prefixation**.

2.1.9 Microscopy and image processing

Images were taken using the Zeiss LSM800 or Nikon A1R confocal microscope. When intensity between samples was compared, the microscope settings were kept constant between samples within the same culture group but adjusted between Transwell and collagen-cultured samples. For experiments in which brightness did not contribute to the result, minor adjustments were taken to avoid overexposure.

Images were processed using ImageJ Version 1.51n. The images were processed differently depending on whether the relevant information was purely reliant on the localization of the stained structures or on the staining intensity.

Where the images contained purely structural information that did not rely on the staining intensity, the brightness and contrast were adjusted to optimize visibility of the stained compartments. In some of these images “salt-and-pepper” noise was removed using a median filter with a radius of 2 pixel. This filter measures the brightness of each pixel within the set radius and sets the brightness of the central pixel to the median value. More diffuse background signal, such as shading, was removed using the “subtract background” function of ImageJ. The function, which is based on the “rolling ball” algorithm (Sternberg, 1983), was used with a radius of 50 pixel. If the signal intensity was relevant to the result, the brightness and contrast were adjusted for better visualization. The settings were then kept constant between control and treated samples. Any intensity measurements were performed on raw images.

2.1.10 Explant size and volume measurement

Explant dimensions were measured using FIJI (Schneider *et al.*, 2012). To measure the maximum diameter, the optical sections of the whole kidney explants were merged in a maximum z-projection image. Subsequently, a circle was drawn around the explant to measure the maximum diameter. The thickness was measured within the orthogonal (yz) view using the line tool. For volume measurement the outline of the explants was traced using the freehand selection tool. Subsequently, any outside signal was removed using the "clear outside" function and a threshold was applied to segment the stained kidneys from the background. The threshold was kept constant between images from the same dataset. The volume measurement was performed using a published macro (Villani, 2018).

2.1.11 Nephron quantification

Nephrons were quantified using the 'surface' tool in Imaris Version 6.2. The surface tool enables the extraction of a 3D structures by rendering a surface along the stained structures and detecting their connections and edges. It also provides the number and measurements of the structures found and therefore can be used for counting. Settings were adjusted for each image individually due to different intensity and background between samples. The precision of the automated quantification was determined for one dataset by manual count. The difference between automated quantification and manual count was about 5 %. For the quantification of the total number of nephrons the data from three independent experiments with 4 kidneys from each experiment in each culture group was pooled (total N = 12). Ass1 positive nephrons were quantified from one dataset containing 4 explants for each culture condition.

2.1.12 Statistical analysis used in Chapter 3

The calculation of confidence intervals was performed using SciPy (Virtanen *et al.*, 2020). Variances were compared using a F-test. The normal distribution for all datasets was verified using a Shapiro-Wilk test. All but one dataset tested positive for normal distribution. In the dataset which tested negative for normal distribution, the Transwell-cultured kidney displayed a significantly reduced nephron number, as determined using a Grubbs outlier test ($p < 0.01$). Exclusion of this kidney from the Shapiro-Wilk test resulted in a positive normality test. The outlier was not excluded for subsequent analysis.

The statistical significance was determined using a two-tailed Student's t-test for independent samples in cases in which variances were similar or by using Welch's t-test in case which the variances displayed a statistically significant difference. For the dataset where normal distribution was affected by the presence of an outlier, the statistical significance, determined using Welch's t-test, was confirmed using a Kruskal-Wallis test.

2.2 Chapter 5 methods

2.2.1 Kidney culture and treatments

E11.5 kidneys were isolated and cultured on top of 50 µl type 1 collagen as described before (**2.1.2 Kidney dissection and culture**) in a 96 well plate. For the induction of *Vegfa* expression, the kidney explants were cultured in 100 µl low serum KCM (LS-KCM, MEM (Merck) supplemented with 1.5% FBS (Biosera) and 1x penicillin/streptomycin (Gibco)). To induce VEGF expression the kidney explants were treated for either 24 h or 72 h, as indicated, with 100 µl LS-KCM containing the indicated concentrations of progesterone (Merck) and Insulin-like growth factor 1

(IGF1, Biolegend) (Neubauer *et al.*, 2009; Slomiany and Rosenzweig, 2004; Swiatek-De Lange *et al.*, 2007).

2.2.2 Immunostaining

Immunostaining was performed as described in chapter 3 methods (**2.1.6 Immunofluorescence staining with PFA prefixation**). For grafted kidneys that were injected with fluorescent dyes and kidney organoids the bleaching step was omitted to prevent bleaching of the fluorescent dye.

2.2.3 RNA isolation, primer design and rtPCR

E11.5 kidneys were cultured for 2 days in LS-KCM and treated for additional 24h with the indicated VEGF inducers (see **2.2.1 Kidney culture and treatments**). The RNA was isolated using an RNA easy mini extraction kit (Qiagen) according to the manufacturer's instructions. For the cDNA synthesis, 100 ng RNA were diluted in 14 µl of water. After addition of 1 µl (50 ng) prediluted oligo d(T) primer (Promega, C110A), the samples were heated to 70 °C for 5 min and cooled on ice to break secondary structures. After addition of 10 µl master mix (**Table 2-1**), the samples were incubated for 1 h at 42 °C. The reaction was inactivated by heating the samples to 95 °C for 5 min.

Table 2-1: reverse transcription master mix

Reagent	**Promega catalogue number**	**Volume (µl/sample)**
RNAsin ribonuclease inhibitor	N251A	0.625
M-MLV RT buffer	M531A	5
M-MLV reverse transcriptase	M170A	1
dNTPs	U144A	1.25
water	From Qiagen RNAeasy kit	2.125

Primers were designed to bind across an exon-exon junction to prevent the amplification of genomic DNA. The specificity of the primers was tested *in silico* using the "pubmed primer blast" (Ye *et al.*, 2012). All selected primers resulted in a single amplicon of the expected size (**Figure 2-1**), which was determined by gel electrophoresis after amplification with GoTaq Green (Promega, for experimental details see Appendix **Table A 3** and **Table A 4**). The annealing temperature was predicted using the "NEB tm calculator" (NEB, 2016). Thereby the primers were chosen to have a predicted annealing temperature of 56 to 58 C. The selected primers were evaluated using "primerstats" (Stothard, 2004). The primer efficiency for each primer pair (**Table 2-2**) was determined by using serial dilutions of RNA.

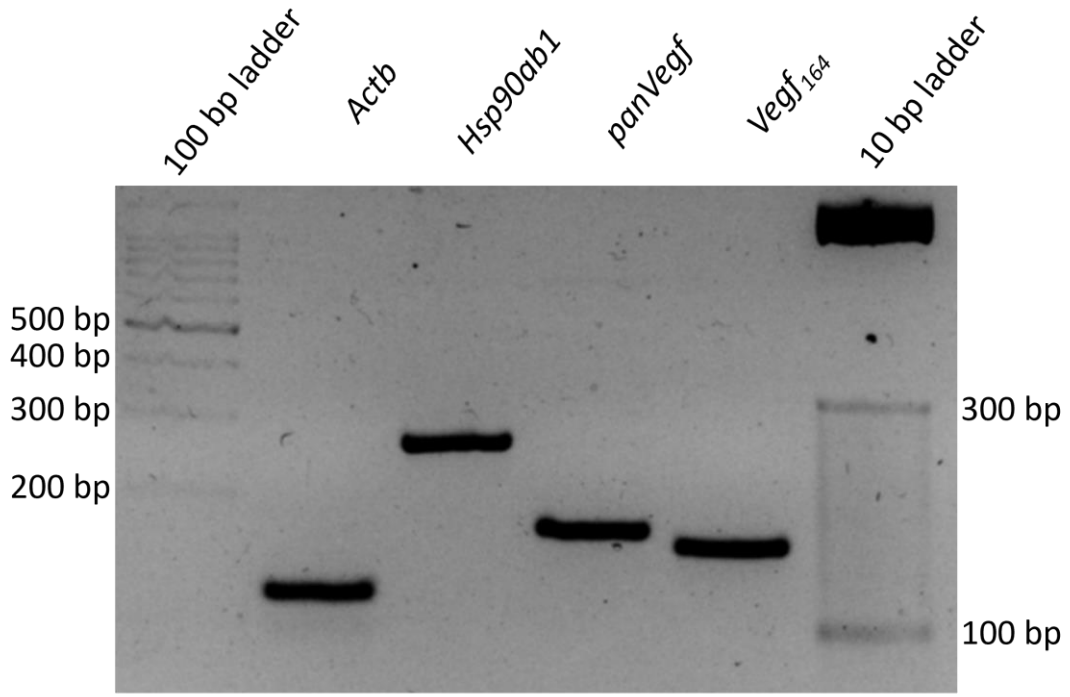

Amplicon	*Actb*	*Hsp90ab1*	*panVegf*	*Vegf*$_{164}$
Predicted size	122	267	166	156

Figure 2-1: Observed amplicon length matches predicted amplicon length

Table 2-2: primer sequences for realtime PCR

Primer	sequence
β-actin fwd	GCCACCAGTTCGCCATGGAT
β-actin rev	GCCCACGATGGAGGGGAATACA
Hsp90ab1 fwd	CACCCTCTATTTGGAGAAGGAAC
Hsp90ab1 rev	CCATACTCCTCCTGCGTGAT
VEGFA$_{164}$ fwd	CCAGAAAATCACTGTGAGCCTT
VEGFA$_{164}$ rev	CCTTGGCTTGTCACATCTGC
panVEGFA fwd	GCCAAGGCGCGCAAGAGA
panVEGFA rev	GCCTGGGACCACTTGGCA

Prior to rtPCR, the cDNA was diluted 1:2 (for VEGF$_{164}$ expression) to 1:4 (for panVEGF expression). The different dilutions were chosen based on the estimated difference of expression.

For the rtPCR, 2 µl of the diluted cDNA were combined with 5 µl 2x PowerUp Sybr Green Master Mix (Invitrogen) and 0.2 µl of each primer. Each sample was used in technical triplicates. The expression was analysed using the ΔΔCt method (Livak and Schmittgen, 2001). Therefore, the Ct values of both housekeeping genes (*Actb* and *Hsp90ab1*) were averaged. Subsequently, the difference between *Vegf$_{164}$*/*panVegf* (ΔCt) for each sample was calculated. The average ΔCt value of the control samples was used to calculate the ΔΔCt value of each sample, including the control samples themselves.

2.2.4 CAM grafting

The grafting experiments were conducted based on advice from Patricia Prado similar to the procedure published by (Garreta *et al.*, 2019).

Hy-line wild-type chicken eggs were obtained from the National Avian Research Facility. The eggs were maintained at 37 °C and 60 % humidity. After one day of culture, 4 ml of albumin was extracted from each egg using a syringe with a 21G needle. On day six of culture, a window was cut in the shell of the eggs and sealed with transparent tape. Prior to grafting on day seven, a small injury in the chorioallantoic membrane (CAM) was made using a wide orifice pipette tip (Starlab, E1011-8400). E11.5 kidneys, cultured for either 24 h or 72 h on type 1 collagen, were placed on the site of injury. After 3 additional days of culture, the CAM containing the grafted kidneys was cut out and fixed with PFA. For some samples, the CAM vasculature was injected with 10 µl dextran-FITC (1 mg/ml, Merck) or Donkey-anti-Mouse AlexaFluor594 conjugated antibody to visualize the blood flow through the kidney prior to extraction.

2.2.5 Calculation of confidence intervals of the difference of the proportion of grafted kidneys

The 95% confidence interval (CI) for the difference between the proportion of grafted kidneys with preculture in grafting and control medium was calculated as described previously (Gardner and Altman, 1986) using the following equation:

$$CI = \left(\frac{g}{t_g} - \frac{c}{t_c}\right) \pm 1.96 \sqrt{\frac{g(t_g - g)}{t_g^3} + \frac{c(t_c - c)}{t_c^3}}$$

g: number of successful grafts of kidneys precultured in grafting medium

t_g: total number of kidneys, precultured in grafting medium, that were detected on CAM after *in ovo* incubation*

c: number of successful grafts precultured in control medium

t_c: total number of kidneys, precultured in control medium, that were detected on CAM after *in ovo* incubation*

*Kidneys that could not be detected on the CAM after *in ovo* incubation (less than 5 %) were excluded from the analysis.

2.3 Chapter 6 methods

General comment on perfusion rates:

Initial perfusion experiments were performed using a Biorad Econo Peristaltic Pump perfusion pump. The flow rate delivered by a peristaltic pump is not only affected by the speed of the pump but also by the diameter of the tubing and therefore requires calibration. The Econo pump offered a pre-calibrated mode for the chosen tubing diameter (0.8 mm) which was used to set the flow rate. The pump was later replaced with a Gilson Minipulse 3 peristaltic pump. As this pump did not have the option to automatically adjust the flow rate to the tubing diameter, it was manually calibrated. For the calibration, the flow rate of this pump was measured once for each type of tubing (F1825101 and 10256022 from Gilson) used, by running the pump three times for 10 minutes at a setting of '1'. During each of the 10-minute cycles the medium was collected to measure the total volume. This volume was used to calculate the setting required to achieve indicated flow rates. However, due to the working mechanism of this pump and minor differences as well as tearing of the tubing the actual flow rate may have been different from the indicated flow rate. An individual adjustment of the flow rate was not feasible because several cultures were run simultaneously and therefore could only be run with constant settings.

2.3.1 Initial bioreactor assembly

Silicone caps (1 cm diameter, Universal Biologicals) were used as a makeshift bioreactor. Two glass capillaries (inner diameter (ID): 0.10 mm, outer diameter (OD): 0.17 mm, CM Scientific, CV1017) were on opposing sides of the silicone cap. The capillaries were either inserted into 270 µm LDPE tubing (VWR) or a 15 ml

polypropylene tube (recycled antibody container from Novus) which functioned as medium reservoir. The glass capillaries were attached using epoxy glue (**Figure 2-2**). To increase stability the reactor was fixed on a standard microscope glass slide using autoclave tape. Sterilization was performed using 70% ethanol. Water based black ink (Tiger Stationery) was used to visualize the flow of liquid.

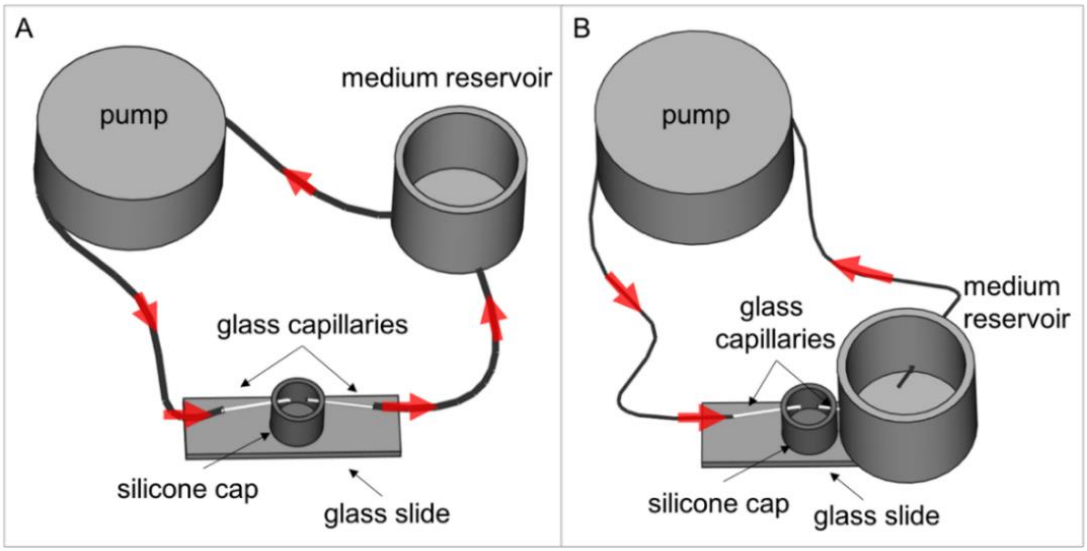

Figure 2-2: Illustration of the flow through bioreactor designs. A: connection of growth chamber to reservoir via outflow tubing. B: direct coupling of growth chamber to reservoir via glass capillary. Red arrows indicate direction of flow.

2.3.2 Bioreactor design, manufacture, and assembly:

The short-term perfusion bioreactor was designed using "FreeCad". The body was 3D printed using ABS plastic (University of Edinburgh, School of Engineering). The surface of the print was sealed by acetone vapour treatment. To enable visualization of the blood vessels, two coverslips were inserted into the bottom of the culture chambers and fixed using aquarium-grade silicone glue. Chambers and reservoir were sealed using silicone O-rings and tied with M2 screws. For the mounting of blood vessels, "MicroFil" tubing (WPI) was inserted into the culture chambers and sealed using aquarium glue (Aqua Mate, Everbuild Everflex). After assembly, the bioreactor was soaked overnight in 70% ethanol and subsequently dried for 24h.

For long-term perfusions, the initial reactor design was revised, and two additional reactors were manufactured by Reinhard Tarnick (Schenkendöbern, Germany) using a custom build Computer numerical control (CNC) machine. RT also provided a custom build pressure control unit, which enables the measurement of the pressure on two sites and the control of the main pump (Minipulse 3, Gilson).

The bioreactor parts were sterilized by soaking in 5 % hydrogen peroxide (acrylic model) or by autoclaving (polycarbonate model). Subsequently, Microfil needles (World Precision Instruments) of appropriate diameter (34G for embryonic aorta, 28G for adult aorta and 20G for adult vena cava), were inserted into the perfusion channels and fixed using aquarium grade silicone glue. The Microfil needles were mounted into silicone tubing (1 mm ID, 2 mm OD obtained from Fisher Scientific or Altec, supplier was changed due to limited availability) using epoxy glue (Araldite 5 min epoxy). After assembly, the bioreactor was left at RT over night to allow the glue to harden.

At the end of the experiment the bioreactor was rinsed with autoclaved water. In case of contamination the bioreactor was incubated overnight in 5 % Dettol and subsequently rinsed several times with autoclaved water, before being left to dry at RT. After drying the Microfil needles were removed by pulling and disposed of and any residues of the silicone glue were scraped out.

2.3.3 Characterization of piezoelectric pump-derived flow

The piezoelectric pumps (Dolomite MicroFluidcs, 3200138) were controlled by a high-voltage function generator, which was kindly custom build by Reinhard Tarnick (Schenkendöbern, Germany). The characterization of the flow provided by the piezoelectric pump was carried out with filtered water. Water was chosen for the calibration for health and safety regulations because it was done outside a laboratory setting while the building was closed for non-essential work. While there is a 41 % difference in viscosity between culture medium and water (preprint by Poon, 2020), its effect on the flow rate is likely to be negligible compared to the influence of other factors such as backpressure caused by elevation of the outflow tubing compared to the location of the pump. Initially, the flow rate was intended to be measured using the Mitos Flow Rate Sensor (Dolomite Microfluidics, 3200097). However due to the high pulsation of the flow it was not possible to use this sensor to determine a flow rate. Instead, the sensor was used to detect backflow in the absence or presence of check valves, which was identified as negative flow rate. The check valves that were evaluated were a Masterflex Inert In-line female check valve (Cole-Parmer, WZ-01355-24) and a One-way luer check valve, SAN with silicone diaphragm (Cole-Parmer, WZ-30505-92).

The flow rate in relation to frequency and voltage was determined by measuring the volume with a glass cylinder. As flow rates per minute were low, the volume was measured after running the pump for 10 to 15 minutes and then dividing the volume by the time. The pressure was measured using a custom-built unit, which was also provided by Reinhard Tarnick (Schenkendöbern, Germany). All measurements were carried out in triplicates.

2.3.4 Isolation of blood vessels

Tissue, including embryos was obtained from CD-1 mice after the animals were culled by a member of the Bioresearch and Veterinary Services (University of Edinburgh) using a method listed under the Schedule 1 of the UK Animals Scientific Procedures Act 1986.

Embryonic aortas (E14.5) where isolated in prechilled (4 °C) MEM. The ventral torso was opened using microdissection scissors. After partial removal of the ribs a 25G needle was inserted above the heart and internal organs were resected by gently scraping along the spine. Subsequently internal organs, with exception of the heart were cut from the aorta. The heart was used to mark the cranial end of the aorta and removed immediately before mounting of the vessel on the perfusion bioreactor.

Adult blood vessels were isolated from midpregnant CD1 mice (P12 +/- 0.75) or age-matched littermates. After sterilization of the carcass with 70% ethanol, the abdomen was opened with a midline incision. Subsequently, the uterine horn containing embryos was removed and placed in a tube of ice-cold PBS for other experiments. After removal of the uterine horn the intestines were gently pushed to the left side of the animal and the connective tissue was pulled away from the aorta and vena cava. The aorta and vena cava were separated from each other caudally to the renal arteries. For the culture of separated vessels, the separation of aorta and vena cava was performed until the point where the aorta branches into the iliac arteries. For experiments in which aorta and vena cava were cultured in direct contact, both vessels were separated in a short region right below the renal arteries and in a short region cranially to the iliac arteries but not between these two sections. After separation aorta and vena cava were isolated by cutting through the iliac artery and vein and through the aorta and vena cava just below the branch point of the renal arteries. The isolated blood vessels were transferred into KCM and any connective tissue was removed using forceps. After cleaning of the vessels, they were transferred into the bioreactor and mounted proximally with a double surgical tie

using size 10 polyamide 6 suture (Ethilon). The branch into the iliac arteries was used to identify the distal end. After mounting of the proximal end, the iliac arteries were trimmed of and the distal end of the aorta and vena cava were mounted using a surgical tie using the same suture.

2.3.5 Characterization of angiogenic potential

Adult blood vessels were isolated as described above. The isolated blood vessels were cut into fragments of approximately 1 mm length and embedded in a matrix of 1 mg/ml type 1 collagen (Masson *et al.*, 2002). The vessels were cultured in KCM supplemented with 20 ng/ml VEGF (BioLegend) and 5 ng/ml FGF2 (BioLegend) (Rohan *et al.*, 2000; Zhu *et al.*, 2003). The medium was replaced every 2 days. On day 7 of the culture, the vessels were imaged using the Leica MSV269.

To compare the angiogenesis in perfused and unperfused blood vessels, two adult mouse aortas were isolated and mounted in the dual channel bioreactor. One of the blood vessels was perfused with MEM (Merck) supplemented with 10 % FBS (Biosera) and 1 % antibiotic-antimycotic (Gibco) while the other one was left unperfused mounted on sealed tubing. Angiogenesis in the culture chamber was stimulated by adding perfusion medium supplemented with VEGF (20 ng/ml, Biolegend) and FGF2 (5 ng/ml, Biolegend). The blood vessels were imaged after 8 days of culture. The experiment was performed 3 times.

2.3.6 Assessment of vascular leakage

To identify potential leakage, embryonic and adult aortas, isolated as described in section **2.3.4 Isolation of blood vessels**, were mounted on MicroFil needles (World Precision Instruments) with a double surgical tie using size 10 sutures (**Figure 2-3**). After a short perfusion with PBS to remove residual blood cells, the vessels were

perfused with 50 % water-based black ink (Tiger Stationery) in PBS using a flow rate of approximately 50 µl/min for adult or 5 µl/min for embryonic aortas until leakage was observed or for a minimum of 10 min.

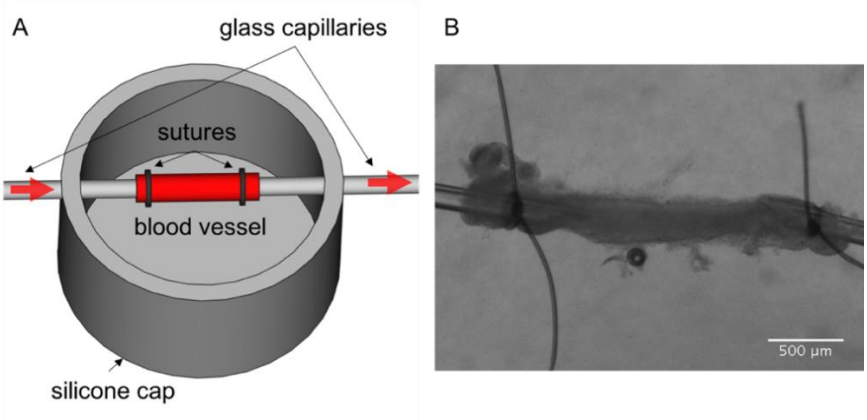

Figure 2-3: mounting of blood vessels. A: Illustration of a mounted blood vessel. Red arrows indicate direction of flow. B: image of a mounted E13.5 aorta

2.3.7 Perfusion culture of blood vessels

After mounting of the blood vessels within the culture chamber, the vessels were surrounded by 1.5 ml type I collagen (1 mg/ml) unless stated otherwise. The collagen was left to polymerize for 1 – 2 h at 37 °C. Subsequently the collagen was overlaid with 1 ml of the chamber medium containing the indicated growth factors (suppliers listed in **Table 2-3**) and the culture chamber was closed.

Table 2-3: list of growth factors used for blood vessel culture.

growth factor	supplier	catalogue number
PDGF-BB	Biolegend	558804
VEGF164	Biolegend	583104
FGF2	Biolegend	579604
HGF	Biolegend	771601
D-erythro Sphingosine-1-phosphate (S1P)	Abcam	ab141748
Phorbol 12-myristate 13-acetate (PMA)	Abcam	ab120297

After closure of the culture chamber, adult blood vessels were perfused with a flow rate of about 50 µl/min. Embryonic blood vessels were perfused with the conditions stated in the results section. Unless otherwise specified, the chamber medium was changed every other day while the perfusion medium was changed after 7 days if the total culture period exceeded 10 days. The exact medium composition can be found in **Table 2-4.**

Table 2-4: culture conditions for perfused blood vessels. All media contained 1x Antibiotic-Antimycotic. NA: not applicable, MEM: minimum essential eagle medium, FBS: fetal bovine serum, VEGF: vascular endothelial growth factor, FGF2: fibroblast growth factor 2, PDGF-BB: platelet-derived growth factor B homodimer, S1P: sphingosine-1-phostphate PMA: Phorbol 12-myristate 13-acetate, HGF: hepatocyte growth factor

Figure	**perfusion settings**	**perfusion medium**	**chamber medium**
6-9A	unperfused	NA	MEM, 10 % FBS, 50 ng/ml VEGF, 50 ng/ml FGF2, 50 ng/ml PDGF-BB, 1 mM S1P, 2 ug/ml PMA
6-9B	Unknown, 170 V, 10 Hz	MEM, 10 % FBS, 50 ng/ml VEGF, 50 ng/ml FGF2, 50 ng/ml PDGF-BB, 1 mM S1P, 2 ug/ml PMA	
6-9C	10 ul/min		
6-11A	10 ul/min	MEM, 10% FBS, 20 ng/ml VEGF, 5 ng/ml FGF2	
6-11B	Daily increase 30 mmHg, 40 mmHg, 50 mmHg	MEM, 10 % FBS, 50 ng/ml VEGF, 50 ng/ml FGF2, 50 ng/ml PDGF-BB, 1 mM S1P, 2 ug/ml PMA	
6-13 6-14	unperfused	NA	MEM, 10 % FBS, 20 mg/ml VEGF, 5 ng/ml FG2
6-15	50 ul/min	MEM, 1.5% FBS, 20 mg/ml VEGF, 5 ng/ml FG2	
6-17A		MEM, 1.5% FBS	MEM, 1.5% FBS, 20 mg/ml VEGF, 5 ng/ml FG2
6-17B			Promocell EGM, 20 ng/ml VEGF, 5 ng/ml FGF2
6-17C 6-18A		MEM, 10 % FBS, 50 ng/ml VEGF, 50 ng/ml FGF2, 50 ng/ml PDGF-BB, 1 mM S1P, 2 ug/ml PMA	
6-18B-F 6-19A-D		MEM, 10 % FBS,	MEM, 10 % FBS, 50 ng/ml VEGF, 50 ng/ml FGF2, 50 ng/ml PDGF-BB, 1 mM S1P, 2 ug/ml PMA
6-19E			MEM, 10 % FBS, 50 ng/ml VEGF, 50 ng/ml FGF2, 50 ng/ml PDGF-BB, 1 mM S1P, 2 ug/ml PMA, **50 ng/ml HGF**
6-19F 6-20			MEM, 10 % FBS, 50 ng/ml VEGF, 50 ng/ml FGF2, 50 ng/ml PDGF-BB, 1 mM S1P, 2 ug/ml PMA, **50% MS-5 conditioned medium**

For the co-culture of embryonic blood vessels with embryonic kidneys the blood vessels were pre-cultured for the indicated time. Subsequently, the medium was aspirated and freshly isolated kidneys were placed nearby the embryonic aorta by making an incision into the collagen using a 25G dissection needle and placing the kidney into the formed pocked. This was done to prevent the kidneys from moving when the chamber medium was added.

For the co-culture of adult blood vessels and embryonic kidneys the blood vessels were pre-cultured for 7 days while the kidneys were precultured for 3 days. Prior to addition to the blood vessel culture the kidneys were pre-soaked in KCM containing 10 µg/ml VEGF (Biolegend) for 2.5 h, as soaking in VEGF has been previously shown to increase the grafting efficiency of kidney organoids *in vivo* (Xinaris *et al.*, 2012). After soaking in VEGF, the kidneys were washed twice with KCM and the chamber medium was aspirated from the blood vessel culture. The kidneys were placed near the vessels by creating a pocket in the collagen as described above. After addition of the kidneys, 1 ml of co-culture medium (MEM supplemented with 10 % FBS, 1x Antibiotic-Antimycotic, 50 ng/ml PDGF-BB and 50 ng/ml HGF) was added into the culture chamber and the vessels were cultured for further 3 days. On the second day of the co-culture, 10 µl of IsolectinB4 conjugated with AlexaFluor594 was added to the culture chamber to visualize the blood vessels. The dye was incubated overnight until termination of the experiment on day 3 of co-culture.

2.3.8 Culture of MS-5 mouse bone marrow stromal cells and generation of conditioned medium

MS-5 cells (obtained from DSMZ-German Collection of Microorganisms and Cell Cultures GmbH, ACC 441), a murine bone marrow stromal cell line, were maintained in αMEM (Thermo Fisher, 22571020) supplemented with 10 % heat inactivated horse serum (Thermo Fisher, 26050070), 1x sodium pyruvate (Thermo Fisher, 11360070) and 1 % Penicillin/Streptomycin (Gibco). The cells were passaged every other day in

a ratio of 1:3 for up to 10 passages considering the vial of cells obtained from the DSMZ as passage “0”.

For the generation of conditioned medium, the cells were grown to confluence in normal growth medium. Once confluence was reached the cells were washed once with PBS and cultured for 3 days in growth medium with a reduced serum concentration of 0.1 %. After conditioning for 3 days, the conditioned medium was harvested, filtered through 0.45 µm syringe filter (Merck, CLS431225-50EA) and stored in 5 ml aliquots at -20 °C for up to 1 month or at -80 °C for long term.

Chapter 3 - Three-dimensional growth of embryonic kidneys in type 1 collagen

3.1 Introduction

3.1.1 Induction of three-dimensional growth

Kidney explants are traditionally cultured on filters or glass, which results in a flat morphology quite different from their *in vivo* growth (Ekblom *et al.*, 1994; Falk *et al.*, 1996; Sebinger *et al.*, 2013).

In general, a more three-dimensional growth can be achieved in two ways, either by (a) culturing cells or tissue in suspension using hanging drops or a surface that does not allow their attachment, or (b) by embedding the cells in a matrix. At the beginning of the 20th century, Harrison *et al.* (1907) developed the hanging drop method which enables the three-dimensional culture of cell aggregates. The hanging drop method is rarely used today, because it is relatively labour intensive, changing medium can be difficult and imaging of the tissues within the drops is challenging due to the light scattering at the curved drop surface. However, the underlying basic principle of stimulating the cells to aggregate by culturing them under non-adhesive conditions, nowadays mostly by using more convenient low-attachment plates, has become a popular culture method for a variety of organoids including kidney organoids (Li *et al.*, 2016; Morizane and Bonventre, 2017; Taguchi and Nishinakamura, 2017; Yuri *et al.*, 2017).

A previous study reported a poor growth of kidney explants in hanging drop culture methods (Sebinger *et al.*, 2010). An alternative method to induce three-dimensional growth is the embedding of cells or tissue fragments into a matrix. The first studies, in 1929, used a clotted mixture of embryo extract and plasma to support the growth and shape maintenance of avian limb buds (Fell and Robison, 1929). The method was later also applied to kidney explants where it resulted in an increased thickness of the explant but did not reproduce the shape of *in situ* grown kidneys (Bentley, 1936). Today a variety of natural and synthetic 3D matrices is available, but most commonly used is Matrigel an extract from Engelbrech-Holm-Swarm sarcoma (reviewed by Fang and Eglen, 2017). Matrigel contains mainly laminin and type IV collagen, but also various growth factors (Kleinman *et al.*, 1982; Vukicevic *et al.*, 1992). While it is possible to purchase growth factor-reduced Matrigel, this would not be completely free of growth factors. Additionally, the ratio between components could vary between batches, which could impact reproducibility of results. Type I collagen, mostly isolate from either bovine skin or rat tails, serves as a more chemically defined natural polymer, it is usually advertised with a purity of 90 % with a specified concentration, and has been shown to promote the growth of kidney explants when applied as a thin coat on polymer films (Sebinger *et al.*, 2013).

Organoids may also be cultured in synthetic hydrogels. However, the use of synthetic hydrogels may require extensive optimization of their mechanical and biochemical properties (Gjorevski *et al.*, 2016). Synthetic hydrogels may require the addition of adhesion peptides to allow the cells to bind to the matrix (Gjorevski *et al.*, 2016).

When embedding kidneys in an extracellular matrix only the outer layer, which is composed of mesenchymal cells, would be exposed to the matrix. Cells bind to the extracellular matrix via Integrins, which are heterodimeric complexes consisting of an α and a β subunit (Barczyk *et al.*, 2010). There are at least 11 integrins expressed within the kidney with some of them having a large impact on kidney development (Appendix, **Table A 5**).

The renal mesenchyme expresses the collagen binding integrin α1β1, the fibronectin receptor integrin α4β1 and integrin α8β1 which binds to fibronectin, vitronectin and nephronectin (Barczyk *et al.*, 2010; Müller *et al.*, 1997; Rahilly and Fleming, 1992). I did not find any record of fibronectin, vitronectin or nephronectin being used individually as a 3D environment, but did find references of them being used as a thin coating or added to type I collagen or fibrin gels to study their effect of cell and organ growth (Arai *et al.*, 2017; Sebinger *et al.*, 2013; Trujillo *et al.*, 2020). Since there is no record of these compounds being used individually as 3D matrix, it is not clear whether they would form a gel suitable for explant culture. Therefore, I did not consider using them for initial experiments.

In contrast, collagens are widely used individually to culture cells and tissues in 3D, whereby type 1 collagen is the most abundantly used type (Nocera *et al.*, 2018). Type I is, together with type III, the most abundant type of collagen expressed during early kidney development, while type IV is the predominant type of collagen in later stages (Ekblom *et al.*, 1981). Due to its frequent use and abundant expression in early developmental stages of the kidney, I decided to use type I collagen to induce a three-dimensional growth of kidney explant.

3.2 Results

3.2.1 Type-1 collagen supports three-dimensional growth

In cell lines and organoids, 3D growth has been previously acquired by embedding the cells in a 3D matrix (Broutier *et al.*, 2016; Gjorevski *et al.*, 2016; Hisha *et al.*, 2013). By embedding the kidneys in an ECM, adhesion sites are provided all around the kidney. To test whether this is sufficient to induce 3D growth of murine kidney explants, I have isolated kidneys from embryonic day (E) 11.5 and embedded the explants in a matrix of type 1 collagen. The explants were cultured for 7 days prior to analysis.

Collagen-cultured explants grew in a more spherical shape than Transwell-cultured kidneys (**Figure 3-1**). To determine the size of the explants, I stained the kidneys for stromal cells which are, second to nephron progenitors, the predominant cell type in the peripheral kidney region (Hum *et al.*, 2014). While the outer layer of collagen-cultured explants stained positive for the stromal markers Meis1/2/3 (Hum *et al.*, 2014), Transwell-cultured explants were usually surrounded by a single layer of cells, which did not stain positive for Meis1/2/3, or for other renal markers used in later experiments. Therefore, this cell-layer was not considered part of the explant when measuring the dimensions of the kidneys.

In Transwell-cultured kidneys the diameter of the explants was measured parallel to the membrane and the thickness was measured perpendicular to the membrane of the Transwell. In collagen-cultured kidneys the x-y plane during imaging was considered as the diameter, while extend of the explant along the z-axis was measured as thickness.

Collagen-cultured kidneys had a thickness of 280 µm (± 30 µm, N = 9) compared to a thickness of 120 µm (± 30 µm, N = 9) of Transwell-cultured kidneys (**Figure 3-1B**). However, Transwell-cultured explants had a larger maximum diameter of 1900 µm (± 600 µm) than collagen cultured explants whose maximum diameters were 500 µm

(± 30 µm) on average, which is about a quarter of the diameters of Transwell-cultured kidneys (**Figure 3-1B**).

Explants cultured in collagen for 7 days had a smaller volume of 0.033 mm^3 (± 0.007 mm^3) compared to Transwell-cultured kidneys which had a volume of 0.285 mm^3 (± 0.113 mm^3) (**Figure 3-1B**). When comparing the volume of Transwell- and collage-cultured explants, it has to be considered that the TO-PRO-3, the nuclear dye which was used to quantify the explant dimensions, displayed non-specific binding to the Transwell membrane. The thickness of the membrane is about 10 µm, which is approximately 10 % of the explant thickness. Assuming a disc-like shape of the explant the actual thickness could be about 10 % lower than the measured one.

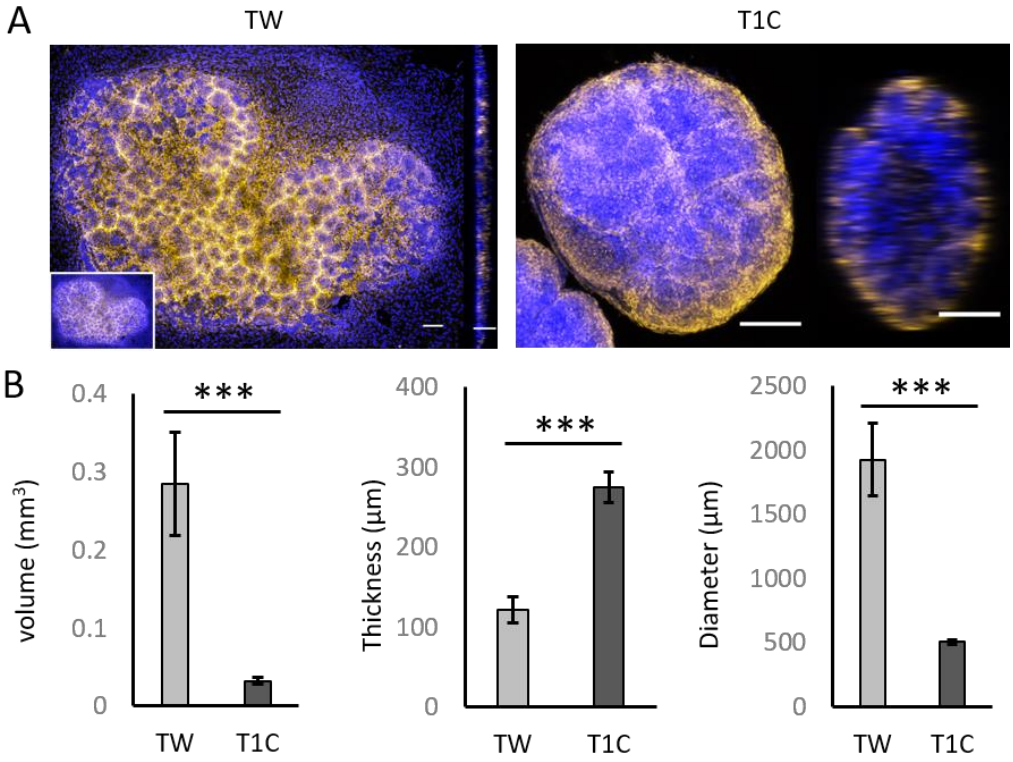

Figure 3-1: Kidney explants grow more three-dimensional when cultured in type 1 collagen. A: front and side views of kidney explants cultured for 7 days on a Transwell (TW) or embedded in type 1 collage (T1C) stained for Meis1/2/3 (yellow) and Topro3 (blue). T1C cultured explants show increased thickness but decreased lateral growth compared to TW cultured explants. Scale bars: 100 µm. B: Quantification of explant volume, maximum explant thickness and maximum explant diameter. Error bars represent standard deviation. *** $p < 0.001$ according Welch's t-test, N=9

3.2.2 3D shape can be acquired after Transwell culture, but collecting duct morphology is affected

For some experiments, the flat growth of kidney explants is an advantage. One example is the generation of asymmetric kidney organoids. This requires the application of a local stimulus of BMP4 to induce the differentiation of a single collecting duct into an unbranched uroplakin-expressing urothelium (Mills *et al.*, 2017).

Applying a local stimulus of BMP4 would be much more difficult in a 3D culture system, because the beads used in 2D experiments are difficult to place in a 3D culture and might move during the culture period. Therefore, I wanted to determine whether 3D growth could be reacquired after several days of 2D culture. For this purpose, murine kidney explants, isolated from E11.5 embryos were cultured on a Transwell for 3 or 6 days (**Figure 3-2A**) and subsequently embedded into type 1 collagen for further 3 days of culture. After fixation, the explants were stained for the collecting duct marker gata3 (Harding *et al.*, 2011) and with the nuclear dye TO-PRO-3.

The collagen-cultured explants adopted a spherical shape (**Figure 3-2A'**). However, the collecting ducts did not display the typical tree-like morphology of a kidney. Instead, the peripheral region appeared to have folded into the centre. (**Figure 3-2B**).

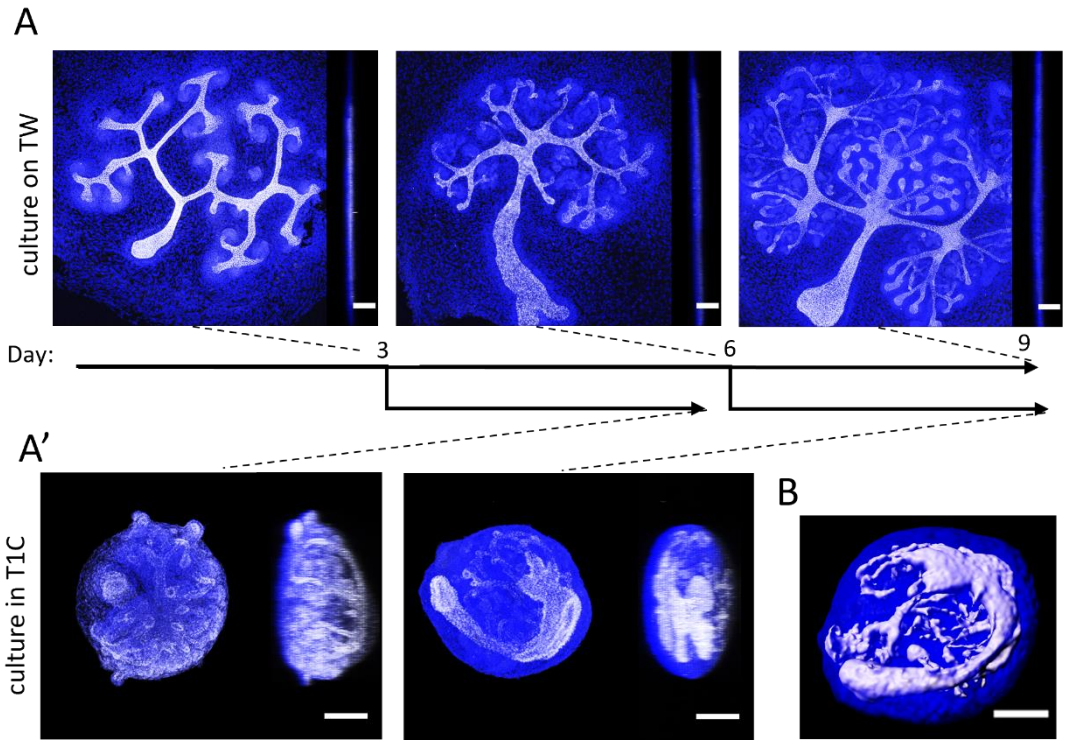

Figure 3-2: Plasticity of 3D growth. A: Kidney explants reacquired 3d growth when embedded into type I collagen (T1C) after culture on a Transwell (TW). Kidney explants were cultured for 3 or 6 days on a TW before embedding into T1C (A') for further 3 day of culture. Top row: front and side views of Transwell-cultured kidneys. Bottom row: front and side vied after embedding in T1C. Explants were stained with TO-PRO-3 (blue) and the collecting duct marker Gata3 (grey). Scale bars: 100 µm. B: 3D rendering of Gata3 staining shows folding of collecting duct system after acquisition of 3D shape. Scale bar 100 µm.

3.2.2 3D culture results in more realistic gross morphology compared to 2D culture

After confirming that a more three-dimensional growth of the kidney explants was possible by embedding kidneys into type 1 collagen, I next aimed to determine whether the 3D culture affected the morphology of the kidney explants. Kidney explants cultured traditionally in 2D acquire several characteristics of kidneys grown *in vivo*. The ureteric bud undergoes several branching cycles to form a tree-like ductal network (**Figure 3-2A**). Nephron progenitor cells form clusters around the collecting

duct tips before they differentiate into nephrons. The stromal cells surround the nephron progenitor caps and collecting ducts.

To identify whether 3D cultured explants display the same morphological characteristics, the explants were cultured for 7 days either on a Transwell, as a 2D-control, or embedded into collagen. Subsequently the explants were fixed and stained for collecting duct, nephron progenitor, nephron and stromal markers.

No gross morphological defects were detected in collagen-cultured explants. Staining with the collecting duct marker revealed that both culture methods allowed branching of the ureteric bud (**Figure 3-3A and B**). Due to the three-dimensionality of collagen-cultured explants counting of the collecting duct tips was rather difficult. Since later experiments identified several limitations of the collagen culture method, I did not spend time on optimizing the staining and image processing for tip counting.

In Transwell as well as collagen-cultured explants, Six2-positive nephron progenitors arranged in cell clusters around the collecting duct tips (**Figure 3-3A'**). As in natural kidneys, the nephron progenitor clusters were surrounded by Meis1-positive stromal cells (**Figure 3-3A'**) (Hilliard *et al.*).

Both culture methods allowed the formation of nephrons as indicated by the detection of Jagged 1, which is a marker for the medial region of the nephron (Liu *et al.*, 2013), and Wilms'-Tumour 1 (WT1), a marker for the proximal region in early nephrons and the glomerular podocytes in more mature nephrons (Harding *et al.*, 2011; Pritchard-Jones *et al.*, 1990), staining. Comma and S-shaped nephrons were frequently observed in both culture methods. Post-S-stage nephrons, defined by the presence of the Loop of Henle, were identified in Transwell-cultured explants, but not in collagen-cultured explants. Due to the high cell density and the lower signal in the core of collagen-cultured kidneys an identification of post-S-stage nephrons was difficult in collagen-cultured kidneys. Therefore, it was not possible to draw robust conclusions about differences in nephron maturity between both culture methods solely based on shape-based identification.

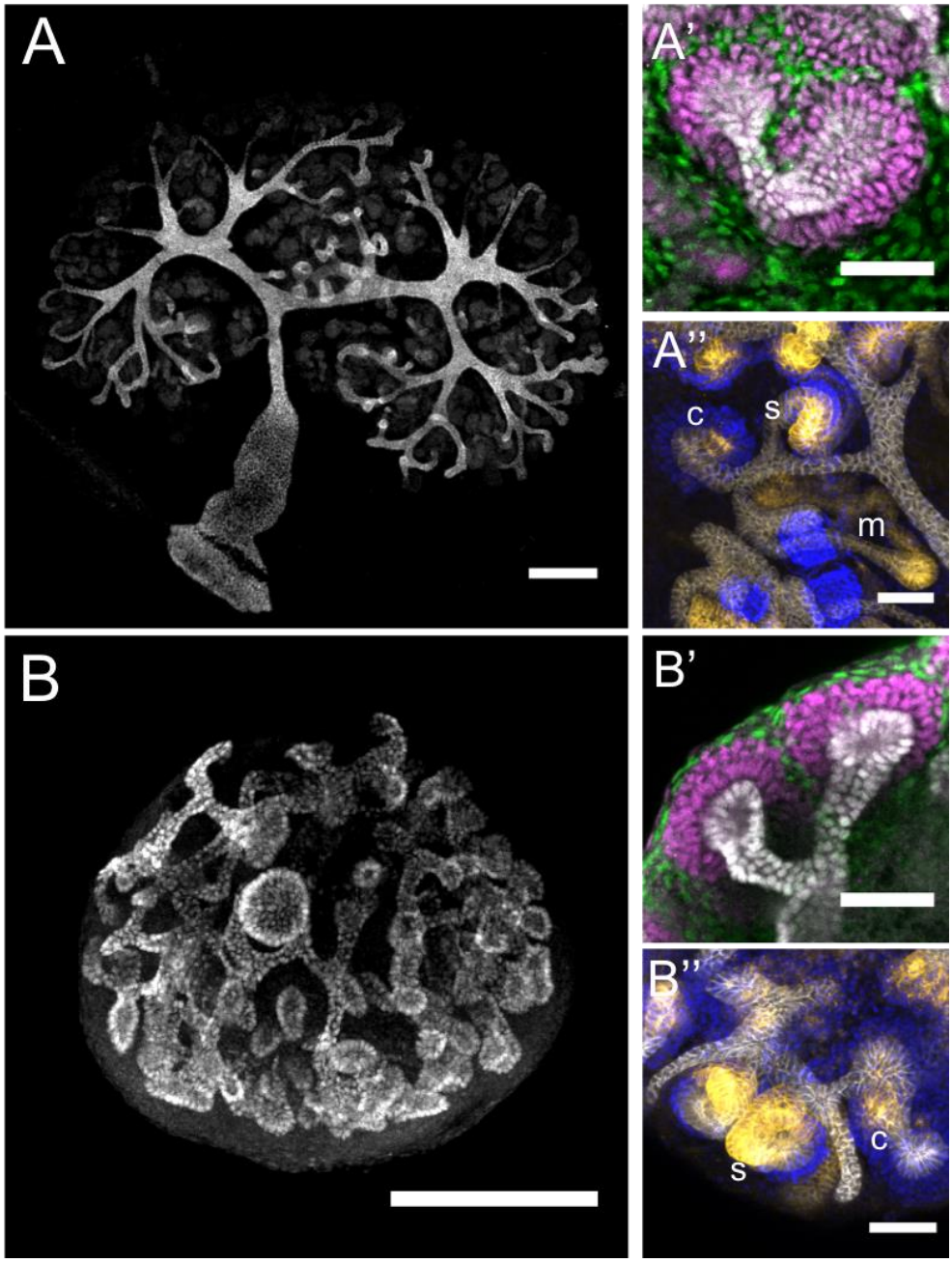

Figure 3-3: morphology of Transwell- and collagen-cultured explants. Gata3 staining (grey) of TW (A) and collagen (B) cultured explants shows branched network of collecting ducts. Scale bars 200 µm. The collecting duct tips of TW (A') and collagen (B') cultured explants are capped with Six2 positive (magenta) nephron progenitors which are surrounded by Meis1 positive (green) stromal progenitor. Scale bars 50 µm Comma shaped (c) and S-shaped (s) nephrons were detected in TW cultures (A'') as well as collagen (B'') cultured explants as indicated by Jagged 1 (yellow) and WT1 (blue) staining. Scale bars 50 µm Mature nephrons (m) were only identified in TW cultured explants.

3.2.3 3D culture leads to a reduced number of nephrons and fewer mature nephrons

After confirming that nephrogenesis is possible in 3D-cultured samples, I next aimed to quantify the number of forming nephrons, because nephrons are essential for the function of the kidney and low nephron numbers have been associated with renal pathologies (reviewed by Bertram *et al.*, 2011). To evaluate whether the culture of kidney explants in collagen affects the number of nephrons, kidney explants were cultured for 7 days and stained for the nephron marker Jagged1. Subsequently, the nephrons were counted using Imaris (see **2.1.11 Nephron quantification**). The nephron count revealed that explants cultured in collagen developed half the number of nephrons (34.7 ±10.3, N = 12) compared to Transwell-cultured kidneys (70.8 ±15.8, N = 12), a difference which was statistically significant ($p < 0.001$) according to the Student's t-test. (**Figure 3-4 A and B**).

To determine whether the reduced number of nephrons is associated with a reduced number of progenitor cells, the explants were stained for the nephron progenitor marker Six2. However, the staining showed a high background in most of the samples. Therefore, quantification was not possible.

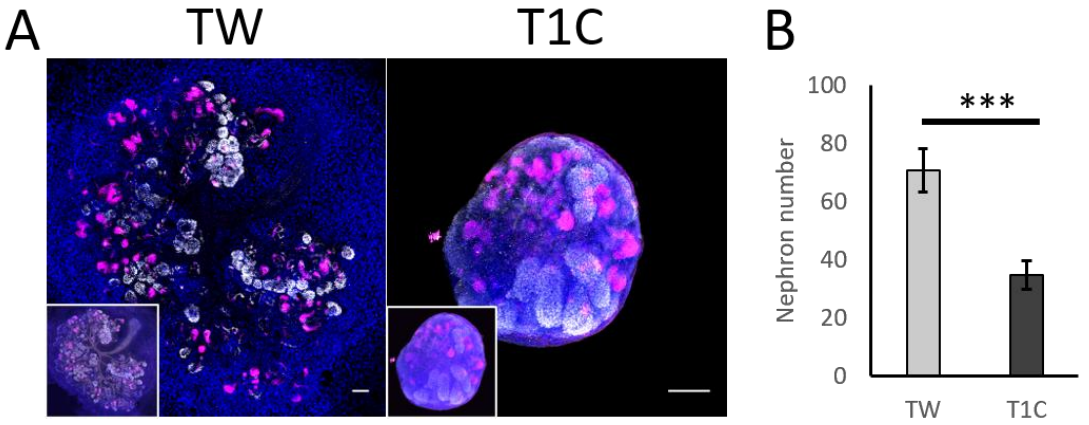

Figure 3-4: 3D culture affects nephron development. A: Kidney explants were cultured on Transwells (TW) or in collagen (T1C) for 7 days prior to staining for Jagged1 (magenta), Six2 (white) and Topro3. Scale bar: 100 um. B: Quantification of the nephron number revealed a lower number of nephrons in collagen-cultured samples. Error bars display standard deviation. N = 12 $p < 0.001$, Student's t-test

The shape-based identification of mature nephrons is difficult in 3D samples. Therefore, a marker expressed only in mature nephrons was required. Fortunately, Sarah Finnie, at the time a PhD student at QMRI, was interested in the expression of Argininosuccinate synthase 1 (Ass1) during kidney development. The staining of isolated kidneys of various ages revealed that Ass1 is absent from early stages of kidney development but appears in the convoluted tubules of mature nephrons after E14.5 indicating that it is expressed in later stages of nephron development (**Figure 3-5A**). The staining of Transwell-cultured kidney confirmed the absence of Ass1 in comma and S-shaped bodies. In contrast, Ass1 was highly expressed in the proximal tubules of Loop of Henle containing nephrons and can therefore be used as a marker for nephron maturity (**Figure 3-5B**).

The staining of cultured kidneys with Ass1 indicates post-S-stage nephrons form in kidneys cultured on Transwells as well as in those embedded in collagen (**Figure 3-5C**). To identify the percentage of Ass1-positive nephrons, the total number of nephrons was quantified based on Jagged1 staining and compared to the number of Ass1 expressing nephrons. The percentage of Ass1-positive nephrons was 62.5 % (± 24.8, N = 4) in Transwell-cultured kidneys and 30.6 % (± 9.9, N = 4) in collagen-cultured kidneys, a difference which was statistically significant according to the Student's t-test ($p < 0.05$) (**Figure 3-5D**).

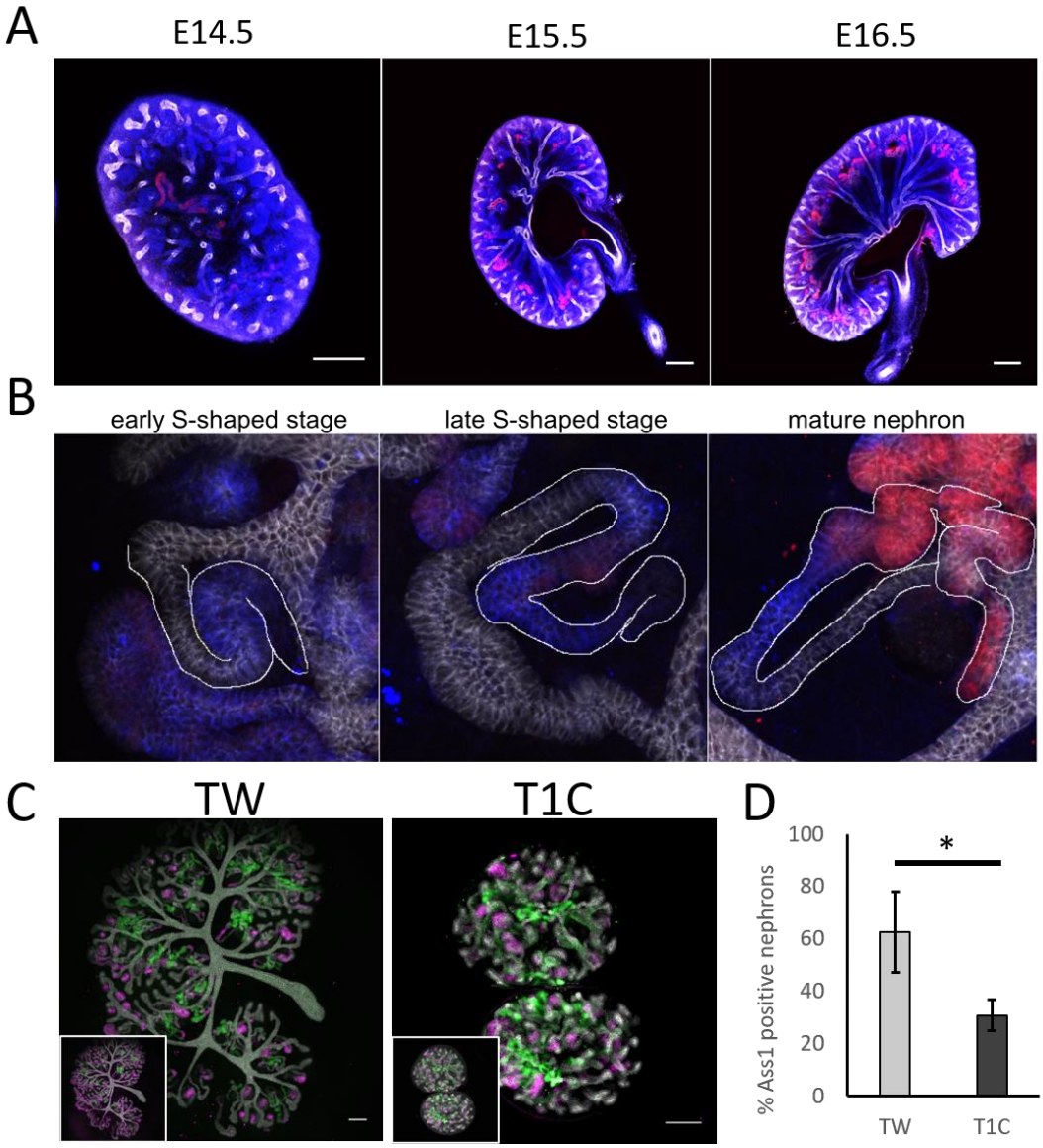

Figure 3-5: 3D-cultured explants contain fewer mature nephrons. A: staining of kidneys from E14.5, E15.5 and E16.5 shows Ass1 (red) expression in convoluted tubules. The explants were co-stained with gata3 (white) and TO-PRO-3 (blue). Scale bars: 200 µm). B: Staining of Transwell-culture explants with E-cadherin (grey), Jagged 1 (blue) and Ass1 (magenta) shows that Ass1 is absent from comma and s-shaped nephrons but expressed highly in mature nephrons. C: Staining of Transwell (TW) and collagen (T1C) cultured explants with E-cadherin (grey), Jagged 1 (magenta) and Ass1 (green). D: Quantification of Ass1 positive nephrons revealed that collagen-cultured explants develop fewer mature nephrons. N = 4, $p < 0.05$, Student's t-test, Error bars display standard deviation.

3.2.4 3D-cultured explants display central cell death

A measurement of the fluorescence signal intensity of TO-PRO-3-stained explants through the central plane (**Figure 3-6A**) shows a decrease of the signal from periphery to the centre (**Figure 3-6B**). Even though the kidney explants have been cleared, a minor signal loss could be expected due to limited light penetration as well as scattering from subcellular components. Additionally, collagen-cultured explants appeared to show a lower cell density in the centre. Due to the limited resolution of the images and the weak staining in the centre, a manual count of the nuclei appeared difficult and would potentially be biased as weakly stained nuclei would be more difficult to see. Therefore, I used the "Find Maxima" function of ImageJ to count the cells. While this will not give an accurate count, it does give an unbiased approximation and seemed therefore more suitable. The detection of maxima revealed that the number of cells in the centre was reduced by 11 % compared to the cell density in the periphery (**Figure 3-6C**). A possible explanation for this is the death of the cells within the explant core, as central necrosis has been observed in other 3D culture systems (Glicklis *et al.*, 2004; McMurtrey, 2016; Sakaguchi *et al.*, 2013).

To test this hypothesis, explants were cultured for either 3, 4 or 5 days on Transwells or embedded in type 1 collagen, followed by staining for the apoptosis marker cleaved caspase 3 (Gown and Willingham, 2002). Transwell-cultured explants displayed few apoptotic cells after three days of culture. On day four, more cells appeared to stain positive. After five days of culture, the fraction of apoptotic cells was visibly lower compared to day four of culture (**Figure 3-6**).

In contrast, collagen-cultured explants displayed a progressive increase in the percentage of apoptotic cells. A direct comparison of the percentage of apoptotic cells between collagen and Transwell-cultured explants was not possible on wholemount samples. The reason for this is that quantification of the stained structures requires an intensity threshold to distinguish between signal and background. Transwell- and collagen-cultured kidney have different optical

parameters, such as absorption and scattering of the light, due to their different thicknesses. As a consequence, they cannot be imaged with the same setting and be processed with the same threshold. As the quantification of dead cells was strongly affected even by minor adjustments of the threshold, it was not possible to compare the volume of dead cells between Transwell- and collagen-cultured kidneys.

The distribution of apoptotic cells differed in Transwell and collagen-cultured explants. In Transwell-cultured explants, dying cells were detected throughout the explant and appeared to be mostly interstitial cells, which were identified by the local density and arrangement of cell-nuclei. Within collagen-cultured explants, apoptotic cells concentrated in the core region of the explant, while few caspase-positive cells were detected in the periphery of the explant. Due to the higher cell density of collagen-cultured explants, it was not possible to identify whether cell death was concentrated to a certain cell type (**Figure 3-6**).

Apoptosis is a normal process during kidney development (Coles *et al.*, 1993; Kim *et al.*, 1996). However, the high number and concentration of dying cells in the core region of collagen-cultured explants differs largely from the *in vivo* situation, where apoptosis is observed mostly in the nephrogenic zone and does not exceed 3.2 % (Coles *et al.*, 1993).

A determination of the apoptotic index of collagen-cultured kidneys was not possible in wholemount samples, because it would require imaging with a greater magnification, which was not possible due to the limited working distance of available objectives. One possibility to determine the apoptotic index of cultured kidney explants would be sectioning of the explant prior to staining. However, this process is relatively time consuming and even without quantification it was obvious that the percentage of apoptotic cells was far above 3 %. Therefore, I did not spend time on sectioning and determining the exact percentage of apoptotic cells.

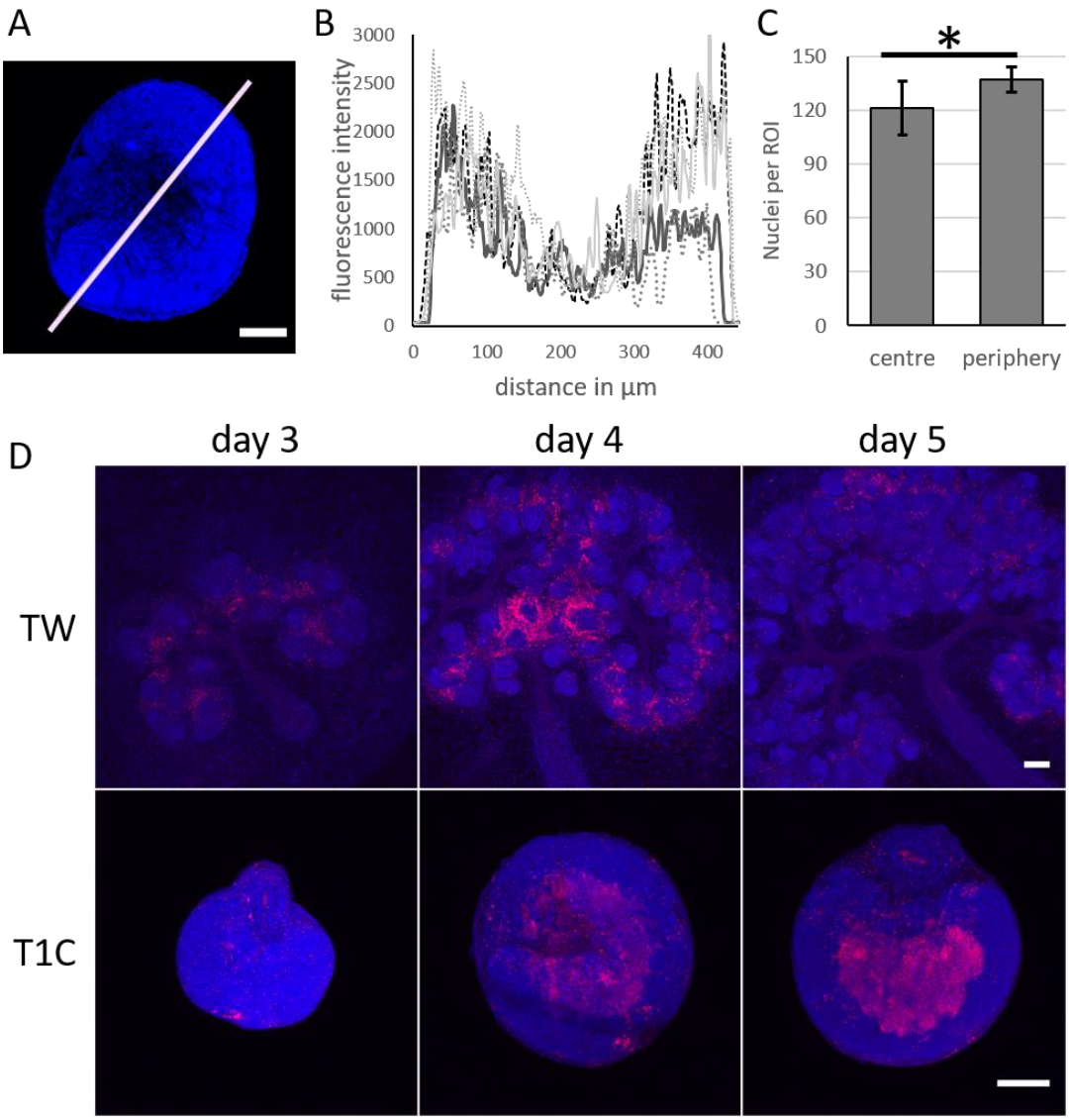

Figure 3-6: Explants cultured in type 1 collagen display central cell death. A: Central plane of a kidney explant stained with TO-PRO-3 shows signal decline from periphery to centre (white line). B: intensity profiles of 5 explants measured through a central plane using line tool in ImageJ (Schneider *et al.*, 2012). Curves were smoothed using a 5-point rolling average. C: Number of nuclei identified per ROI in the centre and periphery of the explant. * $p < 0.05$, paired t-test, error bars display standard deviation, N = 12. D: Kidney explants that were cultured for 3, 4 or 5 day on Transwells (TWs) or in collagen (T1C). After culture period, the explants were stained for cleaved caspase 3 (red) and Topro3 (blue). Scale bar 100 µm.

3.2.5 Collagen-cultured explants show a hypoxic zone after 5 days of culture

A possible cause for the death of cells in the centre of collagen-cultured explants could be hypoxia. Oxygen regulates the degradation of the ubiquitously expressed transcription factor Hypoxia-induced-factor 1α (Hif1α) (Ke and Costa, 2006). When oxygen levels drop, the degradation is less effective and Hif1α accumulates within the cells (Ke and Costa, 2006).

To identify whether the cells in the core of collagen-cultured explants die due to hypoxia, cultured kidney explants were stained for Hif1α. For better visualization of small differences in fluorescence intensity the FIJI "Gem" pseudo colour scale has been used (**Figure 3-7A**).

To verify the specificity of the antibody, kidney explants were cultured on a Transwell for two days followed by an additional day of culture either in the absence or the presence of 400 µM $CoCl_2$. $CoCl_2$ enhances the translation of Hif1α and can therefore induces the accumulation of Hif1α (Chachami *et al.*, 2004). Explants cultured without $CoCl_2$ stained weakly for Hif1α, while explants treated with $CoCl_2$ displayed elevated levels of Hif1α (**Figure 3-7B and C**).

In untreated 5-day collagen-cultured explants, Hif1α was detected throughout the explant. However, an upregulation was found in the medial region of the explant about 80 µm from the periphery. The ring-like hypoxic zone extended for approximately 50 µm into the centre of the explant. The core of the explant stained weakly for Hif1α, potentially due to advanced stages of cell death within the core (**Figure 3-7D**).

Collagen-cultured explants treated with $CoCl_2$ displayed a much higher expression of Hif1α compared to untreated explants. In contrast to the untreated samples, the expression was highest in the periphery of the explant (**Figure 3-7E**).

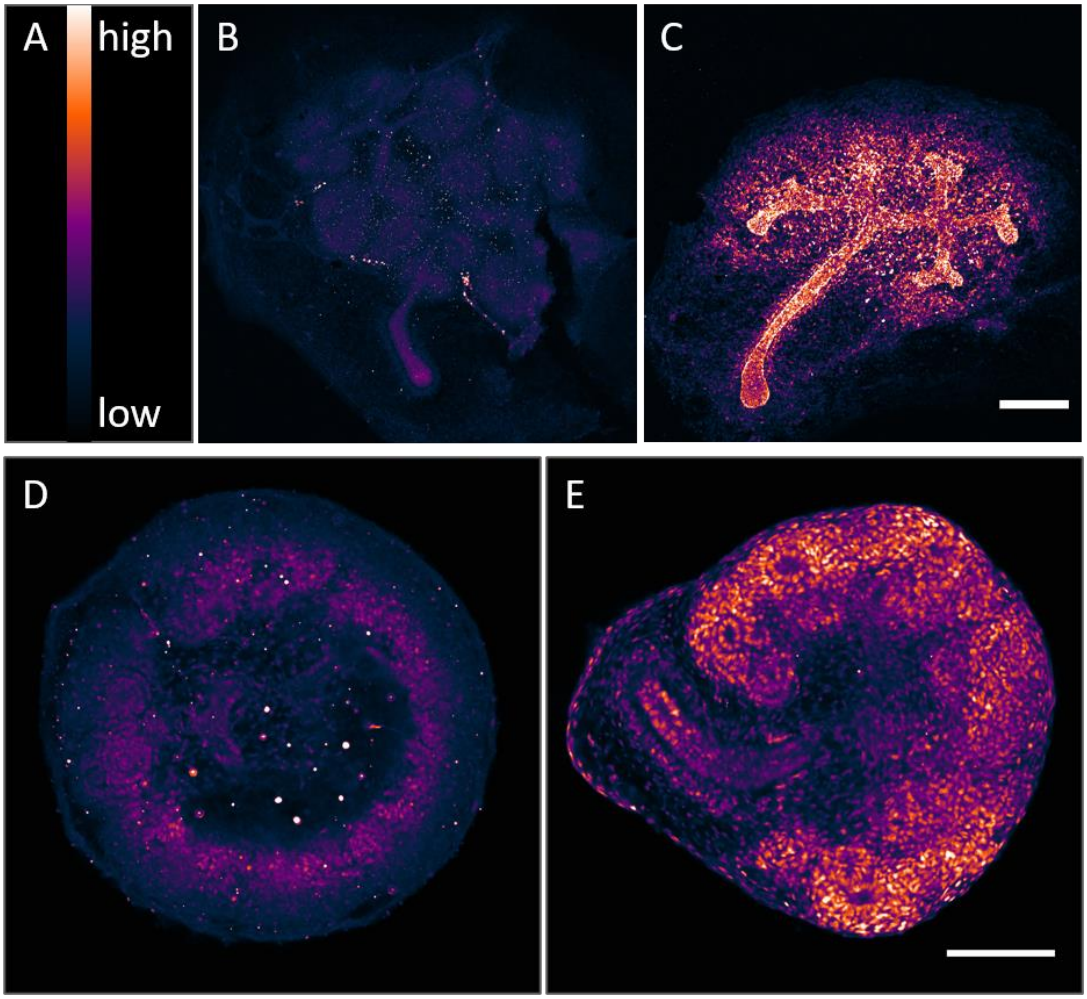

Figure 3-7: Detection of Hypoxia in cultured kidneys. A: FIJI "gem" colour scale used to visualize expression. B: Kidney explant cultured for 3 days on a Transwell following staining for Hif1α. C: Transwell-cultured explant displaying increased levels of Hif1α after treatment with 400 µM $CoCl_2$. Scale bar 200 µm D: Kidney explant cultured for 5 days in collagen showing a moderate increase of Hif1α expression in the medial region. E: Collagen-cultured kidney explant treated with 400 µM $CoCl_2$ to reduce Hif1α degradation. Scale bar 100 µm

3.2.6 Culture of kidney explants in type 1 collagen allows glomerular vascularization

The previous experiments showed that the cells within the core of the explant die and that hypoxia, indicated by increased levels of Hif1α, could be one of the reasons for this. *In vivo*, oxygen, and nutrients, are transported via the circulatory system. The development of blood vessels within the kidney explants could therefore have an effect on nutrient distribution.

Previous studies have established the presence of endothelial cells within reaggregated embryonic and iPSC-derived kidney organoids under standard culture methods (Munro *et al.*, 2017; Takasato *et al.*, 2016). To determine whether the culture in type 1 collagen had an effect on vascular development *in vitro*, I cultured kidney explants and organotypic organoids for 7 days in type I collagen following staining for vascular markers.

Similarly to *in vivo* grown kidneys, the CD31-expressing endothelia in the explants avoided the Six2-positive cap mesenchyme (**Figure 3-8A**). However, in Transwell-cultured kidneys a ring of blood vessels was often seen surrounding the explant. Similarly, in collagen-cultured explants blood vessels were occasionally seen to cover the cap mesenchyme.

Interestingly kidney explants grown in type I collagen contained a small subset of vascularized glomeruli, which were never detected in Transwell-cultured kidneys (**Figure 3-8B**).

To detect whether the blood vessels could mature *in vitro*, I stained the cultured explants for CD31 and smooth muscle actin. In E14.5 kidneys, smooth muscle actin positive cells were arranged around the major blood vessels. In contrast, cultured E11.5 kidneys developed a layer of smooth muscle actin positive cells around the outside of the explant. There was no preferential alignment of smooth muscle cells and endothelial cells (**Figure 3-8C**).

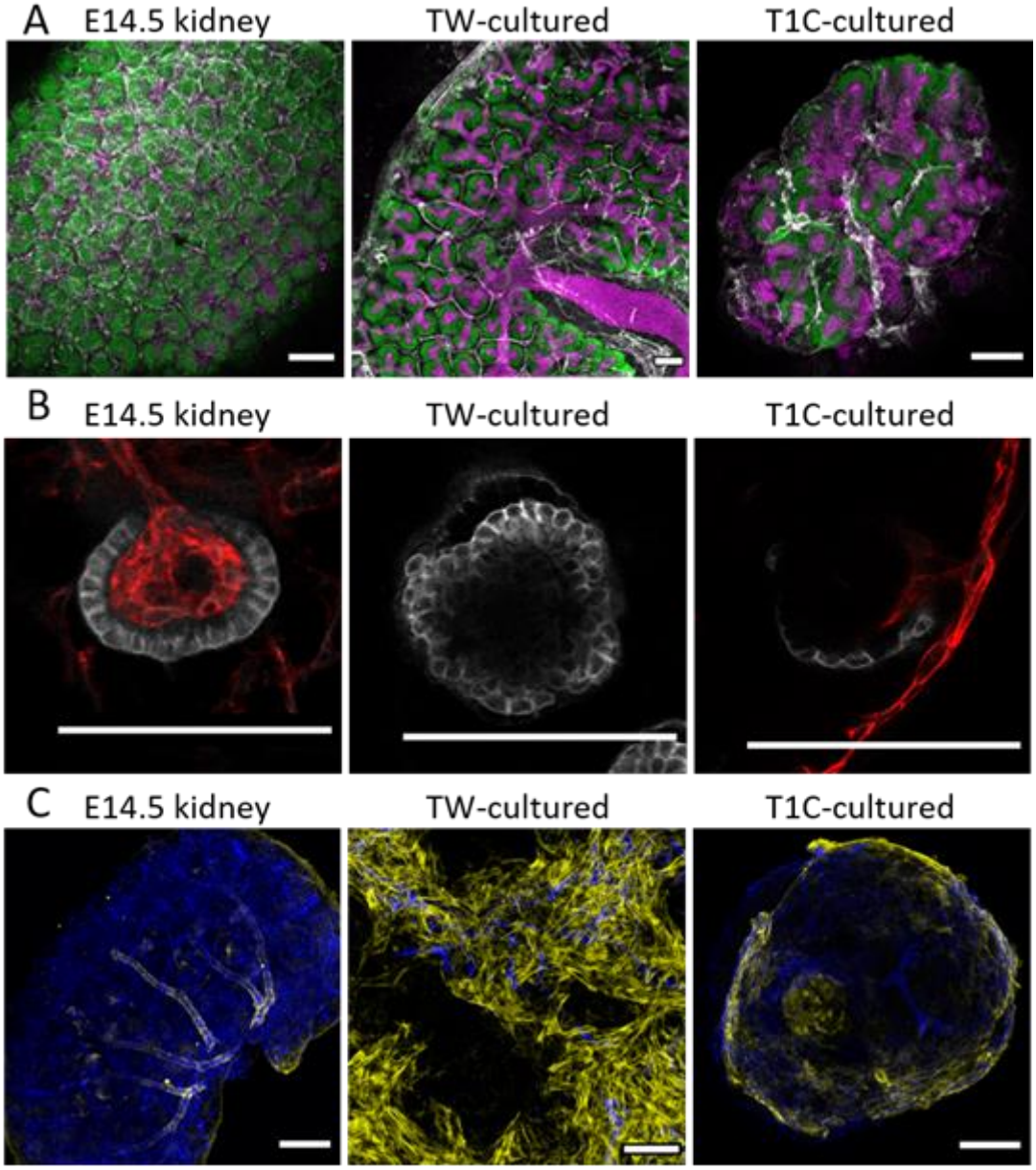

Figure 3-8: vascular development *in vivo* and *in vitro*. E14.5 kidneys, 7-day Transwell (TW)-cultured E11.5 kidneys and 7-day type I collagen (T1C)-cultured E11.5 kidneys were stained for renal and vascular markers. A: Staining for Six2 (green), E-cadherin (magenta) and CD31 (grey) shows blood vessels arranged around the cap mesenchyme. B: Staining with Podocalyxin (grey) and CD31 (red) was used to identify vascularised glomeruli. Vascularised glomeruli were seen in E14.5 kidneys and collagen-cultured kidneys but not in Transwell-cultured kidneys. C: Staining for smooth muscle actin (yellow) and CD31 (blue) reveals recruitment of smooth muscle cells around major blood vessels in E14.5 kidneys but not in cultured E11.5 kidneys. Scale bars: 100 μm

After identifying that kidney explants contain vascularized glomeruli when cultured for 7 days in type I collagen, I wanted to determine whether this was also the case for kidney organoids. Further I wanted to characterize the how closely the *in vitro* forming vasculature resembles the *in vivo* situation in terms of the arrangement around the cap mesenchyme. For this purpose, I generated mouse kidney organoids as described previously (Ganeva *et al.*, 2011), but on the first day of culture these organoids were transferred into type I collagen and cultured for a further 6 days.

To identify whether reaggregation would affect the localization of blood vessels around the cap mesenchyme, the organoids were stained for Six2, CD31 and E-cadherin. The staining revealed the avoidance of the cap mesenchyme by endothelial cells but also showed that blood vessels in the organoids, similar to explant cultures, occasionally grew cortically around the cap mesenchyme (**Figure 3-9A**).

After co-staining of CD31 and Podocalyxin it was confirmed that collagen-cultured organoids contain a subset of vascularized glomeruli (**Figure 3-9B**).

Lastly, I stained the organoids for smooth muscle actin and E-cadherin to identify whether smooth muscle cells were present within the organoids. The staining showed that smooth muscle cells were present but that these did not localize around the blood vessels (**Figure 3-9C**), indicating that the vascular plexus of kidney organoids does not mature into arteries.

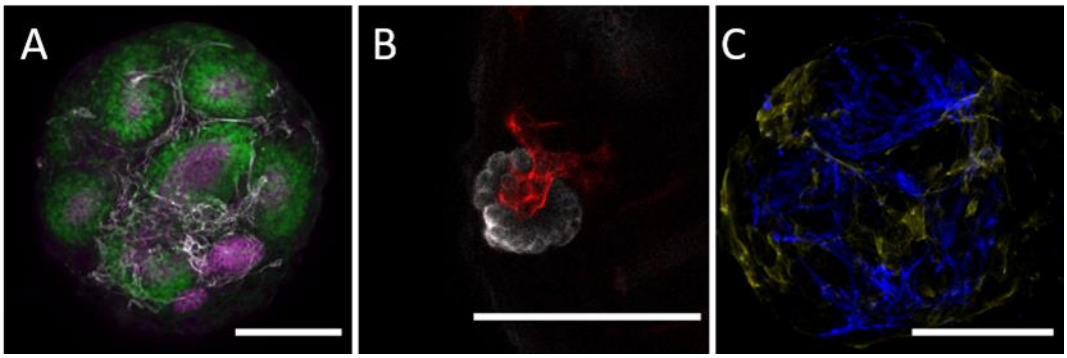

Figure 3-9: Vasculature in Ganeva-organoid. A: Staining of a Ganeva-organoid with Six2 (green), E-cadherin (magenta) and CD31 (grey) shows that the endothelial cells avoid the cap mesenchyme. B: Co-staining of CD31 (red) with Podocalyxin (grey) was used to visualize vascularized glomeruli in Ganeva-organoids. C: Staining for blood vessels (CD31, blue) and smooth muscle cells (smooth muscle actin, yellow) confirms the presence smooth muscle cells and their lack of perivascular alignment. Scale bars: 100 µm

Taken together these results underline the similarity of organotypic kidney organoids and kidney explants. They further demonstrate that culture in type I collagen, in contrast to the traditional culture at the air-liquid-interface, enabled endothelial cells to invade the glomeruli and therefore led to a higher degree of maturity. However, there was no sign of arterial maturation as demonstrated by the lack of smooth muscle cell recruitment.

3.3 Discussion

Type I collagen allowed the three-dimensional growth of kidney explants but had some negative effect on the kidney growth, with the explants exhibiting a reduced overall growth, reduced number of nephrons and fewer mature nephrons compared to traditional 2D culture.

Previous studies of different culture methods for kidney explants linked nephron maturity to surface tension applied from the substrate (Sebinger *et al.*, 2010). Kidneys grown on glass, a very stiff and adhesive surface, developed nephrons with a higher degree of maturity compared to explants cultured on a polycarbonate filter (Sebinger *et al.*, 2010). When embedded in an extracellular matrix, the explants would either be compressed or have to degrade the matrix in order to be able to grow. Therefore, it can be assumed that the kidney explants grown in type 1 collagen are facing compression rather than tensile forces, which might inhibit the nephrons from maturing. A possible way of applying a tension force would be the culture of the embedded explants in stretch chambers (Tokuyama *et al.*, 2015; Tondon and Kaunas, 2014).

The reduced overall growth stands in contrast to a previous study where E12 mouse kidneys displayed no significant difference of total cell mass after 7 days of culture on a filter or in collagen (Rosines *et al.*, 2010). The staining background on the Transwell membrane could account for a fraction of the measured volume of Transwell-cultured kidneys. However, given that the average maximum diameter of Transwell-cultured explants was about 1900 µm and the filter membrane has a thickness of 10 µm, the Transwell membrane would only account for 0.000597 mm^3 which is less than the observed volume difference of 0.252 mm^3 between Transwell and collagen-cultured kidneys. Rosines *et al.* (2010) measured an about 6 times larger volume of collagen-cultured kidneys, which could be explained by their use of a different age since E12 explants are larger than E11.5 explants from the beginning. However, their measured volume of Transwell-cultured kidneys was only about half

of what I measured, a difference that can be explained by different measurement methods. While Rosines *et al.* (2010) computed the volume based on diameter measurement and the assumption of an ellipsoid shape, I quantified the volume based on TO-PRO-3 staining using a published FIJI macro (Villani, 2018).

Rosines *et al.* (2010) further noticed a more realistic branch pattern in explants cultured in type IV collagen compared to type I collagen. Unfortunately, I have not been aware of the study until recently, therefore I did not attempt to culture kidney explants in type IV collagen. The addition of collagen IV could be of interest for studying the branching of isolated ureteric buds. Collagen IV might also improve the growth of renal explants; however, it is unlikely to improve the limited of oxygen and nutrient perfusion, which resulted in central necrosis of the explants.

The central necrosis was detected by staining for the apoptosis marker cleaved caspase 3. Apoptosis occurs naturally during kidney development, mostly within the nephrogenic zone, with a percentage of apoptotic cells around 2.7% and to a lesser extent in the proximal and distal papilla (Coles *et al.*, 1993). However, the distribution of apoptotic cells in type 1 collagen-cultured kidney explants does not reflect the *in vivo* situation and is therefore highly unlikely to represent a normal developmental process. A more likely cause for the cell death is the limited diffusion of oxygen, which was evidenced by increased levels of the hypoxia marker Hif1α. Hypoxia, alongside limited nutrient diffusion, has also been identified to cause cell death in other three-dimensional culture systems (Glicklis *et al.*, 2004; McMurtrey, 2016; Sakaguchi *et al.*, 2013).

There are different strategies to improve the diffusion of oxygen and nutrients within three-dimensional tissues. Some groups decided to seed cells in scaffolds to decrease the density of the tissue and improve diffusion (Ahn *et al.*, 2010; Li *et al.*, 2012; Loh and Choong, 2013; Xu *et al.*, 2018). While this may improve the diffusion rate it could also impact the anatomy of kidney organoids. Other groups cultured organoids under flow: for example, in rotation bioreactor (DiStefano *et al.*, 2018; Homan *et al.*, 2019).

While this will lead to some improvement of oxygen and nutrient diffusion the availability in the core will still be limited due to consumption of oxygen in the peripheral region (DiStefano *et al.*, 2018; Homan *et al.*, 2019; McMurtrey, 2016).

Within vertebrate species oxygen and nutrients are distributed via the circulatory system, whereby the distance of a cell from the nearest capillary does usually not exceed a few hundred micrometres (Krogh, 1919; Pittman, 2011; Pries and Secomb, 2014). In agreement with previous studies (Loughna *et al.*, 1997; Munro *et al.*, 2017) the presence of blood vessels has been confirmed in kidney explants and organoids. Culture in type I collagen allowed the vascularization of glomeruli in culture, which represents an improvement compared to previous culture methods. A previous study linked glomerular maturity to the stiffness of the culture matrix (Garreta *et al.*, 2019; Munro *et al.*, 2017), which could explain the presence of vascularized glomeruli in collagen- but not Transwell-cultured kidneys. However, even with the presence of vascular glomeruli the overall vascular network remained immature as indicated by the lack of arterial maturation.

In this chapter, I improved the 3D growth of kidney explants and organoids by embedding them in type 1 collagen which led to a more natural shape of the explants and organoids. The 3D culture method further enabled the vascularization of glomeruli which can be interpreted as an enhancement of nephron maturity. However, the vascular maturity was limited as evidenced by the lack of arterial smooth muscle cell recruitment.

In some tissues, such as the skin, arterial differentiation is regulated by neuron-derived signals (Li *et al.*, 2013; Mukouyama *et al.*, 2005). In the next chapter, I therefore aim to characterize a potential involvement of the renal neurons during arterial differentiation in the kidney by determining the timing of smooth muscle cell recruitment and innervation of the developing kidney.

Chapter 4 - Development of renal vascular smooth muscle cells *in vivo* and *in vitro*

4.1 Introduction

In the previous chapter, I showed that kidney explants adopt three-dimensional growth when embedded in type I collagen. The 3D culture preserved key morphological characteristics, such as branching of the collecting duct network, but also let to central necrosis most likely due to limited diffusion of oxygen and nutrients. Since oxygen and nutrients are distributed via the circulatory system *in vivo*, I studied the forming vasculature in kidney explants in more detail. In agreement with previous studies (Munro *et al.*, 2017), endothelial cells were present and arranged primarily around the cap mesenchyme. I further showed that culture in type I collagen, in contrast to the traditional method, allowed the vascularisation of the glomeruli of cultured kidneys as well as reaggregated kidney organoids. While this represents an improvement of the vascular realism of kidney organoids, the blood vessels appeared to remain immature as indicated by the lack of arterial smooth muscle cell recruitment.

To address the lack of arterial maturation in kidney explants, this chapter will focus on the timing of smooth muscle cell recruitment *in vivo* and on the potential involvement of renal neurons, as neurons have been demonstrated to regulate arterial differentiation in other tissues (see **4.1.1. Arterial differentiation**). This will give information whether renal neurons are required for arterial differentiation *in vivo*, which could indicate that neuronal signals could drive arterial differentiation *in vitro*.

4.1.1. Arterial differentiation

The specification of endothelial cells into arteries and veins occurs early in development (E9.0) (Wang *et al.*, 1998). The venous marker EphB4 and its artery-specific ligand ephrin-B2 are already expressed in the first primitive blood vessels that form de novo by vasculogenesis (Wang *et al.*, 1998).

A number of factors have been found to be involved in regulating arterio-venous differentiation. It has been showed that Hedgehog signalling is required to form the first intraembryonic artery, the dorsal aorta (Williams *et al.*, 2010). During subsequent development, arterial differentiation is induced by Notch signalling, which most likely acts as a downstream mediator of sonic hedgehog (Lawson *et al.*, 2001).

While the arterio-venous identity is acquired early in development, endothelial cells can adapt to a new environment and transdifferentiate in order to integrate into blood vessels of the opposing vascular type (Moyon *et al.*, 2001). However, transplanted endothelial cells tend to integrate predominantly into blood vessels of the same type (Moyon *et al.*, 2001). Transplantation experiments of quail-derived endothelial cells into 2-day old chick embryos revealed that the percentage of arterial cells that integrated into venous blood vessels drastically decreased post innervation of the arteries (Pardanaud *et al.*, 2016). It has further been shown that adrenergic signalling induces the upregulation of arterial markers indicating that neuron-derived signals can influence vascular identity (Pardanaud *et al.*, 2016). In mice, neurons control the differentiation of blood vessels into arteries in the developing skin via VEGF secretion (Li *et al.*, 2013; Mukouyama *et al.*, 2005).

Taken together, the involvement of neuronal signals in arterial differentiation in the skin, the loss of arterio-venous plasticity of arterial cells post-innervation (Moyon *et al.*, 2001) as well as the upregulation of arterial markers in cultured endothelial cells after treatment with adrenergic compounds (Pardanaud *et al.*, 2016) suggest that

neurons could play an important role in driving arterial differentiation in other tissues such as the kidney.

In human kidneys, innervation starts about two weeks after formation of the definitive renal artery and during formation of the renal vein indicating that neurons are not involved in the differentiation of renal arteries (Mompeo *et al.*, 2019). The formation of renal innervation in the developing mouse kidney has, to my knowledge, not yet been described.

In this chapter, I aim to examine the hypothesis that renal neurons control vascular smooth muscle cell recruitments in the kidney, by characterizing the timing of arterial smooth muscle cell recruitment and renal innervation.

4.2 Results

4.2.1 Maturation of murine renal arteries occurs between E13.5 and E14.5

While kidney explants do contain endothelial cells and smooth muscle cells, the smooth muscle cells do not arrange around the blood vessels, indicating that arterial maturation does not occur in cultured kidneys (**Figure 3-8**). Previous studies dated the appearance of smooth muscle cells in the kidney to E13.5 and the localization of smooth muscle cells around the blood vessels to E15.5 (Hurtado *et al.*, 2015). Hurtado *et al.* (2015) used a FoxD1 linage-tracing mouse line (originated from a B6;129 background) for their study of smooth muscle cell development. Since different mouse strains can display some variability in the timing of development (Miyake *et al.*, 1997), I first aimed to confirm the timing of smooth muscle cell differentiation in wildtype CD1 mice, which are very suitable for developmental studies, because of their large litter size. To characterize the timing of smooth muscle cell development in CD1 mice, I isolated the kidneys of E13.5 (N = 9, from two different females) and E14.5 (N = 6, from two different females) embryos and stained them for smooth muscle actin and CD31. The E13.5 embryos of one of the females used for this experiment appeared less mature than typically observed, for example the separation of digits was not as prominent. This could have been caused by a mistake in setting up the timed mating, but could also be a natural phenomenon as differences of the developmental stage of murine embryos from the same litter are relatively common and have been described before (Yamamura, 1969). To adequately describe the developmental age of the embryos, they were comparatively staged based on previously described characteristics (Theiler, 1989). To keep labelling consistent between experiments the kidneys were relabelled as E12.75 and E13.0 instead, instead of using the Theiler stage.

E12.75 kidneys did not stain for smooth muscle actin. The renal blood vessels displayed clear differences in diameter, indicating that a hierarchical vascular network was formed (**Figure 4-1A**).

E13.0 kidneys contained individual smooth muscle cells that mostly, but not exclusively, localized in the peripheral region of the kidney. There was no preferential association of smooth muscle cells with blood vessels (**Figure 4-1B**).

In E13.5 and E14.5 kidneys, the smooth muscle cells were arranged around large-diameter blood vessels as well as around the ureter (**Figure 4-1C and D**).

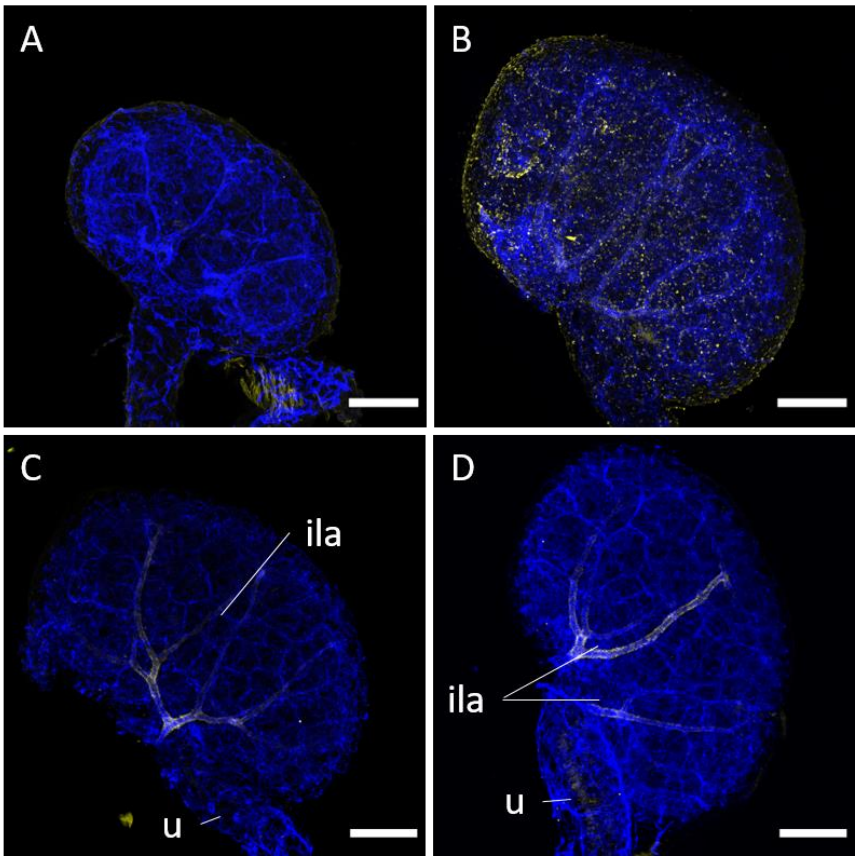

Figure 4-1: Smooth muscle cell development of the kidney *in vivo*. The kidneys have been isolated at E12.75 (A, N = 1), E13.0 (B, N = 1), E13.5 (C, N = 7) and E14.5 (D, N = 6) and were stained for smooth muscle actin (yellow) and CD31 (blue). Smooth muscle cells were visible around the ureter (u) and interlobular arteries (ila) in E13.5 and E14.5 kidneys. Scale bars: 200 um.

4.2.2 The smooth muscle cell marker Calponin1 is expressed later than smooth muscle actin and Transgelin

In agreement with previous studies (Hurtado *et al.*, 2015), I found that smooth muscle actin-positive cells appear and are recruited to the blood vessels between E13.0 and E14.5. In order to characterize the temporal correlation between smooth muscle cell recruitment and innervation, it has to be ensured that the markers used are expressed early during development. Therefore, I wanted to confirm when other smooth muscle cell markers are expressed compared to smooth muscle actin. Two markers that are reported to be expressed during smooth muscle cell development are Transgelin and Calponin 1. Transgelin, also known as Sm22α, is expressed early during development and is hypothesized to have a regulatory function on smooth muscle cell contractility (Xu *et al.*, 2003; Zeidan *et al.*, 2004). Calponin 1 has been shown to regulate smooth muscle cell contractility and is expressed nearly synchronously with Transgelin but after smooth muscle actin in chick embryos (Duband *et al.*, 1993; Winder *et al.*).

To identify in which sequence these markers were expressed during renal development, E13.5 (N = 2) and E14.5 kidneys (N = 2) were co-stained for smooth muscle actin, Calponin1 and Transgelin.

The staining revealed that smooth muscle actin and Transgelin overlapped in artery-shaped structures. Throughout the kidney there were a small number of cells that stained positive for both markers but also cells that expressed either smooth muscle actin or Transgelin but not both. Calponin-1 was expressed in the artery-shaped structures near the ureter, but did not extend as much along them as smooth muscle actin and Transgelin (**Figure 4-2A**). The Calponin-1 staining showed some speckled staining throughout the kidney. Due to the small size and even distribution of these speckles this was identified as background in the form of 'Salt-and-Pepper' noise.

E14.5 kidneys displayed a strong Calponin-1 expression in the ureter and a weaker expression in the vessel-shaped-structures. In contrast, smooth muscle actin was

expressed weakly in the ureter but showed a strong staining of the vessel-shaped-structures, whereas Transgelin appeared to be expressed with similar intensity in both ureteral and vascular smooth muscle cells. Some branches of the vessels showed no detectable expression of Calponin-1 but visible expression of smooth muscle actin and Trangelin (**Figure 4-2B**). Transgelin and Calponin-1 were found in spherical structures that did not express smooth muscle actin.

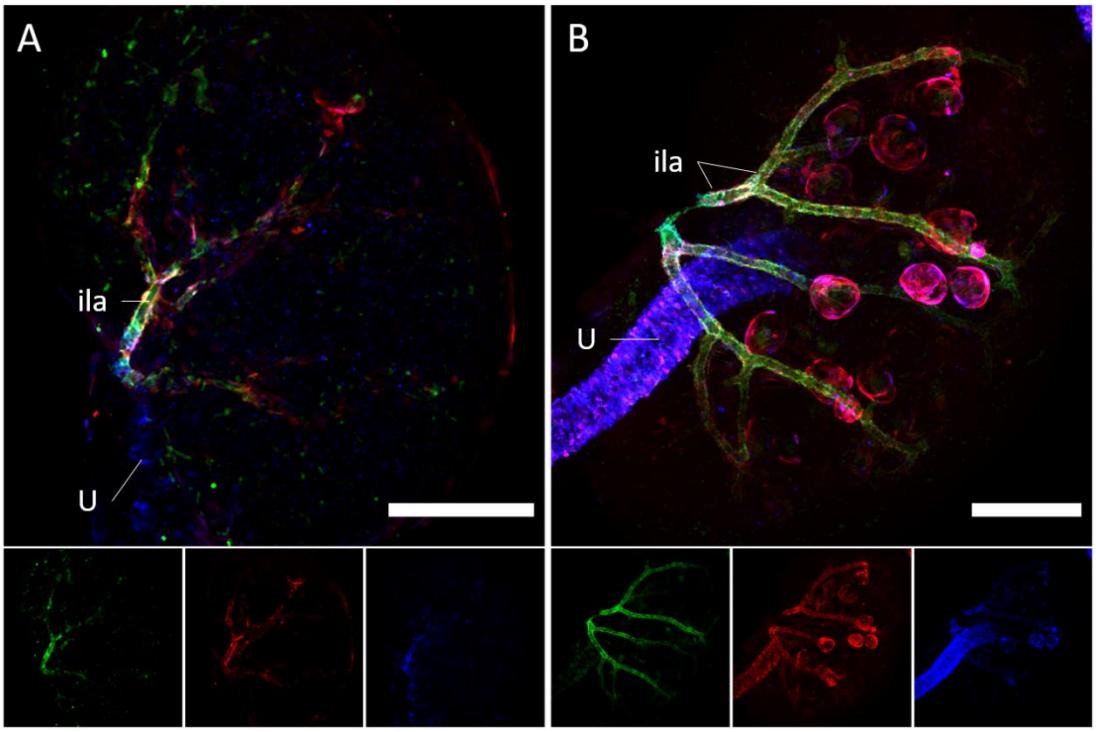

Figure 4-2: Expression of smooth muscle cell markers in the developing kidney. E13.5 (A) and E14.5 (B) kidneys were stained for smooth muscle actin (green), Transgelin (red) and Calponin-1 (blue). U: ureter, ila: interlobular arteries. Scale bars: 200 µm, N = 2

4.2.3 Arterial smooth muscle cell lining is lost in cultured murine E14.5 kidneys

The expression of smooth muscle cell markers seen in embryonic kidneys contrasts with the demonstration that, while smooth muscle cells develop in cultured mouse kidney explants, they do not align along the blood vessels (**Figure 3-8**). Kidneys isolated from E14.5 embryos consistently showed the presence of a smooth muscle cell lining around large-diameter blood vessels (**Figure 4-1**). To see whether arteries formed *in vivo* would maintain the smooth muscle cell lining *in vitro*, I isolated the kidneys of E14.5 embryos and cultured them on a Transwell for 8 to 32 h. Subsequently the explants were stained for the endothelial marker CD31 and the smooth muscle cell markers Calponin 1 and smooth muscle actin. Transgelin was not included because it was also detected in spherical structures, potentially glomeruli, where no smooth muscle cells were expected. Therefore, Transgelin expression might be less specific to smooth muscle cells.

After 8 h of culture all explants (5/5) stained positive for vascular smooth muscle actin and Calponin 1 (**Figure 4-3A**).

After 16 h of culture 5/5 explants showed expression of smooth muscle actin around the blood vessels and 3/5 explants contained blood vessels that stained positive for calponin 1 (**Figure 4-3B**).

After 24 h of culture 3/4 explants contained blood vessels that stained positive for smooth muscle actin and 2/4 explants stained positive for vascular Calponin 1. As well as being around the ureter, Calponin 1 and smooth muscle actin positive cells were detected in the peripheral cell layer of the explants (**Figure 4-3C**).

After 32 h of culture 2/4 explants exhibited a weak staining for smooth muscle actin around the blood vessels and none of the explants had blood vessels that stained positive for Calponin 1. The expression of smooth muscle actin and Calponin 1 in the peripheral cell layer persisted. While in 8 h-cultured samples, some blood vessels had

a larger diameter than others, which can be interpreted as evidence of a hierarchical vascular network, this was no longer visible in samples cultured for 32 h (**Figure 4-3D**).

Within the ureter the expression of smooth muscle actin and Calponin 1 persisted for the entire culture period in all explants, so acted as a positive control.

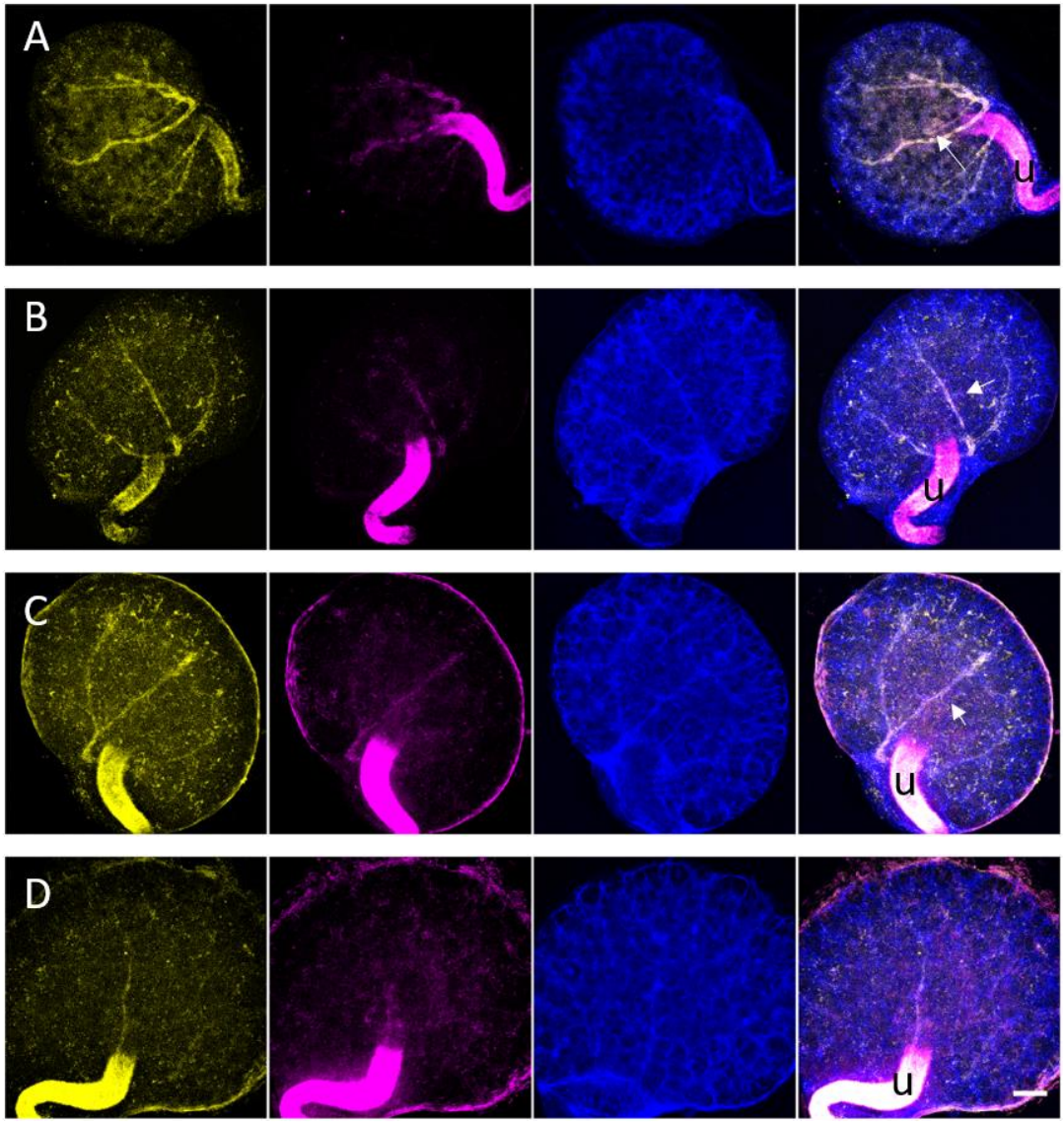

Figure 4-3: Arterial smooth muscle cell lining is lost in culture. E14.5 kidneys were cultured for 8 h (A, N = 5), 16 h (B, N = 5), 24 h (C, N = 4) and 32 h (D, N = 4). subsequently the kidneys were stained for smooth muscle actin (yellow), Calponin-1 (magenta) and CD31 (blue). Smooth muscle cells remain visible around the ureter (u), but are sequentially lost around the arteries (arrows). Scale bars: 100 µm.

4.2.4 Innervation of the mouse kidney occurs after recruitment of smooth muscle actin positive cells

Renal explant cultures fail to develop and maintain arteries lined with smooth muscle cells. In other tissues, such as the skin, the differentiation of arteries and recruitment of smooth muscle cells is regulated by neuron-derived signals. To identify whether neuronal signals might be involved in renal arterial maturation, I stained E13.5 (N = 3) and E14.5 kidneys (N = 3) for smooth muscle actin and the neuronal marker Tuj1 and the vascular marker CD31.

As shown in the earlier experiments the majority of smooth muscle cells align around the blood vessels in E13.5 kidney. Most E13.5 kidneys showed no staining for Tuj1. In a one of E13.5 kidneys Tuj1 expressing axons were seen around the ureter but not along the blood vessels of the kidney (**Figure 4-4A**).

In E14.5 kidneys the Tuj1 positive axons wrapped around the smooth muscle cell layer of the major arteries (**Figure 4-4B**). As Tuj1 is expressed early during neuronal differentiation (Memberg and Hall, 1995), this indicates that the innervation of the kidney occurs after the recruitment of the smooth muscle cells. This strongly suggests that neuron derived signals are not required for the initial formation of the smooth muscle cell lining.

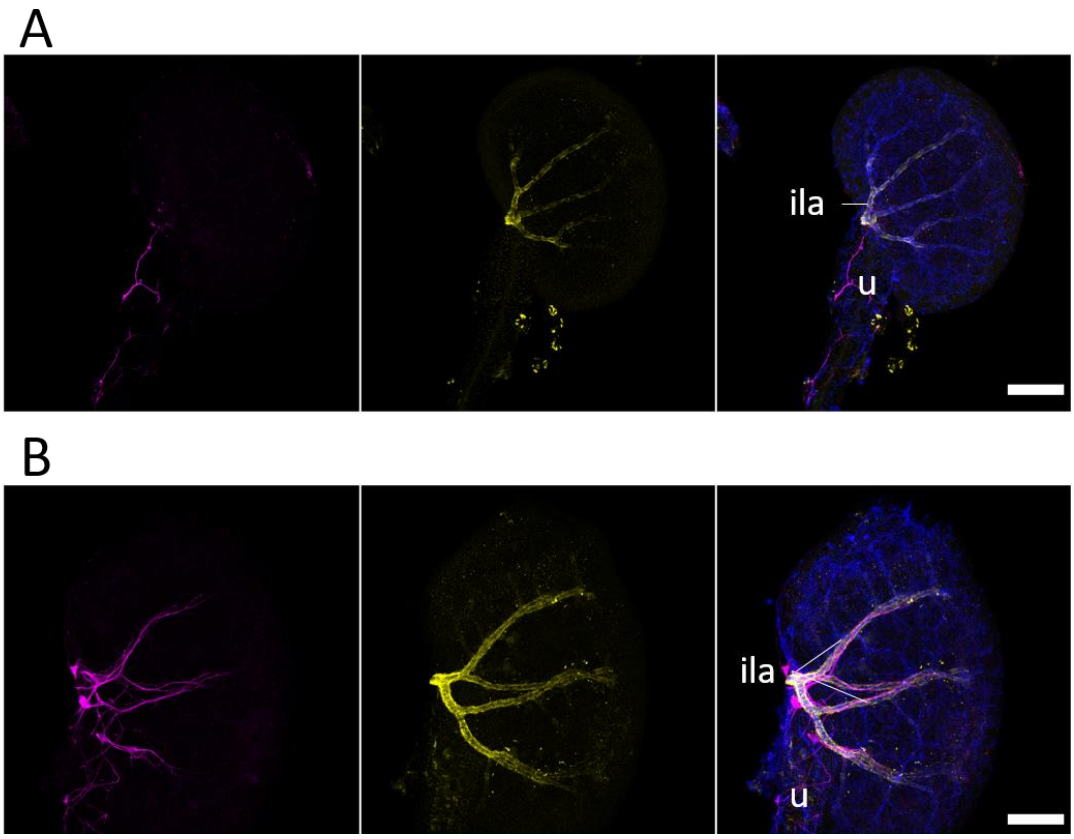

Figure 4-4: Innervation of the developing kidney. To determine the time-point of the innervation of the kidney E13.5 (A) and E14.5 (B) kidneys were stained for the neuronal marker Tuj1 (magenta), smooth muscle actin (yellow) and CD31 (blue). At E13.5 neurons were seen around the ureter (u) but not within the kidney. At E14.5, neurons were seen around the ureter and along the interlobular arteries (ila). Scale bars: 200 µm. N = 3

4.2.5 Neurons develop in cultured murine kidneys, but do not grow exclusively in close proximity to smooth muscle cells

The staining of *in vivo* maturing kidney revealed a close proximity between renal neurons and smooth muscle cells. The neurons invaded the kidney following the formation of the smooth muscle cell lining on major blood vessels. In other tissues, for example the lung, neurons follow smooth muscle cell derived signals such as brain-derived neurotrophic factor (Radzikinas *et al.*, 2011).

As demonstrated earlier (**Figure 3-8**) smooth muscle cells develop in cultured kidney explants. To investigate whether neurons would form in cultured kidney and align closely with the smooth muscle cells, I stained 7-day cultured kidney explants cultured in type 1 collagen for smooth muscle actin and Tuj1. Consistent with previous studies (Karavanov *et al.*, 1995; Sariola *et al.*, 1988) neurons developed in the majority, 7 out of 8, of cultured kidneys (**Figure 4-5**).

The neurons were not exclusively seen in areas with a high density of smooth muscle cells. In turn, smooth muscle cells occupied large areas of the explants that did not contain any neurons. There was no sign of an artery-like arrangement of smooth muscle cells and no sign of any area which was particularly densely populated with smooth muscle cells and neurons. This suggests that neither cell type depends on direct contact with the other for its growth and that their presence is not sufficient for the formation of a hierarchical arterial network (**Figure 4-5A**).

While the neurons in some sections of the kidneys aligned with the blood vessels, they did not exclusively grow in proximity to endothelial cells (**Figure 4-5B**).

In vivo, renal neurons expressed the dopaminergic lineage marker tyrosine hydroxylase (**Figure 4-5C**). Interestingly some neurons formed dense, node-like aggregates of which a subset stained positive for tyrosine hydroxylase indicating the differentiation of the neurons into the dopaminergic linage can occur in explant

cultures (**Figure 4-5A**). Notably tyrosine hydroxylase was rarely seen in the axonal structures.

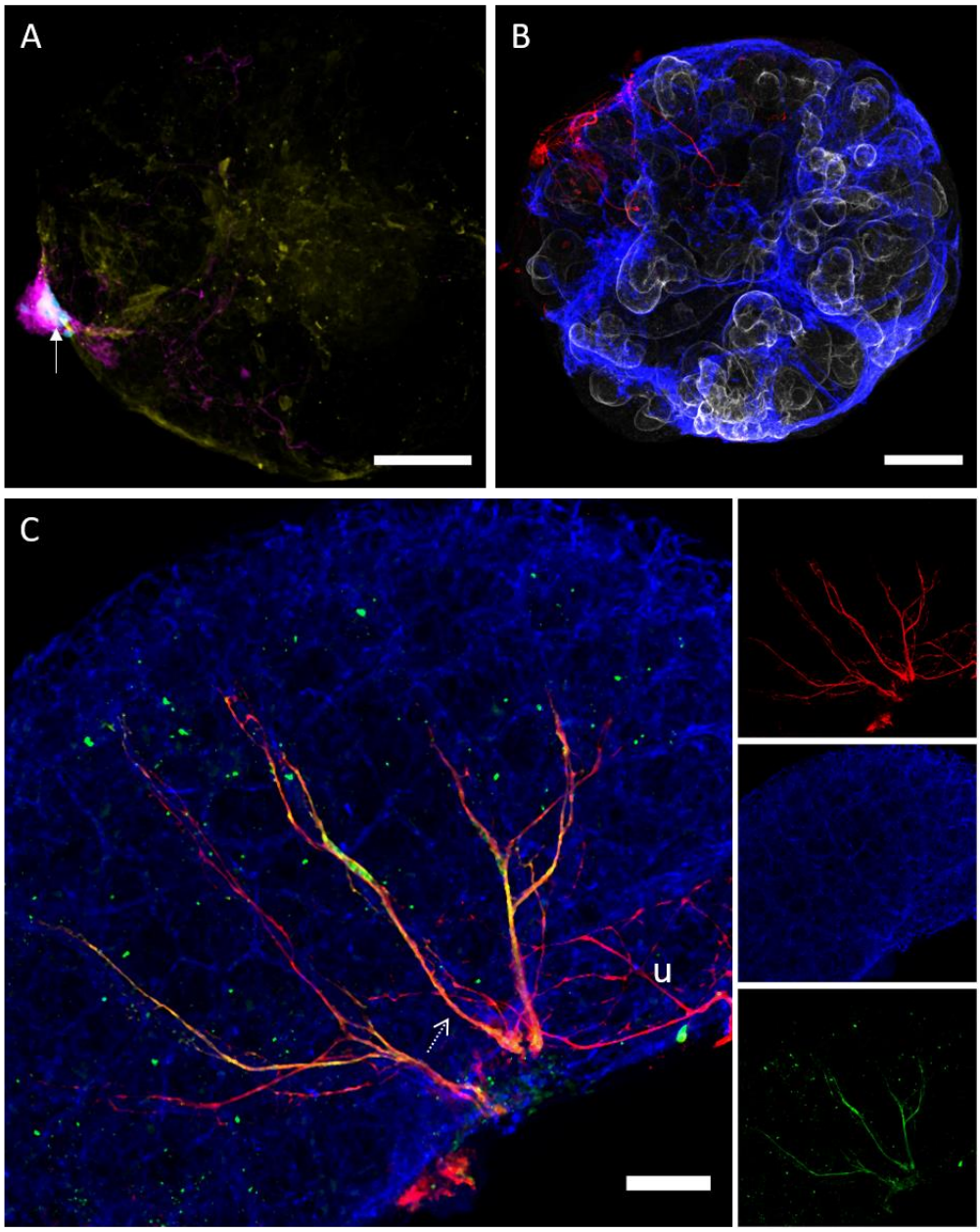

Figure 4-5: Differentiation of neurons in cultured E11.5 kidneys. E11.5 kidneys cultured for 7 days and stained for smooth muscle actin (yellow), Tuj1 (magenta) and Tyrosine hydroxylase (cyan, arrow). N = 5 B: Staining of cultured neurons for Tuj1 (red), CD31 (blue) and laminin (grey). N = 3. C: Staining of E14.5 kidney for Tuj1 (red), CD31 (blue) and Tyrosine hydroxylase (green) shows differentiation if intrarenal neurons (dashed arrow) into dopaminergic lineage, while neurons around the ureter (u) remain negative for tyrosine hydroxylase. N = 3. Scale bars 100 µm

4.2.4 A subset of blood vessel-aligned neurons of murine E14.5 kidneys appears to undergo apoptosis in culture

The previous experiments showed that both neurons and smooth muscle cells develop in culture but the smooth muscle cells fail to align along the renal blood vessels. I also showed that the already formed smooth muscle cell lining in E14.5 kidneys could not be maintained in culture. This raised the question of whether blood vessel associated neurons would also undergo apoptosis in culture. To identify if and when neurons in kidney explants would die, I isolated E14.5 kidneys and cultured them for 8 to 32 h followed by staining them for Tuj1, CD31 and smooth muscle actin (N = 3 per time point).

After 8 h of culture, the usually continuous Tuj1 staining appeared as fragmented lines, indicating fragmentation and cell death of the neurons (**Figure 4-6A**). These fragmented neurons were seen at all time points. Interestingly, while all 8 h-cultured kidneys showed fragmented neurons, some of the longer cultured explants also contained healthy-looking, continuously stained neurons (**Figure 4-6**).

One explanation for this is that the initially present blood vessel-associated neurons die but simultaneously new ones are also formed in culture. However, this hypothesis could only be tested by live imaging, which was not possible because, despite several attempts, I could not source kidneys from transgenic mice expressing a fluorophore within neurons for live imaging.

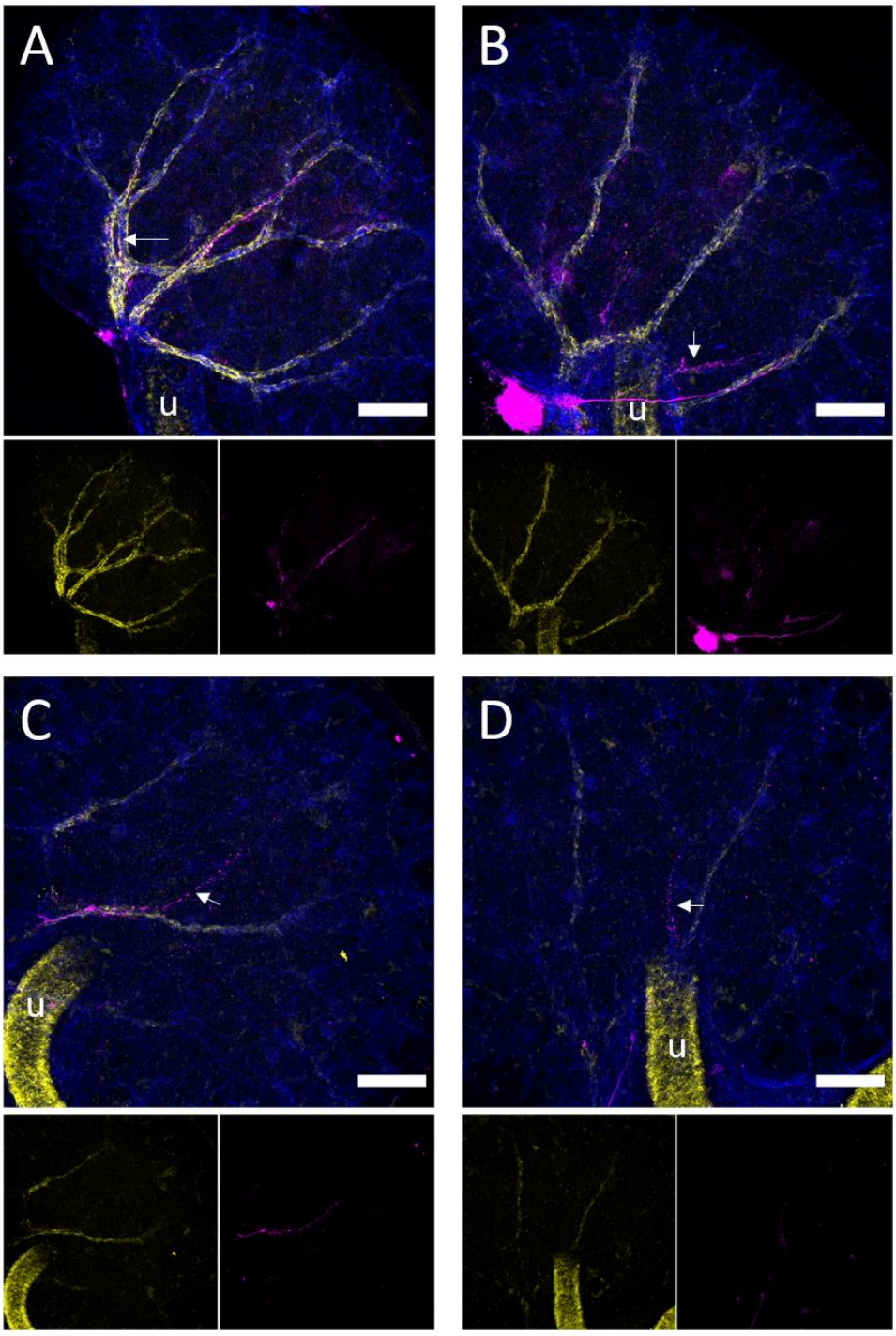

Figure 4-6: Progressive loss of neurons and vascular smooth muscle cells in cultured E14.5 kidneys. E14.5 kidneys have been isolated and cultured on a Transwell for 8 h (A), 16 h (B), 24 h (C) and 32 h (D). Subsequently the kidneys have been stained for smooth muscle actin (yellow), Tuj1 (magenta) and CD31 (blue). Smooth muscle cells remains along the ureter (u) but were but not alon the arteries. Neurons appear fragmented (arrows). Scale bars: 200 µm. N = 3

4.3 Discussion

This chapter gives an important insight into vascular smooth muscle cells in the developing kidney. The staining for the smooth muscle cell markers Transgelin, Calponin-1 and smooth muscle actin revealed that, at at the analyzed stages (E13.5 and E14.5), vascular smooth muscle cells display different relative expression levels of these markers to each other compared to ureteric smooth muscle cells. This heterogenicity of smooth muscle cell types could have important implications for renal engineering. Within the kidney, vascular smooth muscle cells are required to regulate the blood flow, which is essential to prevent damage to the nephrons and to ensure an optimal filtration (Bidani Anil and Griffin Karen, 2004; Hashimoto and Ito, 2015), while the main function of the ureteric smooth muscle cells is to actively transport urine from the kidney to the badder, a process that requieres cordinated contraction along the proximal-distal axis of the ureter (Lang *et al.*, 2002). Engineered kidneys would most likely need to reflect the heterogenicy of smooth muscle cells found *in vivo* in order to function efficiently. The differential expression ratio of smooth muscle actin to calponin-1 could be used as a first step in characterizing smooth muscle cells in engineered kidneys. However, further experiments, for example single-cell transcriptomics, will be requiered to identify how many smooth muscle cell subtypes are found within the kidney and how they can be distiguished.

The main aim of this chapter was to characterize a potential involvement of neurons during arterial differentiation in the kidney. Neurons have been previously shown to drive the differentiation of arteries in the limb skin and to regulate arterio-venous plasticity during avian development (Li *et al.*, 2013; Mukouyama *et al.*, 2005; Pardanaud *et al.*, 2016). In the adult kidney, the renal neurons are closely aligned with the arteries (Marfurt and Echtenkamp, 1991), hinting that one of the tissues depends on the other for its growth.

If neurons were responsible for driving arterial differentiation, they would invade the kidney prior to the formation of the arterial smooth muscle cell lining. However, the

experiments in this chapter demonstrated that the smooth muscle cell recruitment occurs prior to the innervation of the kidney. Therefore, the initiation of arterial differentiation cannot depend on neuronal signals. This suggests that neurons are dispensable for the initial development of a hierachial vascular network. As adult kidneys can function to some degree after at least partial denervation of the renal artery (Sanders *et al.*, 2017), the role of neurons might be neglactable for generating fuctional blood-filtering kidney organoids.

Under culture conditions, neurons as well as smooth muscle cells developed but did not appear exclusively in close proximity, indicating that neither cell type depends on direct contact with the other for its growth. Since all kidney explants examined contained smooth muscle cells but 1/8 explants did not contain any neurons, it can be assumed that smooth muscle cells do not require any neuron-derived secreted factors for their growth. A small proportion of the neurons in cultured E11.5 kidney expressed tyrosine hydroxylase a marker for dopaminergic neurons. *In vivo*, tyrosine hydroxylase was detected in the neurons growing along the interlobular arteries, but not in the neurons forming around the ureter (**Figure 4-5C**), suggesting that ureteric neurons differentiate eihter at a later stage or into a different lineage. In rabbit kidneys, the ureteric neurons express acetylcholine esterase, a marker for adreneric neurons (Gosling and Dixon, 1971), which suggests that the ureteric neurons in mice may also differentiate into a different lineage. Since one function of neurons is to control smooth muscle cell contraction (Gosling and Waas, 1971; Sata *et al.*, 2018), a differentiation into different lineages could be necessary to communicate with the different subpopulations of smooth muscle cells.

Interestingly, the neurons and smooth muscle cells associated with the arteries of isolated E14.5 kidneys were lost within 32 h of culture. The survival of these cell types in cultured E11.5 explants suggests that loss of artery-associated smooth muscle cells and neurons is not caused by the culture conditions themselves. However, more differentiated neurons and smooth muscle cells might require other factors for their survival than more immature smooth muscle and neuronal cells and therefore might

not surive in culture. Neurons commonly depend on targed derived signals for their survival (Hamburger and Levi-Montalcini, 1949). Therefore, the death of neurons might be caused by the loss of input signals from the vascular smooth muscle cells. The loss of smooth muscle cells could be due to a change of the endothelial cell metabolism in culture. *In vivo*, the recruitment of vascular smooth muscle cells is regulated by heamodynamic forces (Padget *et al.*, 2019). Therefore the lack of blood flow in cultured kidneys might cause the loss of the vascular smooth muscle cells around the blood vessels.

The results above refute the hypothesis that the arterial smooth muscle cell recruitment is initiated by neuronal signals. Therefore, neurons may be dispensible for mimicking early developmental stages of vascular development in kidney organoids. However, there appears to be an essential factor missing in cultured kidneys that allows the endothelial cells to differentiate into arteries and recruit smooth muscle cells as well as to maintain already present periarterial smooth musscle cells in cultured E14.5 kidneys.

A likely explanation for the loss of artery-associated smooth muscle cells is the lack of blood flow. Therefore, my next aim was to initiate a flow through the kidney explants by connecting them to the vasculature of a host.

Chapter 5 - Graft-based vascularization of kidney explants

5.1 Introduction

The embedding of kidney explants in type I collagen results in a more three-dimensional growth compared to traditional culture methods but causes central necrosis most likely due to limited oxygen and nutrient perfusion (**Chapter 3**). *In vivo*, this is prevented by the transport of oxygen and nutrients via the blood system. While blood vessels were present within kidney explants, they remained immature as indicated by the lack of smooth muscle cell recruitment (**Figure 3-7**). The smooth muscle cell recruitment to the renal arteries is not initiated by neuronal signals as neurons invade the kidney after the vascular smooth muscle cell wall is formed (**Figure 4-4**). Therefore, other factors, not present in cultured kidney explants, are required for the vascular maturation in the kidney.

Blood flow has been shown to play a critical role during vascular development (Padget *et al.*, 2019). Connecting kidney organoids, or explants to the circulatory system of a host, might therefore increase vascular maturation.

5.1.1 Strategies to vascularise organoids

Several studies show the potential of renal organoids to connect to the vasculature of a host (Low *et al.*, 2019; van den Berg *et al.*, 2018; Xinaris *et al.*, 2012). In some studies the organoids were soaked in VEGF prior to transplantation to enhance the vascularization of kidney organoids (Xinaris *et al.*, 2012). Other groups co-transplanted the organoids with VEGF-soaked rods or aggregated endothelial cells (Sharmin *et al.*, 2016).

The vascularisation of organoids may also be accelerated by pre-treatments with proangiogenic factors upstream of VEGF. Chai *et al.* (2018) treated periosteum-derived mesenchymal stem cells with low dosages of Cobalt chloride (Chai *et al.*, 2018). Cobalt chloride stimulates the translation of Hif1α, a regulator of VEGF expression (Chachami *et al.*, 2004). Pre-treatment of periosteum-derived mesenchymal stem cells with Cobalt chloride supported the vascularisation of the cell aggregate after transplantation (Chai *et al.*, 2018).

An improved vascularization after induction of VEGF expression or direct soaking in VEGF is not surprising given that VEGF is one of the main stimulators of angiogenesis. In humans, at least seven variants of VEGF are generated by alternative splicing or proteolytic cleaving (**Figure 5-1**). The most abundant in humans are $VEGF_{121}$, $VEGF_{165}$ and $VEGF_{189}$ (Tischer *et al.*, 1991). The equivalent murine proteins are one amino acid shorter (Shima *et al.*, 1996). The alternative splicing occurs in the heparin-binding domain resulting in $VEGF_{120}$ having no heparin- binding domain, $VEGF_{164}$ having one and $VEGF_{188}$ having two heparin binding domains (Ruhrberg *et al.*, 2002). Consequentially, $VEGF_{120}$ is highly diffusible while $VEGF_{164}$ has an intermediate and $VEGF_{188}$ a short diffusion range (Ruhrberg *et al.*, 2002). While mice expression either only $VEGF_{120}$ or only $VEGF_{188}$ show severe developmental defects, mice expressing solely $VEGF_{164}$ appear healthy, indicating that $VEGF_{164}$ is the main regulating isoform of cardiovascular development (Carmeliet *et al.*, 1999; Mattot *et al.*, 2002; Stalmans *et al.*, 2003; Stalmans *et al.*, 2002).

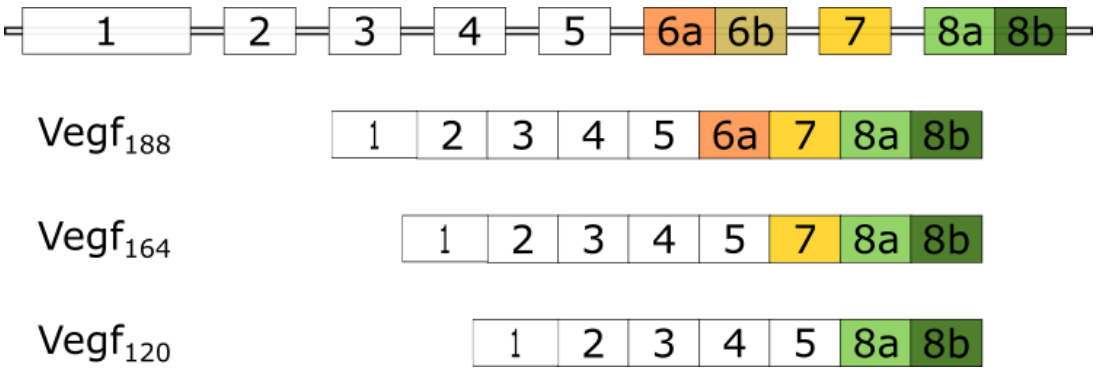

Figure 5-1: Splice variants of Vegf

While grafting kidney explants or organoids into a mammalian host, which may be facilitated by upregulation of *Vegf* expression, could introduce a blood flow through the renal capillary plexus and thereby improve the supplementation with oxygen and nutrients, it would require the use of animals and therefore raises ethical concerns. The transplantation into a host would also make the kidneys less accessible and therefore more difficult to observe their development post-transplantation. Additionally, implanting into a mammalian host may only be successful in immunocompromised animals or might require the use of immune system supressing drugs.

An alternative to mammalian host implantation could be the grafting of kidney explants onto the chick chorioallantoic membrane (CAM). The CAM is a highly vascularized and easy accessible extraembryonic membrane (Nowak-Sliwinska *et al.*, 2014). It starts to develop around day 3 of incubation and reaches its full size around day 10 of incubation after rapid exponential growth (Nowak-Sliwinska *et al.*, 2014). Since chick embryos do not become fully immunocompetent until day 18 of incubation (Janse and Jeurissen, 1991), no administration of immunosuppressants is required when using the CAM to graft tissues.

Kidney organoids and explants have been previously vascularized by engraftment on the CAM (Garreta *et al.*, 2019; Loughna *et al.*, 1997). After 5 days of culture, blood flow was visible within the grafted organoids and the blood vessels reached the

glomerulus (Garreta *et al.*, 2019). However, the anatomical realism of the vascular plexus in grafted kidneys has not been analysed in dept.

Hypothesizing that blood flow is essential for the arterial differentiation of renal blood vessels, I aimed to introduce flow through the kidneys explants by engrafting them onto the chick CAM. I further aimed to characterize the realism of the forming vascular plexus in order to evaluate this method for its potential to generate anatomically realistic vascularized kidney organoids.

5.2 Results

5.2.1 Murine kidneys can be vascularised by engraftment onto the chick CAM, but with low efficiency

While cultured embryonic kidneys do contain endothelial cells, the majority of glomeruli remain avascular (Sariola *et al.*, 1983). Additionally, their vascular plexus appears to remain immature, since there is no sign of formation of a smooth muscle cell lining.

The lack of vascular maturity *in vitro* is likely caused by the lack of blood flow as embryos with a reduced heart rate show an impairment of vascular maturation (Padget *et al.*, 2019). To provide a flow of blood, I placed 3-day cultured E11.5 kidney explants onto the chick CAM (Garreta *et al.*, 2019). After incubation of the eggs for an additional three days, the majority of explants were visible as white discs on top of the CAM without any visible blood vessels (**Figure 5-2A**). About 21 % (N = 42) of the kidneys displayed an at least two-times increase in size and seemed to have sunken into the CAM where they appeared to have connected to the host vasculature (**Figure 5-2B**). Kidneys with an obvious increase in size as well as visible blood vessels growing in and around them were considered as successfully grafted, while kidneys appearing as white disc-like structures were considered as not grafted.

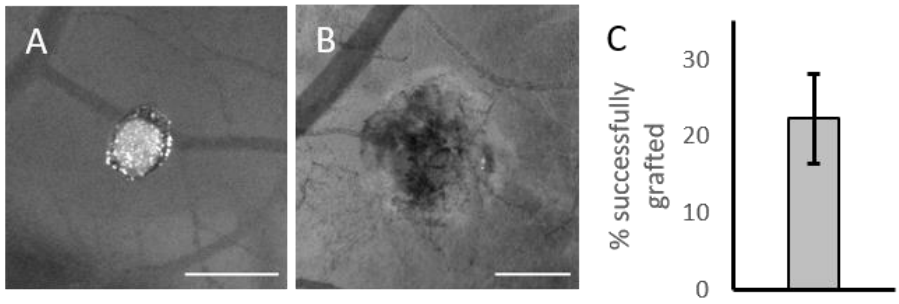

Figure 5-2: grafting efficiency of kidneys is low. A kidney explant which did not engraft into the CAM within 3 days. B: engrafted kidney explant. Scale bars: 500 µm C: Quantification of grafted kidneys. The bar shows the percentage of grafted kidneys calculated from the pooled data of 4 independent experiments. The error bar displays the standard deviation of the grafting efficiency across the 4 experiments.

5.2.2 Pre-treatment of murine kidney explants with VEGF inducers did not increase grafting efficiency

The grafting efficacy of embryonic kidneys onto the chick CAM was low with only about 1 in 5 kidneys connecting to the host vasculature. Some studies state that the vascularization of kidney organoids by implantation requires pre-soaking them in VEGF or co-transplantation of HUVECS while others report successful engraftment of kidney organoids without prior treatment (Sharmin *et al.*, 2016; Xinaris *et al.*, 2012).

Soaking the kidney explant in VEGF, however, could potentially direct blood vessels into compartments that usually remain avascular such as the cap mesenchyme and therefore affect the anatomical realism of the forming vasculature. *In vivo*, VEGF is expressed by the collecting ducts (Simon *et al.*, 1995). To induce the expression of *Vegf* within the collecting duct compartment, I treated E11.5 kidney explants with the known *Vegf* inducers progesterone and Insulin-like growth factor 1 (IGF-1), whose receptors are expressed specifically in the collecting duct compartment (Harding *et al.*, 2011; McMahon *et al.*, 2008). For the induction of *Vegf* expression, the kidney explants were cultured for 2 days and subsequently treated for 24h with 5 µM, 10 µM or 50 µM of progesterone and 10 nM, 50 nM or 100 nM IGF-1. Following this, RNA was extracted and analysed for expression of total *Vegf*, and $Vegf_{164}$ as the main pro-angiogenic isoform.

Treatment with neither progesterone nor IGF-1 alone resulted in a significant increase of the expression of total *Vegf* or $Vegf_{164}$. Combined treatment with 5 µM progesterone and 100 nM IGF-1 (hereafter referred to as 'grafting medium') resulted in a 50% increase of *Vegf* (**Figure 5-3A**) as well as $Vegf_{164}$ expression (**Figure 5-3B**).

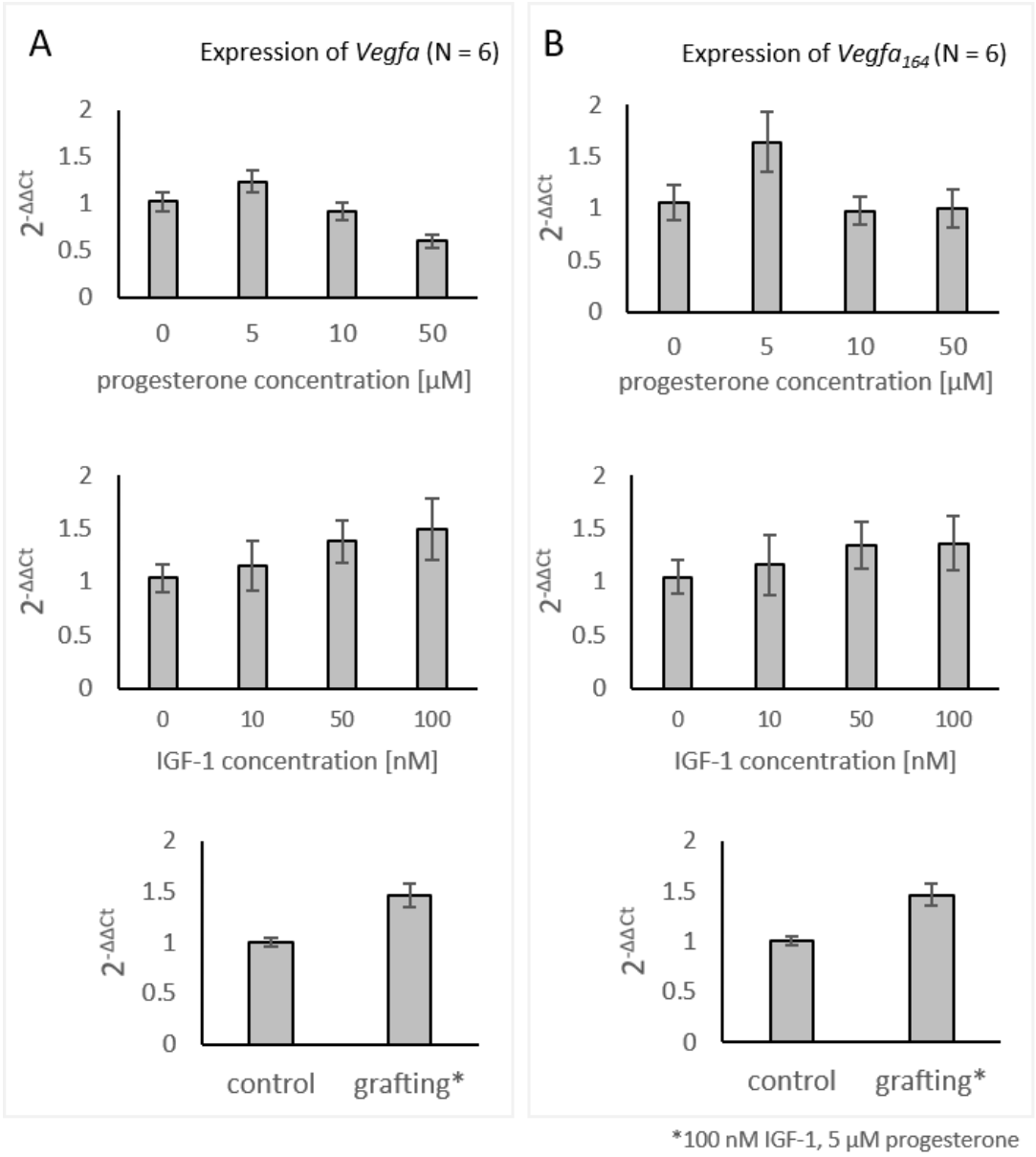

Figure 5-3: Expression of *Vegf* and $Vegf_{164}$ after treatment with IGF-1 and progesterone.A: Expression of *Vegf,* normalized to the averaged expression of *Actb* and *Hsp90ab1*, after treatment with indicated dosages of progesterone and IGF-1 individually resulted in an apparent increase of *Vegf* expression, which was not statistically significant. The combination of 5 µM progesterone and 100 nM IGF-1 (grafting medium) resulted in a significant upregulation of *Vegf* (unpaired Student's t-test, $p < 0.01$, N = 6, data from 2 independent experiments, error bars display standard deviation). B: Expression of $Vegf_{164}$ isoform after treatment with either progesterone or IGF-1 did not result in an increased expression of $Vegf_{164}$ expression. However, $Vegf_{164}$ was significantly upregulated by the combined treatment with 5 µM progesterone and 100 nM IGF-1 (Student's t-test, $p < 0.01$, N = 6, data from 2 independent experiments, error bars display standard deviation).

To test whether the induction of VEGF would increase the grafting efficiency, kidney explants were cultured for 24 h in either grafting or control medium. After treatment, the kidney explants were placed on the CAM and cultured *in ovo* for an additional 3 days (**Figure 5-4A**). Kidney explants cultured in control medium grafted with an efficiency of 8 % (2/25). Explants cultured in the grafting medium grafted with a comparable efficiency of 11 % (4/36) (CI: -0.12, 0.18) (**Figure 5-4B**).

For kidneys cultured in the control medium, the grafting efficiency of 8 % was lower compared to the 21 % from the previous experiments (**Figure 5-2**), however, this difference was not statistically significant (CI: -0.03, 0.30).

For RNA sampling, the kidney explants were cultured for 2 days prior to the treatment period of 24 h. To test whether the lack of an effect of the grafting medium was due to a reduction of the culture time the experiment was repeated with a pre-grafting culture period of 72 h, and then the kidneys were cultured for 2 days in control medium following 24 h in grafting medium (**Figure 5-4A**). After extending the pre-culture time for kidneys in the grafting medium a grafting efficiency of 9 % (3/34) was reached which was comparable to the 11 % that were obtained with a pre-culture time of 24 h (**Figure 5-4B**). The grafting medium had no visible effect on the grafting efficiency for kidneys cultured 72 h prior to grafting (CI: -0.28, 0.03) (**Figure 5-4B**).

In summary, there were no statistically significant differences between any of the culture conditions.

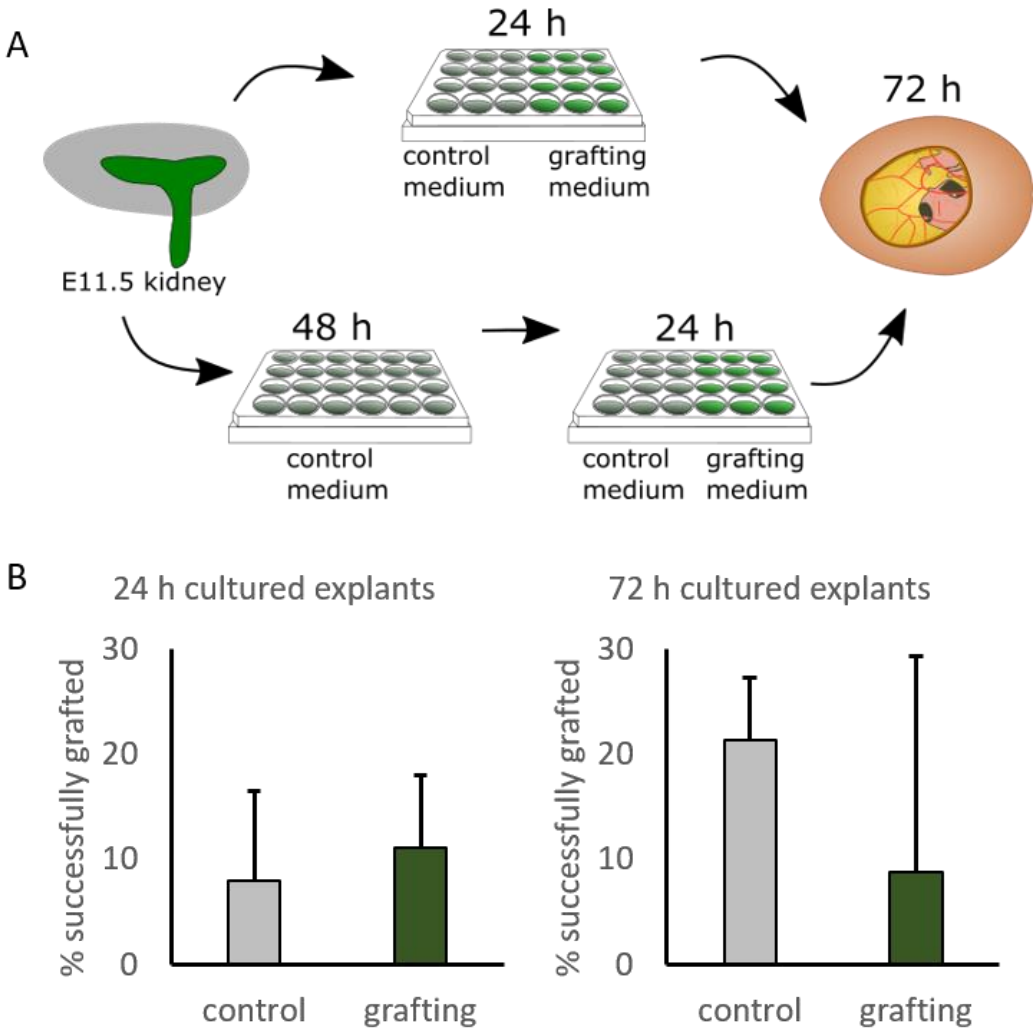

Figure 5-4: Induction of *Vegf* expression did not improve grafting efficiency. A: illustration of grafting procedure. B: Bars represent the grafting efficiency in % after pooling the data from different experiments. Error bars display standard deviation of the percentage of grafted kidneys between different experiments. Sample sizes: 24 h grafting: N = 36, data pooled from 3 independent experiments, 72 h control: N = 42, data from 4 independent experiments, 72 h grafting: N = 34, data from 4 independent experiments

5.2.3 Grafted explants display limited blood vessel maturation and morphological abnormalities

In vivo kidneys become vascularized by a single artery which enters the kidney near the ureter and ramifies to follow the collecting duct branches (Bowman, 1842). Following the onset of blood flow the segmental arteries, the arteries that are branched from the renal artery and further ramify into the interlobular arteries, recruit smooth muscle cells and the glomeruli become vascularized (Bowman, 1842; Hurtado *et al.*, 2015). To determine whether the vasculature in grafted kidneys would mature to form a hierarchical network and vascularized glomeruli, the grafts were fixed and stained for renal and endothelial markers.

In contrast to *in vivo*-grown kidneys, which are vascularized by a single artery and vein originating from the aorta, kidneys grafted onto the CAM were invaded by multiple blood vessels entering from different sites (**Figure 5-5A**). To confirm blood flow through the grafts, the chick vasculature was injected with either Dextran-FITC, Tomato lectin conjugated with DyLight 594, or Donkey-anti-mouse AlexaFluor594 secondary antibody prior to removal and fixation of the graft. Injection with Dextran-FITC indicated flow through the grafted kidney *in ovo* (**Figure 5-5A**). However, the signal was lost after the staining process. The conjugated tomato lectin was visible within the blood vessels but also stained the proximal tubules (data not shown), most probably because the lectin was washed away during the staining and then bound to the proximal tubules. The injected secondary antibody was detectable after co-staining with CD31 and it indicated blood flow mainly through the peripheral vessels of the graft (**Figure 5-5B**).

To determine the maturity of the vascular network within grafts, I stained the kidneys for the smooth muscle cell marker Calponin 1 and with the vascular marker CD31 (Miano and Olson, 1996). The staining revealed that smooth muscle cells developed around the ureter, which served as a positive control for the antibody, but the smooth muscle cells did not arrange around the blood vessels (**Figure 5-5C**). The

staining also showed that the CD31 antibody used for these experiments detected the mouse endothelial cells within the grafted kidney, but not the chick endothelial cells of the CAM, as the arteries of the CAM could be identified by Calponin-1 staining but did not stain with the CD31 antibody used (**Figure 5-5C**). While I tried using two other antibodies to detect endothelial cells in the CAM (anti-VE-cadherin (abcam, ab33168) and anti-CD31 (abcam, ab7388)) those antibodies displayed a high background which made it difficult to distinguish between blood vessels and other tissues (data not shown)

Co-staining of the grafted kidneys with CD31 and one of the glomerular markers, WT1 (not shown) and Podocalyxin showed that a small subset (2/12) of glomeruli contained blood vessels, but the majority remained avascular (**Figure 5-5D**). However, since the CD31 antibody used for this staining displayed specificity to murine endothelial cells, it can not be ruled out that avascular appearing glomeruli were vascularized by galline endothelial cells.

To analyse the overall morphology of the grafted kidneys, two of the grafts were stained for the collecting duct marker E-cadherin, the nephron progenitor marker Six2 and the endothelial marker CD31. The staining showed that, similarly to *in vivo* grown kidneys, the collecting ducts formed a branched network with clusters of nephron progenitor cells around the tips and the blood vessels avoided the region of the cap mesenchyme. However, one of the explants displayed a cluster of nephron progenitor cells within the medullary region (**Figure 5-5E**).

In vivo, the cortical vasculature grows within the interstitium around the nephron progenitor caps but does not grow cortical to them (Munro *et al.*, 2017). In contrast, all explants developed excess vasculature cortical to the nephron progenitor caps, which formed a dense capillary network not present in *in situ* maturing kidneys (**Figure 5-5F**).

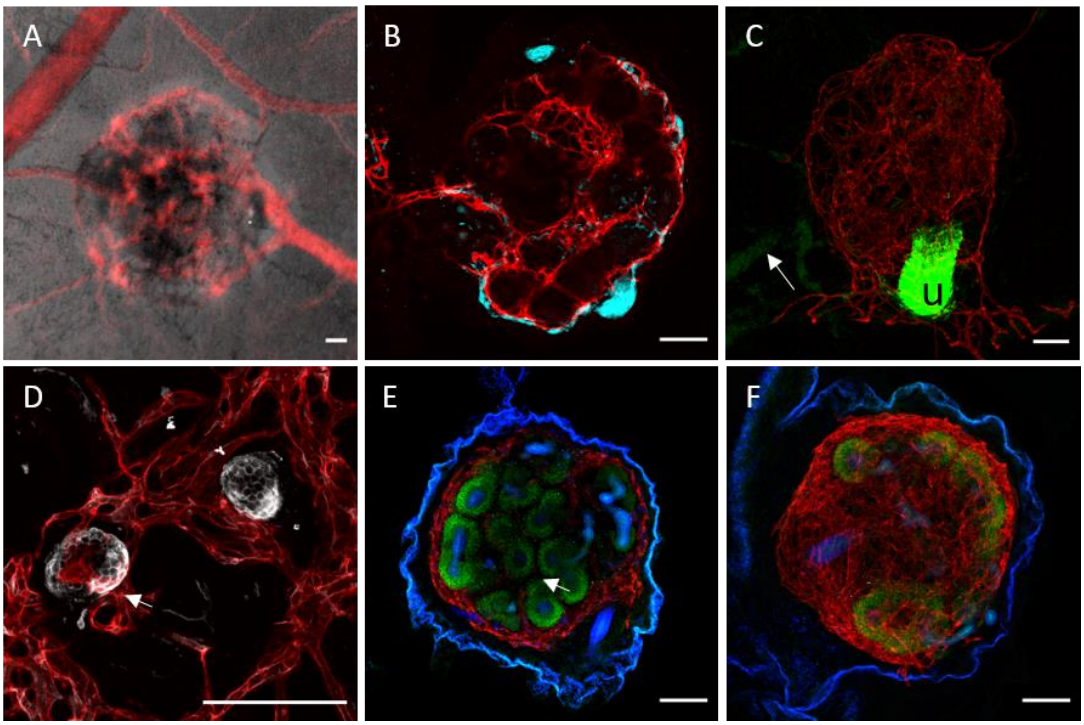

Figure 5-5: morphology of grafted kidneys. A: A grafted kidney was injected with Dextran-FITC (red) via a chorioallantoic membrane (CAM) vessel to visualize blood flow within the graft. B: A grafted kidney was injected with Donkey-anti-mouse AlexaFluor594 (cyan) antibody via a CAM blood vessel. Subsequent staining of the graft with CD31 (red) shows blood flow mainly through the peripheral vessels of the graft. C: Staining of a grafted kidney with CD31 (red) and Calponin1 (green) shows smooth muscle development around the ureter (u) but not around the blood vessels. The staining also revealed that the used CD31 antibody was specific to murine endothelial cells as the arteries of the CAM (arrow) stained for Calponin-1 but not with the used CD31 antibody. D: vascularized (arrow) and non-vascularized glomerulus of a grafted kidney stained with Podocalyxin (white) and CD31 (red). E: single plane of a grafted kidney shows aberrant localization of nephron progenitor cells (Six2, green, arrow) in the medullary region of the explant (Co-stained with CD31, red and E-cadherin blue). F: maximum projection of a grafted kidney stained with E-cadherin (blue), Six2 (green) and CD31 (red) shows development of excess vasculature around the explant. Scale bars 100 µm.

5.2.4 Grafting medium had no obvious effect on branching, nephron progenitor arrangement or blood vessel morphology

Some of the grafts previously cultured in the grafting medium showed an aberrant localization of nephron progenitor cells. To identify whether these might have been caused by compounds within the grafting medium, a subset of kidney explants was excluded from grafting and was instead cultured for three additional days, the time period they would have been cultured *in ovo*, in either the grafting or control medium. Subsequently, the explants were stained for CD31, Six2 and E-cadherin.

Neither kidney explants cultured within the control nor in the grafting medium displayed an aberrant localization of cap mesenchyme. The endothelial cells were mostly confined to the stromal area between the cap mesenchyme, however occasionally blood vessels were visible growing cortical to the nephron progenitor caps (**Figure 5-6**).

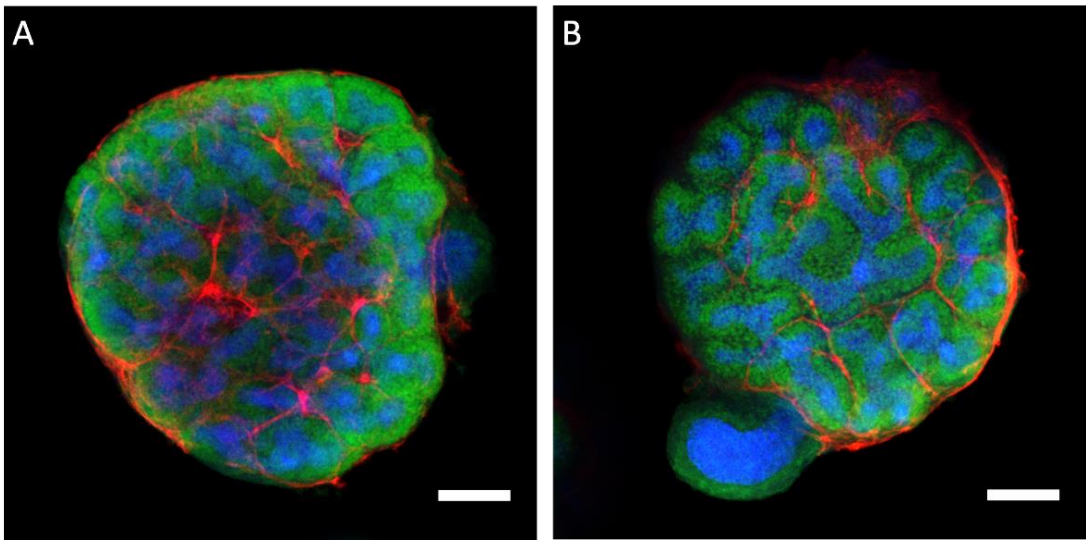

Figure 5-6: Kidney explants cultured in grafting medium did not display dysmorphologies observed in grafted kidneys. Kidney explants were cultured in control (A) or grafting medium (B) for 6 days followed by staining of Six2 (green), CD31 (red) and E-cadherin (blue). Scale bars: 100 µm

5.3 Discussion

Kidney explants and reaggregated kidney organoids have been shown previously to contain blood vessels (Munro *et al.*, 2017). However, the blood vessels remained immature as indicated by the lack of vascular smooth muscle cells (Chapter 3).

I hypothesized that introducing flow through the kidneys by grafting them onto the chick CAM would improve vascular maturity. The kidneys did connect to the CAM vasculature albeit with a low efficiency which was not increased through stimulation of *Vegf* expression. Hypothetically, it might be possible to improve the grafting efficiency with a further increase of *Vegf* expression or by soaking the explants in recombinant VEGF as done previously prior to implantation of kidney explants into rat hosts (Xinaris *et al.*, 2012).

The low efficiency of this assay makes subsequent analysis difficult as only a small number of grafted kidneys can be obtained for downstream assays such as the characterization of the anatomical realism of the graft vasculature. Within the kidney blood vessels, nephrons and collecting ducts need to be arranged in a precise special manner in order to achieve an optimal filtration of blood and concentration of urine (Dantzler *et al.*, 2011). This arrangement could not be reproduced by grafting kidney explants onto the chick CAM, as the grafted kidney displayed several vascular abnormalities. Most prominently the chick blood vessels entered the explants at multiple random locations instead at a single point near the ureter. Secondly, an abnormally dense capillary network was formed around the grafts by murine endothelial cells.

Additionally, one of the grafts showed an aberrant localization of nephron progenitor cells in the medullary region. None of the cultured non-grafted kidneys displayed any aberrant localization of cap mesenchyme, indicating that the mis-localization of nephron progenitors was caused by the grafting environment.

The majority (10/12) of glomeruli of the grafted kidneys did not contain any blood vessels of murine origin (**Figure 5-5D**) as they did not stain with a mouse specific CD31 antibody. Previous grafting experiments demonstrated that the majority of glomeruli were vascularized by cells originating from the host rather than the graft vasculature (Ekblom *et al.*, 1982; Sariola *et al.*, 1983; Sariola *et al.*, 1984a; Sariola *et al.*, 1984b). Therefore, there is a possibility that some glomeruli had been vascularised by blood vessels originating from the chick CAM. Despite multiple attempts there was no antibody found that stained chick endothelial cells with sufficient specificity, as all tested antibodies showed high background in samples of the chick CAM, making it not possible to discriminate between endothelial cells and other cell types.

It has been shown previously that haemodynamic forces caused by blood flow are essential for the maturation of blood vessels (Padget *et al.*, 2019). Injection of the host vasculature with a fluorescent labelled antibody following staining of the grafted kidneys for murine CD31 confirmed the perfusion of the graft vasculature. However, there was no indication of the formation of a smooth muscle cell lining around the graft vessels, indicating that perfusion of the graft by the host circulation is not sufficient to enhance vascular maturity. A reason for this could be differences in the haemodynamic profile of the two species. While some aspects of the circulation such as heart rate and stroke volume can be easily compared between embryonic mice and embryonic chicks (Keller *et al.*, 1996), the forces in individual blood vessels vary depending on local geometry and velocity (Zhou *et al.*, 2014) making it difficult to compare the blood flow of the embryonic kidney to the chick CAM.

Taken together these results demonstrate that the CAM grafting assay neither enabled the formation of a realistic renal vasculature nor improved vascular maturity of the existing capillary plexus. The differences between the vasculature formed in grafts to the one formed *in situ* could be caused by a variety of factors such as differenced in flow dynamics, circulating growth factors or extracellular matrix properties. These factors would be difficult to control *in ovo*.

Mammalian hosts could potentially offer a more suitable growth environment for murine and human tissues. Mice and rats have been previously used as hosts for the transplantation of embryonic kidneys and kidney organoids. Most studies agree that the transplantation into murine hosts improves the glomerular vascularization and maturity compared to *in vitro* grown organoids (Murakami *et al.*, 2019; Nam *et al.*, 2019; van den Berg *et al.*, 2018). It has also been shown that organotypic kidney organoids transplanted into murine hosts displayed expressed the arterial marker Cx40, indicating a higher degree of vascular maturity (Murakami *et al.*, 2019). This suggests that transplanting kidneys or kidney organoids into murine hosts could improve the vasculature of the graft compared to engraftment onto the chick CAM. However, it was noted that the vasculature of transplanted kidney organoids did not completely recapitulate the pattern seen in kidneys developing *in situ* (Murakami *et al.*, 2019).

Similar to *in ovo* cultures, there are several factors, such as the haemodynamic profile of the blood flow or circulating growth factors, that are difficult to control *in vivo* and could impact the forming vasculature. An *in vitro* system to vascularize kidneys and organoids would allow a tighter control over the growth environment as well as facilitate the observation of the growth and forming vasculature. A potential way of vascularizing kidneys *in vitro* would be to co-culture them with isolated perfused blood vessels. In the next chapter I will therefore focus on the optimization of the culture of perfused mouse blood vessels *in vitro* and their potential as a vascular source to improve kidney explant growth.

Chapter 6 - Establishment of an *ex vivo* perfusion culture for whole mouse blood vessels as vascular source for embryonic kidney explants

6.1 Introduction

Kidney explants display limited vascular maturation in culture. *In vivo*, vascular remodelling and maturation are largely controlled by haemodynamic factors However, the vascular maturation of kidney organoids by engraftment on the CAM was limited, despite flow being detected through the peripheral blood vessels. This could be caused by a range of factors such as unfavourable growth conditions or the lack of certain growth factors or differences in the haemodynamic profile of the species.

6.1.1 Mechanical forces regulating vascular development and remodelling

The heart of an adult mouse beats with a frequency of about 7 Hz (Kreissl *et al.*, 2006). During each heart beat, a volume of 45 µl is pushed into the arterial network (Kreissl *et al.*, 2006). While the blood moves within the blood vessels it exerts different types of mechanical strain on the endothelium – circumferential stretch perpendicular to

the direction of flow and shear stress tangential to the endothelium (Chien, 1976; Murray, 1926).

These mechanical forces play important roles during development of the vascular system. During angiogenesis, the pressure caused by flow can trigger lumen formation in angiogenic sprouts (Bazigou *et al.*, 2011). Exposure of the endothelium to linear flow reduces proliferation and induces alignment of the endothelial cells along the direction of flow (Akimoto *et al.*, 2000; Levesque and Nerem, 1985). Flow has been shown to regulate arterial and venous differentiation of the chick yolk sac vasculature (le Noble *et al.*, 2004). Additionally, local changes of the flow pattern play important roles during valve formation in the venous and lymphatic systems as well as within the heart (Bazigou *et al.*, 2011; Heckel *et al.*, 2015; Sabine *et al.*, 2012).

Shear stress and circumferential stress depend largely on vessel diameter and the velocity of blood flow (Chien, 1976; Murray, 1926). In response to high shear stress vessels tend to enlarge (Kuo *et al.*, 1990; Smiesko and Johnson, 1993). According to Bernoulli's principle (a higher velocity of a fluid results in a decreased static pressure), the increased diameter will result in a slower flow and therefore greater static pressure acting on the vessel wall and therefore increased circumferential stress (Bernoulli, 1738; Bernoulli and Flierl, 1965). The increased circumferential stress often induces a thickening of the vessel wall (Wolinsky, 1970). The sensing mechanism for mechanical stress is complex and beyond the scope of this thesis but has been recently reviewed by Fels & Kushe-Vihrog (2020).

In kidneys grown *in vivo*, differences in arterial diameter and the recruitment of smooth muscle cells to form the blood vessel wall can be observed after the onset of blood flow (Daniel *et al.*, 2018). Renal explant cultures lack blood flow and show no formation of a smooth muscle cell wall (**Figure 3-8**). Inducing a flow through renal explants by engraftment onto the CAM was not sufficient to stimulate vascular smooth muscle cell recruitment (**Figure 5-5**). One reason for this could be differences between the haemodynamic profile of the galline and murine blood flow (Keller *et*

al., 1996). A tighter control over the flow would only be possible with an *in vitro* system.

Studies with cardiac cell sheets show two possible mechanisms for implementing a perfused vascular network with a controlled flow rate *in vitro*. One possibility is to stimulate the endothelial cells in the cardiac cell sheet to form a vessel along perfused collagen channels and thereby connect the microvascular plexus to a perfusion pump (Sakaguchi *et al.*, 2013). Alternatively, the cardiac cell sheets can be grafted onto a perfused isolated vascular bed (Sekine *et al.*, 2013). After addition of endothelial cells, the microvascular plexus can connect to the perfused vessels of the vascular bed (Sekine *et al.*, 2013). A similar approach could be used to vascularize kidney organoids but requires the establishment of a perfusion culture system for blood vessels.

6.1.2 Vascular perfusion culture systems

Native and engineered blood vessels have been previously cultured under flow. In simpler systems this was done by mounting the blood vessels onto two needles which were directly connected to a pump system to create a closed loop (Lysyy *et al.*, 2020; Yamagishi *et al.*, 2014). This single loop design was extended by Zhang *et al.*, who implemented a second perfusion loop to exchange the medium in the abluminal space (Zhang *et al.*, 2009). The majority of culture systems are however based on the basic single loop design.

A more complex flow system was implemented by Surowiec et al who used a 3-chamber approach (Surowiec *et al.*, 2000). In this design the medium was aspirated from the lower reservoir chamber using a peristaltic pump and pumped into a compliance chamber to dampen the pulsations from the pump system. This may be preferred even though the blood flow is also considered pulsatile, because the frequency of the pulsations of the peristaltic pump is unlikely to match the one of the

blood flow. Peristaltic pumps also frequently display some degree of back flow, which is not present in arteries. The compliance chamber was directly connected with the growth chamber where the blood vessels was mounted onto stainless steel needles. Their system further allowed the control of the intraluminal pressure through a pinch valve which was inserted between the distal end of the blood vessel and the reservoir chamber (Surowiec *et al.*, 2000). The use of a pinch valve to control the intraluminal pressure was also implemented by Prim *et al.* (2018). However, their study did not mention the use of a compliance chamber to dampen the pulsations from the peristaltic pump (Prim *et al.*, 2018).

Peristaltic pumps are the most widely used pump system (Lysyy *et al.*, 2020; Prim *et al.*, 2018; Surowiec *et al.*, 2000). They might be preferred over other pump system because they are widely available and can deliver a large range of flow rates. Very few whole-blood vessel culture systems use different pump systems for example centrifugal pumps (Yamagishi *et al.*, 2014). Some studies use a combination of pump systems (Moore *et al.*, 1994; Webb *et al.*, 2007). Moore *et al.* combined a peristaltic pump with a diaphragm pump to create a 1 Hz pulsatile flow. Webb *et al.* used a slightly different approach to implement a flow with adjustable pulse rate. They used a peristaltic pump to aspirate the medium from a reservoir and pump it into a compliance chamber which was connected to pressurized air (Webb *et al.*, 2007). By regulating the air flow into the compliance chamber a pulsatile flow of medium was created (Webb *et al.*, 2007). A third method of creating a controlled pulsatile flow was used by Diamantourus *et al.*, who combined a centrifugal pump with a voice-coil actuator. In this system, the centrifugal pump provides a steady flow which is turned into a pulsatile flow through the actuator, a piston that presses onto a silicone membrane (Diamantouros *et al.*, 2013).

The culture system used by Diamantourus *et al.* further contained a range of monitoring devices such as oxygen and carbon dioxide sensors, a flow meter, pressure sensor and a pH meter (Diamantouros *et al.*, 2013), which makes it a rather complex and expensive system that would be challenging to replicate. Most of the

analysed studies did not monitor medium pH, oxygen and carbon dioxide concentrations, however, they did take measures to ensure gas exchange, either through including syringe filters or the use of gas-permeable materials for tubing and growth chambers (Surowiec *et al.*, 2000; Yamagishi *et al.*, 2014).

The systems described above were designed for either engineered, human or porcine blood vessels, which were larger than the blood vessels found in mice. They were also not built with the aim to induce angiogenesis and co-culture the blood vessels with other tissues. In this chapter I aim to design a perfusion system that is suitable for murine blood vessels and allows the co-culture of one or two vessels with embryonic kidneys.

6.2 Results

6.2.1 Characterization of liquid flow through an improvised bioreactor

Kidney explants cultured in 3D systems, display central necrosis and elevated levels of the hypoxia marker Hif1α (**Figure 3-6** and **Figure 3-7**). *In vivo*, oxygen and nutrients are transported into the tissue via the blood flow. *In vitro*, an efficient delivery of oxygen and nutrients may be achieved by co-culturing a tissue with perfused blood vessels, as this had been previously used to enhance the survival of 3D-grown cardiac cell sheets (Sekine *et al.*, 2013). A similar approach, the co-culture of kidneys explants with perfused blood vessels (**Figure 6-1**) could potentially enhance oxygen and nutrient delivery and thereby prevent the central necrosis.

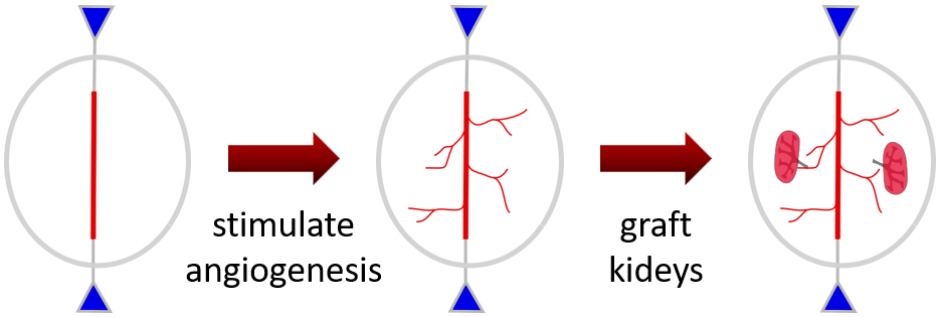

Figure 6-1: Illustration of the *in vitro* attempt to vascularize kidneys. A blood vessel is mounted on two needles (blue) which are connected to a pump system (tubing and pump not shown). The vessels are surrounded by an extracellular matrix allowing angiogenesis, such as type I collagen and overlayed with medium containing pro-angiogenic growth factors. After the blood vessels displays angiogenic sprouting, kidney explants are placed next to it so that the forming sprouts can connect with the microvascular plexus of the kidney and thereby allow flow from the perfused blood vessel through the kidney explant. The details of the experimental approach, such as flow rate and media compositions will be discussed in the following sections.

As a first step to establish a co-culture system with flow-carrying blood vessels, I focussed on the assembly of a perfusion culture system for ex-vivo blood vessels (see **2.3.1 Initial bioreactor assembly**). For this purpose, I built a series of perfusion bioreactors using the issues identified by one design to optimize the subsequent one until I found a design which was suitable for long-term use.

A long-term perfusion without excessive consumption of liquid requires a closed loop between the reservoir and culture chamber in order to recycle the used medium. Any blockage of a closed loop could result in the build-up of excessive pressure inside the blood vessel and affect its viability. Additionally, leakage from the blood vessels could disrupt the loop if the leaked medium was not redirected to the reservoir by some means. Several assembly variants were evaluated in the absence of a blood vessel, to simulate potential leakage from the vessel. The flow of liquid was visualized by adding black ink to the culture chamber and plain water to the reservoir. The experiments were performed with a flow rate of 50 µl/min, which was previously used for the perfusion culture of rat blood vessels (Sekine *et al.*, 2013). The liquid was aspirated from a reservoir holding approximately 20 ml liquid and pumped through fine bore tubing with an inner diameter of 380 µm. Glass capillaries with an inner diameter of 100 µm were connected to the fine bore tubing using epoxy glue and inserted at opposing ends into the reservoir.

When using an open reservoir, liquid was pumped into the open culture chamber. Unsurprisingly, there was no visible flow from the culture chamber back to the reservoir, which led to overflow in the culture chamber (**Figure 6-2**).

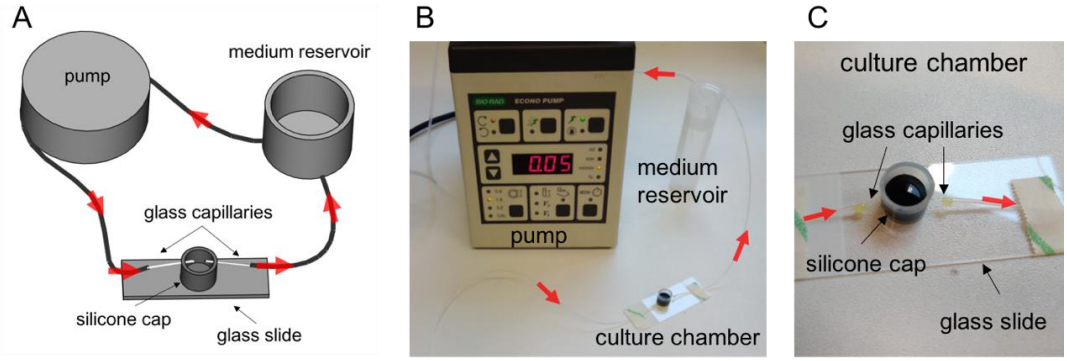

Figure 6-2: A closed loop with equal inflow and outflow cannot be generated using an open reservoir. A: illustration of the open perfusion circuit: The liquid is aspirated from an open reservoir and pumped into the culture chamber. B: image of the perfusion circuit. C: image of a culture chamber, no flow is observed from the culture chamber to the reservoir. Red arrows indicate direction of flow

Closing the reservoir initiated a short flow from the culture chamber towards the reservoir (**Figure 6-3A and B**). However, the liquid did not reach the reservoir, indicating that the aspiration of liquid from the reservoir did not sufficiently reduce the atmospheric pressure to draw back the liquid from the culture chamber. Priming, the removal of air from the outflow tubing, could potentially support the flow of liquid from the culture chamber to the reservoir, by removing air locks. Air locks can block the flow as a part or all of the kinetic energy is used to compress the air instead of moving the liquid (Jordan, 1984). To fill the outflow tubing with liquid, the pressure inside the closed reservoir was decreased below atmospheric pressure with a syringe which led to a flow from the culture vessel to the reservoir (**Figure 6-3C and D**). However, the pressure reduction was not sufficient to avoid overflowing of the culture chamber, as the amount of liquid being pumped in the culture chamber exceeded the amount of liquid returned to the reservoir. While this may not represent an issue in a closed system with a blood vessel, a partial blockage of the outflow due to high resistance in the path could lead to tissue damage as a consequence of an increased pressure within the blood vessel. Additionally, blood vessels could display leakage which would result in an overflow if the culture chamber was left open or in the build-up of pressure inside the culture chamber if it was closed and not otherwise connected to the reservoir.

Hypothesizing that the resistance of outflow tubing impedes the recycling of liquid, I next removed the outflow tubing by directly coupling the culture chamber to the medium reservoir via a glass capillary (**Figure 6-4A**). This leads to shortening of the distance between culture chamber and reservoir and therefore to reduced friction within the flow path. Additionally, the smaller inner diameter of the glass capillary (100 µm) compared to the tubing diameter (380 µm) would lead to enhanced capillary action and thereby promote the flow through the smaller capillary.

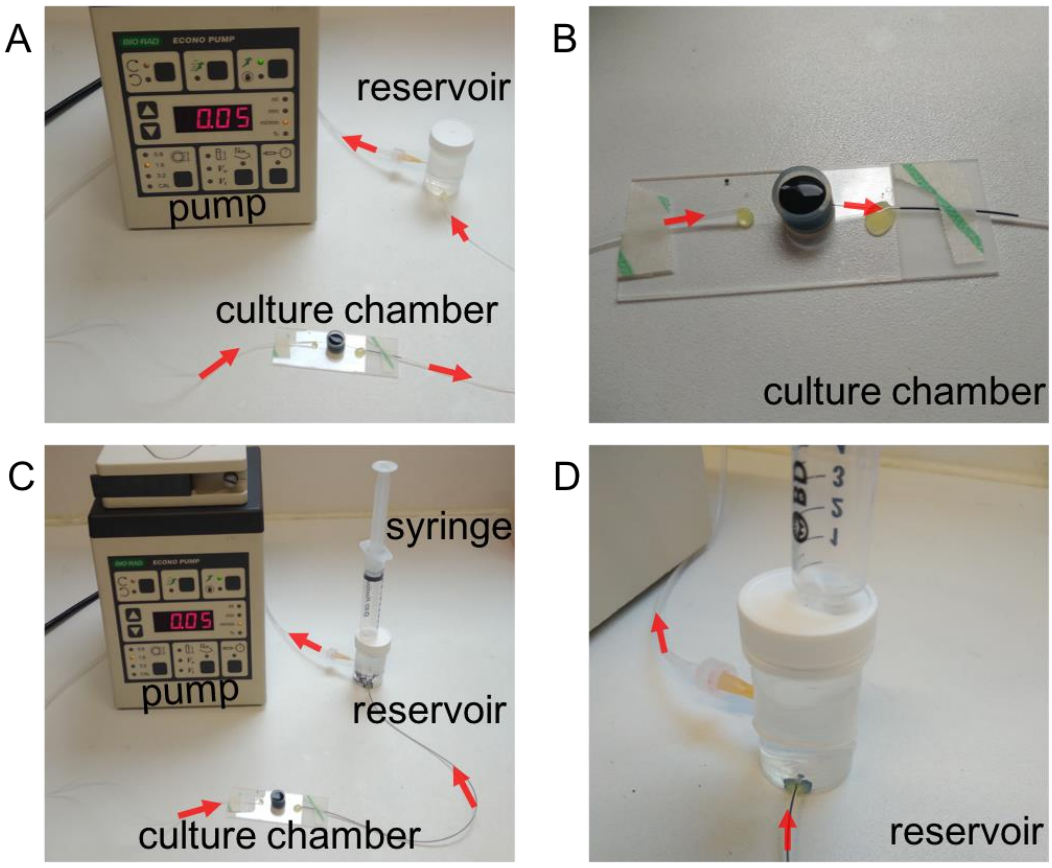

Figure 6-3: A closed reservoir in combination with pressure reduction in the reservoir enables a flow from the culture chamber to the reservoir. When the liquid is aspirated from a closed reservoir and pumped into the culture chamber (A) there is no complete recycling flow between the culture chamber and the reservoir (B). When reducing the pressure inside the reservoir using a syringe (C) a flow from the culture chamber to the reservoir is observed (D).

No flow was visible after directly connecting the culture chamber and medium reservoir with a glass capillary when using a closed reservoir (**Figure 6-4B**). However, after applying a partial vacuum in the reservoir using a syringe, a flow of liquid from the culture chamber to the reservoir was visible (**Figure 6-4C**). After removal of the outflow tubing the syringe only had to be aspirated to a volume of about 3 ml while with the outflow tubing the syringe had to be aspirated to 10 ml in order to drive the flow from the culture chamber back to the reservoir. This indicates that the required aspiration force was lower after removal of the outflow tubing.

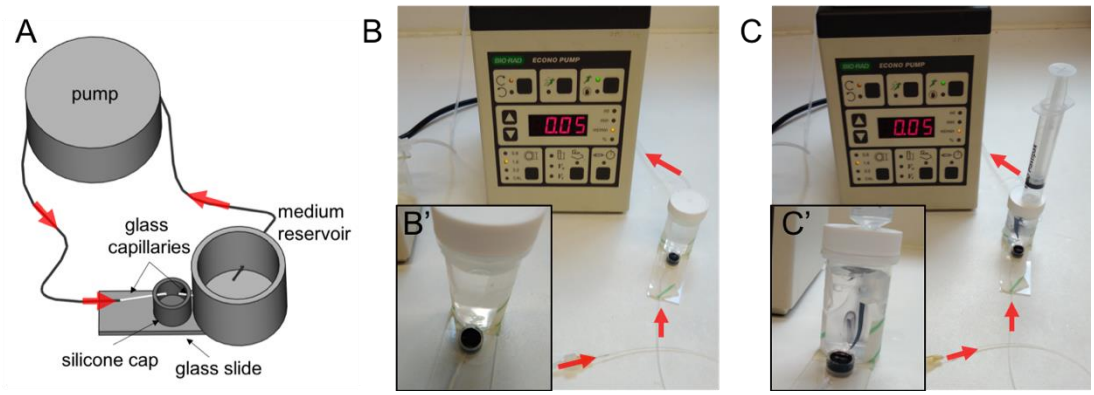

Figure 6-4: Removal of the outflow tubing is not sufficient to enable the flow from the culture vessel to the reservoir. When the liquid is aspirated from a closed reservoir and pumped into a culture chamber directly linked to the reservoir with a capillary (A) no flow between the culture vessel and the reservoir is observed (B and B'). After reducing the pressure inside the reservoir using a syringe (C), a flow from the culture vessel into the reservoir is visible (C'). Red arrows indicate direction of flow. The above results indicate that controlling the pressure inside the reservoir is critical to drive a flow from the culture chamber back to the reservoir. Further it has been shown that a short distance between the culture chamber and the reservoir limited the risk of overflow in the culture chamber.

6.2.2 Initial bioreactor design

Based on these observations, a customized bioreactor (**Figure 6-5**) was designed using "FreeCAD" software (Riegel *et al.*, 2001) and was then 3D printed by the School of Engineering. The bioreactor contained two circular culture chambers and a shared reservoir. A channel was drilled through the culture chambers, connecting them to the reservoir. Within this channel, MicroFil needles were mounted for attaching the blood vessels. The MicroFil needles replaced the glass capillaries used in earlier experiments as they were more flexible and unlikely to break during mounting of the blood vessels. Both culture chambers were designed to be expanded with a cylinder that could be screwed on top of the chamber. The expandable culture chamber design was chosen to facilitate the attachment of the blood vessels as the perfusion needles can be inserted near the top of the lower chamber while the upper chamber part would provide the necessary room to add medium on top of the blood vessels.

The reservoir would hold a volume of approximately 15 ml. The lid of the reservoir contained two ports, one for measuring the pressure inside the reservoir and the other one for applying a vacuum either with a syringe or a pump.

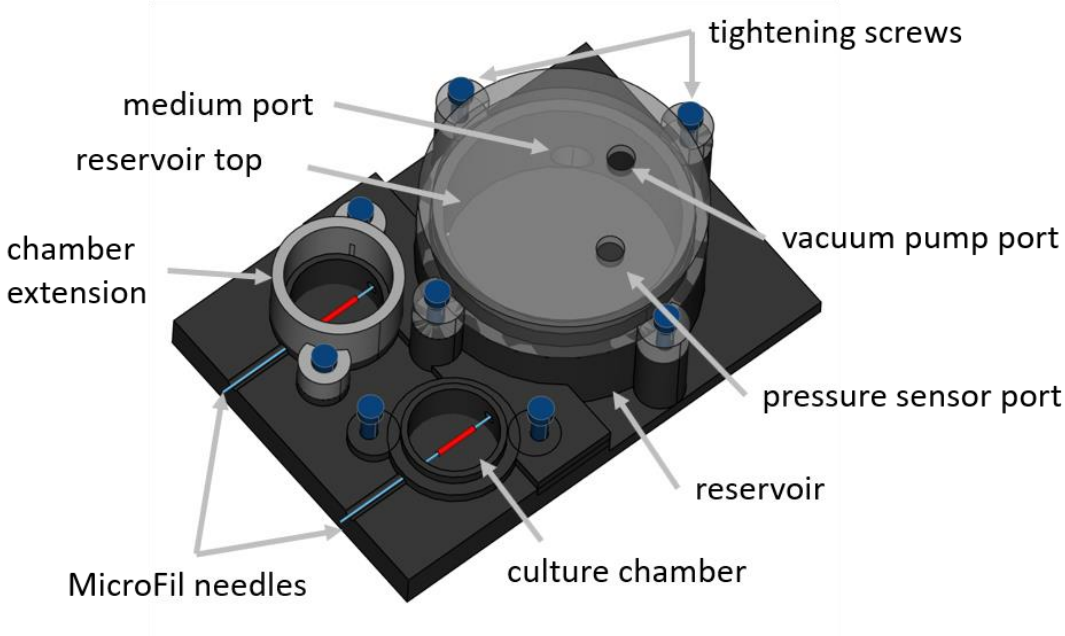

Figure 6-5: initial bioreactor design. The medium is aspirated from a reservoir and pumped into the culture chambers via a MicroFil needle (light blue). A second MicroFil needle connects the culture chambers to the reservoir. A blood vessel (red) can be mounted on both capillary tubes. The culture chambers can be extended vertically to allow the addition of medium on top of the mounted blood vessels. The chamber extension as well as the top of the reservoir can be sealed with an O-ring (not shown) and several screws (dark blue).

6.2.5 3D printed bioreactor is too porous for long term perfusion

While the 3D print could be used for short-term perfusion, the material appeared to be very porous, resulting in diffusion of the medium inside the reactor walls (**Figure 6-6A**). In order to smoothen the surface, the 3D print was incubated in an acetone vapour chamber for several hours to melt the surface and close the pores (Garg *et al.*, 2015). After acetone treatment, the surface was visibly smoother (**Figure 6-6B**) but the overall shape of the print was affected and diffusion of the liquid in the material was still observed during subsequent use.

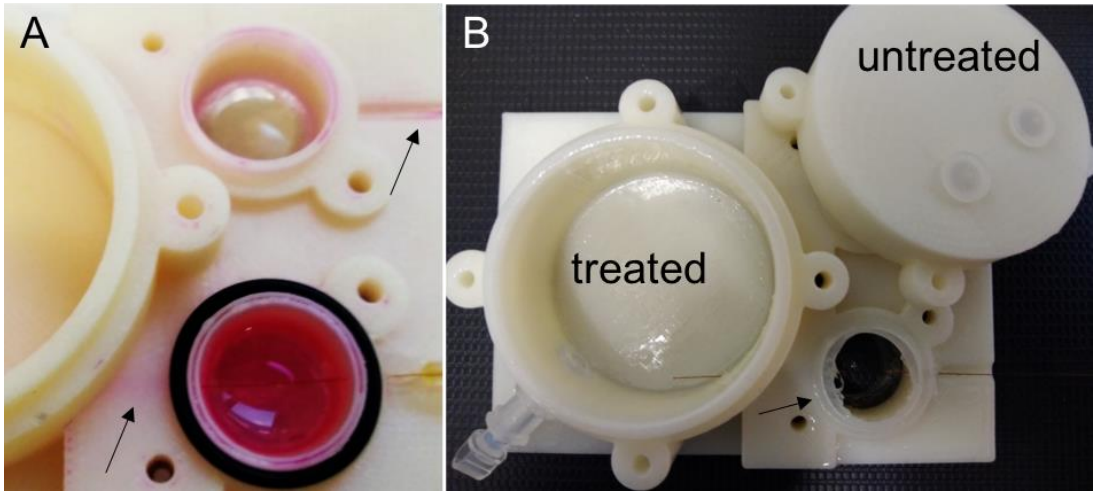

Figure 6-6: The material of the 3D-printed bioreactor is highly porous. A: The medium was soaking into 3D-printed material (indicated by arrows). B: untreated and acetone treated material. Prior to acetone treatment the surface appears coarse. After incubation in acetone vapour the surface appears smooth and reflective. Arrow indicates damage caused by acetone treatment.

6.2.3 Single channel acrylic bioreactor

Due to the porosity of the 3D-printed bioreactor, a second bioreactor was manufactured from acrylic by computer numerical control (CNC) cutting. Prior to manufacturing of the second bioreactor the initial design was revised. Similar to the previous model this design contained two culture chambers connected to a single shared reservoir. Each chamber contained a single channel to mount the perfusion needles, hence one vessel can be cultured per chamber (**Figure 6-7**).

Measurement of the perfusion pressure appeared to be imprecise due to the Bernoulli effect - a reduction of the static pressure (the feature that was measured), due to an increase of the velocity, which could not be measured with the sensor type used. Therefore, the port for the pressure sensor was removed and instead an overflow channel that connected the chamber extension with the reservoir was inserted, to direct any potential leakage from the mounted blood vessel back to the reservoir. Further a tubing holder was included to prevent stretching of the vessels during movement of the bioreactor.

Since acrylic is sensitive to ethanol, the reactor was sterilized by soaking in 5% hydrogen peroxide. However, the peroxide treatment induced rapid corrosion of brass inserts and connecting screws.

During subsequent use, I also noticed that the design with two culture chambers connected to a shared reservoir was impractical for several reasons. Firstly, in case of a contamination occurring within one culture chamber it would spread to the second chamber. Secondly, the two blood vessels would have to be mounted on the same day as otherwise the second culture chamber would have to be sealed in order to prevent medium from leaking out and could therefore not be used.

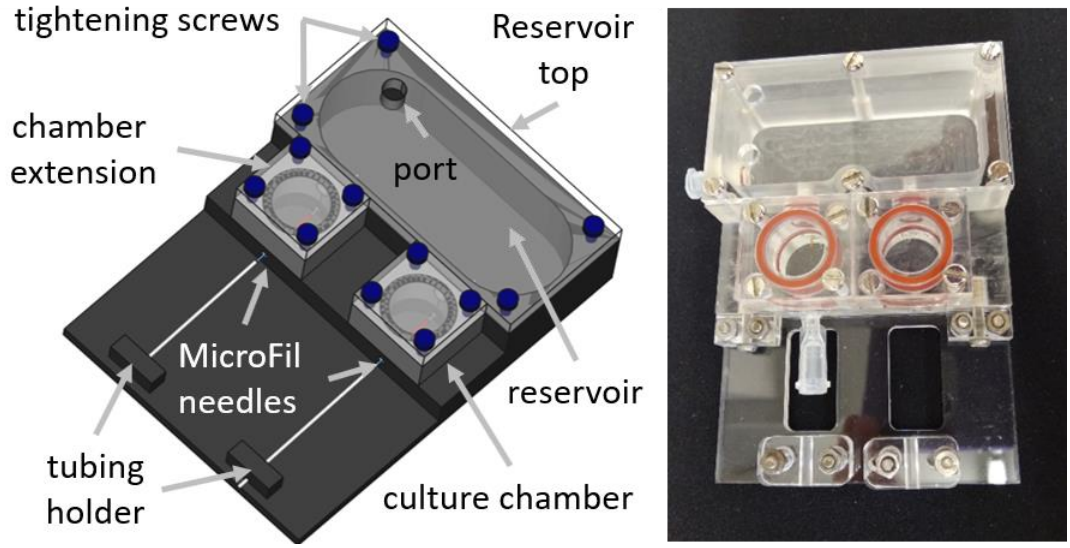

Figure 6-7: single channel perfusion reactor.. This perfusion bioreactor contained two culture chambers connected to a shared reservoir. A channel was drilled through each chamber to allow the insertion of MicroFil needles, which were used to mount one blood vessel in each chamber. After mounting of the blood vessel an extension piece can be screwed on top of each culture chamber. This chamber extension allows room to add culture medium on top the blood vessel. It was designed removable to facilitate the mounting of the blood vessel. The culture chambers and reservoir can be sealed air-tight with a lid and silicone gasket. The front of the bioreactor contained two tubing holders where the tubing connected to the MicroFil needles was fixed in place to prevent any movement of the needles during handling of the bioreactor.

6.2.4 Dual channel polycarbonate bioreactor

As the two-chamber design appeared impractical during use, the design was revised to have a single growth chamber connected to a reservoir (**Figure 6-8A**). This modification also resulted in a smaller reservoir leading to a reduced medium consumption and overall smaller size of the bioreactor, which meant that less material needed for each individual bioreactor. As a consequence, two single-chamber bioreactors could be run individually using nearly the same resources as one dual chamber bioreactor. By using several bioreactors in parallel the risk of cross-contamination was eliminated. To further reduce the contamination risk, the bioreactor material was changed to polycarbonate, which is easier to sterilize than

acrylic. Polycarbonate was considered more suitable due to its heat stability which allows sterilization by autoclaving, its resistance to ethanol and higher CO_2 permeability. Repeated autoclaving had no visible effect on the material. Polycarbonate was chosen over more heat-stable materials, such as polysulfone, due to its higher clarity (**Figure 6-8B**). In order to enable the perfusion of 2 vessels, an artery and a vein, within the same chamber, the revised design contained two channels running parallel 1 mm apart.

During parallel perfusion of two blood vessels, the liquid was aspirated from the reservoir and pumped through the blood vessels mounted in the culture chamber back into the reservoir (**Figure 6-8C**). The two-channel design still allowed the perfusion of one individual blood vessel as the second channel could be sealed with silicone glue.

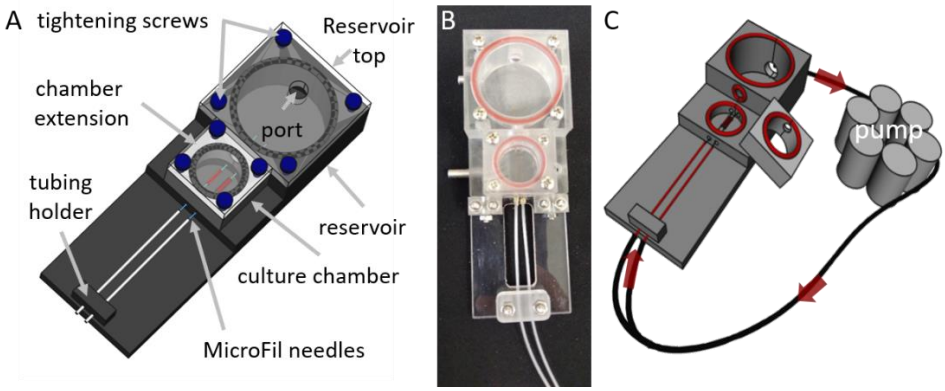

Figure 6-8: double channel perfusion reactor. A: Draft of the bioreactor. This design contained a single culture chamber connected to a reservoir. Two channels were drilled parallelly leading through the culture chamber into the reservoir. Microfil needles were inserted into the channels for mounting the blood vessels into the culture chamber. A chamber extension was screwed on top of the culture chamber to allow room for adding culture medium. The chamber extension and reservoir were connected with a channel that allowed in case of leakage from the blood vessel to redirect medium back from the chamber extension into the reservoir. A lid and silicone gask*et al*lowed an air-tight seal of the culture chamber and reservoir. The front of the bioreactor contained a tubing holder were the tubing connected to the MicroFil needles was fixed in place to prevent any movement of the needles during handling of the bioreactor. B: manufactured bioreactor. C: Parallel perfusion of two blood vessels. The arrows indicate the direction of flow from the reservoir through the blood vessels back into the reservoir.

6.2.5 Comparison of pump systems for the culture of embryonic aortas

For initial flow characterization experiments, the "Econo" peristaltic pump from Biorad was used as one was already present in the laboratory. This pump was replaced with the peristaltic pump "Minipulse 3" from Gilson which, in contrast to the Econo pump, allowed simultaneous perfusion of up to eight cultures by vertical staggering of up to 8 tubes. Peristaltic pumps move the liquid by squeezing a tube with a circulating wheel. This results in a pulsatile flow. The disadvantages of the system are that there is a certain degree of backflow and that the flow rate can be difficult to adjust as it will depend on how tightly the tube is compressed.

As an alternative to the peristaltic pump several piezoelectric pumps were purchased. A piezoelectric pump is a form of diaphragm pump. Two ports, one entry and one exit port, are covered via membrane. The membrane is induced to swing away from the ports by an electric current, resulting in the liquid being drawn into the pump. When the membrane swings back, the liquid is pushed out of the exit port. The extent to which the membrane bends, and therefore the volume of liquid transferred per pulse, is controlled via the amplitude of the electric current, while the interval between pulses is controlled by the frequency. This allows production of a pulsatile flow with high frequency and low stroke volumes. In theory these pumps can closely mimic the blood flow of a mouse with a frequency of about 7 Hz and low stroke volume of 45 µl (Kreissl *et al.*, 2006).

To see the effect of flow on the *in vitro* growth of embryonic blood vessels, E14.5 aortas were isolated and either cultured in the absence of flow or mounted in a perfusion reactor, which was connected to either of the pump systems (see **2.3.7 Perfusion culture of blood vessels**). E14.5 blood vessels were considered a suitable age for this experiment for several reasons. Firstly, they would have already formed a thin smooth muscle cell lining and would therefore be less fragile than younger vessels. Secondly, E14.5 marks the age when a permanent connection between the kidney and the dorsal aorta is formed *in vivo* (Hurtado *et al.*, 2015; Nishimura *et al.*,

2016) therefore using this age would mimic the *in vivo* situation as close as possible. The vessels were attached to the MicroFil needles by suturing them with a double surgical tie. After 3 days of culture in the presence of the proangiogenic factors identified in section (**6.2.13 Sprouting of perfused blood vessels in different media)**, the blood vessels were imaged using a Leica MSV269 microscope. Dr. Vrushali Patil kindly evaluated the sprouting of cultured blood vessels in blind-coded samples using a scale ranging from 0 (no sprouting) to 3 (extensive sprouting).

Embryonic (E14.5) aortas showed visible morphological differences when cultured unperfused or with either of the pump systems. In all (4/4) unperfused aortas, the lumen collapsed and was no longer visible. In response to proangiogenic treatment the unperfused vessels showed extensive sprouting which was rated with a score of 3.0 (**Figure 6-9A**).

When flow was induced by a piezoelectric pump, driven by a potential of 170 V peak to peak/60 V root mean square (V_{rms}) at 10 Hz, the lumen was small but clearly visible in 2 out of 4 samples. Regrettably, I did not determine the flow rate at the time I conducted this experiment and due to rapid wear of the piezoelectric pump as well as its sensitivity to minor changes in the flow path, such as different lumen diameters of the blood vessels, measurements taken at later experiments cannot be used to estimate the flow rate of earlier ones. Sprouting was substantially reduced compared to unperfused aortas and scored with 1.75 (**Figure 6-9B**).

In all (3/3) aortas perfused with the peristaltic pump at a setting of about 10 µl per minute, the lumen remained open and the vascular wall appeared more defined. However, within the perfused section of the blood vessel the response to proangiogenic stimulation was rated 1.0 and very limited compared to unperfused aortas or aortas perfused with piezoelectric pumps (**Figure 6-9C**).

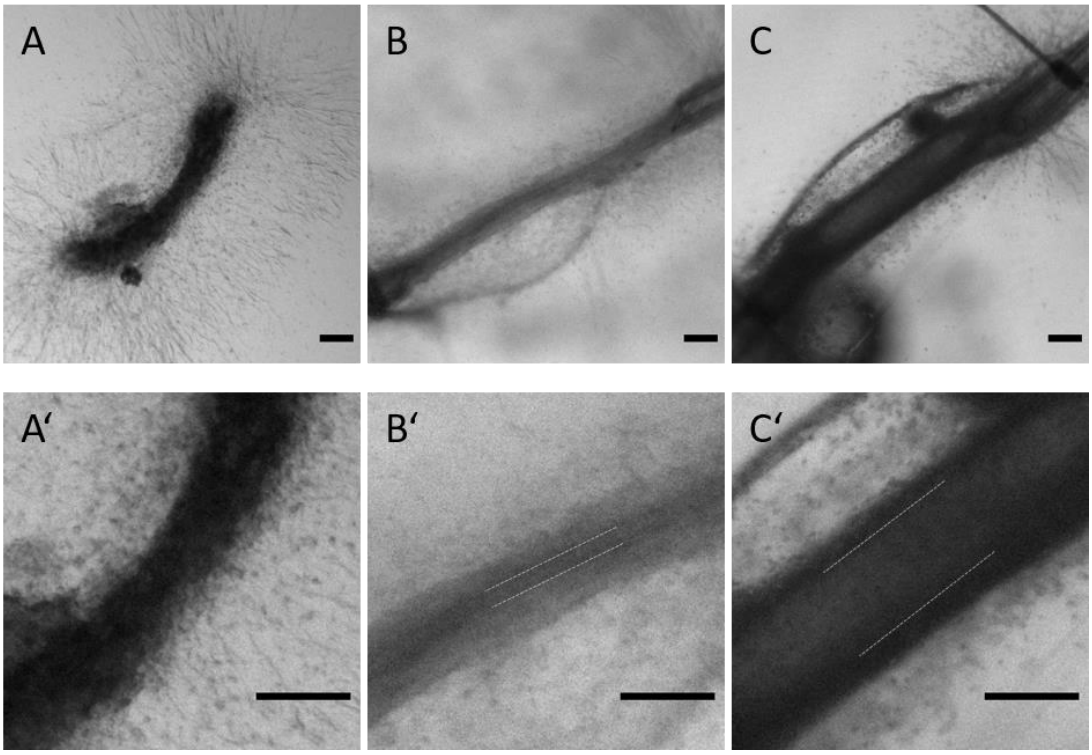

Figure 6-9: Unperfused and perfused E14.5 aortas after 3 days of culture. A, A’: unperfused aorta showing intensive sprouting but no visible lumen. B, B’: aorta perfused with piezoelectric pump displayed reduced sprouting and a visible lumen (highlighted as dashed line in B’). C, C’: Aorta perfused with peristaltic pump had a larger lumen (highlighted with dashed line in C’) but sprouting within the perfused section of the vessel was vastly reduced. Scale bars 200 µm, N = 3

6.2.6 Characterization of flow provided by piezoelectric pumps

Dorsal aortas perfused with piezoelectric pumps showed a good compromise between sprouting and lumen maintenance. Therefore, I wanted to determine the properties of the flow provided by piezoelectric pumps.

Firstly, I measured the relationship between voltage frequency and output pressure. At frequencies between 10 HZ to 30 Hz the output pressure increased proportionally to the voltage reaching 120 mmHg at 60 V_{rms} (**Figure 6-10A**).

To measure the flow rate, I intended to use a flow rate sensor, but this turned out to be not suitable due to the pulsation of the flow (**Figure 6-10B**). However, the flow

rate sensor could be used to visualize the backflow as this showed up as negative flow rates (**Figure 6-10B-E**, highlighted in red).

While backflow plays important roles in heart and lymphatic valve development (Heckel *et al.*, 2015; Sabine *et al.*, 2012), it does not usually occur in arteries and therefore may induce unwanted cell behaviour. To prevent the backflow, I ordered two different types of check valves. Type 1, a check valve with silicone diaphragm, had a minor reducing effect on the backflow (**Figure 6-10C**)

Type 2, an in-line check valve, nearly eliminated the backflow (**Figure 6-10D**) but also greatly reduced the flow rate which was visible after adjusting the y-axis (**Figure 6-10E**). To determine how large the effect of the valves on the flow rate was, I ran the same pump three times with each valve and determined the volume using a precision scale. The type 1 valve slightly reduced the flow rate from 140 µl/min to 110 µl/min. When using the type 2 valve the flow rate with the same settings was only 3 µl/min. (**Figure 6-10F**) I concluded that neither valve was suitable to effectively reduce backflow and permit a sufficient flow rate.

Since the sensor could not be used to determine the flow rate, I measured the volume after 10 minutes of perfusion using a measuring cylinder. While the flow rate increased with higher voltage, its relationship with the voltage was less linear than the one between the output pressure and voltage (**Figure 6-10G**).

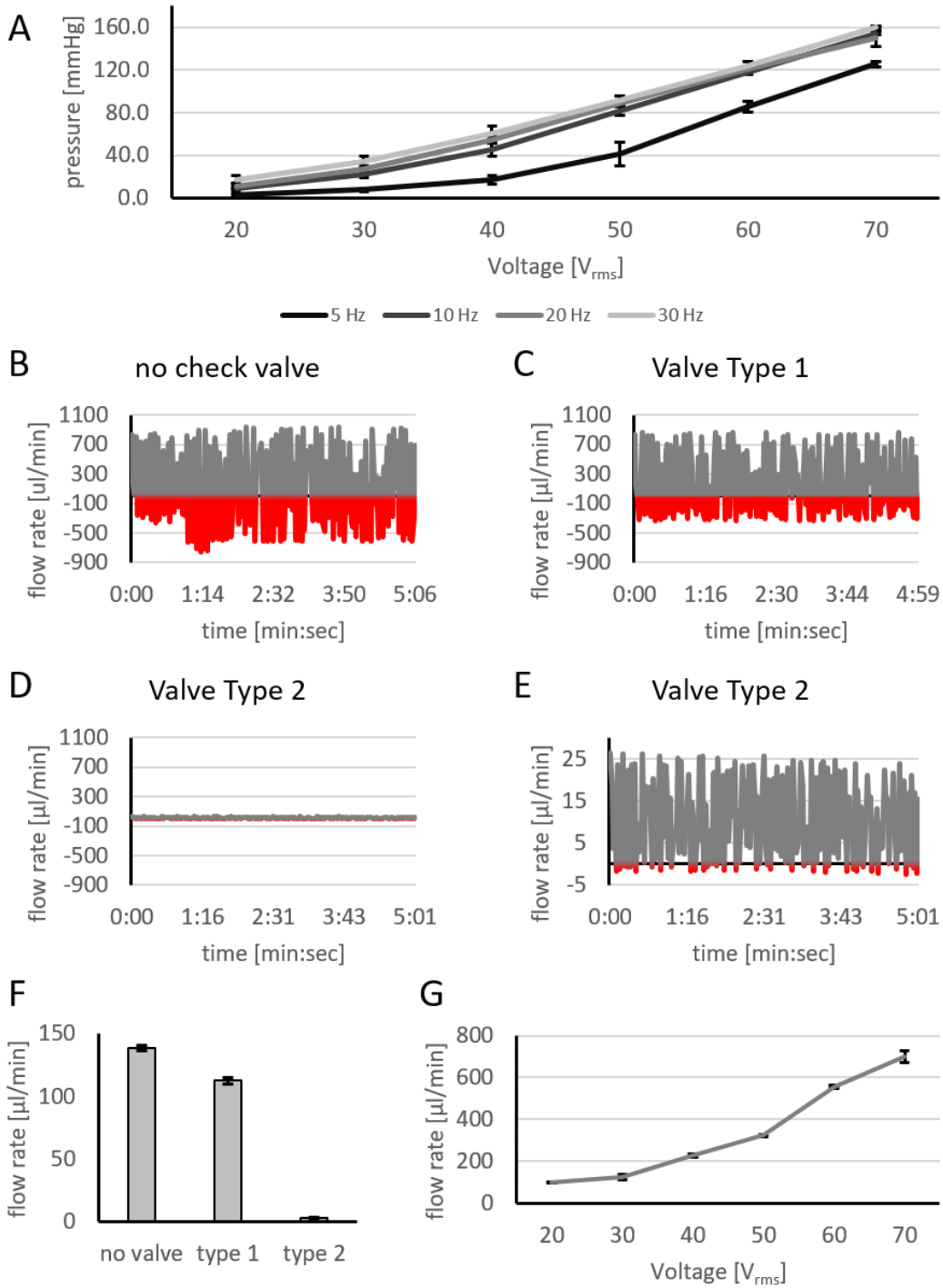

Figure 6-10: Characterization of flow pattern derived from piezoelectric pump. A: relationship between frequency, rms voltage, and output pressure. B-E. Measurement of flow rate using a sensor in absence (B) or presence of either a type 1 (C) or type 2 (D-E) check valve. F: Measurement of the flow rate without and with either check valve using a precision scale. G: Correlation between voltage and flow rate. All measurements were taken in triplicates. Error bars display standard deviation.

6.2.7 Co-culture of embryonic blood vessels with embryonic kidney explants

An initial co-culture experiment (N=1) combining the embryonic aorta and an E11.5 kidney showed sprouting blood vessels connecting the kidney and the aorta which appeared to form a connection (**Figure 6-11A**).

In an attempt to increase the number of connections forming, several changes to the culture conditions were made. Firstly, the medium was supplemented with higher concentrations of VEGF (50 ng/ml) and FGF2 (50 ng/ml) and additional proangiogenic growth factors (PDGF, S1P and PMA). The medium composition was identified as suitable in perfusion experiments executed in parallel with adult blood vessels (see **6.2.13 Sprouting of perfused blood vessels in different media**)

The peristaltic pump was replaced with a piezoelectric pump because previous experiments showed that aortas would sprout more when perfused with a piezoelectric pump (**Figure 6-9**).

Lastly, the voltage was adjusted for the first 3 days of culture to produce an increasing output pressure between 30 mmHg to 50 mmHg, mimicking the increasing blood pressure that would occur *in vivo*. An increasing pressure was chosen because the vascular blood pressure increases over time (Le *et al.*, 2012). The pressure values were higher than those determined for late embryonic development by Kovacs *et al.* because no flow was visible at a lower setting.

On day 3 of culture, an embryonic kidney was added next to the perfused aorta and both tissues were co-cultured for two additional days. After the culture period, a dense network of cells was seen between the kidney and the aorta; a subset of these cells stained positive for Isolectin B4, indicating the presence of endothelial cells or macrophages (Munro *et al.*, 2019). Due to the density of the network, it was difficult to identify individual vessel-like structures. Therefore, it is not clear whether a connection between the kidney and the vessel was formed. One way of detecting a

connection between the vessel and the kidney would be to perfuse the vessel with a dye. However, due to the leakiness of embryonic blood vessels (**Figure 6-11C**) this would not have resulted in a conclusive result as there would be no proof of whether the dye reached the kidney via the blood vessel or was leaking out of the blood vessel to be taken up by the kidney from the surrounding medium.

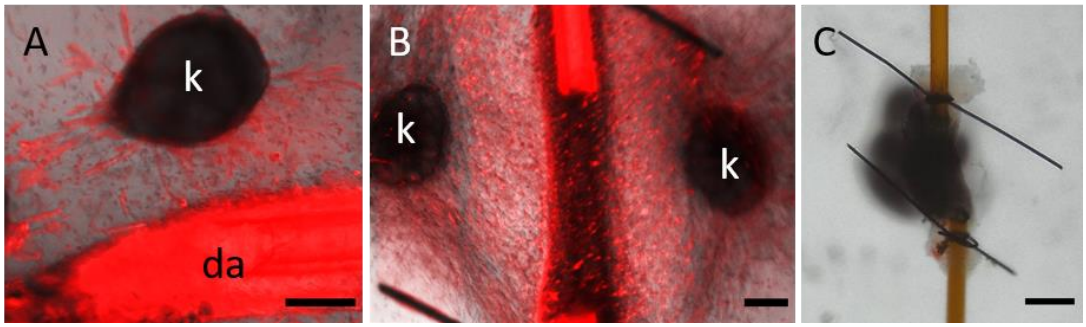

Figure 6-11: Co-culture of embryonic aorta with embryonic kidney. A: An E14.5 dorsal aorta (da) was perfused using a piezoelectric pump and cultured in presence of 20 ng/ml VEGF and 5 ng/ml FGF2. After 24h of co-culture with a kidney explant (k) a connection was formed between the embryonic kidney and the aorta. Staining with Isolectin B4 (red) indicated that the connecting cells are endothelial cells. Scale bar: 200 µm B: An E14.5 aorta was perfused using a piezoelectric pump and cultured in presence of VEGF (50 ng/ml), FGF2 (50 ng/ml), PDGF (50 ng/ml), S1P (1 mM) and PMA (2 µg/ml). The aorta was cultured for 3 days with increasing pressure (30 mmHg on day 1, 40 mmHg on day 2 and 50 mmHg on day 3) prior to addition of E11.5 kidney explants (k). After 2 days of co-culture a dense network of sprouting cells was visible between the kidneys and the aorta. A large proportion of cells stained positive for Isolectin B4 (red) Scale bar: 200 µm C: Perfusion of embryonic aorta with black ink reveals leakage. Scale bar: 500 µm.

The voltage setting required to reach the desired output pressure varied between pumps (**Figure A 7**) as well as between different repeats using the same pump, indicating a rapid decline of the functionality of piezoelectric pumps. Therefore, all further experiment were executed using the “Minipulse 3” peristaltic pump

6.2.8 Assessment of vascular leakage in adult aortas

Determining whether there is flow between the kidney and the co-cultured blood vessel is critical in evaluating the success of the co-culture system in terms of vascularizing kidneys and promoting 3D growth. The largest vessel in the embryo is the dorsal aorta. However, the embryonic aorta had many site branches that were too small to ligate at the age used (E14.5) and a less defined smooth muscle cell layer which made it more difficult to isolate it without causing damage. As a consequence, all embryonic aortas examined showed visible leakage. In contrast adult blood vessels have a mature vessel wall and major blood vessels such as the aorta have visible side branches. Therefore, I considered adult blood vessels would be less likely to display leakage. To facilitate the identification of leakage, I perfused the adult blood vessels with 50 % black ink in PBS. Leakage of the adult aorta was observed in 1/3 samples (**Figure 6-12**), and most likely caused by damaging the blood vessel during the isolation from the mouse.

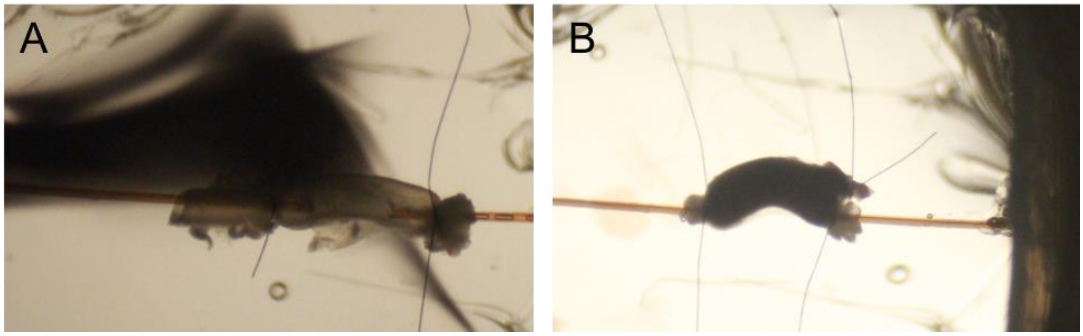

Figure 6-12: leakage recording of the abdominal aorta. The blood vessels were fixed to MicroFil needles using size 10 suture and perfused with 50% black ink at a flow rate of 50 µl/min. A: Detection of vascular leakage by perfusion with 50% ink. B: A subset of samples showed no visible leakage within 30 min of perfusion

6.2.9 Characterization of in vitro *angiogenic potential of adult murine blood vessels*

In contrast to embryonic aortas, adult ones rarely showed leakage, which is beneficial for co-culture experiments with kidneys as it allows flow through potentially forming connections to be visualized. The formation of connecting sprouting vessels would require the perfused blood vessel to undergo angiogenesis. To identify the response of adult mouse blood vessels to proangiogenic stimulation, I isolated several blood vessels and compared them in terms of their ability to sprout *in vitro* (hereafter referred to as "angiogenic capacity").

In order to reduce the number of animals used, the vessels were isolated from mid-pregnant mice (P12 +/- 0.75), as their embryos were required for other experiments. After embedding in 1 mg/ml type 1 collagen, the blood vessels were cultured for 7 days in kidney culture medium (KCM) supplemented with 20 ng/ml VEGF and 5 ng/ml FGF2 which had been shown to induce angiogenesis in an aortic ring assay (Rohan *et al.*, 2000; Zhu *et al.*, 2003).

After 7 days of culture, the blood vessels were imaged (**Figure 6-13**) and sprouting was scored on a scale from 0 (no sprouting) to 3 (extensive sprouting). Among the arteries the aorta showed the highest sprouting with an average score of 2.2 (N = 13). The femoral and uterine arteries showed a considerably lower sprouting with average scores of 0.2 (N = 12) and 0.6 (N = 15) respectively. Due to the much lower sprouting compared to the aorta, the uterine and femoral arteries were excluded from further analysis.

Of the analysed veins the femoral vein showed the lowest angiogenic capacity with a score of 0.4 (N = 10). The uterine vein and vena cava displayed a high angiogenic capacity with sprouting scores of 2.9 (N = 15) and 2.5 (N =13) respectively.

All blood vessels were isolated from mid-pregnant mice as their embryos were needed for other experiments. To identify whether the high angiogenic capacity of

the uterine vein was caused by the pregnancy, I next determined whether the sprouting of blood vessels from non-pregnant females was comparable to those of blood vessels isolated from pregnant mice.

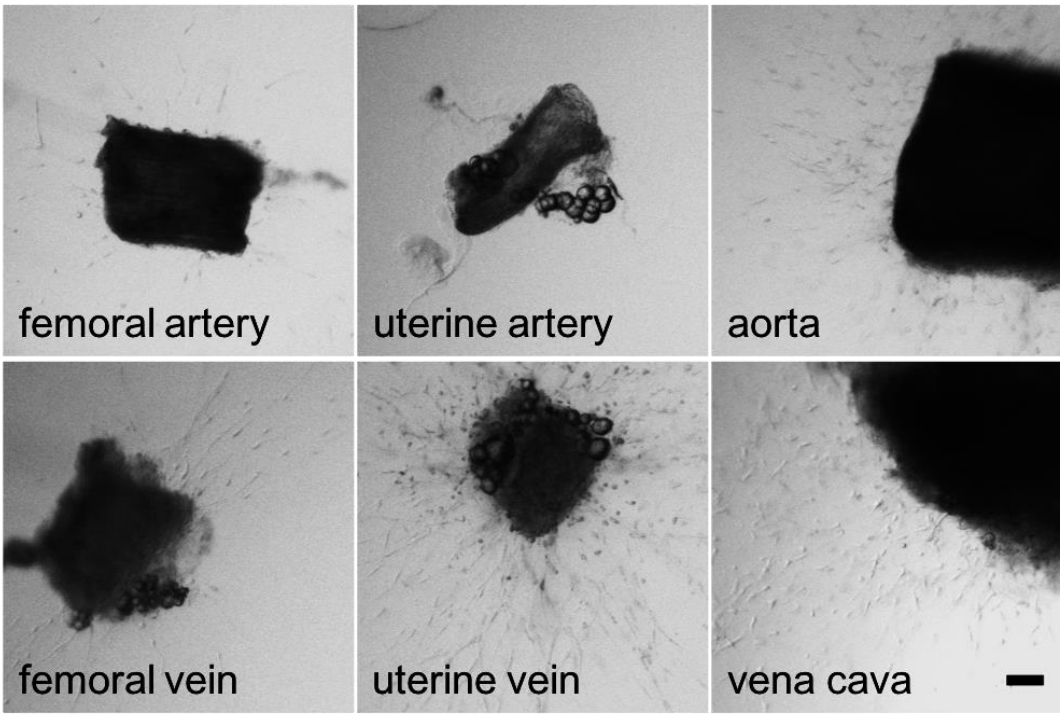

Figure 6-13: comparison of *in vitro* angiogenesis of different blood vesselsfrom midterm pregnant CD1. After 7 days of culture sprouting is observed in cultured aortic rings as well as all cultured veins (data from 3 independent experiments with a minimum of 3 rings per vessel). Scale bar 100 μm.

6.2.10 Pregnancy leads to enhanced in vitro *angiogenesis of the uterine vein but not aorta*

While using blood vessels from pregnant females is convenient for vascularising embryonic organs, the use of non-pregnant mice as a vascular source may seem more suited when no embryos are needed. To evaluate whether the blood vessels from non-pregnant mice show the same angiogenic capacity, I next isolated blood vessels from pregnant and non-pregnant littermates.

Aortas isolated from pregnant (N = 3) as well as non-pregnant females (N = 3) showed a consistently reduced sprouting compared to previous experiments, with no visible difference caused by the state of pregnancy (**Figure 6-14**). The difference to earlier experiments might have been caused by batch-to-batch variability in the activity of VEGF and FGF2 which were used to induce angiogenesis.

After 5 days of culture sprouting was observed in the uterine vein of pregnant but not of non-pregnant mice (**Figure 6-14A**). After 7 days of culture, no sprouts were observed in the uterine vein of non-pregnant females while the uterine veins of pregnant females showed extensive sprouting (**Figure 6-14B**). Additionally, the uterine vein was difficult to isolate and often got visibly damaged during the process. Due to the dependency on pregnancy for the uterine veins to undergo sprouting *in vitro*, which would inconvenient when no embryonic tissue was needed, and the difficulty isolating them, I decided not to proceed with this blood vessel.

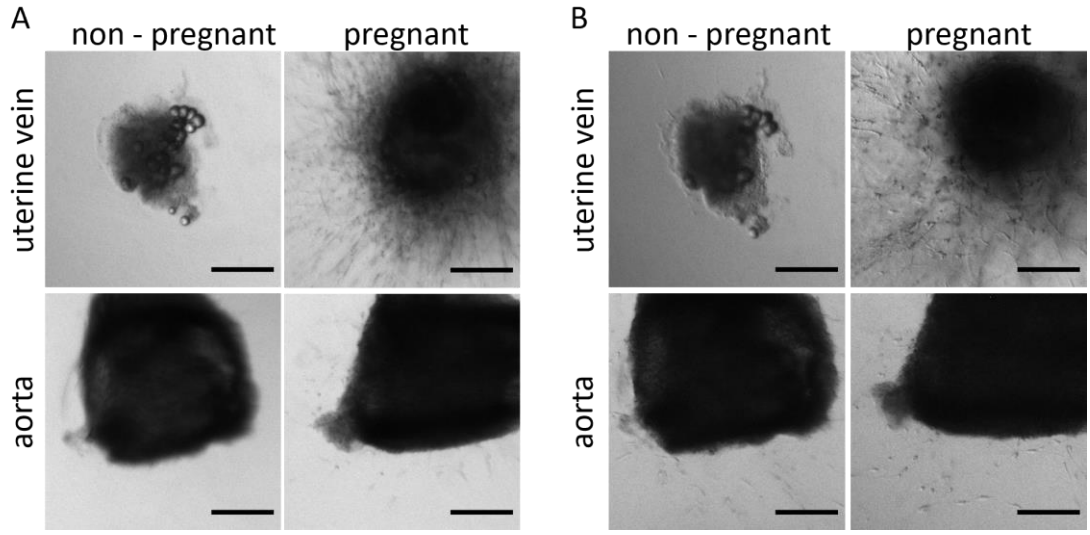

Figure 6-14: *in vitro* angiogenesis of blood vessels from pregnant and non-pregnant mice. A: after 5 days of culture the uterine vein of pregnant mice shows angiogenesis. B: After 7 days of culture extensive sprouting is observed in uterine vein cultures of pregnant but not non-pregnant mice. The aorta showed little sprouting in cultures of pregnant as well as non-pregnant mice. Scale bars: 200 µm. Data from 3 independent experiments.

6.2.11 Evaluation of sprouting capacity of individual perfused aortas

Previous experiments showed that adult mouse aortas can be perfused without displaying major leakage (**Figure 6-12**) and respond to proangiogenic stimulation when cultured without flow (**Figure 6-14**). To see whether the perfusion of aortas had an effect on angiogenesis, I mounted two aortas within the same culture chamber. One of the blood vessels was perfused with a rate of approximately 50 ul/min while the other blood vessel was cultured without perfusion. Angiogenesis was stimulated by supplementing the medium in the culture chamber with VEGF (20 ng/ml) and FGF2 (5 ng/ml) (Rohan *et al.*, 2000; Zhu *et al.*, 2003). After 8 days few sprouting blood vessels were visible around both blood vessels. The perfusion had no visible effect on the angiogenic response (**Figure 6-15**). Minor differences could not be detected because the imaging quality within the chamber was insufficient to perform a quantification of forming sprouts and removal of the blood vessels from the chamber caused damage to the sprouting vessels.

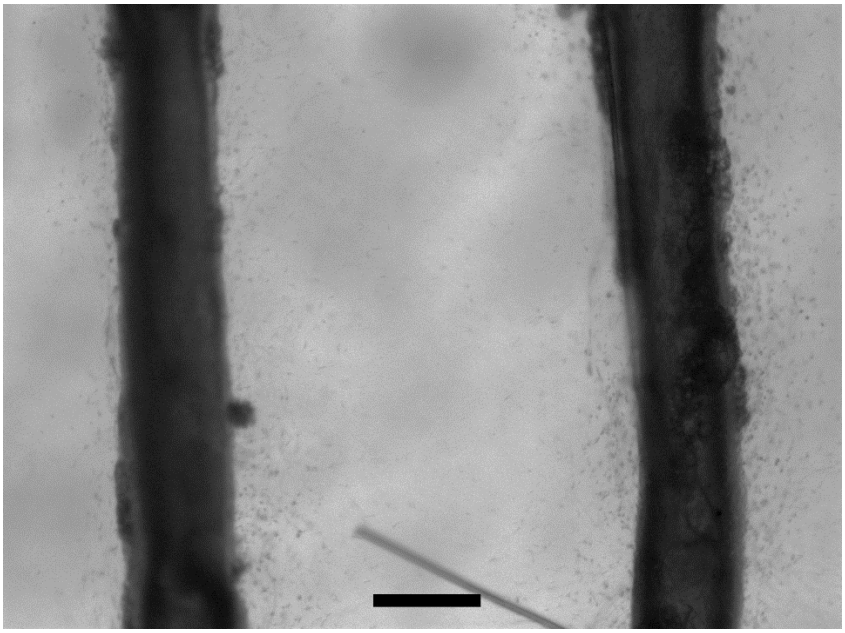

Figure 6-15: Perfusion had not visible effect on angiogenic sprouting. Culture of an unperfused (left) and perfused (right) aorta for 8 days. Scale bar 500 um, N = 3

6.2.12 antiparallel perfusion of aorta and vena cava

The previous experiments showed that adult aortas can be perfused without exhibiting major leakage and are able to respond to proangiogenic stimulation, which is essential for forming a perfused capillary bed. However, to obtain a closed loop it is likely that two blood vessels, for example an artery and a vein, would be required to sufficiently mimic the *in vivo* situation. The two-channel bioreactor can be used to mount two blood vessels. However, *in vivo*, the flow through arteries and veins goes in the opposite direction. To mimic the antiparallel flow through both blood vessels, some modifications had to be made. Firstly, a secondary reservoir was introduced. From this secondary reservoir the liquid was aspirated and through the first blood vessel, the aorta, into the main reservoir. Due to the airtight seal of the main reservoir, the pressure rises and drives the liquid back through the second blood vessel, the vena cava, into the secondary reservoir (**Figure 6-16**). The antiparallel perfusion also required sealing of the overflow channel to ensure that a pressure rise occurred only in the reservoir and not in the culture chamber. An advantage of the antiparallel perfusion is that it ensured the same amount of liquid passing through both blood vessels. In contrast, during parallel perfusion the flow of liquid would be affected by the diameter of the blood vessels, therefore a larger amount of liquid would pass through blood vessels with a larger diameter.

In theory, it would also be possible to connect both reservoirs via a secondary pump and thereby regulate the venous flow independently from the arterial flow (**Figure A 8**). However, this would have had complicated the experimental design and required several additional pressure sensors and pumps. Since previous studies surgically created an arteriovenous fistula, a connection between an artery and a vein, to vascularize tissues (Dong *et al.*, 2012; Wong *et al.*, 2019), I did not consider it necessary to regulate the venous flow separately from the arterial flow at this stage.

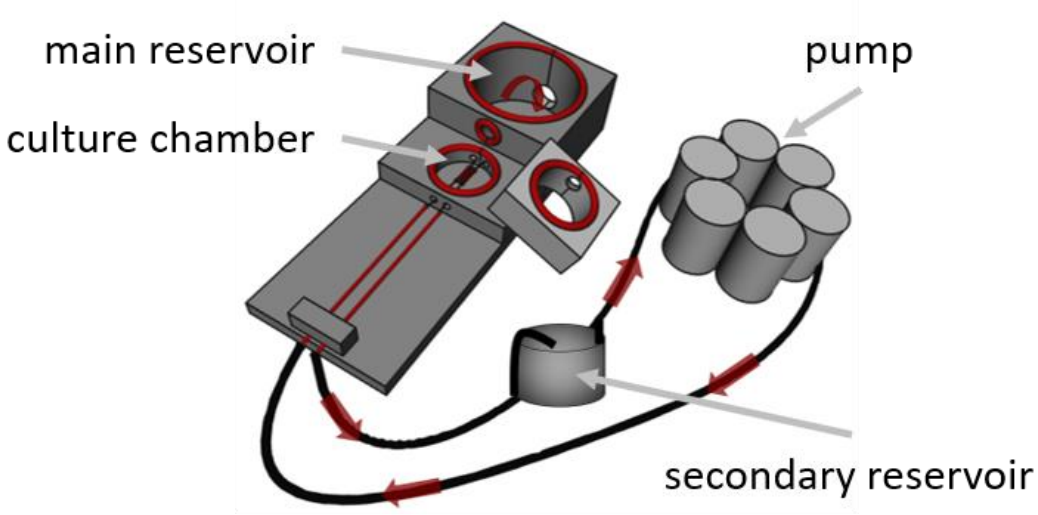

Figure 6-16: Antiparallel perfusion: The medium is aspirated from the secondary reservoir and pumped though the artery into the main reservoir. The resulting pressure increase in the main reservoir drives the medium through the vein back into the secondary reservoir.

6.2.13 Sprouting of perfused blood vessels in different media

While angiogenesis was observed in perfused blood vessel cultures, the number and length of sprouting blood vessels were low. Therefore, I tested different media to see whether angiogenesis could be enhanced in culture. To compare the growth in different media aorta and vena cava were isolated from mid-pregnant mice without separating both blood vessels from each other. After 14 days of culture, the blood vessels were imaged and angiogenesis was qualitatively assessed. Initial experiments were performed by perfusion of the blood vessels with MEM containing 1.5 % FBS ('base medium'). Angiogenesis was induced by addition of VEGF (20 ng/ml) and FGF2 (5 ng/ml) to base medium the culture chamber, but not to the perfusion medium. After 14 days of culture, limited angiogenesis was visible (**Figure 6-17A**).

Subsequently, the medium in the culture chamber was replaced with Promocell Endothelial Growth Medium (EGM). In one preliminary experiment no sprouting of the blood vessels was visible. Since the EGM was composed to be used for human cells and might not work as well on murine cells, I decided to supplement it with

murine VEGF (20 ng/ml) and FGF2 (5 ng/ml) which stimulated angiogenesis in previous experiments. The perfusion medium was not changed. Angiogenesis was not visibly improved by using EGM (**Figure 6-17B**).

In my next attempt to enhance angiogenesis, the FBS concentration was increased to 10 %. To promote angiogenesis, the medium was further supplemented with VEGF (50 ng/ml), FGF2 (50 ng/ml), PDGF-BB (50 ng/ml), sphingosine 1 phosphate (S1P, 1 mM) and PMA (2 ug/ml), a combination which hereafter is referred to as VFPSP medium. As described earlier, PDGF-BB was added to promote pericyte growth and vessel maturation (Stratman *et al.*, 2010; Tomkowicz *et al.*, 2010) while S1P and PMA had been shown to promote VEGF induced-angiogenesis of HUVECs seeded in a microfluidics chip (van Duinen *et al.*, 2019). The VFPSP medium was used as perfusion and growth chamber medium. Blood vessels cultured with this medium composition displayed an increased angiogenic capacity (**Figure 6-17C**).

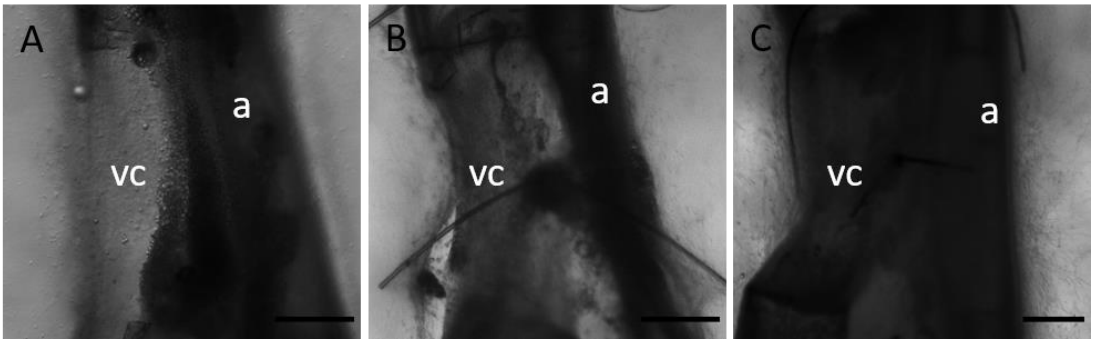

Figure 6-17: adult mouse aorta (a) and vena cava (vc) cultured in different media after 14 days of culture. The blood vessels were cultured without separating the aorta from the vena cava. A: Sprouting in blood vessels perfused with MEM supplemented with 1.5 % FBS. To induce angiogenesis the blood vessels in the culture chamber were overlaid with perfusion medium supplemented with VEGF (20 ng/ml) and FGF2 (5 ng/ml). B: Sprouting in blood vessels perfused with MEM containing 1.5 % FBS. To stimulate angiogenesis, Promocell medium supplemented with additional VEGF (20 ng/ml) and FGF2 (5 ng/ml) was added to the culture chamber. C: Blood vessels were perfused with MEM containing 10 % FBS, VEGF (50 ng/ml), FGF2 (50 ng/ml), PDGF-BB (50 ng/ml), S1P (1 mM) and PMA (2 ug/ml). Angiogenesis was induced with the same medium. Scale bars: 500 um.

6.2.14 Effect of removal of growth factors from perfusion medium

The adult blood vessel displayed an increased angiogenic response when cultured in the VFPSP medium, compared to other media. However, for the perfusion of blood vessels a rather large volume of 20-30 ml was required and consequentially larger quantities of costly growth factors are needed to maintain the cultures. To reduce the experimental costs, I tested whether a similar growth could be achieved with a perfusion medium only contained 10 % FBS, hereafter referred to as base medium.

The first culture which was perfused with the base medium showed growth that was not reduced from that seen in blood vessels perfused with the complete VFPSP medium (**Figure 6-18A and B**). However, the following cultures displayed nearly no angiogenic response (**Figure 6-18C**). Between these two experiments, I ordered a new set of growth factors, which might have been less efficient in stimulating angiogenesis. Since the perfusion experiments are time consuming and only a limited number can be run in parallel, I decided to modify the culture conditions rather than testing each growth factor individually.

Using antiparallel perfusion, the aorta and vena cava can be cultured either after separation of the aorta from the vena cava (**Figure 6-18D, F**) or without separation from each other (non-separated) (**Figure 6-18A-C, E**). When culturing both blood vessels with separation, longer angiogenic sprouts were visible in the space between both blood vessels compared to cultures in which the blood vessels were not separated from each other (**Figure 6-18D**). However, the dissection to separate the aorta from the vena cava was more difficult that isolating non-separated blood vessels together and therefore more likely to induce damage to the blood vessels resulting in subsequent leakage. This was detected by perfusion of dextran-FITC. In all (3/3) separated but only 1/3 non-separated blood vessel cultures, leakage was observed (**Figure 6-18E and F**).

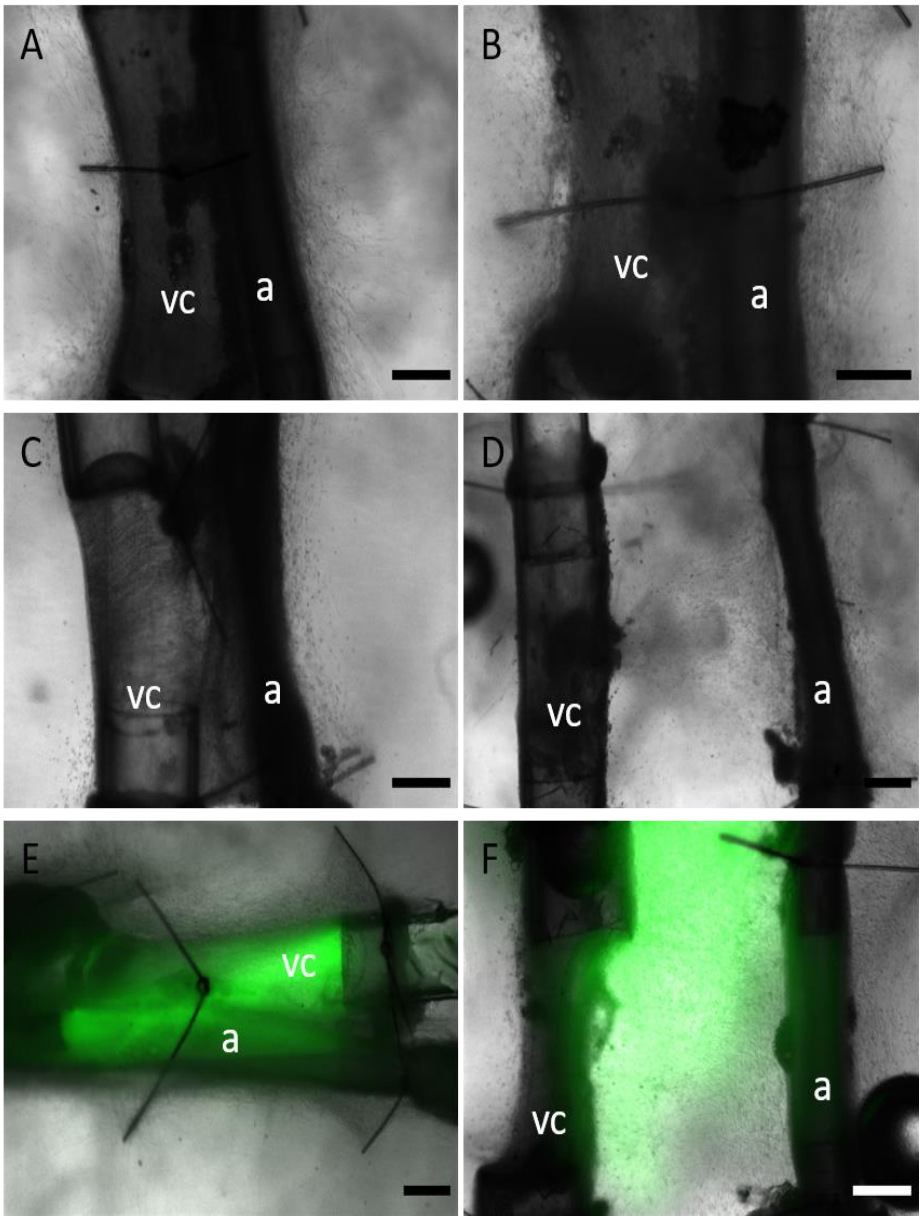

Figure 6-18: Removal of growth factors from perfusion medium while maintaining them in the chamber medium resulted in initially comparable angiogenesis. A: adult aorta (a) and vena cava (vc) were perfused with complete VFPSP medium. B: Aorta and vena cava were perfused with the base medium while the complete VFPSP medium was added to the growth chamber. C: Repeat of the perfusion experiment with the base medium after ordering a new set of growth factors. Angiogenesis was reduced compared to the previous experiment. D: separation of the aorta and vena cava resulted in visibly increased sprouting. E: Perfusion of unseparated aorta and vena cava with dextran-FITC revealed no leakage from the blood vessels. E: When separated blood vessels were perfused with dextran-FITC, leakage was observed from the vena cava. Scale bars: 500 µm

Due to the lack of leakage, leaving the blood vessels unseparated would be advantageous for determining whether the angiogenic sprout carried flow as there would be no background caused by dye leaking out. However, since the separated blood vessels displayed a stronger angiogenic response, they appear to be more suitable for optimizing the culture conditions in terms of maximizing angiogenic growth. Therefore, I decided to carry out further optimization experiments using separated blood vessels.

6.2.15 Further optimization of culture conditions

To test whether the angiogenesis in cultured mouse blood vessels could be further enhanced, I varied the extracellular matrix and medium composition of the blood vessel cultures. Overall, the differences observed were minor. The bioreactor used for these experiments had a 3 mm-thick, unpolished polycarbonate bottom which caused scattering of the light and therefore poor image quality. Due to the limited resolution of the images and the variable distance between the blood vessels it did not seem sensible to carry out any automated quantifications. In addition, the cells grew too densely to carry out a manual count or measurement of the forming sprouts. Therefore, angiogenesis could only be qualitatively assessed.

During sprouting, the blood vessel sprouts have to degrade the surrounding matrix in order to gain space for their growth. To test whether lower concentrations of collagen would facilitate the matrix degradation and enhance the growth, I embedded them in 1 mg/ml, 0.75 mg/ml and 0.5 mg/ml type I collagen. Reducing the collagen concentration from 1 mg/ml (**Figure 6-19A**) to 0.75 mg/ml (**Figure 6-19B**) appeared to improve angiogenesis slightly. Using an even lower concentration of 0.5 mg/ml had no beneficial effects on the sprouting capacity (**Figure 6-19C**). I also noted that collagen gels at this concentration did not polymerize evenly and were frequently covered with a liquid layer.

In an aortic ring assay, the addition of type IV collagen had been previously shown to increase sprout diameter and length compared type I collagen alone (Bonanno *et al.*, 2000). The addition of 100 µg/ml collagen type IV to 1 mg/ml collagen type I seemed to slightly decrease the area covered by angiogenic sprouts, but also appeared to increase the diameter of individual sprouts (**Figure 6-19D and D'**).

In parallel to different extracellular matrix compositions, I tested additional medium supplements. Hepatocyte growth factor (HGF) has been previously shown to promote angiogenesis at a concentration of 25 ng/ml (Ding *et al.*, 2003). The addition of HGF had no visible beneficial effect on angiogenesis (**Figure 6-19E**).

Angiogenesis may also be increased by the addition of MS-5 conditioned medium as MS-5 cells, a murine bone marrow stromal cell line, secrete a range of pro-angiogenic factors (Zhou *et al.*, 2012). In addition to adding MS-5 conditioned medium, I increased the VEGF concentration to 100 ng/ml to reduce the impact of the batch-to-batch variability in the growth factor activity. The concentration of FGF2 was not increased as it had been previously shown to effectively induce angiogenesis at much lower concentrations (Pepper *et al.*, 1992) and also induces the proliferation of other cell types such as fibroblasts (Tsuji *et al.*, 2009; Yu *et al.*, 2012) and therefore could potentially induce the overgrowth of other cell types. The concentration of PDGF-BB had not been increased because in addition to several studies that describe the proangiogenic effect of PDGF-BB (Brogi *et al.*, 1994; Nauck *et al.*, 1998) there are others that report an anti-angiogenic effect (Greenberg *et al.*, 2008; Tang *et al.*, 2016).

While adding MS-5 conditioned medium and increasing the VEGF concentration appeared to increase the overall area covered by sprouting cells, it was difficult to see individual vessel-like structures (**Figure 6-19F**).

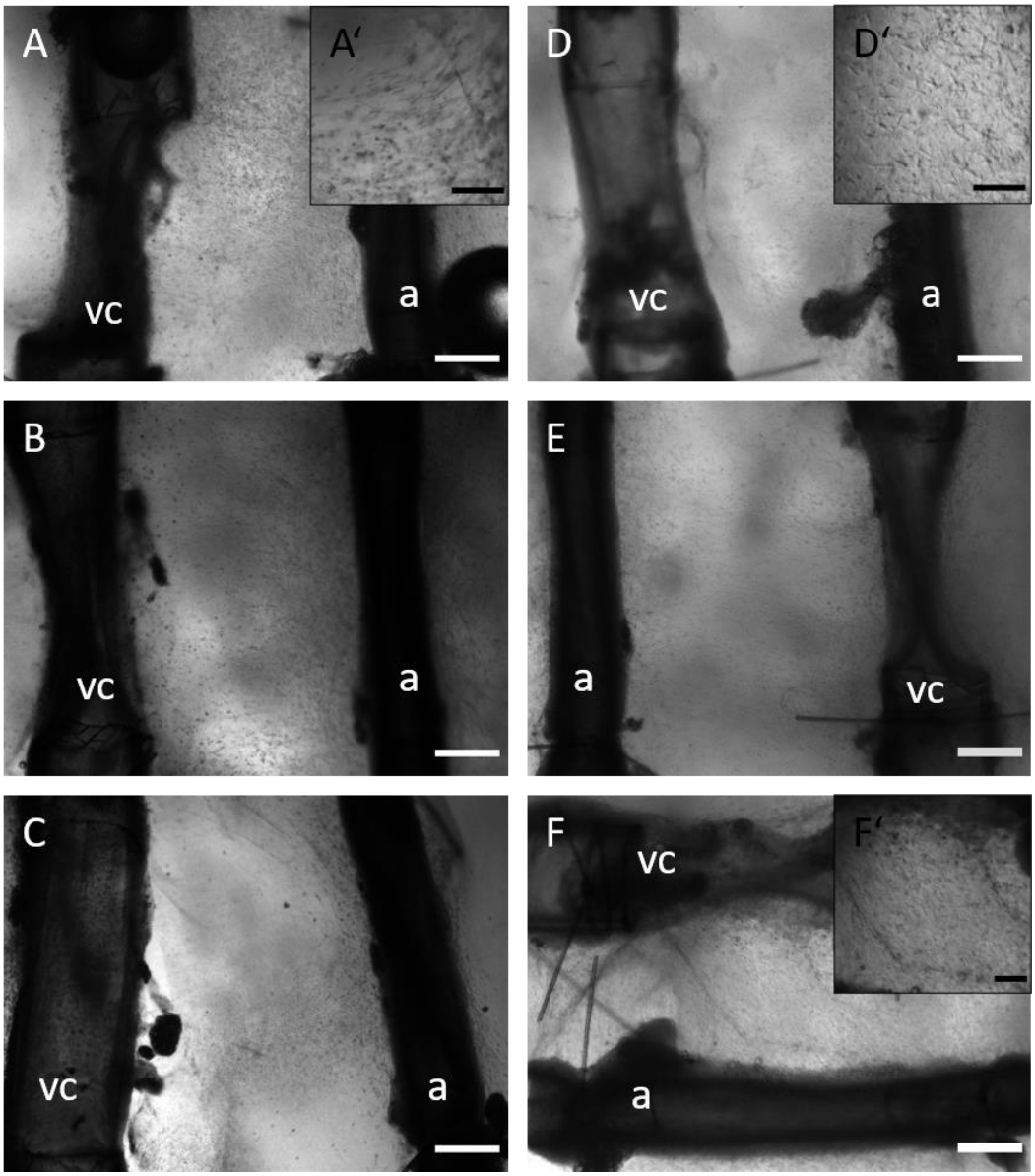

Figure 6-19: Modifications of medium and extracellular matrix to enhance angiogenesis. A: Aorta (a) and vena cava (vc) were embedded in 1 mg/ml type I collagen and cultured in VFPSP medium. A': forming sprouts at higher magnification. B: Reduction of the collagen concentration to 0.75 mg/ml appeared to slightly enhance angiogenesis. C: Reduction of the collagen concentration to 0.5 mg/ml did not improve angiogenesis. D: Addition of 100 µg/ml collagen type IV to 1 mg/ml collagen type I appeared to decrease the area covered by forming sprouts but seemed to slightly increase diameter of forming sprouts (D'). E: Addition of HGF (50 µg/ml) had no visible effect on angiogenesis. F: After increasing the VEGF concentration to 100 ng/ml and adding MS-5 conditioned medium a dense cellular sheet formed between both blood vessels. It was not possible to detect individual vessel-like structures (F'). A-F: scale bar 500 µm, A', D', F': scale bar. 200 µm

6.2.16 Co-culture of adult blood vessels and embryonic kidneys

All culture conditions tested in the previous experiment supported angiogenesis to some degree with minor differences (**Figure 6-19**). To test whether angiogenic sprouts originating from the adult blood vessels could connect with embryonic kidneys, I co-cultured the aorta and vena cava with E11.5 kidneys. The two blood vessels were precultured in VFPSP medium as chamber medium for 7 days. In parallel the kidneys were precultured for 3 days in KCM. The pre-culture period of 3 days was chosen because kidney precultured for this time had a higher probability of grafting onto the chick CAM compared to kidneys cultured for a shorter time (Chapter 5). On the day of grafting the kidneys were soaked in VEGF (10 ug/ml) for 2.5 h, because soaking kidneys in VEGF has been shown to improve vascularization after transplantation into murine hosts (Xinaris *et al.*, 2012). After washing the kidneys twice with KCM they were placed into a small incision in the collagen in the space between the aorta and vena cava. The chamber medium was replaced with MEM containing 10 % FBS, 50 ng/ml PDGF-BB and 50 ng/ml HGF. PDGF-BB was added to promote the growth of pericytes which are required for the stabilization of angiogenic sprouts (Stratman *et al.*, 2010). HGF has been previously shown to promote smooth muscle cell recruitment (Kobayashi *et al.*, 2006) and was also added to increase stability and maturity of the angiogenic sprouts.

On day 2 of the co-culture, Isolectin B4 was added to the chamber medium to stain the endothelial cells, and albumin-FITC (1 mg/ml) was added to the perfusion chamber to visualize the medium flow and determine wither the angiogenic sprouts were perfused. After 3 days of co-culture, Isolectin B4-positive vessel-like structures were seen between the kidneys and the blood vessels (**Figure 6-20**). The albumin-FITC had leaked out of the blood vessels and stained the collagen (data not shown). Therefore, it was not possible to determine whether there was any flow between the perfused blood vessels and the kidney.

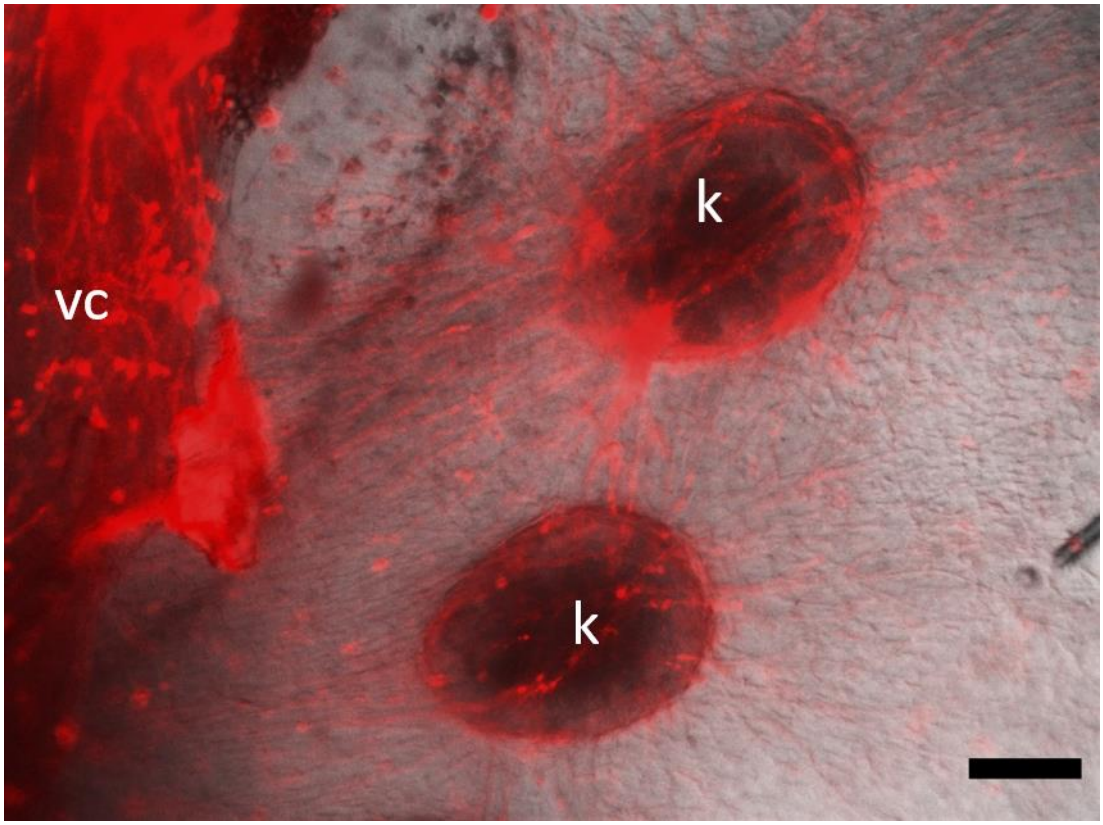

Figure 6-20: Co-culture of adult aorta and vena cava with embryonic kidney. The aorta (not visible) and vena cava (vc) were cultured for 7 days in VFPSP medium with increased VEGF concentration (100 ng/ml). Subsequently E11.5 kidneys (k) that had been precultured for 3 days in KCM were added to the blood vessels culture. After 2 additional days of culture Isolectin B4 (red) was added to the culture chamber and incubated overnight. On the following days angiogenic sprouts between the kidneys and the aorta were visible. Scale bar: 200 µm

6.3 Discussion

In this Chapter, I described the establishment of a perfusion culture system for primary blood vessels. This system is different from commercially available culture systems as it allows the antiparallel perfusion of arteries and veins, similar to blood flow *in vivo*. Additionally, the cultured vessels are easily accessible and can therefore be co-cultured with other tissues such as kidney explants. Therefore, this culture system has the potential to be used for vascularizing organ explants or organoids *in vitro*.

6.3.1 Inducing angiogenesis in vitro

Using cultured primary blood vessels for the *in vitro* vascularization of other tissues requires angiogenic stimulation to induce the blood vessels to form sprouting capillaries that connect with the other tissue. Angiogenesis is a well-studied process and can be induced by a range of chemicals and growth factors ((reviewed by Marech *et al.*, 2016), see table **Table 6-1**).

In agreement with earlier angiogenesis studies (Jaquet *et al.*, 2002; Zhu *et al.*, 2003), addition of solely VEGF and FGF2 resulted in the formation of angiogenic sprouts, although sprouting was limited in adult blood vessels. Similar to a previous microfluidic study (van Duinen *et al.*, 2019), the addition of PMA and S1P greatly enhanced sprouting. S1P was added because it had been previously shown to promote angiogenesis by facilitating the invasion of collagen matrices (Bayless *et al.*, 2009). According to the authors PMA was added to promote lumen formation in the absence of pericytes. PMA promotes lumen formation by stimulating the secretion of Weibel-Palade Body components such as Angiopoietin-2 (Ang-2) which is essential for lumen formation through activation of the receptor Tie-2 (Francis *et al.*, 2021)

Table 6-1: Selection of pro-angiogenic factors

growth factor	actions	reference
Angiopoietin 1	activation of Tie2 receptor resulting in angiogenic sprouting *in vitro*, *in vivo* required for vascular remodelling	(Koblizek *et al.*, 1998; Suri *et al.*, 1996)
Angiopoietin 2	inhibition of Tie2, *in vivo* expressed at sites of vascular remodelling, *in vitro* induces sprout formation and promoted pericyte detachment	(Brudno *et al.*, 2013; Maisonpierre *et al.*, 1997)
FGF2	activation of FGFR1 and in rare case FGFR2, often autocrine, induces EC proliferation and supports cell migration via ECM degradation through promotion of MMP secretion	(reviewed by Presta *et al.*, 2005)
Heparin-binding EGF	enhances endothelial migration in tube formation by increasing expression of eNOS and through PI-3K and MAPK pathways, stimulates pericyte recruitment	(Mehta and Besner, 2007; Stratman *et al.*, 2010)
HGF	induces EC proliferation after binding to MET receptor, mediates Ang-1 induces smooth muscle cell recruitment	(Ding *et al.*, 2003; Kobayashi *et al.*, 2006)
IGF-1	promotes proliferation and migration of ECs as well as tube formation via PI-3K in presence of D-glucose, induces VEGF expression	(Shigematsu *et al.*; Slomiany and Rosenzweig, 2004)
Interleukin-8	activates CXCR2 receptor leading to enhanced EC proliferation and migration	(Heidemann *et al.*, 2003)
MCP-1	chemotactic attraction of endothelial cells mediated by CCR2 receptor	(Salcedo *et al.*, 2000)
PDGF-BB	binding to PDGF-Rβ, can induce expression of VEGF and FGF in smooth muscle cells, smooth muscle cell recruitment to blood vessels	(Brogi *et al.*, 1994)
PMA	induced tube formation in HUVECs, action mediated by PKC which activates SPK which phosphorylates sphingosine to S1P	(Taylor *et al.*, 2006)
S1P	increases invasion of collagen matrices via integrinα2β1 signalling	(Bayless *et al.*, 2009)
Tryptase	secreted by mast cells, induce angiogenesis in CAM assay, activates PAR-2 receptor on endothelial cells	(Itoh *et al.*, 2005; Ribatti *et al.*, 2011)
Tumour necrosis factor TNF	induces VEGF independent angiogenesis through Etk or BMX activation	(Zhang *et al.*, 2003)
VEGF-A	binding to VEGF tyrosine kinase receptors in endothelial cells, promotes EC proliferation and migration, essential for vascular development *in vivo*	(Neufeld *et al.*, 1999)

In my cultures the addition S1P and PMA, along with other growth factors, greatly increased angiogenesis but there was no sign of lumen formation, as perfused albumin-FITC could not be detected in the angiogenic sprouts. Assuming that PMA is critical for the lumen formation, it could possibly be improved by increasing the concentration of PMA, which was described ambiguously as 2 ng/ml in the results section and 2 µg/ml in the methods section within the article published by van Duinen *et al.* (2019). A similar study which showed lumen formation in endothelial cells seeded in a microfluidics device by Nguyen *et al.* (2013) used a concentration of 75 ng/ml, which is much higher than the 2 ng/ml that I used in my experiments. Interestingly, Nguyen *et al.* (2013) observed the sprouting of single cells in cultures that contain S1P and no PMA and the collective migration of cells forming larger sprouts in cultures that contained only PMA (Nguyen *et al.*, 2013). The sprouting I observed appeared more like individual cells, which is another indicator that the concentration of PMA might have been too low.

In addition to VEGF, FGF2, PMA and S1P, Nguyen *et al.* (2013) further supplemented their media with HGF and monocyte chemotactic protein-1 (MCP-1) and found that a combination of MCP-1, S1P and PMA was most beneficial for the induction of angiogenesis (Nguyen *et al.*, 2013). MCP-1 is a chemokine that enhances endothelial cell migration and has be shown to induce angiogenesis in the CAM assay (Salcedo *et al.*, 2000). The addition of MCP-1 could potentially enhance angiogenesis in blood vessel cultures.

The expression of MCP-1 can also be induced by treatment with angiopoietin-1 (Ang-1) (Aplin *et al.*, 2010). Ang-1 had also been shown to induce the sprouting of endothelial cells *in vitro* and plays and important role in vascular remodelling *in vivo*, which is evidenced by a reduced number of large blood vessels and less distinct size differences between small and large blood vessels (Koblizek *et al.*, 1998; Suri *et al.*, 1996). Paradoxically, Ang-2 which, in contrast to Ang-1, acts as an antagonist of their receptor (Tie-2) has also been shown to be pro-angiogenic *in vitro* (Brudno *et al.*, 2013). While Ang-2 only was weakly proangiogenic when used alone, it greatly

enhanced the pro-angiogenic effects of VEGF treatment, in the study conducted by Brudno *et al.* (2013). As the pro-angiogenic effect of Ang-2 was inhibited by addition of Ang-1 (Brudno *et al.*, 2013), potentially through competition for the Tie2 receptor (Maisonpierre *et al.*, 1997), both compounds should not be used simultaneously.

Brudno *et al.* (2013) suggested the sequential use of VEGF and Ang-2 to induce angiogenesis followed by treatment with PDGF-BB and Ang-1 to stabilize the forming sprouts. A phased experimental design consisting of a sprouting phase followed by the grafting of the kidney and a vascular maturation phase appears to be a sensible approach for future experiments. Due to the large number of growth factors involved in angiogenesis, an extensive optimization may be required to induce a sufficient growth of cultured blood vessels.

Another possibility to induce angiogenesis would be to culture the blood vessels under hypoxic conditions. Hypoxia leads to an accumulation of hypoxia induced transcription factors such as Hif1α, which is degraded in the presence of oxygen (Ke and Costa, 2006). Hif1α has been shown to induce angiogenesis *in vivo* and *in vitro* (Humar *et al.*, 2002; Nakamura-Ishizu *et al.*, 2012; Toffoli *et al.*, 2009). The effect of hypoxia on angiogenesis was not evaluated in this work, because it requires specialized equipment which is usually not build to accommodate perfusion cultures and therefore would have had to be custom build. Additionally, previous studies suggest that reducing the surrounding oxygen concentration from 21 % to 5 % has negative effects on renal explant growth as it results in reduced size, reduced branching and a lower number of glomeruli (Rymer *et al.*, 2014; Schley *et al.*, 2015).

6.3.2 In vitro models of angiogenesis need to consider the effect of smooth muscle cells on vascular sprouting.

One difficulty with the optimization of the angiogenesis medium using perfused blood vessels is the low throughput of this method. Traditionally, the most frequently

used methods to identify the angiogenic potential of compounds are the tube formation assay, bead assay and the aortic ring assay. During a tube formation assay, an endothelial cell line, such as HUVEC, are seeded on an extracellular matrix- coated dish and treated with the compound of interest (Akiyama *et al.*, 2014; Frontini *et al.*, 2011; Kubota *et al.*, 1988). If the cells arrange in tubules, this compound is classified as "pro-angiogenic". However, other cell types such as Madin-Darby Canine Kidney (MDCK) cells (Hellmuth *et al.*, 2008) also form a tubular networks in response to certain growth factors. Therefore, the tube formation assay might not be very specific. An alternative approach id the bead assay during which beads coated with endothelial cells are placed in an extracellular matrix (Nehls and Drenckhahn, 1995). Upon proangiogenic stimulation the endothelial cells start to form sprouts from the bead (Nehls and Drenckhahn, 1995). The bead assay facilitates quantification of angiogenesis compared to the tube formation assay since the length of the sprouts originating from the beads can be easily measured therefore minor differences in the amplitude of a proangiogenic response can be easier detected in the bead assay compared to the tube-formation assay (Carpentier *et al.*, 2020).

In an aortic ring assay a blood vessel, in most cases the aorta, hence the name, is isolated and cut into rings. These rings are then placed on top or embedded in an extracellular matrix replacement such as collagen or Matrigel and treated with the compound of interest and observed for the formation of sprouting capillaries (Nicosia and Ottinetti, 1990; Nicosia *et al.*, 1982). In contrast to the previously mentioned *in vitro* assays, the aortic ring assays allows the interaction between different cell types, since the aortic rings contain apart from endothelial cells also smooth muscle cells, fibroblasts and adventitial inflammatory cells. The interplay between these cell types can affect angiogenesis. For example, adventitial macrophages have been shown to be essential in mediating injury-induces angiogenesis in the aortic ring assay (Gelati *et al.*, 2008) and fibroblasts have been shown to stabilize the forming microvessels (Villaschi and Nicosia, 1994).

There is a major difference between these assays and the angiogenic stimulation of the perfused blood vessels. In the traditional assays the endothelial cells are directly exposed to the compound. In contrast, when mounted in the perfusion bioreactor only the vessel wall is exposed to the surrounding proangiogenic factors. Therefore, some compounds, which had been identified as proangiogenic using traditional methods, might not work for perfused blood vessels. Adding the growth factors to the perfusate, where they would be in direct contact with the endothelium, could potentially improve angiogenesis. However, a previous study showed that in the ischemic hind limb model an intramuscular administration of VEGF resulted in a better restoration of blood flow compared to intravenous administration of VEGF (Lee *et al.*, 2014) suggesting that VEGF might be less efficient when added to the perfusate.

A model that more closely resembles the *in vivo* situation to study angiogenesis is the chick chorioallantoic membrane (CAM) which contains a dense, hierarchical network of blood vessels (Nowak-Sliwinska *et al.*, 2014). There are two major factors that need to be taken into consideration when comparing the CAM model to perfused blood vessel cultures. Firstly, factors that induce angiogenesis in the chick might not have the same effect on mouse blood vessels or might only act in a pro-angiogenic way in combination with factors that are already present in the CAM, but not in cultures of murine blood vessels. Secondly, the CAM consist mostly of microcapillaries with very thin vessel walls (Nowak-Sliwinska *et al.*, 2014), meaning that the endothelial cells are more exposed to compounds added to the CAM than they would be if they were surrounded by a thicker smooth muscle cell coat as in a mature mouse blood vessels. While the CAM assay gives a good representation of angiogenesis during development, it might not be as helpful in identifying factors to induce angiogenesis a mature murine blood vessel which is coated with a thick smooth muscle cell layer.

There are some studies that focus on the interplay between smooth muscle cells and endothelial cells. Smooth muscle cells have been shown to secrete pro-angiogenic factors as smooth muscle cell-conditioned medium induced tube formation in

cultured endothelial cells (Kuzuya *et al.*, 1995). One study showed an upregulation of pro-angiogenic factors (VEGF, PDGF-AA, PDGF-BB, TGFβ, but downregulated FGF2) in smooth muscle cells when these were co-cultured with a layer of endothelial cells. In these experiments a confluent layer of smooth muscle cells was overlayed with a sheet of endothelial cells. The endothelial cells were directly exposed to the medium. The methods section of that paper was unclear about whether control cultures were also layered. Therefore, differences could potentially be caused by reduced medium exposure (Heydarkhan-Hagvall *et al.*, 2003).

The secretion of proangiogenic factors can be increased through TGFβ and PMA, which have been shown to enhance the expression of the pro-angiogenic factors VEGF and FGF2 in smooth muscle cells (Brogi *et al.*, 1994; Winkles and Gay, 1991). In contrast other pro-angiogenic factors such as S1P have been shown to inhibit angiogenesis in co-cultures of smooth muscle cells and endothelial cells by stimulating the secretion of the angiogenesis inhibiting protein TIMP-2 in smooth muscle cells (Mascall *et al.*, 2012).

There are conflicting results about the effect of PDGF-BB on angiogenesis in the presence of smooth muscle cells. While some studies suggest that the treatment with PDGF-BB promotes angiogenesis by increasing the expression of VEGF and FGF (Brogi *et al.*, 1994; Nauck *et al.*, 1998), another found that treatment with PDGF-BB inhibits the secretion of several pro-angiogenic factors from smooth muscle cells (Tang *et al.*, 2016). In the study by Tang *et al.* VEGF and FGF2 expression were not determined, therefore it does not necessarily contradict the earlier experiments by Brogi *et al.* and Nauck *et al.* who confirmed the enhanced secretion of VEGF and FGF but did not assess whether this would enhance angiogenesis. In the CAM assay, PDGF-BB treatment alone has been shown to promote angiogenesis, but in combination with VEGF suppresses angiogenesis (Greenberg *et al.*, 2008). Therefore, an increased expression of VEGF from the smooth muscle cells in response to PDGF-BB does not necessarily lead to enhanced endothelial cell proliferation and migration. Based on this information, the addition of PDGF-BB might not be beneficial for the initiation of

angiogenesis. However, due to its involvement in smooth muscle cell recruitment (Hellstrom *et al.*, 1999; Lindahl *et al.*, 1997), PDGF-BB could play an important role in enhancing the maturity of forming sprouts which will be discussed below (**6.3.3 Overcoming limited vascular maturation *in vitro***).

Tang *et al.* (2016) noticed that smooth muscle cells could transdifferentiate into a pro-angiogenic phenotype when treated with cyclopentenyl cytosine. This trans-differentiation, which is mediated through activation of the adenosine receptors A1 and A2a, leads to upregulation of the pro-angiogenic CXCL1 and downregulation of the anti-angiogenic endostatin. Using several compounds that target different receptors in parallel may induce a stronger angiogenic response than using compounds that target the same receptor of work either upstream or downstream of one another. Therefore, cyclopentenyl cysteine could be a strong candidate to be used in addition to more traditional pro-angiogenic factors.

There is evidence that the pro-angiogenic effect of smooth muscle cells is also mediated by the Tweak receptor (TweakR), which can be induced by several pro-angiogenic growth factors such as PMA, Ang-2 and FGF2 (Wiley *et al.*, 2001). Determining the expression of TweakR in smooth muscle cell cultures after treatment with a pro-angiogenic compound might be a useful intermediate step in determining growth factors that induce angiogenesis in a smooth muscle cell-dependent way.

6.3.3 Overcoming limited vascular maturation in vitro

When the adult aorta and vena cava were co-cultured in the presence of pro-angiogenic growth factors, an endothelial network was visible between the blood vessels. However, there was no evidence of a medium flow as the added albumin-FITC could not be detected within the capillaries. One reason for this could be that the sprouting of individual cells dominated over the formation of a continuous network, an effect which might be prevented with an optimization of the surrounding

medium. The visible capillaries were most likely formed from vasa vasorum, a network of microvessels which delivers nutrients to the vessel wall of major blood vessels such as the aorta (Heistad *et al.*, 1981). Therefore, it is possible that the capillaries were not able to connect to the endothelium of the major blood vessels. This could be facilitated by partial enzymatic degradation of the extracellular matrix of the vessel wall, which is assumed to be a critical step during angiogenesis (Stetler-Stevenson, 1999). An upregulation of the matrix-metalloproteinase 9 (MMP9), which is involved in pathological weakening of the vessels wall during an aortic aneurism, could be achieved by treatment of the vessels with Tumour necrosis factor α (TNFα) (Ramella *et al.*, 2017; Xiao *et al.*, 2011). The permeability of the vessel wall may also be increased by elevating the levels of nitric oxide (NO) through activation of the endothelial NO synthase (eNOS) (Fukumura *et al.*, 2001). This could be achieved by increasing the flow rate (Lam *et al.*, 2006) and by addition of heparin-binding epidermal growth factor-like growth factor (HB-EGF) to the perfusate (Mehta *et al.*, 2008).

Another reason for the lack of flow through the capillary plexus could be a limited maturation of the blood vessels, meaning a failure to recruit pericytes and smooth muscle cells which are essential in order to stabilize the vessel (Hellstrom *et al.*, 1999; Lindahl *et al.*, 1997). *In vivo*, pericytes and smooth muscle cells are recruited through PDGF-BB which is secreted from the endothelial cells and binds to the PDGF-Rβ on the pericytes (Hellstrom *et al.*, 1999; Lindahl *et al.*, 1997). The co-expression of PDGF-BB and VEGF in a precise localization and fixed ratio have been shown to play an important role in the formation of eumorphic vascular networks that permit the flow of blood (Banfi *et al.*, 2012). While PDGF-BB is undoubtedly an important factor for vascular maturation, adding it to the culture medium could possibly interfere with the recruitments of pericytes to the endothelial cells, as it would distribute everywhere rather than form a gradient that directs the pericytes to the endothelial cells. Therefore, it may be more beneficial to induce PDGF-BB expression within the

endothelial cells. VEGF had been shown to induce the expression of PDGF-BB in HUVECS (Arkonac *et al.*, 1998; Reinmuth *et al.*, 2004).

However, the activation of the VEGF-receptor 2 (VEGF-R2) trough VEGF has also been shown to inhibit PDGF-Rβ-signalling in vascular smooth muscle cells (Greenberg *et al.*, 2008) and therefore could impair the vascular maturation. This could possibly be compensated by addition of FGF9, which has been shown to enhance PDGF-Rβ expression in vascular smooth muscle cells and to increase smooth muscle cell recruitment in a tissue implant model *in vivo* (Frontini *et al.*, 2011). Additionally, VEGF could be added to the perfusion medium rather than the surrounding medium, which would deliver it specifically to the endothelial cells.

Arterial maturation could also be improved by treatment with Ang-1. Ang-1 is a strong candidate for improving smooth muscle cell recruitment as it has been shown to induce at least three different growth factors, MCP-1, Heparin-binding EGF and HGF, which are each involved in smooth muscle cell recruitment (Aplin *et al.*, 2010; Iivanainen *et al.*, 2003; Kobayashi *et al.*, 2006).

6.3.4 Summary of recommended future experimental design

The cultured blood vessels were able to respond to angiogenic stimulation and in co-cultures with embryonic kidneys sprouts that seemingly connect the kidney and the blood vessels were visible. However, there was no evidence of a flow of medium through the renal vascular capillaries. The reasons for the lack of flow could be the formation of a discontinuous vascular network caused by the sprouting of individual cells rather than collective cell migration and a limited maturation of the forming capillaries. There are several factors that could enhance the maturation of the forming capillary plexus. However, some of these may impede endothelial cell sprouting and migration. This could be prevented by using a phased approach consisting of an initial sprouting phase followed by a maturation phase (**Figure 6-21**).

Thereby the composition of the medium would be varied between both phases in order to maximize vessel growth during the initial phase and to promote vessel maturation during the second phase.

To allow the initial sprouting of the blood vessels, endothelial cell proliferation and migration, as well as the detachment of mural cells and the degradation of the surrounding matrix, should be supported. To support endothelial cell proliferation, VEGF and FGF2 (Pepper *et al.*, 1992) should be added. Cyclopentenyl cytosine could induce the expression of additional proangiogenic growth factors within the smooth muscle cells (Tang *et al.*, 2016). The endothelial cell migration could be enhanced by addition of MCP-1 (Salcedo *et al.*, 2000). S1P and PMA should be added as they play important roles in the ECM degradation and thereby the invasion of collagen gels (Bayless *et al.*, 2009; Nguyen *et al.*, 2013). Lastly, Ang-2 has been shown to promote pericyte detachment (Brudno *et al.*, 2013) which is also an essential step to allow sprouting of the blood vessels.

Once the forming capillary plexus appears to form a continuous network between the aorta and vena cava, the maturation phase should be initiated. The expression of the smooth muscle cell chemoattractant PDGF-BB in the endothelial cells could be enhanced by adding VEGF to the perfusion medium (Arkonac *et al.*, 1998; Reinmuth *et al.*, 2004). Its respective receptor PDGF-Rβ could be upregulated in the smooth muscle cells through addition of FGF9 to the surrounding medium (Frontini *et al.*, 2011). The smooth muscle cell recruitment could further be supported by addition of Ang-1 (Aplin *et al.*, 2010; Iivanainen *et al.*, 2003; Kobayashi *et al.*, 2006).

It further has to be determined when would be the ideal time point for grafting a kidney, or kidney organoid. One possibility would be to graft the kidney in-between the sprouting and maturation phase (**Figure 6-21A**). Another option would be to add the kidney after the maturation phase and possibly insert a second sprouting phase to establish a connection between the capillary network and the renal vascular plexus followed by a second maturation phase (**Figure 6-21B**). The first option has the

advantage that fewer phases are needed. However, depending how long the maturation phase takes, it might take too long to establish a flow through the grafted kidney leading to advanced stages of central necrosis within the kidney. Additionally, the onset of flow might induce a remodelling of the capillary plexus (Chapman, 1918; Murray, 1926; Thoma, 1893) which could lead to losing the connection between the renal vascular network and the co-cultured blood vessels. Taking these points into account, it appears more promising to graft the kidney after a flow through the capillary plexus is established.

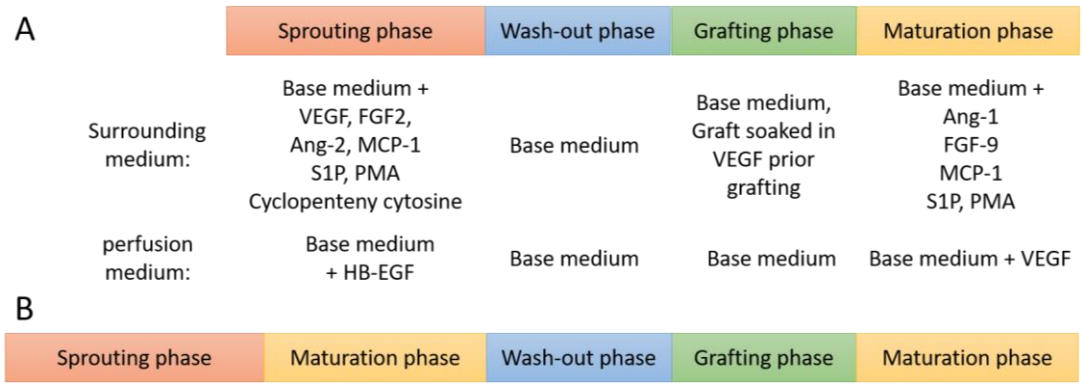

Figure 6-21: Proposed future experimental design. Vascular growth may be improved by a sequential treatment with different growth factors. The initial phase would be focus on promoting sprouting angiogenesis and pericyte detachment ("sprouting phase"). This phase could either be followed by a wash out phase to remove residual growth factors which could affect the growth of the kidney and the grafting phase during which a kidney soaked in VEGF would be placed near the blood vessels (A). To direct the angiogenic sprouts towards the VEGF-soaked kidney, no further growth factors would be added during that phase. After vascular sprouts are appearing to connect with the kidneys a maturation phase would follow. The aim of this phase would be to promote pericyte and smooth muscle cell recruitments and thereby allow perfusion of the pro-angiogenic sprouts. An alternative design would be to include a second maturation phase directly after the initial sprouting phase and prior to grafting of the kidney (B). The advantage of this design is that the presence of flow could be determined without the need of grafting the kidney first. This would facilitate the optimization of the sprouting and maturation media in absence of a kidney.

Limitations of the perfusion system and experimental design

There are several limitations of the experimental design to be noted. One of these limitations is the unphysiological flow profile. While the aortic blood flow is highly pulsatile, the frequency and amplitude of the pulsatile flow originating from the peristaltic pump do not match those of the blood flow found *in vivo*. A more realistic pulsation pattern could be achieved by firstly removing the pulsations of the peristaltic pump using a flow dampener and subsequently use an actuator to create a new pulsatile flow with the frequency of the aortic flow of about 6 Hz (Diamantouros *et al.*, 2013; Tovar Perez *et al.*, 2021).

In contrast the aortic flow, the venous blood flow is less pulsatile (Crouch *et al.*, 2020). While it can be assumed that the reservoir between the aorta and the vena cava acts to some degree as a flow dampener due the presence of compressible air, the degree to which the flow is dampened needs to be verified. It would be further advisable to use computational fluid dynamics to model which reservoir size would be required to reduce the pulsations sufficiently. It may also be required to replace the solid reservoir lid with a flexible membrane.

An additional variation from the physiological flow parameters is the flow rate, which was substantially lower than the *in vivo* flow rate of 2.6 ml/min (Crouch *et al.*, 2020). The lower flow rate was chosen under the assumption that perfusing the vessel at a lower rate would impose less strain on the vessels wall and therefore could result a reduction of smooth muscle cell layers (Thoma, 1893) which may aid angiogenesis. The initial rate of 50 µl/min was considered suitable as a starting value because it was used in a published study aiming to induce angiogenesis *in vitro* using similar sized blood vessels (Sakaguchi *et al.*, 2013). In future work the flow rate should be optimized to initially allow sprouting of the blood vessels and subsequently gradually raised to physiological values to mechanically condition the vessels and make them suitable for transplantation.

The flow within the vessel is also affected by the size of the needles leading to and from the blood vessels. The smaller diameter of the needles compared to the tubing will result in an increase of the flow velocity and a decrease of the pressure. The reduction of the pressure is dependent on the flow rate (Q), viscosity of the fluid (μ), length (L) and radius (R) of the needles and can be calculated using Poiseuille's equation (eq. (1)) (Sutera and Skalak, 1993).

$$\Delta p = 8\mu \frac{LQ}{\pi R^4} \quad (1)$$

In the present experimental design the needle length would be a variable parameter and its importance needs to be taken into account for future experiment. Since the blood vessel is mounted on two needles, one at the entrance and one at the exit, the influence of the needle length and diameter may be limited by cutting entrance and exit needles to the same length. According to the concept of electronic-hydraulic analogy this situation would be comparable to a potential divider where the two needles would act as identical resistors. This implies that the pressure is an analogue of the voltage and within the blood vessel would be at half of the output pressure of the pump system (Robbins, 2021).

The needles do not only affect the pressure within the blood vessels they also influence the turbulence of the flow entering the vessel. To mount the vessels onto the needles, the needles had to have a diameter smaller than that of the blood vessels. However, if the diameter of the needle lumen is substantially smaller than the blood vessel the vorticity of the flow will be increased due to the sudden enlargement of the flow path . The average inner diameter of the mouse aortas was about 360 µm, therefore the chosen MicroFil needles with an outer diameter of 350 µm and an inner diameter of 250 µm appeared to be the most suitable option available. However, there was some variation in the aortic lumen size between blood vessels, therefore, the needle size should have ideally been adjusted based on the lumen diameter of each individual blood vessel. This was not possible with this

system because the needles had to be mounted into the bioreactor on the day before isolation of the blood vessels to allow the silicone sealant that was used for mounting to polymerize.

Another issue with mounting the blood vessels onto the needles is that the terminal ends of the vessel that overlap with the needles are not perfused. This could affect the growth of the blood vessel as the cells from the unperfused section may secrete factors that impact the growth of the blood vessel, especially if a large section of the vessel is not exposed to the flow of medium. A preferred method would be to end-to-end anastomose the blood vessels. With larger vessels that could for example be done by suturing the vessel end-to-end to a soft tubing. However, this would be challenging to do with murine blood vessels due to their small size. A potential alternative could be to use a magnetic compression device as described in a recent study by Lu *et al.* (2020). During this procedure the end of the blood vessels is passed through a magnetic ring and rivet-like ring and everted onto the cylindrical structure of the rivet-like ring. Subsequently, a second magnetic ring are placed over the everted blood vessel to allow magnetic attraction between both vessels (Lu *et al.*, 2020). The now magnetized ends of the blood vessel could then be used to mount the vessels onto metallic perfusion needles.

Perhaps it would also be feasible to construct a metallic perfusion channel with an aperture that can be used to adjust the inner diameter of the flow channel to the lumen diameter of the blood vessel. This option would also enable to culture two blood vessels within a fixed distance. With the current system the distance between both blood vessels cultured separately from each other varied considerably. The difference in distance could affect the growth of angiogenic sprout as this may involve the exchange of paracrine signals between both blood vessels. Placing both vessels closer to each other would results in a higher concentration of signalling molecules reaching the opposite blood vessels. The difference in distance occurs through the process of manually inserting and gluing the needles into the bioreactor. If the installation of a metal perfusion channel with aperture is not possible, this could

be prevented in two different ways. One possibility would be to choose autoclavable needles that do not have to be exchanged after each use and therefore would have to be adjusted only once to a fixed distance. The disadvantage of having permanently mounted perfusion needles would be that the needle size was no longer adjustable which can impact the flow within the blood vessels if the size of the vessel changes. Alternatively, instead of gluing the needles into the bioreactors, ferrules could be used to mount them. Preparing ferrules with different inner diameters would allow the use of different needle sizes. This would further remove the need to let the silicone polymerize overnight and therefore enable adjusting the needle size after isolation of the blood vessels based on the dimensions of the blood vessel. However, it would have to be established whether the ferrules can provide a tight enough seal to prevent leakage.

There are some limitations arising from the complexity of the experimental design. For example, the use of two different blood vessels, the aorta and vena cava, leads to an increased biological variability. The system was designed to accommodate an artery and a vein because the aim was to reconstruct a capillary network between both vessels with a directional flow from the artery through newly-forming capillaries into the vein. The larger cross-sectional area of the vena cava compared to the aorta would result in a lower resistance in the vein and thereby allow the liquid to flow from the aorta through newly forming capillaries into the vein. When using two same-sized blood vessels, the resistance would still be slightly lower in the second vessel further down the flow path due to the pressure loss caused by friction, but the difference would be less pronounced, which may make it more difficult to establish a directional flow through a capillary bed from one vessel to the other. Another reason for choosing the vena cava as a second vessel was the thinner smooth muscle cell wall, which may facilitate angiogenesis through a more efficient detachment of smooth-muscle cells which is the initial step during sprouting (Stetler-Stevenson, 1999). This theory was supported by a study on angiogenesis of an artificially created arterio-venous fistula where the majority of newly forming vessels originated from

the venous side (Wong *et al.*, 2019). Conducting the experiment with two veins would not have been feasible, because the veins are more difficult to isolate and therefore less likely to get damaged and become leaky. Extensive leakage within the growth chamber would have resulted in a pressure rise which would in turn compress the veins and block the outflow of the growth chamber.

Additional variability was introduced in the co-culture experiments of the embryonic kidneys with adult and embryonic blood vessels as the number of co-cultured explants varied between experiments. Further the explants were placed manually with a variable distance to the blood vessels. The variation in number and distance could affected the growth of the kidneys as well the blood vessels. A higher number of explants could lead to an accumulation of growth factors secreted by the kidneys which could either have positive or negative effects on the forming vasculature. Placing the explants closed to the blood vessels would also result in a higher concentration of factors secreted by the kidney affecting the blood vessels.

The co-culture experiment could further be improved by using transgenic tissue that expresses a fluorescent marker. When using wild-type tissue, it is not possible to tell from where the sprouting vessels originate and whether they connect with sprouts coming from the other tissue. By using fluorescent kidney tissue, it would be possible to identify sprouts originating from the kidney and to identify whether these connect with angiogenic sprouts from the blood vessel.

The establishment of a functional, flow carrying vascular system is a critical step in growing healthy three-dimensional kidney explants. This chapter explored the possibility of establishing flow through kidney explants by using a co-culture system with perfused blood vessels. While still requiring extensive optimization, the device developed in this chapter sets the basis for an accessible long-term culture of blood vessels and thereby establishes a new model system to study vascular function and growth under the influence of flow *in vitro*.

Chapter 7 – Discussion

The aim of this thesis was to improve renal explant growth by inducing a more physiological, three-dimensional shape. This was achieved by embedding the explants in type I collagen. However, the explants displayed central necrosis, most likely due to a limited diffusion of oxygen and nutrients. *In vivo*, oxygen and nutrients are transported via the circulatory system. In agreement with previous studies, kidney organoids were shown to contain endothelial cells which formed an immature capillary network. To test the hypothesis that blood flow was needed in order to induce the maturation of the explant vasculature, I grafted kidneys onto the chick CAM. However, the establishment of flow in the grafted kidneys, which was confirmed by injection with a fluorescent antibody, was not sufficient to enhance the maturity of the renal vasculature, suggesting that the growth environment provided by the CAM was not suitable for the vascular maturation of the graft. In order to establish a more controlled environment, I aimed to optimize the *in vitro* culture conditions for isolated blood vessels which could potentially be used as a source for vascularizing kidney explants. When the explants were co-cultured with perfused primary blood vessels under proangiogenic stimulation, vascular sprouts were detected between the kidney and the blood vessels appearing to have formed a connection between both tissues. However, there was no evidence of flow through the renal plexus and further experiments are needed to determine whether the evidenced connection is formed by a continuous endothelium.

7.1 Enhancement of oxygen and nutrient diffusion without vascularization

The 3D growth of kidney explants is limited by the diffusion of oxygen. One possibility to increase the availability of oxygen in the core of 3D-cultured explants would be to increase its concentration in the culture environment. However, kidney explants are already cultured at higher oxygen levels than *in vivo* (Simon and Keith, 2008; Tsuji *et al.*, 2014) and further increasing the oxygen concentration could result in excessive oxidative stress in the periphery of the explant. Additionally, oxygen is highly flammable and therefore represents a fire hazard in high concentrations.

The availability of oxygen may also be enhanced by culturing kidney explants under flow (Barisam *et al.*, 2018; Sharifi *et al.*, 2019). In a recent study, kidney organoids were cultured within a millifluidic chip and subjected to flow shear stress (Homan *et al.*, 2019). The culture under flow shear stress led to enhanced endothelial cell growth and the peripheral vessels were shown to take up fluorescent beads from the perfusion medium (Homan *et al.*, 2019). However, the authors did not analyse cell death or hypoxia within the core of the organoids. Therefore, it cannot be concluded whether the culture under flow improved nutrient availability within the core. Additionally, the organoids used in this study did not represent the overall architecture of a kidney with a single collecting duct tree and a ureter, which makes it difficult to estimate the realism of the forming vasculature.

7.2 Limitations of implantation-based vascularization

Kidney explants and organoids have previously been vascularized by implantation into murine hosts or grafting on the chick chorioallantoic membrane (Ekblom *et al.*, 1982; Hyink *et al.*, 1996; Loughna *et al.*, 1997). However, there is limited control over the development of kidney organoids after implantation. In chapter 5, I have shown

that grafting of kidney explants onto the chick chorioallantoic membrane leads to abnormal vascular development and an aberrant localization of nephron progenitor cells in at least one of the grafts.

Some aspects of the abnormal vascular development could perhaps be prevented by pre-treatment of the kidney explants. For example, coating the one side of the explant (or organoid) in anti-angiogenic factors may prevent the ingrowth of blood vessels from this side. Other aspects, such as the lack of vascular smooth muscle cell recruitment, may be solved by choosing a different, closer related host species to rule out that the limited vascular maturity is caused by differences in the haemodynamic profile or species differences of circulation growth factors. A previous study showed the expression of the arterial marker Cx40 in kidney organoids transplanted into mice (Murakami *et al.*, 2019), which indicated a higher degree of vascular maturity. Whether the maturation of the vascular network in kidney organoids transplanted into murine hosts would be sufficient to induce smooth muscle cell recruitment remains to be identified.

However, even if a realistic vasculature were formed in implanted kidney organoids, the use of host animals for human regenerative medicine would still be problematic for various reasons. Firstly, it raises ethical concerns by causing pain and suffering to the host animal during implantation and removal of the organoid. Secondly, the implantation of human organoids into postnatal animal hosts would either require specialized breeds that are not immunocompetent or the administration of immune system suppressing drugs, to prevent rejection of the implant. Lastly, it is likely that the implanted organoids would contain at least some host derived cells (Murakami *et al.*, 2019; Sariola *et al.*, 1984b) resulting in chimeric organs which could increase the risk of rejection when transplanted into humans.

7.3 Alternative strategies for *in vitro* vascularization

Vascularizing kidney explants *in vitro* has several advantages compared to implantation-based experiments. The culture environment allows control over circulating growth factors as well as over mechanical properties of the surrounding matrix and flow dynamics.

While co-culturing kidney explants with perfused primary blood vessels is one possible method, there are other approaches to vascularize tissues *in vitro* (**Figure 7-1**). Cardiac cell sheets have been previously vascularized by culturing them on a block of collagen, that contained microchannels through which medium containing proangiogenic factors was perfused (Sakaguchi *et al.*, 2013). The perfused proangiogenic factors stimulated endothelial cells from the cardiac cell sheet to migrate towards the channel and form a vessel-like structure around it. This led to connection of the cardiac cell sheet with the perfusion medium, allowing the cardiac tissue to grow to greater thickness (Sakaguchi *et al.*, 2013) (**Figure 7-1**). As kidney explants and organoids contain endothelial cells (Munro *et al.*, 2017; Takasato *et al.*, 2015), this approach could also be used to vascularize renal organoids. I did try to replicate these experiments by creating a perfusable channel within the collagen in the bioreactor. However, when perfusing the channel with black ink, the ink quickly distributed within the entire culture chamber instead of remaining within the channel (Appendix, **Figure A 9**). It should be noted that in my replication attempt the size of the channels as well as the overall geometry of the bioreactor was different to the parameters used by Sakaguch *et al.* (2013) because I did not have the necessary resources to precisely reproduce their work. With further optimization it may be possible to use their approach for vascularizing renal tissue.

Another possibility to create a flow through the organoids could be to culture within microfluid chips that contain a network of endothelial cells (**Figure 7-1**). This approach has been used to vascularize human lung fibroblast spheroids and successfully prevented necrosis in the core of the spheroids (Nashimoto *et al.*, 2017).

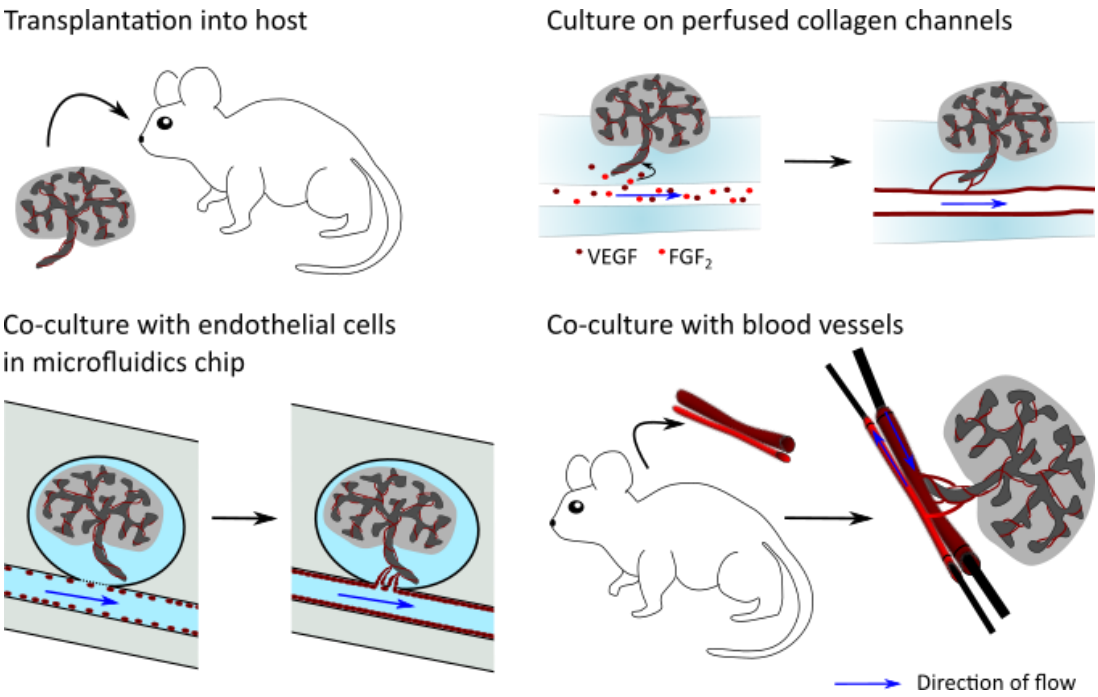

Figure 7-1: Overview of vascularization methods. One way of vascularizing kidneys would be the transplantation into a host. Alternatively, culturing the kidneys in a collagen gel that contains channels which are perfused with proangiogenic growth factory might stimulate the endothelial cells to migrate towards and anastomose with the channels to allow flow from the channel through the kidney. A slightly different approach would be to co-culture kidneys with endothelial cells on a microfluidics chip. Lastly, the kidneys could potentially be vascularized by co-culture with isolated perfused blood vessels.

The use of commercially available endothelial cells seeded within microfluids chips might reduce the variability between experiments. Compared to endothelial cell lines, the ability of freshly isolated blood vessels to undergo angiogenesis depends on a range of factors such as age and strain of the mouse used (Rohan *et al.*, 2000; Zhu *et al.*, 2003) as well as varying degrees of damage to the blood vessel during isolation or differences in the amount of connective tissue surrounding the vessel. The advantage of using whole isolated blood vessels is that they contain, aside from endothelial cells, also other vascular cells such as pericytes and smooth muscle cells which play an important role during vascular maturation (Teichert *et al.*, 2017) and by regulating mechanical strength and patency of the blood vessels (Bacakova *et al.*, 2018; Hamilton *et al.*, 2010). The use of a complete blood vessel also has practical

advantages because it could be directly ligated to the host vasculature. In contrast, a rather immature endothelium formed in a microfluidics chip may be difficult to harvest and to transplant.

7.4 Future work

7.4.1 Potential applicability of co-culture with primary blood vessels to vascularize iPSC-derived organoids

In this work, I used embryonic murine kidney explants to detect whether these would become vascularized when co-cultured with adult murine blood vessels. However, while vascularized embryonic mouse kidneys may be able to offer interesting insights into kidney development, their use for medical applications such as drug testing or regenerative medicine would be limited due to differences between mice and humans.

Human iPSC-derived kidney organoids on the other hand, have great potential to detect nephrotoxicity during drug discovery and to be used in regenerative medicine. To date, several protocols exist that induce differentiation of iPSCs into a variety of kidney cells including the three populations that give rise to the majority of renal cell types – ureteric bud cells, nephron progenitors and stromal progenitors (Low *et al.*, 2019; Przepiorski *et al.*, 2018; Takasato *et al.*, 2015). These organoids share some morphological characteristics, such as patterning of the nephrons in proximal, medial and distal segments, with natural kidneys, but they lack the overall structure of a kidney with a single collecting duct network and a ureter (Low *et al.*, 2019). In order to be used for transplantation, the kidney organoids would require a more organotypic anatomy and a perfusable vascular system.

Several research groups have confirmed the presence of endothelial cells within iPSC-derived kidney organoids (Takasato *et al.*, 2015; van den Berg *et al.*, 2018). Additionally, endothelial cells, for example HUVECs, may be added to dissociated organoids in order to integrate upon reaggregation, similar to a previously published "self-condensation"-approach (Takahashi *et al.*, 2018).

One major difference between kidney explants and iPSC-derived organoids is the overall anatomic realism. Since non-organotypic kidney organoids can be vascularized by implantation (Garreta *et al.*, 2019; Low *et al.*, 2019; Xinaris *et al.*, 2012), the lack of overall anatomical realism, meaning the lack of a single, asymmetric collecting duct network, is unlikely to prevent vascularization *in vitro* by co-culture with primary blood vessels. However, without any macroscopic anatomic realism, the functionality of the kidney organoids may be impaired as for optimal filtration and urine concentration a precise arrangement of collecting ducts, blood vessels and nephrons is required (Dantzler *et al.*, 2011).

A more organotypic organoid could potentially be achieved, by sorting and recombining ureteric bud cells, nephron progenitors and stromal progenitors. It has been shown previously that combining engineered ureteric buds and nephron progenitors from mouse iPSC with primary stromal progenitors resulted in an organoid that contained a single, branched collecting duct network (Taguchi and Nishinakamura, 2017). A similar approach may be applicable to generate anatomically more realistic human kidney organoids.

One limitation of this approach is the lack of a ureter. *In vivo*, blood vessels enter the kidney near the ureter and subsequently ramify to follow the branched collecting duct network (Munro *et al.*, 2017). Therefore, the absence of a ureter could potentially affect the arrangement of the forming vasculature. The development of the ureter is regulated by the expression of BMP4 within the periureteric mesenchyme (Brenner-Anantharam *et al.*, 2007; Cain *et al.*, 2005). A localized application of BMP4 coated sepharose beads resulted in the formation of an

asymmetric collecting duct tree with an unbranched, uroplakin expressing urothelium-like structure in renal cell-derived organoids (Mills *et al.*, 2017). Using a localized stimulus of BMP4 could on reconstituted organoids from sorted iPSC-derived renal cells could potentially generate human organotypic kidney organoids, which then could be vascularized by co-culturing with primary blood vessels.

One complication of this approach is the timing of BMP4 treatment. Mills *et al.* (2017) treated the kidney organoids for 5 days during which the organoids were cultured on a Transwell. However, kidney explants cultured for several days on a Transwell, displayed an aberrant arrangement of the collecting duct network when subsequently embedded in type 1 collagen (Chapter 3). Therefore, the treatment with BMP4 would either have to be done for a shorter time period, which may not be sufficient to induce urothelial differentiation, or a local BMP4 stimulus would have to be applied to the organoids after embedding in type 1 collagen. Given that BMP4 can act proangiogenic (Rezzola *et al.*, 2019), embedding the organoids nearby a perfused blood vessel may be the preferred approach as it could also facilitate the vascularization of the blood vessel.

7.4.2 Engineering of blood vessels

The co-culture of embryonic kidneys with adult murine blood vessels showed evidence of a vascular connection being formed between the vessel and the kidney (Chapter 6). While the use of murine blood vessels to vascularize human kidney organoids could work in theory, it raises similar concerns to the ones occurring when vascularizing kidney organoids by implantation into a host animal (see section **7.2 Limitations of implantation-based vascularization**). The isolation of a human peripheral blood vessel is possible in principle, but it would represent an invasive procedure connected with risks for the blood vessel donor.

A better option would be to engineer blood vessels with iPSC-derived vascular cells. Endothelial cells have been reported to identified in kidney organoids differentiated from iPSCs (Takasato *et al.*, 2015). Since the generation of organotypic organoids requires sorting of renal cell populations it may be convenient to also sort out endothelial cells from the organoids to engineer blood vessels. Alternatively, human iPSCs can be directed to efficiently differentiate into vascular organoids containing endothelial cells (34 %) and pericytes (64 %) (Wimmer *et al.*, 2019). Human iPSCs have also been differentiated into contractile vascular smooth muscle cells that secrete basement membrane components such as elastin, collagen type I and III as well as fibronectin, which play important roles in vascular elasticity (Eoh *et al.*, 2017).

There are different strategies to combine vascular cells to form a blood vessel. One way of obtaining a multi-layered spherical engineered vessel is to seed fibroblasts and smooth muscle cells in two compartments next to each other and culture them until a dense cell sheet is formed and a thick layer of extracellular matrix is deposited. Subsequently, the sheet can be detached and rolled on a rod to form a layer of smooth muscle cells surrounded by a layer of fibroblasts (Gauvin *et al.*, 2010) (**Figure 7-2A**). This method may also be used to create a 3D extracellular matrix scaffold for seeding endothelial cells. For this purpose, fibroblasts are cultured for several weeks to form a dense cell sheet and secrete extracellular matrix compounds. Subsequently, the fibroblast sheet is rolled on a stainless steal rod and cultured for a minimum of 10 weeks. By dehydration an acellular scaffold is obtained, which can be populated with vascular cells (L'Heureux *et al.*, 2006).

There are various other, less time-consuming methods for creating cylindrical scaffolds such as electrospinning (Ju *et al.*, 2017; Zhang *et al.*, 2008), moulding (Roh *et al.*, 2008) or sewing from sheets (Niklason *et al.*, 2001; Niklason *et al.*, 1999). These cylindrical casts can then be populated by sequential seeding of fibroblasts, smooth muscle cells and endothelial cells to create an engineered blood vessel (**Figure 7-2B**). Electrospun poly(ε-caprolactone) (PCL)/collagen scaffolds populated with smooth muscle cells and endothelial cells displayed a vessel-like morphology with elongated

endothelial cells and limited contractility *in vitro* (Ju *et al.*, 2017). After implantation into the carotid artery of sheep, these grafts remained patent and displayed no signs of forming aneurisms or dilation during the 6-month observation period (Ju *et al.*, 2017). Additionally, contractility of the grafts was greatly improved, reaching physiological levels, 6 months after implantation (Ju *et al.*, 2017).

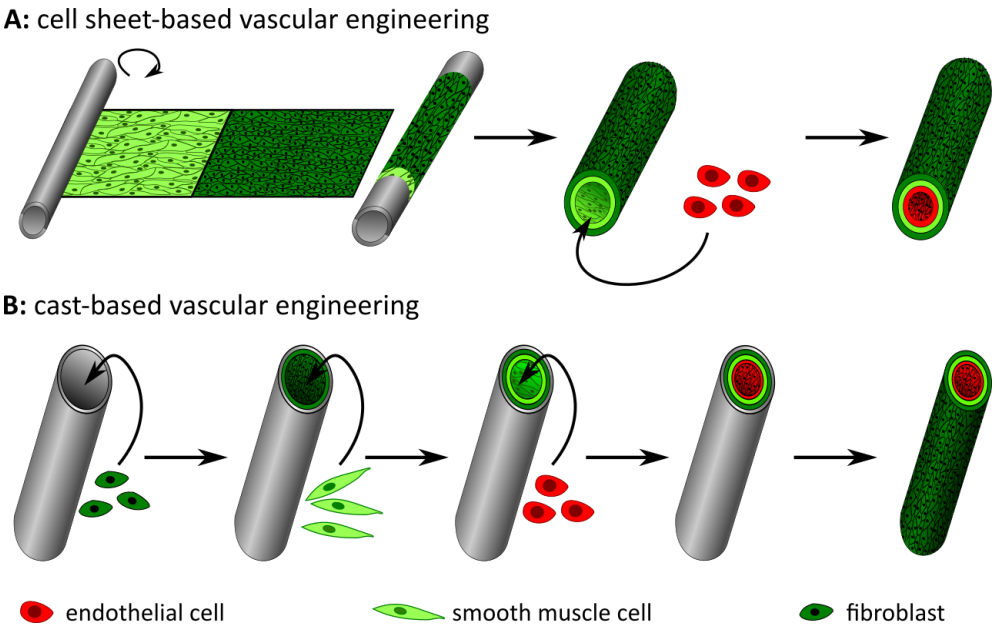

Figure 7-2: Methods to engineer blood vesselsFor the sheet-based method smooth muscle cells and pericytes are seeded next to each other and grown until a confluent cell sheet is formed. The sheet is then rolled onto a rod. After removal of the rod, endothelial cells are seeded inside the tube resulting in a three-layered engineered blood vessel. The cast-based method differs slightly. Instead of rolling a cell sheet onto a rod vascular cells are seeded sequentially starting with fibroblasts followed by smooth muscle cells and endothelial cells inside a tube-shaped cast. After removal of the cast a three-layered engineered blood vessel is left.

An efficient contractility of the renal artery is required to regulate the blood flow within the kidney and thereby optimize renal filtration and prevent damage to the kidney (Chang *et al.*, 2015). Therefore, it will be necessary to optimize the culture conditions for engineered blood vessels to obtain near physiological contractility, when using them to vascularize kidney organoids for future transplantation. It also

remains an open question whether engineered blood vessels with a dense smooth muscle cell layer can respond to pro-angiogenic stimulation in order to form capillaries sprouting and connecting with co-cultured kidney organoids.

7.5 Final remarks

In this thesis, I have shown that isolated and perfused blood vessels respond to proangiogenic stimulation. The presence of angiogenic sprouts between the blood vessel and the kidney suggest that the formation of a connection between both tissues is formed. However further experiments are required to establish whether the endothelium of the sprouts between the kidney and blood vessel is continuous and whether a lumen allowing flow is formed. Further modification of this culture method may improve the maturity of forming endothelial sprouts to allowing a flow between the perfused vessel and the kidney explant. This could lead to improved 3D growth of kidney explants.

In the future, this method may enable *in vitro* vascularization of kidney organoids, which could improve their growth in culture as well as enable the determination of their filtration efficiency.

Chapter 8 - References

Ahn, G., Park, J. H., Kang, T., Lee, J. W., Kang, H. W. and Cho, D. W. (2010). Effect of pore architecture on oxygen diffusion in 3D scaffolds for tissue engineering. *J Biomech Eng* **132**, https://doi.org/10.1115/1.4002429

Akimoto, S., Mitsumata, M., Sasaguri, T. and Yoshida, Y. (2000). Laminar shear stress inhibits vascular endothelial cell proliferation by inducing cyclin-dependent kinase inhibitor p21(Sdi1/Cip1/Waf1). *Circ Res* **86**, https://doi.org/10.1161/01.res.86.2.185

Akiyama, I., Yoshino, O., Osuga, Y., Shi, J., Harada, M., Koga, K., Hirota, Y., Hirata, T., Fujii, T., Saito, S., *et al.* (2014). Bone morphogenetic protein 7 increased vascular endothelial growth factor (VEGF)-a expression in human granulosa cells and VEGF receptor expression in endothelial cells. *Reprod Sci* **21**, https://doi.org/10.1177/1933719113503411

Almquist, M., Isaksson, E. and Clyne, N. (2020). The treatment of renal hyperparathyroidism. *Endocr Relat Cancer* **27**, https://doi.org/10.1530/ERC-19-0284

Alport, A. C. (1927). Hereditary Familial Congenital Haemorrhagic Nephritis. *Br Med J* **1**, https://doi.org/10.1136/bmj.1.3454.504

Aplin, A. C., Fogel, E. and Nicosia, R. F. (2010). MCP-1 promotes mural cell recruitment during angiogenesis in the aortic ring model. *Angiogenesis* **13**, https://doi.org/10.1007/s10456-010-9179-8

Arai, C., Yoshizaki, K., Miyazaki, K., Saito, K., Yamada, A., Han, X., Funada, K., Fukumoto, E., Haruyama, N., Iwamoto, T., *et al.* (2017). Nephronectin plays critical roles in Sox2 expression and proliferation in dental epithelial stem cells via EGF-like repeat domains. *Scientific Reports* **7**, https://doi.org/10.1038/srep45181

Arkonac, B. M., Foster, L. C., Sibinga, N. E., Patterson, C., Lai, K., Tsai, J. C., Lee, M. E., Perrella, M. A. and Haber, E. (1998). Vascular endothelial growth factor induces heparin-binding epidermal growth factor-like growth factor in vascular endothelial cells. *J Biol Chem* **273**, https://doi.org/10.1074/jbc.273.8.4400

Ausprunk, D. H. and Folkman, J. (1977). Migration and proliferation of endothelial cells in preformed and newly formed blood vessels during tumor angiogenesis. *Microvasc Res* **14**, https://doi.org/10.1016/0026-2862(77)90141-8

Bacakova, L., Travnickova, M., Filova, E., Matějka, R., Stepanovska, J., Musilkova, J., Zarubova, J. and Molitor, M. (2018). The Role of Vascular Smooth Muscle Cells in the Physiology and Pathophysiology of Blood Vessels. In *Muscle Cell and Tissue - Current Status of Research Field*: InTech.

Baker, K. M., Campanile, C. P., Trachte, G. J. and Peach, M. J. (1984). Identification and characterization of the rabbit angiotensin II myocardial receptor. *Circ Res* **54**, https://doi.org/10.1161/01.res.54.3.286

Banfi, A., von Degenfeld, G., Gianni-Barrera, R., Reginato, S., Merchant, M. J., McDonald, D. M. and Blau, H. M. (2012). Therapeutic angiogenesis due to balanced single-

vector delivery of VEGF and PDGF-BB. *FASEB J* **26**, https://doi.org/10.1096/fj.11-197400

Barczyk, M., Carracedo, S. and Gullberg, D. (2010). Integrins. *Cell Tissue Res* **339**, https://doi.org/10.1007/s00441-009-0834-6

Barisam, M., Saidi, M. S., Kashaninejad, N. and Nguyen, N. T. (2018). Prediction of Necrotic Core and Hypoxic Zone of Multicellular Spheroids in a Microbioreactor with a U-Shaped Barrier. *Micromachines (Basel)* **9**, https://doi.org/10.3390/mi9030094

Bayless, K. J., Kwak, H. I. and Su, S. C. (2009). Investigating endothelial invasion and sprouting behavior in three-dimensional collagen matrices. *Nat Protoc* **4**, https://doi.org/10.1038/nprot.2009.221

Bazigou, E., Lyons, O. T., Smith, A., Venn, G. E., Cope, C., Brown, N. A. and Makinen, T. (2011). Genes regulating lymphangiogenesis control venous valve formation and maintenance in mice. *J Clin Invest* **121**, https://doi.org/10.1172/JCI58050

Benjamin, L., Hemo, I. and Keshet, E. (1998). A plasticity for blood vessel remodelling is defined by pericyte coverage of the performed endothelial network and is regulated by PDGF-B and VEGF. *Development* **125**, https://dev.biologists.org/content/125/9/1591

Bentley, F. H. (1936). Wound Healing in vitro. *J Anat* **70**, https://www.ncbi.nlm.nih.gov/pubmed/17104610

Bernoulli, D. (1738). *Danielis Bernoulli ... Hydrodynamica, sive, De viribus et motibus fluidorum commentarii : opus academicum ab auctore, dum Petropoli ageret, congestum*. Argentorati: Sumptibus Johannis Reinholdi Dulseckeri.

Bernoulli, D. and Flierl, K. (1965). *Hydrodynamik oder Kommentare über die Kräfte und Bewegungen der Flüssigkeiten: Anm. b*: Forschungsinst. d. Dt. Museums f.d. Geschichte d. Naturwissenschaften u.d. Technik.

Bertram, J. F., Douglas-Denton, R. N., Diouf, B., Hughson, M. D. and Hoy, W. E. (2011). Human nephron number: implications for health and disease. *Pediatr Nephrol* **26**, https://doi.org/10.1007/s00467-011-1843-8

Bidani Anil, K. and Griffin Karen, A. (2004). Pathophysiology of Hypertensive Renal Damage. *Hypertension* **44**, https://doi.org/10.1161/01.HYP.0000145180.38707.84

Bolton, G. R., Deen, W. M. and Daniels, B. S. (1998). Assessment of the charge selectivity of glomerular basement membrane using Ficoll sulfate. *Am J Physiol* **274**, https://doi.org/10.1152/ajprenal.1998.274.5.F889

Bonanno, E., Iurlaro, M., Madri, J. A. and Nicosia, R. F. (2000). Type IV collagen modulates angiogenesis and neovessel survival in the rat aorta model. *In Vitro Cell Dev Biol Anim* **36**, https://doi.org/10.1290/1071-2690(2000)036*<0336:TICMAA>2.0.CO;2*

Boute, N., Gribouval, O., Roselli, S., Benessy, F., Lee, H., Fuchshuber, A., Dahan, K., Gubler, M. C., Niaudet, P. and Antignac, C. (2000). NPHS2, encoding the glomerular protein podocin, is mutated in autosomal recessive steroid-resistant nephrotic syndrome. *Nat Genet* **24**, https://doi.org/10.1038/74166

Bowman, W. (1842). On the Structure and Use of the Malpighian Bodies of the Kidney, with Observations on the Circulation through That Gland. *Philosophical Transactions of the Royal Society of London* **132**, http://www.jstor.org/stable/108143

Braun-Menendez, E., Fasciolo, J. C., Leloir, L. F. and Munoz, J. M. (1940). The substance causing renal hypertension. *J Physiol* **98**, https://doi.org/10.1113/jphysiol.1940.sp003850

Brenner-Anantharam, A., Cebrian, C., Guillaume, R., Hurtado, R., Sun, T. T. and Herzlinger, D. (2007). Tailbud-derived mesenchyme promotes urinary tract segmentation via BMP4 signaling. *Development* **134**, https://doi.org/10.1242/dev.004234

Brogi, E., Wu, T., Namiki, A. and Isner, J. M. (1994). Indirect angiogenic cytokines upregulate VEGF and bFGF gene expression in vascular smooth muscle cells, whereas hypoxia upregulates VEGF expression only. *Circulation* **90**, https://doi.org/10.1161/01.cir.90.2.649

Broutier, L., Andersson-Rolf, A., Hindley, C. J., Boj, S. F., Clevers, H., Koo, B. K. and Huch, M. (2016). Culture and establishment of self-renewing human and mouse adult liver and pancreas 3D organoids and their genetic manipulation. *Nat Protoc* **11**, https://doi.org/10.1038/nprot.2016.097

Brown, A. C., Adams, D., de Caestecker, M., Yang, X., Friesel, R. and Oxburgh, L. (2011). FGF/EGF signaling regulates the renewal of early nephron progenitors during embryonic development. *Development* **138**, https://doi.org/10.1242/dev.065995

Brown, A. C., Muthukrishnan, S. D. and Oxburgh, L. (2015). A synthetic niche for nephron progenitor cells. *Dev Cell* **34**, https://doi.org/10.1016/j.devcel.2015.06.021

Brudno, Y., Ennett-Shepard, A. B., Chen, R. R., Aizenberg, M. and Mooney, D. J. (2013). Enhancing microvascular formation and vessel maturation through temporal control over multiple pro-angiogenic and pro-maturation factors. *Biomaterials* **34**, https://doi.org/10.1016/j.biomaterials.2013.08.007

Burke, M., Pabbidi, M. R., Farley, J. and Roman, R. J. (2014). Molecular mechanisms of renal blood flow autoregulation. *Curr Vasc Pharmacol* **12**, https://doi.org/10.2174/15701611113116660149

Burri, P. H. and Djonov, V. (2002). Intussusceptive angiogenesis--the alternative to capillary sprouting. *Mol Aspects Med* **23**, https://doi.org/10.1016/s0098-2997(02)00096-1

Cain, J. E., Nion, T., Jeulin, D. and Bertram, J. F. (2005). Exogenous BMP-4 amplifies asymmetric ureteric branching in the developing mouse kidney in vitro. *Kidney Int* **67**, https://doi.org/10.1111/j.1523-1755.2005.67098.x

Carmeliet, P., Ng, Y. S., Nuyens, D., Theilmeier, G., Brusselmans, K., Cornelissen, I., Ehler, E., Kakkar, V. V., Stalmans, I., Mattot, V., *et al.* (1999). Impaired myocardial angiogenesis and ischemic cardiomyopathy in mice lacking the vascular endothelial growth factor isoforms VEGF164 and VEGF188. *Nat Med* **5**, https://doi.org/10.1038/8379

Carpentier, G., Berndt, S., Ferratge, S., Rasband, W., Cuendet, M., Uzan, G. and Albanese, P. (2020). Angiogenesis Analyzer for ImageJ — A comparative morphometric analysis of "Endothelial Tube Formation Assay" and "Fibrin Bead Assay". *Scientific Reports* **10**, https://doi.org/10.1038/s41598-020-67289-8

Carroll, T. J., Park, J. S., Hayashi, S., Majumdar, A. and McMahon, A. P. (2005). Wnt9b plays a central role in the regulation of mesenchymal to epithelial transitions underlying organogenesis of the mammalian urogenital system. *Dev Cell* **9**, https://doi.org/10.1016/j.devcel.2005.05.016

Chachami, G., Simos, G., Hatziefthimiou, A., Bonanou, S., Molyvdas, P. A. and Paraskeva, E. (2004). Cobalt induces hypoxia-inducible factor-1alpha expression in airway smooth muscle cells by a reactive oxygen species- and PI3K-dependent mechanism. *Am J Respir Cell Mol Biol* **31**, https://doi.org/10.1165/rcmb.2003-0426OC

Chai, Y. C., Mendes, L. F., van Gastel, N., Carmeliet, G. and Luyten, F. P. (2018). Fine-tuning pro-angiogenic effects of cobalt for simultaneous enhancement of vascular endothelial growth factor secretion and implant neovascularization. *Acta Biomater* **72**, https://doi.org/10.1016/j.actbio.2018.03.048

Chang, N. K., Gu, J., Gu, S., Osorio, R. W., Concepcion, W. and Gu, E. (2015). Arterial flow regulator enables transplantation and growth of human fetal kidneys in rats. *Am J Transplant* **15**, https://doi.org/10.1111/ajt.13149

Chang, R. L., Deen, W. M., Robertson, C. R. and Brenner, B. M. (1975). Permselectivity of the glomerular capillary wall: III. Restricted transport of polyanions. *Kidney Int* **8**, https://doi.org/10.1038/ki.1975.104

Chang, S. H., Kanasaki, K., Gocheva, V., Blum, G., Harper, J., Moses, M. A., Shih, S. C., Nagy, J. A., Joyce, J., Bogyo, M., *et al.* (2009). VEGF-A induces angiogenesis by perturbing the cathepsin-cysteine protease inhibitor balance in venules, causing basement membrane degradation and mother vessel formation. *Cancer Res* **69**, https://doi.org/10.1158/0008-5472.CAN-08-4539

Chapman, W. B. (1918). The effect of the heart-beat upon the development of the vascular system in the chick. *American Journal of Anatomy* **23**, https://doi.org/10.1002/aja.1000230107

Chi, X., Michos, O., Shakya, R., Riccio, P., Enomoto, H., Licht, J. D., Asai, N., Takahashi, M., Ohgami, N., Kato, M., *et al.* (2009). Ret-dependent cell rearrangements in the Wolffian duct epithelium initiate ureteric bud morphogenesis. *Dev Cell* **17**, https://doi.org/10.1016/j.devcel.2009.07.013

Chien, S. (1976). Significance of macrorheology and microrheology in atherogenesis. *Ann N Y Acad Sci* **275**, https://doi.org/10.1111/j.1749-6632.1976.tb43335.x

Cho, E. A., Patterson, L. T., Brookhiser, W. T., Mah, S., Kintner, C. and Dressler, G. R. (1998). Differential expression and function of cadherin-6 during renal epithelium development. *Development* **125**, https://www.ncbi.nlm.nih.gov/pubmed/9449663

Clark, E. R. and Clark, E. L. (1940). Microscopic observations on the extra-endothelial cells of living mammalian blood vessels. *American Journal of Anatomy* **66**, https://doi.org/10.1002/aja.1000660102

Coffin, J. D. and Poole, T. J. (1988). Embryonic vascular development: immunohistochemical identification of the origin and subsequent morphogenesis of the major vessel primordia in quail embryos. *Development* **102**, https://www.ncbi.nlm.nih.gov/pubmed/3048971

Coles, H. S., Burne, J. F. and Raff, M. C. (1993). Large-scale normal cell death in the developing rat kidney and its reduction by epidermal growth factor. *Development* **118**, https://www.ncbi.nlm.nih.gov/pubmed/8076517

Costantini, F. and Shakya, R. (2006). GDNF/Ret signaling and the development of the kidney. *Bioessays* **28**, https://doi.org/10.1002/bies.20357

Crouch, A. C., Cao, A. A., Scheven, U. M. and Greve, J. M. (2020). In Vivo MRI Assessment of Blood Flow in Arteries and Veins from Head-to-Toe Across Age and Sex in C57BL/6 Mice. *Annals of Biomedical Engineering* **48**, https://doi.org/10.1007/s10439-019-02350-w

Curthoys, N. P. and Moe, O. W. (2014). Proximal tubule function and response to acidosis. *Clin J Am Soc Nephrol* **9**, https://doi.org/10.2215/CJN.10391012

Dane, M. J., van den Berg, B. M., Avramut, M. C., Faas, F. G., van der Vlag, J., Rops, A. L., Ravelli, R. B., Koster, B. J., van Zonneveld, A. J., Vink, H., *et al.* (2013). Glomerular endothelial surface layer acts as a barrier against albumin filtration. *Am J Pathol* **182**, https://doi.org/10.1016/j.ajpath.2013.01.049

Daniel, E., Azizoglu, D. B., Ryan, A. R., Walji, T. A., Chaney, C. P., Sutton, G. I., Carroll, T. J., Marciano, D. K. and Cleaver, O. (2018). Spatiotemporal heterogeneity and

patterning of developing renal blood vessels. *Angiogenesis* **21**, https://doi.org/10.1007/s10456-018-9612-y

Dantzler, W. H., Pannabecker, T. L., Layton, A. T. and Layton, H. E. (2011). Urine concentrating mechanism in the inner medulla of the mammalian kidney: role of three-dimensional architecture. *Acta Physiol (Oxf)* **202**, https://doi.org/10.1111/j.1748-1716.2010.02214.x

Davies, J. A., Hohenstein, P., Chang, C. H. and Berry, R. (2014). A self-avoidance mechanism in patterning of the urinary collecting duct tree. *BMC Dev Biol* **14**, https://doi.org/10.1186/s12861-014-0035-8

Diamantouros, S. E., Hurtado-Aguilar, L. G., Schmitz-Rode, T., Mela, P. and Jockenhoevel, S. (2013). Pulsatile Perfusion Bioreactor System for Durability Testing and Compliance Estimation of Tissue Engineered Vascular Grafts. *Annals of Biomedical Engineering* **41**, https://doi.org/10.1007/s10439-013-0823-5

Ding, S., Merkulova-Rainon, T., Han, Z. C. and Tobelem, G. (2003). HGF receptor up-regulation contributes to the angiogenic phenotype of human endothelial cells and promotes angiogenesis in vitro. *Blood* **101**, https://doi.org/10.1182/blood-2002-06-1731

DiStefano, T., Chen, H. Y., Panebianco, C., Kaya, K. D., Brooks, M. J., Gieser, L., Morgan, N. Y., Pohida, T. and Swaroop, A. (2018). Accelerated and Improved Differentiation of Retinal Organoids from Pluripotent Stem Cells in Rotating-Wall Vessel Bioreactors. *Stem Cell Reports* **10**, https://doi.org/10.1016/j.stemcr.2017.11.001

Djonov, V. G., Kurz, H. and Burri, P. H. (2002). Optimality in the developing vascular system: branching remodeling by means of intussusception as an efficient adaptation mechanism. *Dev Dyn* **224**, https://doi.org/10.1002/dvdy.10119

Dong, Q.-s., Shang, H.-t., Wu, W., Chen, F.-l., Zhang, J.-r., Guo, J.-p. and Mao, T.-q. (2012). Prefabrication of axial vascularized tissue engineering coral bone by an arteriovenous loop: A better model. *Materials Science and Engineering: C* **32**, https://doi.org/10.1016/j.msec.2012.04.039

Donoviel, D. B., Freed, D. D., Vogel, H., Potter, D. G., Hawkins, E., Barrish, J. P., Mathur, B. N., Turner, C. A., Geske, R., Montgomery, C. A., *et al.* (2001). Proteinuria and perinatal lethality in mice lacking NEPH1, a novel protein with homology to NEPHRIN. *Mol Cell Biol* **21**, https://doi.org/10.1128/MCB.21.14.4829-4836.2001

Dorer, F. E., Kahn, J. R., Lentz, K. E., Levine, M. and Skeggs, L. T. (1975). Formation of angiotensin II from tetradecapeptide renin substrate by angiotensin-converting enzyme. *Biochem Pharmacol* **24**, https://doi.org/10.1016/0006-2952(75)90207-5

Drake, C. J. and Fleming, P. A. (2000). Vasculogenesis in the day 6.5 to 9.5 mouse embryo. *Blood* **95**, https://www.ncbi.nlm.nih.gov/pubmed/10688823

Duband, J. L., Gimona, M., Scatena, M., Sartore, S. and Small, J. V. (1993). Calponin and SM 22 as differentiation markers of smooth muscle: spatiotemporal distribution during avian embryonic development. *Differentiation* **55**, https://doi.org/10.1111/j.1432-0436.1993.tb00027.x

Dudley, A. T., Godin, R. E. and Robertson, E. J. (1999). Interaction between FGF and BMP signaling pathways regulates development of metanephric mesenchyme. *Genes Dev* **13**, https://doi.org/10.1101/gad.13.12.1601

Ekblom, P., Ekblom, M., Fecker, L., Klein, G., Zhang, H. Y., Kadoya, Y., Chu, M. L., Mayer, U. and Timpl, R. (1994). Role of mesenchymal nidogen for epithelial morphogenesis in vitro. *Development* **120**, https://www.ncbi.nlm.nih.gov/pubmed/7925005

Ekblom, P., Lehtonen, E., Saxen, L. and Timpl, R. (1981). Shift in collagen type as an early response to induction of the metanephric mesenchyme. *J Cell Biol* **89**, https://doi.org/10.1083/jcb.89.2.276

Ekblom, P., Sariola, H., Karkinen-Jaaskelainen, M. and Saxen, L. (1982). The origin of the glomerular endothelium. *Cell Differ* **11**, https://doi.org/10.1016/0045-6039(82)90014-8

Eknoyan, G., Lameire, N., Eckardt, K., Kasiske, B., Wheeler, D., Levin, A., Stevens, P. E., Bilous, R. W., Lamb, E. J. and Coresh, J. (2013). KDIGO 2012 clinical practice guideline for the evaluation and management of chronic kidney disease. *Kidney Int* **3**, https://kdigo.org/guidelines/ckd-evaluation-and-management/

Eoh, J. H., Shen, N., Burke, J. A., Hinderer, S., Xia, Z., Schenke-Layland, K. and Gerecht, S. (2017). Enhanced elastin synthesis and maturation in human vascular smooth muscle tissue derived from induced-pluripotent stem cells. *Acta Biomater* **52**, https://doi.org/10.1016/j.actbio.2017.01.083

Eremina, V., Sood, M., Haigh, J., Nagy, A., Lajoie, G., Ferrara, N., Gerber, H. P., Kikkawa, Y., Miner, J. H. and Quaggin, S. E. (2003). Glomerular-specific alterations of VEGF-A expression lead to distinct congenital and acquired renal diseases. *J Clin Invest* **111**, https://doi.org/10.1172/JCI17423

Falk, M., Salmivirta, K., Durbeej, M., Larsson, E., Ekblom, M., Vestweber, D. and Ekblom, P. (1996). Integrin alpha 6B beta 1 is involved in kidney tubulogenesis in vitro. *Journal of Cell Science* **109**, https://jcs.biologists.org/content/109/12/2801.long

Fang, Y. and Eglen, R. M. (2017). Three-Dimensional Cell Cultures in Drug Discovery and Development. *SLAS Discov* **22**, https://doi.org/10.1177/1087057117696795

Farquhar, M. G., Wissig, S. L. and Palade, G. E. (1961). Glomerular permeability. I. Ferritin transfer across the normal glomerular capillary wall. *J Exp Med* **113**, https://doi.org/10.1084/jem.113.1.47

Fell, H. B. and Robison, R. (1929). The growth, development and phosphatase activity of embryonic avian femora and limb-buds cultivated in vitro. *Biochem J* **23**, https://doi.org/10.1042/bj0230767

Fels, B. and Kusche-Vihrog, K. (2020). It takes more than two to tango: mechanosignaling of the endothelial surface. *Pflugers Arch* **472**, https://doi.org/10.1007/s00424-020-02369-2

Fierlbeck, W., Liu, A., Coyle, R. and Ballermann, B. J. (2003). Endothelial cell apoptosis during glomerular capillary lumen formation in vivo. *J Am Soc Nephrol* **14**, https://doi.org/10.1097/01.asn.0000061779.70530.06

Francis, C. R., Claflin, S. and Kushner, E. J. (2021). Synaptotagmin-like protein 2a regulates lumen formation via Weibel-Palade body apical secretion of angiopoietin-2 during angiogenesis. *bioRxiv*, https://doi.org/10.1101/2021.02.15.431296

Fraser, D. R. and Kodicek, E. (1970). Unique biosynthesis by kidney of a biological active vitamin D metabolite. *Nature* **228**, https://doi.org/10.1038/228764a0

Frontini, M. J., Nong, Z., Gros, R., Drangova, M., O'Neil, C., Rahman, M. N., Akawi, O., Yin, H., Ellis, C. G. and Pickering, J. G. (2011). Fibroblast growth factor 9 delivery during angiogenesis produces durable, vasoresponsive microvessels wrapped by smooth muscle cells. *Nat Biotechnol* **29**, https://doi.org/10.1038/nbt.1845

Fukumura, D., Gohongi, T., Kadambi, A., Izumi, Y., Ang, J., Yun, C.-O., Buerk, D. G., Huang, P. L. and Jain, R. K. (2001). Predominant role of endothelial nitric oxide synthase in vascular endothelial growth factor-induced angiogenesis and vascular permeability.

Proceedings of the National Academy of Sciences **98**, https://doi.org/10.1073/pnas.041359198

Ganeva, V., Unbekandt, M. and Davies, J. A. (2011). An improved kidney dissociation and reaggregation culture system results in nephrons arranged organotypically around a single collecting duct system. *Organogenesis* **7**, https://doi.org/10.4161/org.7.2.14881

Gardner, M. J. and Altman, D. G. (1986). Confidence intervals rather than P values: estimation rather than hypothesis testing. *Br Med J (Clin Res Ed)* **292**, https://doi.org/10.1136/bmj.292.6522.746

Garg, A., Bhattacharya, A. and Batish, A. (2015). On Surface Finish and Dimensional Accuracy of FDM Parts after Cold Vapor Treatment. *Materials and Manufacturing Processes* **31**, https://www.tandfonline.com/doi/abs/10.1080/10426914.2015.1070425

Garreta, E., Prado, P., Tarantino, C., Oria, R., Fanlo, L., Marti, E., Zalvidea, D., Trepat, X., Roca-Cusachs, P., Gavalda-Navarro, A., *et al.* (2019). Fine tuning the extracellular environment accelerates the derivation of kidney organoids from human pluripotent stem cells. *Nat Mater* **18**, https://doi.org/10.1038/s41563-019-0287-6

Gauvin, R., Ahsan, T., Larouche, D., Levesque, P., Dube, J., Auger, F. A., Nerem, R. M. and Germain, L. (2010). A novel single-step self-assembly approach for the fabrication of tissue-engineered vascular constructs. *Tissue Eng Part A* **16**, https://doi.org/10.1089/ten.TEA.2009.0313

Gelati, M., Aplin, A. C., Fogel, E., Smith, K. D. and Nicosia, R. F. (2008). The angiogenic response of the aorta to injury and inflammatory cytokines requires macrophages. *J Immunol* **181**, https://doi.org/10.4049/jimmunol.181.8.5711

Georgas, K., Rumballe, B., Valerius, M. T., Chiu, H. S., Thiagarajan, R. D., Lesieur, E., Aronow, B. J., Brunskill, E. W., Combes, A. N., Tang, D., *et al.* (2009). Analysis of early nephron patterning reveals a role for distal RV proliferation in fusion to the ureteric tip via a cap mesenchyme-derived connecting segment. *Dev Biol* **332**, https://doi.org/10.1016/j.ydbio.2009.05.578

Gerhardt, H., Golding, M., Fruttiger, M., Ruhrberg, C., Lundkvist, A., Abramsson, A., Jeltsch, M., Mitchell, C., Alitalo, K., Shima, D., *et al.* (2003). VEGF guides angiogenic sprouting utilizing endothelial tip cell filopodia. *J Cell Biol* **161**, https://doi.org/10.1083/jcb.200302047

Gjorevski, N., Sachs, N., Manfrin, A., Giger, S., Bragina, M. E., Ordonez-Moran, P., Clevers, H. and Lutolf, M. P. (2016). Designer matrices for intestinal stem cell and organoid culture. *Nature* **539**, https://doi.org/10.1038/nature20168

Glicklis, R., Merchuk, J. C. and Cohen, S. (2004). Modeling mass transfer in hepatocyte spheroids via cell viability, spheroid size, and hepatocellular functions. *Biotechnol Bioeng* **86**, https://doi.org/10.1002/bit.20086

Goldblatt, H., Lynch, J., Hanzal, R. F. and Summerville, W. W. (1934). Studies on Experimental Hypertension : I. The Production of Persistent Elevation of Systolic Blood Pressure by Means of Renal Ischemia. *J Exp Med* **59**, https://doi.org/10.1084/jem.59.3.347

Gosling, J. A. and Dixon, J. S. (1971). Morphologic evidence that the renal calyx and pelvis control ureteric activity in the rabbit. *American Journal of Anatomy* **130**, https://doi.org/10.1002/aja.1001300403

Gosling, J. A. and Waas, A. N. C. (1971). The behaviour of the isolated rabbit renal calix and pelvis compared with that of the ureter. *European Journal of Pharmacology* **16**, https://www.sciencedirect.com/science/article/pii/0014299971900616

Gown, A. M. and Willingham, M. C. (2002). Improved detection of apoptotic cells in archival paraffin sections: immunohistochemistry using antibodies to cleaved caspase 3. *J Histochem Cytochem* **50**, https://doi.org/10.1177/002215540205000401

Gray, R., Boyle, I. and DeLuca, H. F. (1971). Vitamin D metabolism: the role of kidney tissue. *Science* **172**, https://doi.org/10.1126/science.172.3989.1232

Greenberg, J. I., Shields, D. J., Barillas, S. G., Acevedo, L. M., Murphy, E., Huang, J., Scheppke, L., Stockmann, C., Johnson, R. S., Angle, N., *et al.* (2008). A role for VEGF as a negative regulator of pericyte function and vessel maturation. *Nature* **456**, https://doi.org/10.1038/nature07424

Grobstein, C. (1956). Trans-filter induction of tubules in mouse metanephrogenic mesenchyme. *Exp Cell Res* **10**, https://doi.org/10.1016/0014-4827(56)90016-7

Hamburger, V. and Levi-Montalcini, R. (1949). Proliferation, differentiation and degeneration in the spinal ganglia of the chick embryo under normal and experimental conditions. *Journal of Experimental Zoology* **111**, https://doi.org/10.1002/jez.1401110308

Hamilton, N. B., Attwell, D. and Hall, C. N. (2010). Pericyte-mediated regulation of capillary diameter: a component of neurovascular coupling in health and disease. *Front Neuroenergetics* **2**, https://doi.org/10.3389/fnene.2010.00005

Harding, S. D., Armit, C., Armstrong, J., Brennan, J., Cheng, Y., Haggarty, B., Houghton, D., Lloyd-MacGilp, S., Pi, X., Roochun, Y., *et al.* (2011). The GUDMAP database--an online resource for genitourinary research. *Development* **138**, https://doi.org/10.1242/dev.063594

Harrison, R. G., Greenman, M. J., Mall, F. P. and Jackson, C. M. (1907). Observations of the living developing nerve fiber. *The Anatomical Record* **1**, https://doi.org/10.1002/ar.1090010503

Hashimoto, J. and Ito, S. (2015). Aortic Blood Flow Reversal Determines Renal Function. *Hypertension* **66**, https://doi.org/10.1161/HYPERTENSIONAHA.115.05236

Heckel, E., Boselli, F., Roth, S., Krudewig, A., Belting, H. G., Charvin, G. and Vermot, J. (2015). Oscillatory Flow Modulates Mechanosensitive klf2a Expression through trpv4 and trpp2 during Heart Valve Development. *Curr Biol* **25**, https://doi.org/10.1016/j.cub.2015.03.038

Heidemann, J., Ogawa, H., Dwinell, M. B., Rafiee, P., Maaser, C., Gockel, H. R., Otterson, M. F., Ota, D. M., Lugering, N., Domschke, W., *et al.* (2003). Angiogenic effects of interleukin 8 (CXCL8) in human intestinal microvascular endothelial cells are mediated by CXCR2. *J Biol Chem* **278**, https://doi.org/10.1074/jbc.M208231200

Heistad, D. D., Marcus, M. L., Larsen, G. E. and Armstrong, M. L. (1981). Role of vasa vasorum in nourishment of the aortic wall. *Am J Physiol* **240**, https://doi.org/10.1152/ajpheart.1981.240.5.H781

Hellmuth, K., Grosskopf, S., Lum, C., Würtele, M., Röder, N., Kries, J., Rosário, M., Rademann, J. and Birchmeier, W. (2008). Specific inhibitors of the protein tyrosine phosphatase Shp2 identified by high-throughput docking. *Proceedings of the National Academy of Sciences of the United States of America* **105**, https://doi.org/10.1073/pnas.0710468105

Hellstrom, M., Kalen, M., Lindahl, P., Abramsson, A. and Betsholtz, C. (1999). Role of PDGF-B and PDGFR-beta in recruitment of vascular smooth muscle cells and pericytes during embryonic blood vessel formation in the mouse. *Development* **126**, https://www.ncbi.nlm.nih.gov/pubmed/10375497

Hellstrom, M., Phng, L. K., Hofmann, J. J., Wallgard, E., Coultas, L., Lindblom, P., Alva, J., Nilsson, A. K., Karlsson, L., Gaiano, N., *et al.* (2007). Dll4 signalling through Notch1 regulates formation of tip cells during angiogenesis. *Nature* **445**, https://doi.org/10.1038/nature05571

Henle, J. (1862). *Zur Anatomie der Niere*. Göttingen: Univ.-Bibl.

Heydarkhan-Hagvall, S., Helenius, G., Johansson, B. R., Li, J. Y., Mattsson, E. and Risberg, B. (2003). Co-culture of endothelial cells and smooth muscle cells affects gene expression of angiogenic factors. *J Cell Biochem* **89**, https://doi.org/10.1002/jcb.10583

Hilliard, S. A., Yao, X. and El-Dahr, S. S. (2014). Mdm2 is required for maintenance of the nephrogenic niche. https://doi.org/10.1016/j.ydbio.2014.01.009

Hironaka, K., Makino, H., Yamasaki, Y. and Ota, Z. (1993). Pores in the glomerular basement membrane revealed by ultrahigh-resolution scanning electron microscopy. *Nephron* **64**, https://doi.org/10.1159/000187418

His, W. (1900). *Lecithoblast und Angioblast der Wirbeltiere: histogenetische Studien*. Leipzig: Teubner.

Hisha, H., Tanaka, T., Kanno, S., Tokuyama, Y., Komai, Y., Ohe, S., Yanai, H., Omachi, T. and Ueno, H. (2013). Establishment of a novel lingual organoid culture system: generation of organoids having mature keratinized epithelium from adult epithelial stem cells. *Sci Rep* **3**, https://doi.org/10.1038/srep03224

Hjalmarsson, C., Johansson, B. R. and Haraldsson, B. (2004). Electron microscopic evaluation of the endothelial surface layer of glomerular capillaries. *Microvasc Res* **67**, https://doi.org/10.1016/j.mvr.2003.10.001

Homan, K. A., Gupta, N., Kroll, K. T., Kolesky, D. B., Skylar-Scott, M., Miyoshi, T., Mau, D., Valerius, M. T., Ferrante, T., Bonventre, J. V., *et al.* (2019). Flow-enhanced vascularization and maturation of kidney organoids in vitro. *Nat Methods* **16**, https://doi.org/10.1038/s41592-019-0325-y

Hum, S., Rymer, C., Schaefer, C., Bushnell, D. and Sims-Lucas, S. (2014). Ablation of the renal stroma defines its critical role in nephron progenitor and vasculature patterning. *PLoS One* **9**, https://doi.org/10.1371/journal.pone.0088400

Humar, R., Kiefer, F. N., Berns, H., Resink, T. J. and Battegay, E. J. (2002). Hypoxia enhances vascular cell proliferation and angiogenesis in vitro via rapamycin (mTOR) -dependent signaling. *The FASEB Journal* **16**, https://doi.org/10.1096/fj.01-0658com

Hurtado, R., Zewdu, R., Mtui, J., Liang, C., Aho, R., Kurylo, C., Selleri, L. and Herzlinger, D. (2015). Pbx1-dependent control of VMC differentiation kinetics underlies gross renal vascular patterning. *Development* **142**, https://doi.org/10.1242/dev.124776

Hyink, D. P., Tucker, D. C., St John, P. L., Leardkamolkarn, V., Accavitti, M. A., Abrass, C. K. and Abrahamson, D. R. (1996). Endogenous origin of glomerular endothelial and mesangial cells in grafts of embryonic kidneys. *Am J Physiol* **270**, https://doi.org/10.1152/ajprenal.1996.270.5.F886

Iivanainen, E., Nelimarkka, L., Elenius, V., Heikkinen, S. M., Junttila, T. T., Sihombing, L., Sundvall, M., Maatta, J. A., Laine, V. J., Yla-Herttuala, S., *et al.* (2003). Angiopoietin-regulated recruitment of vascular smooth muscle cells by endothelial-derived heparin binding EGF-like growth factor. *FASEB J* **17**, https://doi.org/10.1096/fj.02-0939com

Isogai, S., Horiguchi, M. and Hitomi, J. (2010). The para-aortic ridge plays a key role in the formation of the renal, adrenal and gonadal vascular systems. *J Anat* **216**, https://doi.org/10.1111/j.1469-7580.2010.01230.x

Itoh, Y., Sendo, T. and Oishi, R. (2005). Physiology and pathophysiology of proteinase-activated receptors (PARs): role of tryptase/PAR-2 in vascular endothelial barrier function. *J Pharmacol Sci* **97**, https://doi.org/10.1254/jphs.fmj04005x3

Jacobson, L. O., Goldwasser, E., Fried, W. and Plzak, L. (1957). Role of the kidney in erythropoiesis. *Nature* **179**, https://doi.org/10.1038/179633a0

Jacobson, L. O., Plazak, L., Fried, W. and Goldwasser, E. (1956). Plasma factor(s) influencing red cell production. *Nature* **177**, https://doi.org/10.1038/1771240a0

Janse, E. M. and Jeurissen, S. H. (1991). Ontogeny and function of two non-lymphoid cell populations in the chicken embryo. *Immunobiology* **182**, https://doi.org/10.1016/s0171-2985(11)80211-1

Jaquet, K., Krause, K., Tawakol-Khodai, M., Geidel, S. and Kuck, K. H. (2002). Erythropoietin and VEGF exhibit equal angiogenic potential. *Microvasc Res* **64**, https://doi.org/10.1006/mvre.2002.2426

Johnson, A. K., Mann, J. F., Rascher, W., Johnson, J. K. and Ganten, D. (1981). Plasma angiotensin II concentrations and experimentally induced thirst. *Am J Physiol* **240**, https://doi.org/10.1152/ajpregu.1981.240.3.R229

Jordan, T. D. (1984). *A handbook of gravity-flow water systems for small communities*. London, UK: IT Publications.

Ju, Y. M., Ahn, H., Arenas-Herrera, J., Kim, C., Abolbashari, M., Atala, A., Yoo, J. J. and Lee, S. J. (2017). Electrospun vascular scaffold for cellularized small diameter blood vessels: A preclinical large animal study. *Acta Biomater* **59**, https://doi.org/10.1016/j.actbio.2017.06.027

Karavanov, A., Sainio, K., Palgi, J., Saarmat, M., Saxen, L., Sariola, H. and Dawid, I. B. (1995). Neurotrophin 3 rescues neuronal precursors from apoptosis and promotes neuronal differentiation in the embryonic metanephric kidney. **92**, https://doi.org/10.1073/pnas.92.24.11279

Ke, Q. and Costa, M. (2006). Hypoxia-inducible factor-1 (HIF-1). *Mol Pharmacol* **70**, https://doi.org/10.1124/mol.106.027029

Keller, B. B., MacLennan, M. J., Tinney, J. P. and Yoshigi, M. (1996). In vivo assessment of embryonic cardiovascular dimensions and function in day-10.5 to -14.5 mouse embryos. *Circ Res* **79**, https://doi.org/10.1161/01.res.79.2.247

Kerjaschki, D., Sharkey, D. J. and Farquhar, M. G. (1984). Identification and characterization of podocalyxin--the major sialoprotein of the renal glomerular epithelial cell. *J Cell Biol* **98**, https://doi.org/10.1083/jcb.98.4.1591

Kestilä, M., Lenkkeri, U., Männikkö, M., Lamerdin, J., McCready, P., Putaala, H., Ruotsalainen, V., Morita, T., Nissinen, M., Herva, R., *et al.* (1998). Positionally Cloned Gene for a Novel Glomerular Protein—Nephrin—Is Mutated in Congenital Nephrotic Syndrome. *Molecular Cell* **1**, https://doi.org/10.1016/s1097-2765(00)80057-x

Kim, J., Lee, G. S., Tisher, C. C. and Madsen, K. M. (1996). Role of apoptosis in development of the ascending thin limb of the loop of Henle in rat kidney. *Am J Physiol* **271**, https://doi.org/10.1152/ajprenal.1996.271.4.F831

Kleinman, H. K., McGarvey, M. L., Liotta, L. A., Robey, P. G., Tryggvason, K. and Martin, G. R. (1982). Isolation and characterization of type IV procollagen, laminin, and heparan sulfate proteoglycan from the EHS sarcoma. *Biochemistry* **21**, https://doi.org/10.1021/bi00267a025

Klingberg, A., Hasenberg, A., Ludwig-Portugall, I., Medyukhina, A., Mann, L., Brenzel, A., Engel, D. R., Figge, M. T., Kurts, C. and Gunzer, M. (2017). Fully Automated

Evaluation of Total Glomerular Number and Capillary Tuft Size in Nephritic Kidneys Using Lightsheet Microscopy. *J Am Soc Nephrol* **28**, https://doi.org/10.1681/ASN.2016020232

Knepper, M. A. (1982). Measurement of osmolality in kidney slices using vapor pressure osmometry. *Kidney Int* **21**, https://doi.org/10.1038/ki.1982.73

Kobayashi, H., DeBusk, L. M., Babichev, Y. O., Dumont, D. J. and Lin, P. C. (2006). Hepatocyte growth factor mediates angiopoietin-induced smooth muscle cell recruitment. *Blood* **108**, https://doi.org/10.1182/blood-2005-09-012807

Koblizek, T. I., Weiss, C., Yancopoulos, G. D., Deutsch, U. and Risau, W. (1998). Angiopoietin-1 induces sprouting angiogenesis in vitro. *Curr Biol* **8**, https://doi.org/10.1016/s0960-9822(98)70205-2

Kohlstaedt, K. G. and Page, I. H. (1940). The Liberation of Renin by Perfusion of Kidneys Following Reduction of Pulse Pressure. *J Exp Med* **72**, https://doi.org/10.1084/jem.72.2.201

Kreissl, M. C., Wu, H. M., Stout, D. B., Ladno, W., Schindler, T. H., Zhang, X., Prior, J. O., Prins, M. L., Chatziioannou, A. F., Huang, S. C., *et al.* (2006). Noninvasive measurement of cardiovascular function in mice with high-temporal-resolution small-animal PET. *J Nucl Med* **47**, https://www.ncbi.nlm.nih.gov/pubmed/16741307

Krogh, A. (1919). The number and distribution of capillaries in muscles with calculations of the oxygen pressure head necessary for supplying the tissue. *J Physiol* **52**, https://doi.org/10.1113/jphysiol.1919.sp001839

Kubota, Y., Kleinman, H. K., Martin, G. R. and Lawley, T. J. (1988). Role of laminin and basement membrane in the morphological differentiation of human endothelial cells into capillary-like structures. *J Cell Biol* **107**, https://doi.org/10.1083/jcb.107.4.1589

Kuhn, W. (1959). [Hairpin countercurrent principle as the basis of urine concentration in the kidney]. *Klin Wochenschr* **37**, https://doi.org/10.1007/BF01483206

Kumar, S. V., Er, P. X., Lawlor, K. T., Motazedian, A., Scurr, M., Ghobrial, I., Combes, A. N., Zappia, L., Oshlack, A., Stanley, E. G., *et al.* (2019). Kidney micro-organoids in suspension culture as a scalable source of human pluripotent stem cell-derived kidney cells. *Development* **146**, https://doi.org/10.1242/dev.172361

Kuo, L., Davis, M. J. and Chilian, W. M. (1990). Endothelium-dependent, flow-induced dilation of isolated coronary arterioles. *Am J Physiol* **259**, https://doi.org/10.1152/ajpheart.1990.259.4.H1063

Kuzuya, M., Satake, S., Esaki, T., Yamada, K., Hayashi, T., Naito, M., Asai, K. and Iguchi, A. (1995). Induction of angiogenesis by smooth muscle cell-derived factor: possible role in neovascularization in atherosclerotic plaque. *J Cell Physiol* **164**, https://doi.org/10.1002/jcp.1041640324

L'Heureux, N., Dusserre, N., Konig, G., Victor, B., Keire, P., Wight, T. N., Chronos, N. A., Kyles, A. E., Gregory, C. R., Hoyt, G., *et al.* (2006). Human tissue-engineered blood vessels for adult arterial revascularization. *Nat Med* **12**, https://doi.org/10.1038/nm1364

Lam, C.-F., Peterson, T. E., Richardson, D. M., Croatt, A. J., d'Uscio, L. V., Nath, K. A. and Katusic, Z. S. (2006). Increased blood flow causes coordinated upregulation of arterial eNOS and biosynthesis of tetrahydrobiopterin. *American Journal of Physiology-Heart and Circulatory Physiology* **290**, https://doi.org/10.1152/ajpheart.00759.2005

Lang, R. J., Davidson, M. E. and Exintaris, B. (2002). Pyeloureteral motility and ureteral peristalsis: essential role of sensory nerves and endogenous prostaglandins. *Exp Physiol* **87**, https://doi.org/10.1113/eph8702290

Lawson, N. D., Scheer, N., Pham, V. N., Kim, C.-H., Chitnis, A. B., Campos-Ortega, J. A. and Weinstein, B. M. (2001). Notch signaling is required for arterial-venous differentiation during embryonic vascular development. *Development* **128**, https://dev.biologists.org/content/128/19/3675.long

le Noble, F., Moyon, D., Pardanaud, L., Yuan, L., Djonov, V., Matthijsen, R., Breant, C., Fleury, V. and Eichmann, A. (2004). Flow regulates arterial-venous differentiation in the chick embryo yolk sac. *Development* **131**, https://doi.org/10.1242/dev.00929

Le, V. P., Kovacs, A. and Wagenseil, J. E. (2012). Measuring left ventricular pressure in late embryonic and neonatal mice. *J Vis Exp*, https://doi.org/10.3791/3756

Lee, T. K., Hwang, H., Na, K. S., Kwon, J., Jeong, H.-S., Oh, P., Kim, H. K., Lim, S. T., Sohn, M.-H., Jeong, H.-J., *et al.* (2014). Effect of angiogenesis induced by consecutive intramuscular injections of vascular endothelial growth factor in a hindlimb ischemic mouse model. *Nucl Med Mol Imaging* **48**, https://doi.org/10.1007/s13139-014-0273-5

Levesque, M. J. and Nerem, R. M. (1985). The elongation and orientation of cultured endothelial cells in response to shear stress. *J Biomech Eng* **107**, https://doi.org/10.1115/1.3138567

Levin, A., Bakris, G. L., Molitch, M., Smulders, M., Tian, J., Williams, L. A. and Andress, D. L. (2007). Prevalence of abnormal serum vitamin D, PTH, calcium, and phosphorus in patients with chronic kidney disease: results of the study to evaluate early kidney disease. *Kidney Int* **71**, https://doi.org/10.1038/sj.ki.5002009

Li, H., Wijekoon, A. and Leipzig, N. D. (2012). 3D differentiation of neural stem cells in macroporous photopolymerizable hydrogel scaffolds. *PLoS One* **7**, https://doi.org/10.1371/journal.pone.0048824

Li, W., Kohara, H., Uchida, Y., James, J. M., Soneji, K., Cronshaw, D. G., Zou, Y. R., Nagasawa, T. and Mukouyama, Y. S. (2013). Peripheral nerve-derived CXCL12 and VEGF-A regulate the patterning of arterial vessel branching in developing limb skin. *Dev Cell* **24**, https://doi.org/10.1016/j.devcel.2013.01.009

Li, Z., Araoka, T., Wu, J., Liao, H. K., Li, M., Lazo, M., Zhou, B., Sui, Y., Wu, M. Z., Tamura, I., *et al.* (2016). 3D Culture Supports Long-Term Expansion of Mouse and Human Nephrogenic Progenitors. *Cell Stem Cell* **19**, https://doi.org/10.1016/j.stem.2016.07.016

Lindahl, P., Johansson, B. R., Leveen, P. and Betsholtz, C. (1997). Pericyte loss and microaneurysm formation in PDGF-B-deficient mice. *Science* **277**, https://doi.org/10.1126/science.277.5323.242

Lindstrom, N. O., Chang, C. H., Valerius, M. T., Hohenstein, P. and Davies, J. A. (2015a). Node retraction during patterning of the urinary collecting duct system. *J Anat* **226**, https://doi.org/10.1111/joa.12239

Lindstrom, N. O., Lawrence, M. L., Burn, S. F., Johansson, J. A., Bakker, E. R., Ridgway, R. A., Chang, C. H., Karolak, M. J., Oxburgh, L., Headon, D. J., *et al.* (2015b). Integrated beta-catenin, BMP, PTEN, and Notch signalling patterns the nephron. *Elife* **3**, https://doi.org/10.7554/eLife.04000

Liu, Z., Chen, S., Boyle, S., Zhu, Y., Zhang, A., Piwnica-Worms, D. R., Ilagan, M. X. G. and Kopan, R. (2013). The extracellular domain of Notch2 increases its cell-surface abundance and ligand responsiveness during kidney development. *Dev Cell* **25**, https://doi.org/10.1016/j.devcel.2013.05.022

Livak, K. J. and Schmittgen, T. D. (2001). Analysis of relative gene expression data using real-time quantitative PCR and the 2(-Delta Delta C(T)) Method. *Methods* **25**, https://doi.org/10.1006/meth.2001.1262

Loh, Q. L. and Choong, C. (2013). Three-dimensional scaffolds for tissue engineering applications: role of porosity and pore size. *Tissue Eng Part B Rev* **19**, https://doi.org/10.1089/ten.TEB.2012.0437

Loughna, S., Hardman, P., Landels, E., Jussila, L., Alitalo, K. and Woolf, A. S. (1997). A molecular and genetic analysis of renalglomerular capillary development. *Angiogenesis* **1**, https://doi.org/10.1023/A:1018357116559

Low, J. H., Li, P., Chew, E. G. Y., Zhou, B., Suzuki, K., Zhang, T., Lian, M. M., Liu, M., Aizawa, E., Rodriguez Esteban, C., *et al.* (2019). Generation of Human PSC-Derived Kidney Organoids with Patterned Nephron Segments and a De Novo Vascular Network. *Cell Stem Cell* **25**, https://doi.org/10.1016/j.stem.2019.06.009

Lu, Q., Liu, K., Zhang, W., Li, T., Shi, A.-H., Ding, H.-F., Yan, X.-P., Zhang, X.-F., Wu, R.-Q., Lv, Y., *et al.* (2020). End-to-end vascular anastomosis using a novel magnetic compression device in rabbits: a preliminary study. *Scientific Reports* **10**, https://doi.org/10.1038/s41598-020-62936-6

Lysyy, T., Bracaglia, L. G., Qin, L., Albert, C., Pober, J. S., Tellides, G., Saltzman, W. M. and Tietjen, G. T. (2020). Ex vivo isolated human vessel perfusion system for the design and assessment of nanomedicines targeted to the endothelium. *Bioengineering & Translational Medicine* **5**, https://doi.org/10.1002/btm2.10154

Maisonpierre, P. C., Suri, C., Jones, P. F., Bartunkova, S., Wiegand, S. J., Radziejewski, C., Compton, D., McClain, J., Aldrich, T. H., Papadopoulos, N., *et al.* (1997). Angiopoietin-2, a natural antagonist for Tie2 that disrupts in vivo angiogenesis. *Science* **277**, https://doi.org/10.1126/science.277.5322.55

Makanya, A. N., Stauffer, D., Ribatti, D., Burri, P. H. and Djonov, V. (2005). Microvascular growth, development, and remodeling in the embryonic avian kidney: the interplay between sprouting and intussusceptive angiogenic mechanisms. *Microsc Res Tech* **66**, https://doi.org/10.1002/jemt.20169

Mamo, T. M., Wittern, A. B., Kleppa, M. J., Bohnenpoll, T., Weiss, A. C. and Kispert, A. (2017). BMP4 uses several different effector pathways to regulate proliferation and differentiation in the epithelial and mesenchymal tissue compartments of the developing mouse ureter. *Hum Mol Genet* **26**, https://doi.org/10.1093/hmg/ddx242

Mao, Y., Francis-West, P. and Irvine, K. D. (2015). Fat4/Dchs1 signaling between stromal and cap mesenchyme cells influences nephrogenesis and ureteric bud branching. *Development* **142**, https://doi.org/10.1242/dev.122630

Marech, I., Leporini, C., Ammendola, M., Porcelli, M., Gadaleta, C. D., Russo, E., De Sarro, G. and Ranieri, G. (2016). Classical and non-classical proangiogenic factors as a target of antiangiogenic therapy in tumor microenvironment. *Cancer Lett* **380**, https://doi.org/10.1016/j.canlet.2015.07.028

Marfurt, C. F. and Echtenkamp, S. F. (1991). Sensory innervation of the rat kidney and ureter as revealed by the anterograde transport of wheat germ agglutinin-horseradish peroxidase (WGA-HRP) from dorsal root ganglia. *J Comp Neurol* **311**, https://doi.org/10.1002/cne.903110309

Mascall, K. S., Small, G. R., Gibson, G. and Nixon, G. F. (2012). Sphingosine-1-phosphate-induced release of TIMP-2 from vascular smooth muscle cells inhibits angiogenesis. *J Cell Sci* **125**, https://doi.org/10.1242/jcs.099044

Masson, V. V., Devy, L., Grignet-Debrus, C., Bernt, S., Bajou, K., Blacher, S., Roland, G., Chang, Y., Fong, T., Carmeliet, P., *et al.* (2002). Mouse Aortic Ring Assay: A New

Approach of the Molecular Genetics of Angiogenesis. *Biol Proced Online* **4**, https://doi.org/10.1251/bpo30

Mattot, V., Moons, L., Lupu, F., Chernavvsky, D., Gomez, R. A., Collen, D. and Carmeliet, P. (2002). Loss of the VEGF(164) and VEGF(188) isoforms impairs postnatal glomerular angiogenesis and renal arteriogenesis in mice. *J Am Soc Nephrol* **13**, https://doi.org/10.1097/01.asn.0000013925.19218.7b

McMahon, A. P., Aronow, B. J., Davidson, D. R., Davies, J. A., Gaido, K. W., Grimmond, S., Lessard, J. L., Little, M. H., Potter, S. S., Wilder, E. L., *et al.* (2008). GUDMAP: the genitourinary developmental molecular anatomy project. *J Am Soc Nephrol* **19**, https://doi.org/10.1681/ASN.2007101078

McMurtrey, R. J. (2016). Analytic Models of Oxygen and Nutrient Diffusion, Metabolism Dynamics, and Architecture Optimization in Three-Dimensional Tissue Constructs with Applications and Insights in Cerebral Organoids. *Tissue Eng Part C Methods* **22**, https://doi.org/10.1089/ten.TEC.2015.0375

Mehta, V. B. and Besner, G. E. (2007). HB-EGF promotes angiogenesis in endothelial cells via PI3-kinase and MAPK signaling pathways. *Growth Factors* **25**, https://doi.org/10.1080/08977190701773070

Mehta, V. B., Zhou, Y., Radulescu, A. and Besner, G. E. (2008). HB-EGF stimulates eNOS expression and nitric oxide production and promotes eNOS dependent angiogenesis. *Growth Factors* **26**, https://doi.org/10.1080/08977190802393596

Memberg, S. P. and Hall, A. K. (1995). Dividing neuron precursors express neuron-specific tubulin. *J Neurobiol* **27**, https://doi.org/10.1002/neu.480270104

Miano, J. M. and Olson, E. N. (1996). Expression of the smooth muscle cell calponin gene marks the early cardiac and smooth muscle cell lineages during mouse embryogenesis. *J Biol Chem* **271**, https://doi.org/10.1074/jbc.271.12.7095

Michos, O., Goncalves, A., Lopez-Rios, J., Tiecke, E., Naillat, F., Beier, K., Galli, A., Vainio, S. and Zeller, R. (2007). Reduction of BMP4 activity by gremlin 1 enables ureteric bud outgrowth and GDNF/WNT11 feedback signalling during kidney branching morphogenesis. *Development* **134**, https://doi.org/10.1242/dev.02861

Michos, O., Panman, L., Vintersten, K., Beier, K., Zeller, R. and Zuniga, A. (2004). Gremlin-mediated BMP antagonism induces the epithelial-mesenchymal feedback signaling controlling metanephric kidney and limb organogenesis. *Development* **131**, https://doi.org/10.1242/dev.01251

Mills, C. G., Lawrence, M. L., Munro, D. A. D., Elhendawi, M., Mullins, J. J. and Davies, J. A. (2017). Asymmetric BMP4 signalling improves the realism of kidney organoids. *Sci Rep* **7**, https://doi.org/10.1038/s41598-017-14809-8

Miyake, T., Cameron, A. M. and Hall, B. K. (1997). Variability of embryonic development among three inbred strains of mice. *Growth, development, and aging : GDA* **61**, http://www.ncbi.nlm.nih.gov/pubmed/9546105

Miyazaki, Y., Oshima, K., Fogo, A., Hogan, B. L. and Ichikawa, I. (2000). Bone morphogenetic protein 4 regulates the budding site and elongation of the mouse ureter. *J Clin Invest* **105**, https://doi.org/10.1172/JCI8256

Miyazaki, Y., Oshima, K., Fogo, A. and Ichikawa, I. (2003). Evidence that bone morphogenetic protein 4 has multiple biological functions during kidney and urinary tract development. *Kidney Int* **63**, https://doi.org/10.1046/j.1523-1755.2003.00834.x

Moe, S., Drueke, T., Cunningham, J., Goodman, W., Martin, K., Olgaard, K., Ott, S., Sprague, S., Lameire, N., Eknoyan, G., *et al.* (2006). Definition, evaluation, and classification

of renal osteodystrophy: a position statement from Kidney Disease: Improving Global Outcomes (KDIGO). *Kidney Int* **69**, https://doi.org/10.1038/sj.ki.5000414

Mompeo, B., Maranillo, E., Garcia-Touchard, A. and Sanudo, J. R. (2019). The morphogenesis of the renal plexus: Renal artery and sympathetic fibers. *Clin Anat* **32**, https://doi.org/10.1002/ca.23297

Moore, J. E., Jr., Bürki, E., Suciu, A., Zhao, S., Burnier, M., Brunner, H. R. and Meister, J. J. (1994). A device for subjecting vascular endothelial cells to both fluid shear stress and circumferential cyclic stretch. *Ann Biomed Eng* **22**, https://doi.org/10.1007/bf02368248

Moore, M. W., Klein, R. D., Farinas, I., Sauer, H., Armanini, M., Phillips, H., Reichardt, L. F., Ryan, A. M., Carver-Moore, K. and Rosenthal, A. (1996). Renal and neuronal abnormalities in mice lacking GDNF. *Nature* **382**, https://doi.org/10.1038/382076a0

Morizane, R. and Bonventre, J. V. (2017). Generation of nephron progenitor cells and kidney organoids from human pluripotent stem cells. *Nat Protoc* **12**, https://doi.org/10.1038/nprot.2016.170

Moyon, D., Pardanaud, L., Yuan, L., Breant, C. and Eichmann, A. (2001). Plasticity of endothelial cells during arterial-venous differentiation in the avian embryo. *Development* **128**, https://www.ncbi.nlm.nih.gov/pubmed/11546752

Mukouyama, Y. S., Gerber, H. P., Ferrara, N., Gu, C. and Anderson, D. J. (2005). Peripheral nerve-derived VEGF promotes arterial differentiation via neuropilin 1-mediated positive feedback. *Development* **132**, https://doi.org/10.1242/dev.01675

Müller, U., Wang, D., Denda, S., Meneses, J. J., Pedersen, R. A. and Reichardt, L. F. (1997). Integrin α8β1 Is Critically Important for Epithelial–Mesenchymal Interactions during Kidney Morphogenesis. *Cell* **88**, https://www.sciencedirect.com/science/article/pii/S0092867400819030?via%3Dihub#TBL1

Munro, D. A. D., Hohenstein, P. and Davies, J. A. (2017). Cycles of vascular plexus formation within the nephrogenic zone of the developing mouse kidney. *Sci Rep* **7**, https://doi.org/10.1038/s41598-017-03808-4

Munro, D. A. D., Wineberg, Y., Tarnick, J., Vink, C. S., Li, Z., Pridans, C., Dzierzak, E., Kalisky, T., Hohenstein, P. and Davies, J. A. (2019). Macrophages restrict the nephrogenic field and promote endothelial connections during kidney development. *Elife* **8**, https://doi.org/10.7554/eLife.43271

Murakami, Y., Naganuma, H., Tanigawa, S., Fujimori, T., Eto, M. and Nishinakamura, R. (2019). Reconstitution of the embryonic kidney identifies a donor cell contribution to the renal vasculature upon transplantation. *Sci Rep* **9**, https://doi.org/10.1038/s41598-018-37793-z

Murray, C. D. (1926). The Physiological Principle of Minimum Work: I. The Vascular System and the Cost of Blood Volume. *Proc Natl Acad Sci U S A* **12**, https://doi.org/10.1073/pnas.12.3.207

Naiman, N., Fujioka, K., Fujino, M., Valerius, M. T., Potter, S. S., McMahon, A. P. and Kobayashi, A. (2017). Repression of Interstitial Identity in Nephron Progenitor Cells by Pax2 Establishes the Nephron-Interstitium Boundary during Kidney Development. *Dev Cell* **41**, https://doi.org/10.1016/j.devcel.2017.04.022

Nakamura-Ishizu, A., Kurihara, T., Okuno, Y., Ozawa, Y., Kishi, K., Goda, N., Tsubota, K., Okano, H., Suda, T. and Kubota, Y. (2012). The formation of an angiogenic astrocyte template is regulated by the neuroretina in a HIF-1-dependent manner. *Dev Biol* **363**, https://doi.org/10.1016/j.ydbio.2011.12.027

Nam, S. A., Seo, E., Kim, J. W., Kim, H. W., Kim, H. L., Kim, K., Kim, T.-M., Ju, J. H., Gomez, I. G., Uchimura, K., *et al.* (2019). Graft immaturity and safety concerns in transplanted human kidney organoids. *Experimental & Molecular Medicine* **51**, https://doi.org/10.1038/s12276-019-0336-x

Nashimoto, Y., Hayashi, T., Kunita, I., Nakamasu, A., Torisawa, Y. S., Nakayama, M., Takigawa-Imamura, H., Kotera, H., Nishiyama, K., Miura, T., *et al.* (2017). Integrating perfusable vascular networks with a three-dimensional tissue in a microfluidic device. *Integr Biol (Camb)* **9**, https://doi.org/10.1039/c7ib00024c

Nauck, M., Karakiulakis, G., Perruchoud, A. P., Papakonstantinou, E. and Roth, M. (1998). Corticosteroids inhibit the expression of the vascular endothelial growth factor gene in human vascular smooth muscle cells. *Eur J Pharmacol* **341**, https://doi.org/10.1016/s0014-2999(97)01464-7

NEB.(2016).Tm Calculator. https://tmcalculator.neb.com/#!/main: https://tmcalculator.neb.com/#!/main

Nehls, V. and Drenckhahn, D. (1995). A novel, microcarrier-based in vitro assay for rapid and reliable quantification of three-dimensional cell migration and angiogenesis. *Microvasc Res* **50**, https://doi.org/10.1006/mvre.1995.1061

Neubauer, H., Adam, G., Seeger, H., Mueck, A. O., Solomayer, E., Wallwiener, D., Cahill, M. A. and Fehm, T. (2009). Membrane-initiated effects of progesterone on proliferation and activation of VEGF in breast cancer cells. *Climacteric* **12**, https://doi.org/10.1080/13697130802635637

Neufeld, G., Cohen, T., Gengrinovitch, S. and Poltorak, Z. (1999). Vascular endothelial growth factor (VEGF) and its receptors. *FASEB J* **13**, https://www.ncbi.nlm.nih.gov/pubmed/9872925

Nguyen, D. H., Stapleton, S. C., Yang, M. T., Cha, S. S., Choi, C. K., Galie, P. A. and Chen, C. S. (2013). Biomimetic model to reconstitute angiogenic sprouting morphogenesis in vitro. *Proc Natl Acad Sci U S A* **110**, https://doi.org/10.1073/pnas.1221526110

Nicosia, R. F. and Ottinetti, A. (1990). Growth of microvessels in serum-free matrix culture of rat aorta. A quantitative assay of angiogenesis in vitro. *Lab Invest* **63**, https://www.ncbi.nlm.nih.gov/pubmed/1695694

Nicosia, R. F., Tchao, R. and Leighton, J. (1982). Histotypic angiogenesis in vitro: light microscopic, ultrastructural, and radioautographic studies. *In Vitro* **18**, https://doi.org/10.1007/BF02810077

Niklason, L. E., Abbott, W., Gao, J., Klagges, B., Hirschi, K. K., Ulubayram, K., Conroy, N., Jones, R., Vasanawala, A., Sanzgiri, S., *et al.* (2001). Morphologic and mechanical characteristics of engineered bovine arteries. *J Vasc Surg* **33**, https://doi.org/10.1067/mva.2001.111747

Niklason, L. E., Gao, J., Abbott, W. M., Hirschi, K. K., Houser, S., Marini, R. and Langer, R. (1999). Functional arteries grown in vitro. *Science* **284**, https://doi.org/10.1126/science.284.5413.489

Nishimura, Y., Hsu, H. H. and Wang, P. C. (2016). Detection of initial angiogenesis from dorsal aorta into metanephroi and elucidation of its role in kidney development. *Regen Ther* **4**, https://doi.org/10.1016/j.reth.2016.01.003

Nocera, A. D., Comin, R., Salvatierra, N. A. and Cid, M. P. (2018). Development of 3D printed fibrillar collagen scaffold for tissue engineering. *Biomed Microdevices* **20**, https://doi.org/10.1007/s10544-018-0270-z

Nowak-Sliwinska, P., Segura, T. and Iruela-Arispe, M. L. (2014). The chicken chorioallantoic membrane model in biology, medicine and bioengineering. *Angiogenesis* **17**, https://doi.org/10.1007/s10456-014-9440-7

OpenStax (2016). *Anatomy and Physiology*: OpenStax.

Padget, R. L., Mohite, S. S., Hoog, T. G., Justis, B. S., Green, B. E. and Udan, R. S. (2019). Hemodynamic force is required for vascular smooth muscle cell recruitment to blood vessels during mouse embryonic development. *Mech Dev* **156**, https://doi.org/10.1016/j.mod.2019.02.002

Page, I. H. and Helmer, O. M. (1940). A Crystalline Pressor Substance (Angiotonin) Resulting from the Reaction between Renin and Renin-Activator. *J Exp Med* **71**, https://doi.org/10.1084/jem.71.1.29

Palit, S. and Kendrick, J. (2014). Vascular calcification in chronic kidney disease: role of disordered mineral metabolism. *Curr Pharm Des* **20**, https://doi.org/10.2174/13816128206661402121949 26

Pan, X., Suzuki, N., Hirano, I., Yamazaki, S., Minegishi, N. and Yamamoto, M. (2011). Isolation and characterization of renal erythropoietin-producing cells from genetically produced anemia mice. *PLoS One* **6**, https://doi.org/10.1371/journal.pone.0025839

Pankhurst, L., Robb, M. and Mumford, L. (2019). Kidney transplantation in the UK: a UK Transplant Registry analysis. *Journal of Kidney Care* **4**, http://www.magonlinelibrary.com/doi/10.12968/jokc.2019.4.1.12

Pardanaud, L., Pibouin-Fragner, L., Dubrac, A., Mathivet, T., English, I., Brunet, I., Simons, M. and Eichmann, A. (2016). Sympathetic Innervation Promotes Arterial Fate by Enhancing Endothelial ERK Activity. *Circ Res* **119**, https://doi.org/10.1161/CIRCRESAHA.116.308473

Park, J., Shrestha, R., Qiu, C., Kondo, A., Huang, S., Werth, M., Li, M., Barasch, J. and Suszták, K. (2018). Single-cell transcriptomics of the mouse kidney reveals potential cellular targets of kidney disease. In *Science*, pp. 1-10: American Association for the Advancement of Science.

Pepper, M. S., Ferrara, N., Orci, L. and Montesano, R. (1992). Potent synergism between vascular endothelial growth factor and basic fibroblast growth factor in the induction of angiogenesis in vitro. *Biochemical and Biophysical Research Communications* **189**, https://pubmed.ncbi.nlm.nih.gov/1281999/

https://pubmed.ncbi.nlm.nih.gov/1281999/?dopt=Abstract

Phipson, B., Er, P. X., Combes, A. N., Forbes, T. A., Howden, S. E., Zappia, L., Yen, H. J., Lawlor, K. T., Hale, L. J., Sun, J., *et al.* (2019). Evaluation of variability in human kidney organoids. *Nat Methods* **16**, https://doi.org/10.1038/s41592-018-0253-2

Pichel, J. G., Shen, L., Sheng, H. Z., Granholm, A. C., Drago, J., Grinberg, A., Lee, E. J., Huang, S. P., Saarma, M., Hoffer, B. J., *et al.* (1996). GDNF is required for kidney development and enteric innervation. *Cold Spring Harbor symposia on quantitative biology* **61**, http://www.ncbi.nlm.nih.gov/pubmed/9246473

Pittman, R. N. (2011). The Circulatory System and Oxygen Transport. https://www.ncbi.nlm.nih.gov/books/NBK54112/

Poon, C. (2020). Measuring the density and viscosity of culture media for optimized computational fluid dynamics analysis of in vitro devices. https://doi.org/10.1101/2020.08.25.266221

Potter, E. L. (1972). *Normal and abnormal development of the kidney*: Year Book Medical Publishers.

Presta, M., Dell'Era, P., Mitola, S., Moroni, E., Ronca, R. and Rusnati, M. (2005). Fibroblast growth factor/fibroblast growth factor receptor system in angiogenesis. *Cytokine Growth Factor Rev* **16**, https://doi.org/10.1016/j.cytogfr.2005.01.004

Pries, A. R. and Secomb, T. W. (2014). Making microvascular networks work: angiogenesis, remodeling, and pruning. *Physiology (Bethesda)* **29**, https://doi.org/10.1152/physiol.00012.2014

Prim, D. A., Menon, V., Hasanian, S., Carter, L., Shazly, T., Potts, J. D. and Eberth, J. F. (2018). Perfusion Tissue Culture Initiates Differential Remodeling of Internal Thoracic Arteries, Radial Arteries, and Saphenous Veins. *J Vasc Res* **55**, https://doi.org/10.1159/000492484

Pritchard-Jones, K., Fleming, S., Davidson, D., Bickmore, W., Porteous, D., Gosden, C., Bard, J., Buckler, A., Pelletier, J., Housman, D., *et al.* (1990). The candidate Wilms' tumour gene is involved in genitourinary development. *Nature* **346**, https://doi.org/10.1038/346194a0

Przepiorski, A., Sander, V., Tran, T., Hollywood, J. A., Sorrenson, B., Shih, J. H., Wolvetang, E. J., McMahon, A. P., Holm, T. M. and Davidson, A. J. (2018). A Simple Bioreactor-Based Method to Generate Kidney Organoids from Pluripotent Stem Cells. *Stem Cell Reports* **11**, https://doi.org/10.1016/j.stemcr.2018.06.018

Radzikinas, K., Aven, L., Jiang, Z., Tran, T., Paez-Cortez, J., Boppidi, K., Lu, J., Fine, A. and Ai, X. (2011). A Shh/miR-206/BDNF cascade coordinates innervation and formation of airway smooth muscle. *J Neurosci* **31**, https://doi.org/10.1523/JNEUROSCI.2745-11.2011

Rahilly, M. A. and Fleming, S. (1992). Differential expression of integrin alpha chains by renal epithelial cells. *J Pathol* **167**, https://doi.org/10.1002/path.1711670311

Ramella, M., Boccafoschi, F., Bellofatto, K., Follenzi, A., Fusaro, L., Boldorini, R., Casella, F., Porta, C., Settembrini, P. and Cannas, M. (2017). Endothelial MMP-9 drives the inflammatory response in abdominal aortic aneurysm (AAA). *Am J Transl Res* **9**, https://pubmed.ncbi.nlm.nih.gov/29312500

https://www.ncbi.nlm.nih.gov/pmc/articles/PMC5752898/

Reinmuth, N., Rensinghoff, S., Hintelmann, H., Bisping, G., Hilberg, F., Roth, G. J., Berdel, W. E., Thomas, M. and Mesters, R. M. (2004). Induction of PDGF-B expression in HUVECs by growth factors and conditioned medium derived from lung cancer cells. *Cancer Research* **64**, https://cancerres.aacrjournals.org/content/64/7_Supplement/829.4

Reiser, J., Kriz, W., Kretzler, M. and Mundel, P. (2000). The glomerular slit diaphragm is a modified adherens junction. *Journal of the American Society of Nephrology* **11**, https://jasn.asnjournals.org/content/11/1/1

Rennke, H. G. and Venkatachalam, M. A. (1977). Glomerular permeability: in vivo tracer studies with polyanionic and polycationic ferritins. *Kidney Int* **11**, https://doi.org/10.1038/ki.1977.6

Rezzola, S., Di Somma, M., Corsini, M., Leali, D., Ravelli, C., Polli, V. A. B., Grillo, E., Presta, M. and Mitola, S. (2019). VEGFR2 activation mediates the pro-angiogenic activity of BMP4. *Angiogenesis* **22**, https://doi.org/10.1007/s10456-019-09676-y

Ribatti, D., Ranieri, G., Nico, B., Benagiano, V. and Crivellato, E. (2011). Tryptase and chymase are angiogenic in vivo in the chorioallantoic membrane assay. *Int J Dev Biol* **55**, https://doi.org/10.1387/ijdb.103138dr

Riegel, J., Mayer, W. and van Havre, Y. (2001). FreeCAD.

Robbins, M. F. (2021). *Ultimate Electronics: Practical Circuit Design and Analysis*: CircuitLab, Inc.

Rocha, A. S. and Kokko, J. P. (1973). Sodium chloride and water transport in the medullary thick ascending limb of Henle. Evidence for active chloride transport. *J Clin Invest* **52**, https://doi.org/10.1172/JCI107223

Roh, J. D., Nelson, G. N., Brennan, M. P., Mirensky, T. L., Yi, T., Hazlett, T. F., Tellides, G., Sinusas, A. J., Pober, J. S., Saltzman, W. M., *et al.* (2008). Small-diameter biodegradable scaffolds for functional vascular tissue engineering in the mouse model. *Biomaterials* **29**, https://doi.org/10.1016/j.biomaterials.2007.11.041

Rohan, R. M., Fernandez, A., Udagawa, T., Yuan, J. and D'Amato, R. J. (2000). Genetic heterogeneity of angiogenesis in mice. *FASEB J* **14**, https://doi.org/10.1096/fasebj.14.7.871

Rosines, E., Johkura, K., Zhang, X., Schmidt, H. J., Decambre, M., Bush, K. T. and Nigam, S. K. (2010). Constructing kidney-like tissues from cells based on programs for organ development: toward a method of in vitro tissue engineering of the kidney. *Tissue Eng Part A* **16**, https://doi.org/10.1089/ten.TEA.2009.0548

Ruhrberg, C., Gerhardt, H., Golding, M., Watson, R., Ioannidou, S., Fujisawa, H., Betsholtz, C. and Shima, D. T. (2002). Spatially restricted patterning cues provided by heparin-binding VEGF-A control blood vessel branching morphogenesis. *Genes Dev* **16**, https://doi.org/10.1101/gad.242002

Rymer, C., Paredes, J., Halt, K., Schaefer, C., Wiersch, J., Zhang, G., Potoka, D., Vainio, S., Gittes, G. K., Bates, C. M., *et al.* (2014). Renal blood flow and oxygenation drive nephron progenitor differentiation. *Am J Physiol Renal Physiol* **307**, https://doi.org/10.1152/ajprenal.00208.2014

Rymer, C. C. and Sims-Lucas, S. (2015). In utero intra-cardiac tomato-lectin injections on mouse embryos to gauge renal blood flow. *J Vis Exp*, https://doi.org/10.3791/52398

Sabine, A., Agalarov, Y., Maby-El Hajjami, H., Jaquet, M., Hagerling, R., Pollmann, C., Bebber, D., Pfenniger, A., Miura, N., Dormond, O., *et al.* (2012). Mechanotransduction, PROX1, and FOXC2 cooperate to control connexin37 and calcineurin during lymphatic-valve formation. *Dev Cell* **22**, https://doi.org/10.1016/j.devcel.2011.12.020

Sainio, K., Suvanto, P., Davies, J., Wartiovaara, J., Wartiovaara, K., Saarma, M., Arumae, U., Meng, X., Lindahl, M., Pachnis, V., *et al.* (1997). Glial-cell-line-derived neurotrophic factor is required for bud initiation from ureteric epithelium. **124**, http://www.ncbi.nlm.nih.gov/pubmed/9374404

Sakaguchi, K., Shimizu, T., Horaguchi, S., Sekine, H., Yamato, M., Umezu, M. and Okano, T. (2013). In vitro engineering of vascularized tissue surrogates. *Sci Rep* **3**, https://doi.org/10.1038/srep01316

Sakai, T. and Kriz, W. (1987). The structural relationship between mesangial cells and basement membrane of the renal glomerulus. *Anat Embryol (Berl)* **176**, https://doi.org/10.1007/BF00310191

Salcedo, R., Ponce, M. L., Young, H. A., Wasserman, K., Ward, J. M., Kleinman, H. K., Oppenheim, J. J. and Murphy, W. J. (2000). Human endothelial cells express CCR2 and respond to MCP-1: direct role of MCP-1 in angiogenesis and tumor progression. *Blood* **96**, https://www.ncbi.nlm.nih.gov/pubmed/10891427

Sanders, M. F., Reitsma, J. B., Morpey, M., Gremmels, H., Bots, M. L., Pisano, A., Bolignano, D., Zoccali, C. and Blankestijn, P. J. (2017). Renal safety of catheter-based renal denervation: systematic review and meta-analysis. *Nephrol Dial Transplant* **32**, https://doi.org/10.1093/ndt/gfx088

Sands, J. M., Nonoguchi, H. and Knepper, M. A. (1987). Vasopressin effects on urea and H2O transport in inner medullary collecting duct subsegments. *Am J Physiol* **253**, https://doi.org/10.1152/ajprenal.1987.253.5.F823

Sariola, H., Ekblom, P., Lehtonen, E. and Saxen, L. (1983). Differentiation and vascularization of the metanephric kidney grafted on the chorioallantoic membrane. *Dev Biol* **96**, https://doi.org/10.1016/0012-1606(83)90180-x

Sariola, H., Holm, K. and Henke-Fahle, S. (1988). Early innervation of the metanephric kidney. *Development* **104**, https://www.ncbi.nlm.nih.gov/pubmed/3268404

Sariola, H., Peault, B., LeDouarin, N., Buck, C., Dieterlen-Lievre, F. and Saxen, L. (1984a). Extracellular matrix and capillary ingrowth in interspecies chimeric kidneys. *Cell Differ* **15**, https://doi.org/10.1016/0045-6039(84)90028-9

Sariola, H., Timpl, R., von der Mark, K., Mayne, R., Fitch, J. M., Linsenmayer, T. F. and Ekblom, P. (1984b). Dual origin of glomerular basement membrane. *Dev Biol* **101**, https://doi.org/10.1016/0012-1606(84)90119-2

Sata, Y., Head, G. A., Denton, K., May, C. N. and Schlaich, M. P. (2018). Role of the Sympathetic Nervous System and Its Modulation in Renal Hypertension. *Front Med (Lausanne)* **5**, https://doi.org/10.3389/fmed.2018.00082

Saxén, L. (1987). *Organogenesis of the Kidney*. Cambridge: Cambridge University Press.

Schley, G., Scholz, H., Kraus, A., Hackenbeck, T., Klanke, B., Willam, C., Wiesener, M. S., Heinze, E., Burzlaff, N., Eckardt, K.-U., *et al.* (2015). Hypoxia inhibits nephrogenesis through paracrine Vegfa despite the ability to enhance tubulogenesis. *Kidney International* **88**, https://doi.org/10.1038/ki.2015.214

Schneider, C. A., Rasband, W. S. and Eliceiri, K. W. (2012). NIH Image to ImageJ: 25 years of image analysis. *Nature Methods* **9**, https://doi.org/10.1038/nmeth.2089

Schoefl, G. I. (1963). Studies on inflammation. *Virchows Archiv für Pathologische Anatomie und Physiologie und für Klinische Medizin* **337**, https://www.ncbi.nlm.nih.gov/pubmed/14098690

Sebinger, D. D., Ofenbauer, A., Gruber, P., Malik, S. and Werner, C. (2013). ECM modulated early kidney development in embryonic organ culture. *Biomaterials* **34**, https://doi.org/10.1016/j.biomaterials.2013.05.031

Sebinger, D. D., Unbekandt, M., Ganeva, V. V., Ofenbauer, A., Werner, C. and Davies, J. A. (2010). A novel, low-volume method for organ culture of embryonic kidneys that allows development of cortico-medullary anatomical organization. *PLoS One* **5**, https://doi.org/10.1371/journal.pone.0010550

Sekine, H., Shimizu, T., Sakaguchi, K., Dobashi, I., Wada, M., Yamato, M., Kobayashi, E., Umezu, M. and Okano, T. (2013). In vitro fabrication of functional three-dimensional tissues with perfusable blood vessels. *Nat Commun* **4**, https://doi.org/10.1038/ncomms2406

Sharifi, F., Firoozabadi, B. and Firoozbakhsh, K. (2019). Numerical Investigations of Hepatic Spheroids Metabolic Reactions in a Perfusion Bioreactor. *Front Bioeng Biotechnol* **7**, https://doi.org/10.3389/fbioe.2019.00221

Sharmin, S., Taguchi, A., Kaku, Y., Yoshimura, Y., Ohmori, T., Sakuma, T., Mukoyama, M., Yamamoto, T., Kurihara, H. and Nishinakamura, R. (2016). Human Induced Pluripotent Stem Cell-Derived Podocytes Mature into Vascularized Glomeruli upon Experimental Transplantation. *J Am Soc Nephrol* **27**, https://doi.org/10.1681/ASN.2015010096

Shigematsu, S., Yamauchi, K., Nakajima, K., Iijima, S., Aizawa, T. and Hashizume, K. (1999). IGF-1 regulates migration and angiogenesis of human endothelial cells. pp. 59-62: Japan Endocrine Society.

Shima, D. T., Kuroki, M., Deutsch, U., Ng, Y. S., Adamis, A. P. and D'Amore, P. A. (1996). The mouse gene for vascular endothelial growth factor. Genomic structure, definition of the transcriptional unit, and characterization of transcriptional and post-transcriptional regulatory sequences. *J Biol Chem* **271**, https://doi.org/10.1074/jbc.271.7.3877

Short, K. M., Combes, A. N., Lefevre, J., Ju, A. L., Georgas, K. M., Lamberton, T., Cairncross, O., Rumballe, B. A., McMahon, A. P., Hamilton, N. A., *et al.* (2014). Global quantification of tissue dynamics in the developing mouse kidney. *Dev Cell* **29**, https://doi.org/10.1016/j.devcel.2014.02.017

Shultz, T. D., Fox, J., Heath, H., 3rd and Kumar, R. (1983). Do tissues other than the kidney produce 1,25-dihydroxyvitamin D3 in vivo? A reexamination. *Proc Natl Acad Sci U S A* **80**, https://doi.org/10.1073/pnas.80.6.1746

Simon, M., Grone, H. J., Johren, O., Kullmer, J., Plate, K. H., Risau, W. and Fuchs, E. (1995). Expression of vascular endothelial growth factor and its receptors in human renal ontogenesis and in adult kidney. *Am J Physiol* **268**, https://doi.org/10.1152/ajprenal.1995.268.2.F240

Simon, M. C. and Keith, B. (2008). The role of oxygen availability in embryonic development and stem cell function. *Nat Rev Mol Cell Biol* **9**, https://doi.org/10.1038/nrm2354

Skeggs, L. T., Jr., Marsh, W. H., Kahn, J. R. and Shumway, N. P. (1954). The existence of two forms of hypertensin. *J Exp Med* **99**, https://doi.org/10.1084/jem.99.3.275

Slomiany, M. G. and Rosenzweig, S. A. (2004). IGF-1-induced VEGF and IGFBP-3 secretion correlates with increased HIF-1 alpha expression and activity in retinal pigment epithelial cell line D407. *Invest Ophthalmol Vis Sci* **45**, https://doi.org/10.1167/iovs.03-0565

Smiesko, V. and Johnson, P. C. (1993). The Arterial Lumen Is Controlled by Flow-Related Shear Stress. *Physiology* **8**, https://doi.org/10.1152/physiologyonline.1993.8.1.34

Stalmans, I., Lambrechts, D., De Smet, F., Jansen, S., Wang, J., Maity, S., Kneer, P., von der Ohe, M., Swillen, A., Maes, C., *et al.* (2003). VEGF: a modifier of the del22q11 (DiGeorge) syndrome? *Nat Med* **9**, https://doi.org/10.1038/nm819

Stalmans, I., Ng, Y. S., Rohan, R., Fruttiger, M., Bouche, A., Yuce, A., Fujisawa, H., Hermans, B., Shani, M., Jansen, S., *et al.* (2002). Arteriolar and venular patterning in retinas of mice selectively expressing VEGF isoforms. *J Clin Invest* **109**, https://doi.org/10.1172/JCI14362

Sternberg (1983). Biomedical Image Processing. *Computer* **16**, http://ieeexplore.ieee.org/document/1654163/

Stetler-Stevenson, W. G. (1999). Matrix metalloproteinases in angiogenesis: a moving target for therapeutic intervention. *J Clin Invest* **103**, https://doi.org/10.1172/JCI6870

Stothard, P.(2004).PCR Primer Stats. https://www.bioinformatics.org/sms2/pcr_primer_stats.html: https://www.bioinformatics.org/sms2/pcr_primer_stats.html

Stratman, A. N., Schwindt, A. E., Malotte, K. M. and Davis, G. E. (2010). Endothelial-derived PDGF-BB and HB-EGF coordinately regulate pericyte recruitment during vasculogenic tube assembly and stabilization. *Blood* **116**, https://doi.org/10.1182/blood-2010-05-286872

Strilic, B., Kucera, T., Eglinger, J., Hughes, M. R., McNagny, K. M., Tsukita, S., Dejana, E., Ferrara, N. and Lammert, E. (2009). The molecular basis of vascular lumen formation

in the developing mouse aorta. *Dev Cell* **17**, https://doi.org/10.1016/j.devcel.2009.08.011

Suri, C., Jones, P. F., Patan, S., Bartunkova, S., Maisonpierre, P. C., Davis, S., Sato, T. N. and Yancopoulos, G. D. (1996). Requisite role of angiopoietin-1, a ligand for the TIE2 receptor, during embryonic angiogenesis. *Cell* **87**, https://doi.org/10.1016/s0092-8674(00)81813-9

Surowiec, S. M., Conklin, B. S., Li, J. S., Lin, P. H., Weiss, V. J., Lumsden, A. B. and Chen, C. (2000). A new perfusion culture system used to study human vein. *J Surg Res* **88**, https://doi.org/10.1006/jsre.1999.5759

Sutera, S. P. and Skalak, R. (1993). The History of Poiseuille's Law. *Annual Review of Fluid Mechanics* **25**, https://doi.org/10.1146/annurev.fl.25.010193.000245

Swiatek-De Lange, M., Stampfl, A., Hauck, S. M., Zischka, H., Gloeckner, C. J., Deeg, C. A. and Ueffing, M. (2007). Membrane-initiated effects of progesterone on calcium dependent signaling and activation of VEGF gene expression in retinal glial cells. *Glia* **55**, https://doi.org/10.1002/glia.20523

Taguchi, A. and Nishinakamura, R. (2017). Higher-Order Kidney Organogenesis from Pluripotent Stem Cells. In *Cell Stem Cell*, pp. 730-746.e736: Elsevier.

Takahashi, Y., Sekine, K., Kin, T., Takebe, T. and Taniguchi, H. (2018). Self-Condensation Culture Enables Vascularization of Tissue Fragments for Efficient Therapeutic Transplantation. *Cell Rep* **23**, https://doi.org/10.1016/j.celrep.2018.03.123

Takasato, M., Er, P. X., Chiu, H. S. and Little, M. H. (2016). Generation of kidney organoids from human pluripotent stem cells. *Nat Protoc* **11**, https://doi.org/10.1038/nprot.2016.098

Takasato, M., Er, P. X., Chiu, H. S., Maier, B., Baillie, G. J., Ferguson, C., Parton, R. G., Wolvetang, E. J., Roost, M. S., Chuva de Sousa Lopes, S. M., *et al.* (2015). Kidney organoids from human iPS cells contain multiple lineages and model human nephrogenesis. *Nature* **526**, https://doi.org/10.1038/nature15695

Takeda, T., Go, W. Y., Orlando, R. A. and Farquhar, M. G. (2000). Expression of podocalyxin inhibits cell-cell adhesion and modifies junctional properties in Madin-Darby canine kidney cells. *Mol Biol Cell* **11**, https://doi.org/10.1091/mbc.11.9.3219

Tang, R., Zhang, G. and Chen, S. Y. (2016). Smooth Muscle Cell Proangiogenic Phenotype Induced by Cyclopentenyl Cytosine Promotes Endothelial Cell Proliferation and Migration. *J Biol Chem* **291**, https://doi.org/10.1074/jbc.M116.741967

Tanigawa, S., Taguchi, A., Sharma, N., Perantoni, A. O. and Nishinakamura, R. (2016). Selective In Vitro Propagation of Nephron Progenitors Derived from Embryos and Pluripotent Stem Cells. *Cell Rep* **15**, https://doi.org/10.1016/j.celrep.2016.03.076

Taugner, C., Poulsen, K., Hackenthal, E. and Taugner, R. (1979). Histochemistry Immunocytochemical Localization of Renin in Mouse Kidney. **62**, https://doi.org/10.1007/BF00537003

Taylor, C. J., Motamed, K. and Lilly, B. (2006). Protein kinase C and downstream signaling pathways in a three-dimensional model of phorbol ester-induced angiogenesis. *Angiogenesis* **9**, https://doi.org/10.1007/s10456-006-9028-y

Te Riet, L., van Esch, J. H., Roks, A. J., van den Meiracker, A. H. and Danser, A. H. (2015). Hypertension: renin-angiotensin-aldosterone system alterations. *Circ Res* **116**, https://doi.org/10.1161/CIRCRESAHA.116.303587

Teichert, M., Milde, L., Holm, A., Stanicek, L., Gengenbacher, N., Savant, S., Ruckdeschel, T., Hasanov, Z., Srivastava, K., Hu, J., *et al.* (2017). Pericyte-expressed Tie2 controls

angiogenesis and vessel maturation. *Nat Commun* **8**, https://doi.org/10.1038/ncomms16106

Theiler, K. (1989). *The House Mouse: Atlas of Embryonic Development*: Springer-Verlag.

Thoma, R. (1893). *Untersuchungen über die Histogenese und Histomechanik des Gefässsystems*: Enke.

Tischer, E., Mitchell, R., Hartman, T., Silva, M., Gospodarowiczs, D., Fiddes, J. C. and Abrahamll, J. A. (1991). The Human Gene for Vascular Endothelial Growth Factor MULTIPLE PROTEIN FORMS ARE ENCODED THROUGH ALTERNATIVE EXON SPLICING*. *THE JOURNAL OF BIOLOGICAL CHEMISTRY* **266**, http://www.jbc.org/content/266/18/11947.full.pdf

Tobian, L., Coffee, K., Ferreira, D. and Meuli, J. (1964). The Effect of Renal Perfusion Pressure on the Net Transport of Sodium out of Distal Tubular Urine as Studied with the Stop-Flow Technique. *J Clin Invest* **43**, https://doi.org/10.1172/JCI104886

Toffoli, S., Roegiers, A., Feron, O., Van Steenbrugge, M., Ninane, N., Raes, M. and Michiels, C. (2009). Intermittent hypoxia is an angiogenic inducer for endothelial cells: role of HIF-1. *Angiogenesis* **12**, https://doi.org/10.1007/s10456-009-9131-y

Tokuyama, E., Nagai, Y., Takahashi, K., Kimata, Y. and Naruse, K. (2015). Mechanical Stretch on Human Skin Equivalents Increases the Epidermal Thickness and Develops the Basement Membrane. *PLoS One* **10**, https://doi.org/10.1371/journal.pone.0141989

Tomkowicz, B., Rybinski, K., Sebeck, D., Sass, P., Nicolaides, N. C., Grasso, L. and Zhou, Y. (2010). Endosialin/TEM-1/CD248 regulates pericyte proliferation through PDGF receptor signaling. *Cancer Biol Ther* **9**, https://doi.org/10.4161/cbt.9.11.11731

Tondon, A. and Kaunas, R. (2014). The direction of stretch-induced cell and stress fiber orientation depends on collagen matrix stress. *PLoS One* **9**, https://doi.org/10.1371/journal.pone.0089592

Tovar Perez, J. E., Ortiz-Urbina, J., Heredia, C. P., Pham, T. T., Madala, S., Hartley, C. J., Entman, M. L., Taffet, G. E. and Reddy, A. K. (2021). Author Correction: Aortic acceleration as a noninvasive index of left ventricular contractility in the mouse. *Scientific Reports* **11**, https://doi.org/10.1038/s41598-021-87101-5

Trowell, O. A. (1954). A modified technique for organ culture in vitro. *Exp Cell Res* **6**, https://doi.org/10.1016/0014-4827(54)90169-x

Trujillo, S., Gonzalez-Garcia, C., Rico, P., Reid, A., Windmill, J., Dalby, M. J. and Salmeron-Sanchez, M. (2020). Engineered 3D hydrogels with full-length fibronectin that sequester and present growth factors. *Biomaterials* **252**, https://www.sciencedirect.com/science/article/pii/S0142961220303501

Tsuji, K., Kitamura, S. and Makino, H. (2014). Hypoxia-inducible factor 1alpha regulates branching morphogenesis during kidney development. *Biochem Biophys Res Commun* **447**, https://doi.org/10.1016/j.bbrc.2014.03.111

Tsuji, W., Inamoto, T., Yamashiro, H., Ueno, T., Kato, H., Kimura, Y., Tabata, Y. and Toi, M. (2009). Adipogenesis induced by human adipose tissue-derived stem cells. *Tissue Eng Part A* **15**, https://doi.org/10.1089/ten.tea.2007.0297

Udan, R. S., Culver, J. C. and Dickinson, M. E. (2013). Understanding vascular development. *Wiley Interdiscip Rev Dev Biol* **2**, https://doi.org/10.1002/wdev.91

Unbekandt, M. and Davies, J. A. (2010). Dissociation of embryonic kidneys followed by reaggregation allows the formation of renal tissues. *Kidney Int* **77**, https://doi.org/10.1038/ki.2009.482

van den Berg, C. W., Ritsma, L., Avramut, M. C., Wiersma, L. E., van den Berg, B. M., Leuning, D. G., Lievers, E., Koning, M., Vanslambrouck, J. M., Koster, A. J., *et al.* (2018). Renal Subcapsular Transplantation of PSC-Derived Kidney Organoids Induces Neo-

vasculogenesis and Significant Glomerular and Tubular Maturation In Vivo. *Stem Cell Reports* **10**, https://doi.org/10.1016/j.stemcr.2018.01.041

van Duinen, V., Zhu, D., Ramakers, C., van Zonneveld, A. J., Vulto, P. and Hankemeier, T. (2019). Perfused 3D angiogenic sprouting in a high-throughput in vitro platform. *Angiogenesis* **22**, https://doi.org/10.1007/s10456-018-9647-0

Vaughan, M. R. and Quaggin, S. E. (2008). How do mesangial and endothelial cells form the glomerular tuft? *J Am Soc Nephrol* **19**, https://doi.org/10.1681/ASN.2007040471

Villani, T. (2018). Loading and Measurement of Volumes in 3D Confocal Image Stacks with ImageJ | Visikol. In *Visicol*.

Villaschi, S. and Nicosia, R. F. (1994). Paracrine interactions between fibroblasts and endothelial cells in a serum-free coculture model. Modulation of angiogenesis and collagen gel contraction. *Lab Invest* **71**, https://www.ncbi.nlm.nih.gov/pubmed/7521446

Virtanen, P., Gommers, R., Oliphant, T. E., Haberland, M., Reddy, T., Cournapeau, D., Burovski, E., Peterson, P., Weckesser, W., Bright, J., *et al.* (2020). SciPy 1.0: fundamental algorithms for scientific computing in Python. *Nature Methods* **17**, https://doi.org/10.1038/s41592-019-0686-2

Vukicevic, S., Kleinman, H. K., Luyten, F. P., Roberts, A. B., Roche, N. S. and Reddi, A. H. (1992). Identification of multiple active growth factors in basement membrane Matrigel suggests caution in interpretation of cellular activity related to extracellular matrix components. *Exp Cell Res* **202**, https://doi.org/10.1016/0014-4827(92)90397-q

Wainwright, E. N., Wilhelm, D., Combes, A. N., Little, M. H. and Koopman, P. (2015). ROBO2 restricts the nephrogenic field and regulates Wolffian duct-nephrogenic cord separation. *Dev Biol* **404**, https://doi.org/10.1016/j.ydbio.2015.05.023

Wang, H. U., Chen, Z.-F. and Anderson, D. J. (1998). Molecular Distinction and Angiogenic Interaction between Embryonic Arteries and Veins Revealed by ephrin-B2 and Its Receptor Eph-B4. *Cell* **93**, https://www.sciencedirect.com/science/article/pii/S0092867400814361?via%3Dihub

Webb, A. R., Macrie, B. D., Ray, A. S., Russo, J. E., Siegel, A. M., Glucksberg, M. R. and Ameer, G. A. (2007). In Vitro Characterization of a Compliant Biodegradable Scaffold with a Novel Bioreactor System. *Annals of Biomedical Engineering* **35**, https://doi.org/10.1007/s10439-007-9304-z

Wiley, S. R., Cassiano, L., Lofton, T., Davis-Smith, T., Winkles, J. A., Lindner, V., Liu, H., Daniel, T. O., Smith, C. A. and Fanslow, W. C. (2001). A Novel TNF Receptor Family Member Binds TWEAK and Is Implicated in Angiogenesis. *Immunity* **15**, https://doi.org/10.1016/S1074-7613(01)00232-1

Williams, C., Kim, S. H., Ni, T. T., Mitchell, L., Ro, H., Penn, J. S., Baldwin, S. H., Solnica-Krezel, L. and Zhong, T. P. (2010). Hedgehog signaling induces arterial endothelial cell formation by repressing venous cell fate. *Dev Biol* **341**, https://doi.org/10.1016/j.ydbio.2010.02.028

Wimmer, R. A., Leopoldi, A., Aichinger, M., Wick, N., Hantusch, B., Novatchkova, M., Taubenschmid, J., Hammerle, M., Esk, C., Bagley, J. A., *et al.* (2019). Human blood vessel organoids as a model of diabetic vasculopathy. *Nature* **565**, https://doi.org/10.1038/s41586-018-0858-8

Winder, S. J., Allen, B. G., Clement-Chomienne, O. and Walsh, M. P. (1998). Regulation of smooth muscle actin-myosin interaction and force by calponin. *Acta Physiol Scand* **164**, https://doi.org/10.1111/j.1365-201x.1998.tb10697.x

Winkles, J. A. and Gay, C. G. (1991). Serum, phorbol ester, and polypeptide mitogens increase class 1 and 2 heparin-binding (acidic and basic fibroblast) growth factor gene expression in human vascular smooth muscle cells. *Cell Growth Differ* **2**, https://www.ncbi.nlm.nih.gov/pubmed/1726053

Wolfe, R. A., Ashby, V. B., Milford, E. L., Ojo, A. O., Ettenger, R. E., Agodoa, L. Y., Held, P. J. and Port, F. K. (1999). Comparison of mortality in all patients on dialysis, patients on dialysis awaiting transplantation, and recipients of a first cadaveric transplant. *N Engl J Med* **341**, https://doi.org/10.1056/NEJM199912023412303

Wolinsky, H. (1970). Response of the rat aortic media to hypertension. Morphological and chemical studies. *Circ Res* **26**, https://doi.org/10.1161/01.res.26.4.507

Wong, R., Donno, R., Leon-Valdivieso, C. Y., Roostalu, U., Derby, B., Tirelli, N. and Wong, J. K. (2019). Angiogenesis and tissue formation driven by an arteriovenous loop in the mouse. *Scientific Reports* **9**, https://doi.org/10.1038/s41598-019-46571-4

Wu, H., Uchimura, K., Donnelly, E. L., Kirita, Y., Morris, S. A. and Humphreys, B. D. (2018). Comparative Analysis and Refinement of Human PSC-Derived Kidney Organoid Differentiation with Single-Cell Transcriptomics. *Cell Stem Cell* **23**, https://doi.org/10.1016/j.stem.2018.10.010

Xiao, Z., Liu, Q., Mao, F., Wu, J. and Lei, T. (2011). TNF-alpha-induced VEGF and MMP-9 expression promotes hemorrhagic transformation in pituitary adenomas. *Int J Mol Sci* **12**, https://doi.org/10.3390/ijms12064165

Xinaris, C., Benedetti, V., Rizzo, P., Abbate, M., Corna, D., Azzollini, N., Conti, S., Unbekandt, M., Davies, J. A., Morigi, M., *et al.* (2012). In vivo maturation of functional renal organoids formed from embryonic cell suspensions. *J Am Soc Nephrol* **23**, https://doi.org/10.1681/ASN.2012050505

Xu, R., Ho, Y. S., Ritchie, R. P. and Li, L. (2003). Human SM22 alpha BAC encompasses regulatory sequences for expression in vascular and visceral smooth muscles at fetal and adult stages. *Am J Physiol Heart Circ Physiol* **284**, https://doi.org/10.1152/ajpheart.00737.2002

Xu, Y., Guo, X., Yang, S., Li, L., Zhang, P., Sun, W., Liu, C. and Mi, S. (2018). Construction of bionic tissue engineering cartilage scaffold based on three-dimensional printing and oriented frozen technology. *J Biomed Mater Res A* **106**, https://doi.org/10.1002/jbm.a.36368

Yamagishi, Y., Masuda, T., Matsusaki, M., Akashi, M., Yokoyama, U. and Arai, F. (2014). Microfluidic perfusion culture system for multilayer artery tissue models. *Biomicrofluidics* **8**, https://doi.org/10.1063/1.4903210

Yamamura, H. (1969). [Variability in developmental stage of mouse embryos (C 5 7 BL) in the early period of organogenesis]. *Wilhelm Roux Arch Entwickl Mech Org* **162**, https://doi.org/10.1007/BF00576930

Ye, J., Coulouris, G., Zaretskaya, I., Cutcutache, I., Rozen, S. and Madden, T. L. (2012). Primer-BLAST: a tool to design target-specific primers for polymerase chain reaction. *BMC Bioinformatics* **13**, https://doi.org/10.1186/1471-2105-13-134

Yoshikawa, N., Cameron, A. H. and White, R. H. (1981). The glomerular basal lamina in hereditary nephritis. *J Pathol* **135**, https://doi.org/10.1002/path.1711350305

Young, D. B. and Rostorfer, H. H. (1973). Renin release responses to acute alterations in renal arterial osmolarity. *Am J Physiol* **225**, https://doi.org/10.1152/ajplegacy.1973.225.5.1009

Yu, A., Matsuda, Y., Takeda, A., Uchinuma, E. and Kuroyanagi, Y. (2012). Effect of EGF and bFGF on fibroblast proliferation and angiogenic cytokine production from cultured dermal substitutes. *J Biomater Sci Polym Ed* **23**, https://doi.org/10.1163/092050611X580463

Yuri, S., Nishikawa, M., Yanagawa, N., Jo, O. D. and Yanagawa, N. (2017). In Vitro Propagation and Branching Morphogenesis from Single Ureteric Bud Cells. *Stem Cell Reports* **8**, https://doi.org/10.1016/j.stemcr.2016.12.011

Zeidan, A., Sward, K., Nordstrom, I., Ekblad, E., Zhang, J. C., Parmacek, M. S. and Hellstrand, P. (2004). Ablation of SM22alpha decreases contractility and actin contents of mouse vascular smooth muscle. *FEBS Lett* **562**, https://doi.org/10.1016/S0014-5793(04)00220-0

Zhang, R., Xu, Y., Ekman, N., Wu, Z., Wu, J., Alitalo, K. and Min, W. (2003). Etk/Bmx transactivates vascular endothelial growth factor 2 and recruits phosphatidylinositol 3-kinase to mediate the tumor necrosis factor-induced angiogenic pathway. *J Biol Chem* **278**, https://doi.org/10.1074/jbc.M310678200

Zhang, X., Baughman, C. B. and Kaplan, D. L. (2008). In vitro evaluation of electrospun silk fibroin scaffolds for vascular cell growth. *Biomaterials* **29**, https://doi.org/10.1016/j.biomaterials.2008.01.022

Zhang, X., Wang, X., Keshav, V., Wang, X., Johanas, J. T., Leisk, G. G. and Kaplan, D. L. (2009). Dynamic culture conditions to generate silk-based tissue-engineered vascular grafts. *Biomaterials* **30**, https://doi.org/10.1016/j.biomaterials.2009.02.002

Zhou, B., Tsaknakis, G., Coldwell, K. E., Khoo, C. P., Roubelakis, M. G., Chang, C. H., Pepperell, E. and Watt, S. M. (2012). A novel function for the haemopoietic supportive murine bone marrow MS-5 mesenchymal stromal cell line in promoting human vasculogenesis and angiogenesis. *Br J Haematol* **157**, https://doi.org/10.1111/j.1365-2141.2012.09050.x

Zhou, Y. Q., Cahill, L. S., Wong, M. D., Seed, M., Macgowan, C. K. and Sled, J. G. (2014). Assessment of flow distribution in the mouse fetal circulation at late gestation by high-frequency Doppler ultrasound. *Physiol Genomics* **46**, https://doi.org/10.1152/physiolgenomics.00049.2014

Zhu, W. H., Iurlaro, M., MacIntyre, A., Fogel, E. and Nicosia, R. F. (2003). The mouse aorta model: influence of genetic background and aging on bFGF- and VEGF-induced angiogenic sprouting. *Angiogenesis* **6**, https://doi.org/10.1023/B:AGEN.0000021397.18713.9c

Appendix

List of abbreviations

Ang-1	Angiopoietin-1
Ang-2	Angiopoietin-2
Ass1	Argininosuccinate synthase 1
ATP	adenosine triphosphate
BMP	bone morphogenic protein
CAM	chorioallantoic membrane
CI	confidence interval
CNC	Computer numerical control
$CoCl_2$	cobalt chloride
DMSO	Dimethyl sulfoxide
E	embryonic day
ECM	extracellular matrix
EDTA	Ethylenediaminetetraacetic acid
EGM	endothelial growth medium
eNOS	endothelial NO synthase
ES	embryonic stem cell
FBS	foetal bovine serum
FGF	fibroblast growth factor
FITC	Fluorescein isothiocyanate
GBM	glomerular basement membrane
GDNF	Glial cell-derived neurotrophic factor
HGF	Hepatocyte growth factor
Hif1α	Hypoxia-induced-factor 1α
ID	inner diameter
ID	inner diameter
IGF	insulin-like growth factor
INS	interstitial nodal space
iPSC	induced pluripotent stem cell
KCM	kidney culture medium
LoH	loop of Henle
MCP	monocyte chemotactic protein
MCP-1	monocyte chemotactic protein-1
MEM	Minimum essential Eagle Medium
MM	metanephric mesenchyme
NaCl	sodium chloride
NO	nitric oxide
NPC	nephron progenitor cell
OD	outer diameter
OD	outer diameter
PBS	phosphate buffered saline
PDGF	Platelet-derived growth factor
PFA	paraformaldehyde
PMA	Phorbol 12-myristate 13-acetate
PMW	periwolffian mesenchyme
rms	root mean square
rpm	round per minute
RT	room temperature
RT	room temperature
S1P	Sphingosine-1-phosphate
T1C	type 1 collagen

Tuj1	neuron-specific class III beta-tubulin
TW	Transwell
UB	ureteric bud

VEGF	vascular endothelial growth factor
WD	Wolffian duct
WT1	Wilm's Tumour 1

List of antibodies

Table A 1: List of primary antibodies. All antibodies were used in a 1:200 dilution

Antibody	species raised	catalogue number (supplier)
Ass1	rabbit	ab170952 (abcam)
Calponin 1	rabbit	ab46794 (abcam
CD31	goat	AF3628 (R&D)
cleaved caspase 3	rabbit	9661s (cell signalling)
E-cadherin	mouse	610182 (BD)
Gata3	goat	AF2605 (R&D)
Hif1α	rabbit	ab179483 (abcam)
Jagged 1	goat	AF599 (R&D)
Meis1/2/3	mouse	39796 (active motif)
Podocalyxin	rat	MAB1556 (R&D)
Six2	rabbit	11562-1-AP (proteintec)
smooth muscle actin	goat	nb300-978 (Novus)
smooth muscle actin	rabbit	ABT1487 (Merck)
smooth muscle actin-FITC	mouse	A7607 (Merck)
Transgelin	sheep	AF7886-SP (R&D)
Tuj1	mouse	801201 (Biolegend)
Tyrosine hydroxylase	rabbit	AB152 (Merck)
WT1	rabbit	ab89901 (abcam)

Table A 2: List of secondary antibodies. All antibodies were used in a 1:200 dilution

Antibody	catalogue number (supplier)
Donkey-anti-mouse AlexaFluor488	A21202 (Thermo Fisher)
Donkey-anti-rabbit-AlexaFluor555	A31572 (Thermo Fisher)
Donkey-anti-rabbit-AlexaFluor594	A21207 (Thermo Fisher)
Chicken-anti-rat-AlexaFluor594	A21471 (Thermo Fisher)
Donkey-anti-goat-AlexaFluor647	A21447 (Thermo Fisher)
Donkey-anti-mouse-AlexaFluor555	A31570 (Thermo Fisher)
Donkey-anti-mouse-AlexaFluor647	A31571 (Thermo Fisher)
Donkey-anti-rabbit-AlexaFluor488	A21206 (Thermo Fisher)
Donkey-anti-rabbit-AlexaFluor647	A31573 (Thermo Fisher)
Donkey-anti-goat-AlexaFluor488	A11055 (Thermo Fisher)
Donkey-anti-sheep-AlexaFluor594	A11016 (Thermo Fisher)

Supplemental Methods

Table A 3: GoTaq Green PCR reaction Mix to validate amplicon size

GoTaq Green PCR Mix	volume per sample in µl
5x Green GoTaq Reaction buffer (Promega, M7911)	5
forward primer (Invitrogen)	1
reverse primer (Invitrogen)	1
template cDNA	2
dNTPs (Promega, U144A)	0.5
GoTaq G2 Polymerase (Promega, M7841	0.25
dH_2O	15.25

Table A 4: GoTaq Green PCR Program

temperature	duration (min:sec)	repeats
95 °C	2:00	x1
95 °C	0:15	
60 °C	0:30	x35
72 °C	0:20	
72 °C	5:00	x1

Supporting information

Table A 5: Integrin expression in the kidney

Integrin subunit	Expression	renal defects	references
α1 (α1β1)	nephron, glomerulus, metanephric mesenchyme	no morphological or functional abnormalities	(H. Gardner *et al.*, 1996; Korhonen *et al.*, 1990; Rahilly & Fleming, 1992)
α2 (α2β1)	nephron, glomerulus, collecting duct	aberrant podocyte morphology, mild proteinuria	(Girgert *et al.*, 2010; Korhonen *et al.*, 1990; Rahilly & Fleming, 1992)
α3 (α3β1)	nephron, glomerulus, collecting duct, endothelium	defects in podocyte development, reduced branching	(Korhonen *et al.*, 1990; Kreidberg *et al.*, 1996; Rahilly & Fleming, 1992)
α4 (α4β1)	metanephric mesenchyme	unknown, knockout is embryonic lethal	(Rahilly & Fleming, 1992; J. T. Yang *et al.*, 1995)
α6 (α6β1, α6β6)	nephron, collecting ducts, glomerulus, endothelium	decreased tubulogenesis in vitro, but no morphological effect in vivo	(Falk *et al.*, 1996; Georges-Labouesse *et al.*, 1996)
a8 (α8β1)	metanephric mesenchyme	renal agenesis	(Humbert *et al.*, 2014; Müller *et al.*, 1997)
αv (αvβ1, αvβ3, αvβ4, αvβ5, αvβ6)	glomerulus, collecting duct, nephron, endothelium	decreased branching in vitro, but no morphological changes in vivo	(Bader *et al.*, 1998; Wada *et al.*, 1996)
β1 (α1β1, αvβ1)	abundant	branching and nephron development defects	(Rahilly & Fleming, 1992; Xi Zhang *et al.*, 2009)
β3 (αvβ3)	glomerular endothelium	unknown	(Rahilly & Fleming, 1992; Wada *et al.*, 1996)
b4 (αvβ4)	collecting duct (not in adult)	reduced branching in vitro	(Zent *et al.*, 2001)
β5 (αvβ5)	glomerulus	unknown	(Wada *et al.*, 1996)
β6 (αvβ6)	nephron, collecting duct, glomerulus	reduced branching in vitro, no morphological defects in vivo	(Arend *et al.*, 2000; Wada *et al.*, 1996)

Supporting data

Secondary antibody controls:

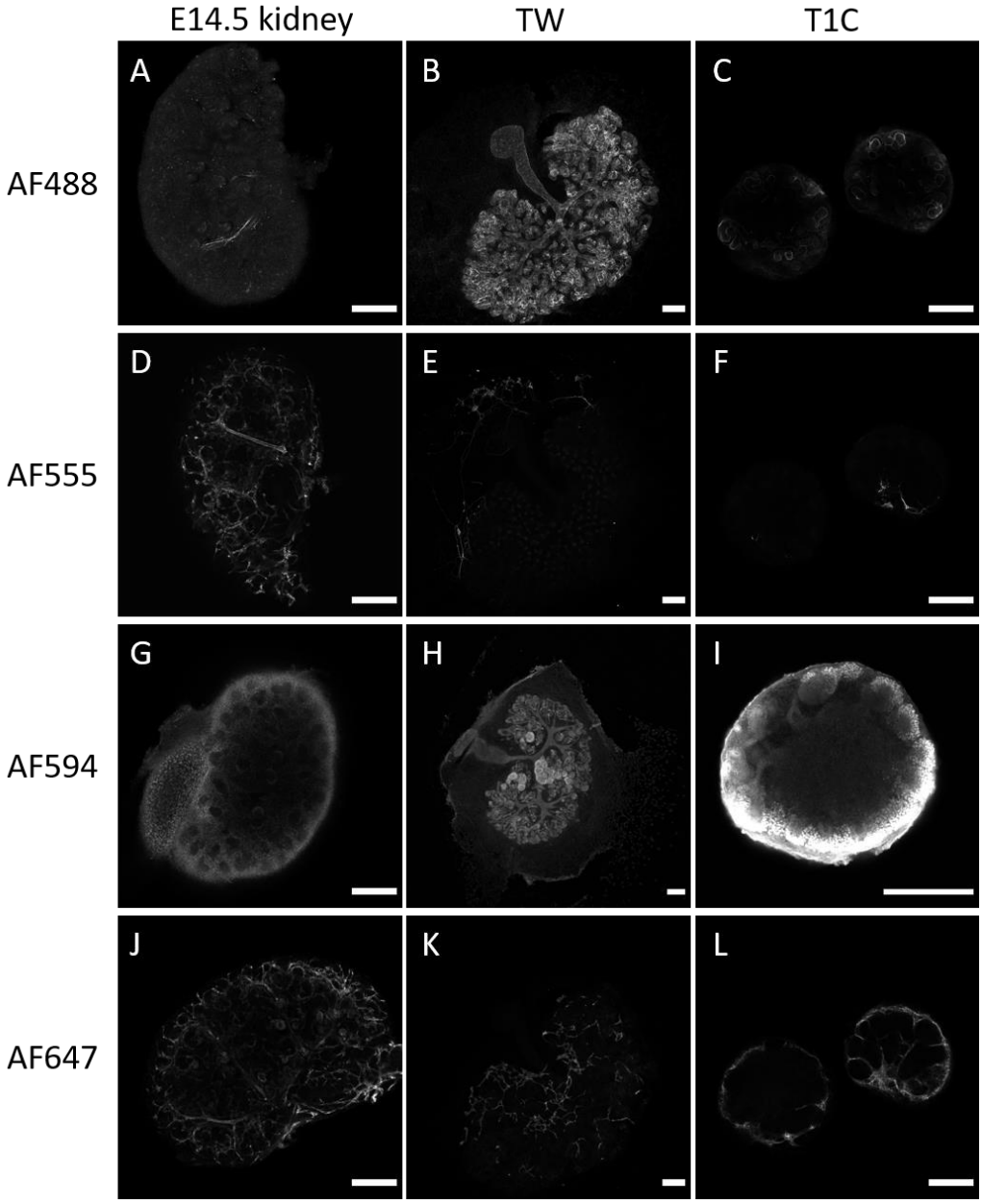

Figure A 1: Examples of exposure controls. Samples of uncultured (A, D, G, J), Transwell-cultured (B, E, H, K) and collagen-cultured kidneys (C, F, I, J) were stained with primary and secondary antibodies and used to set the exposure for the channels AlexaFluor488 (A-C), AlexaFluor555 (D-F), AlexaFluor594 (G-I) and AlexaFluor647 (J-K) to image the secondary only antibody controls. Scale bars: 200 µm

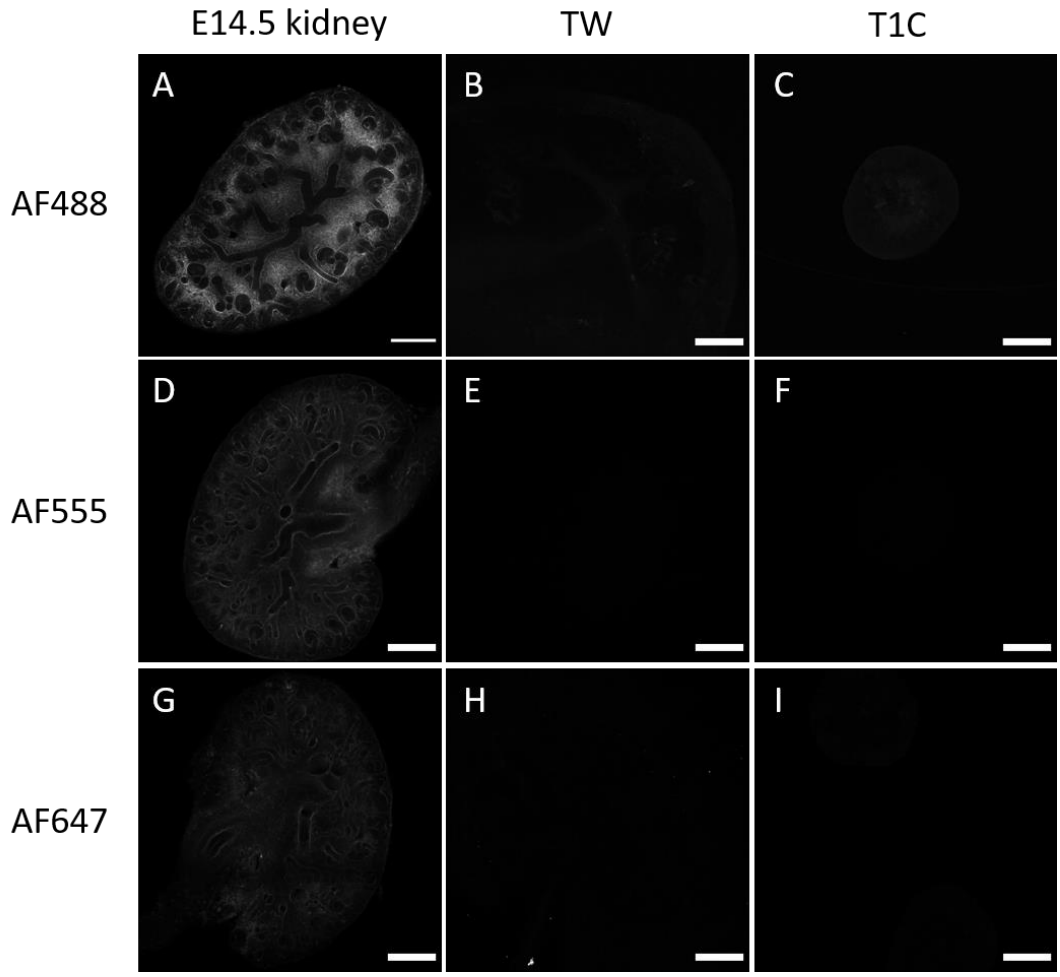

Figure A 2: Secondary-only control: Donkey-anti-mouse secondary antibodies. The antibodies with the conjugates AlexaFluor488 (A-C), AlexaFluor555 (D-F) and AlexaFluor647 (G-I) were tested on an E13.5 kidney (A, D, G), Transwell-cultured kidneys (B, E, H) and kidneys cultured in type 1 collagen (C, F, I). Scale bars: 200 µm

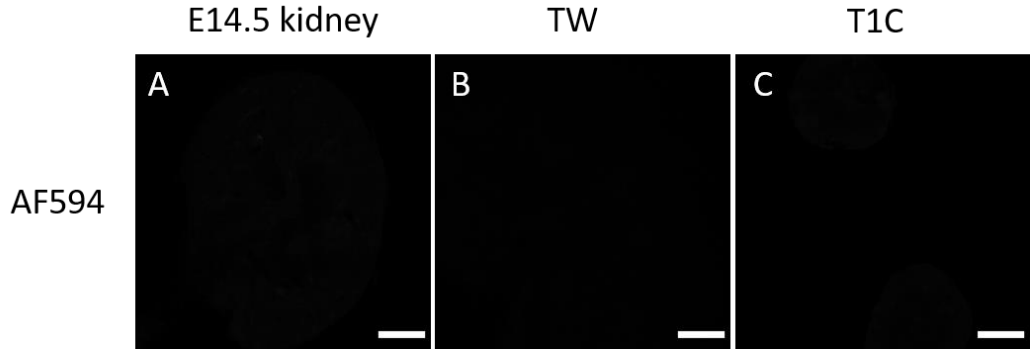

Figure A 3: Secondary-only control: Chicken-anti-rat-AlexaFluor594 antibody. The antibody was tested on an E13.5 kidney (A), a Transwell-cultured kidney (B) and a kidney cultured in type 1 collagen (C). Scale bars: 200 µm

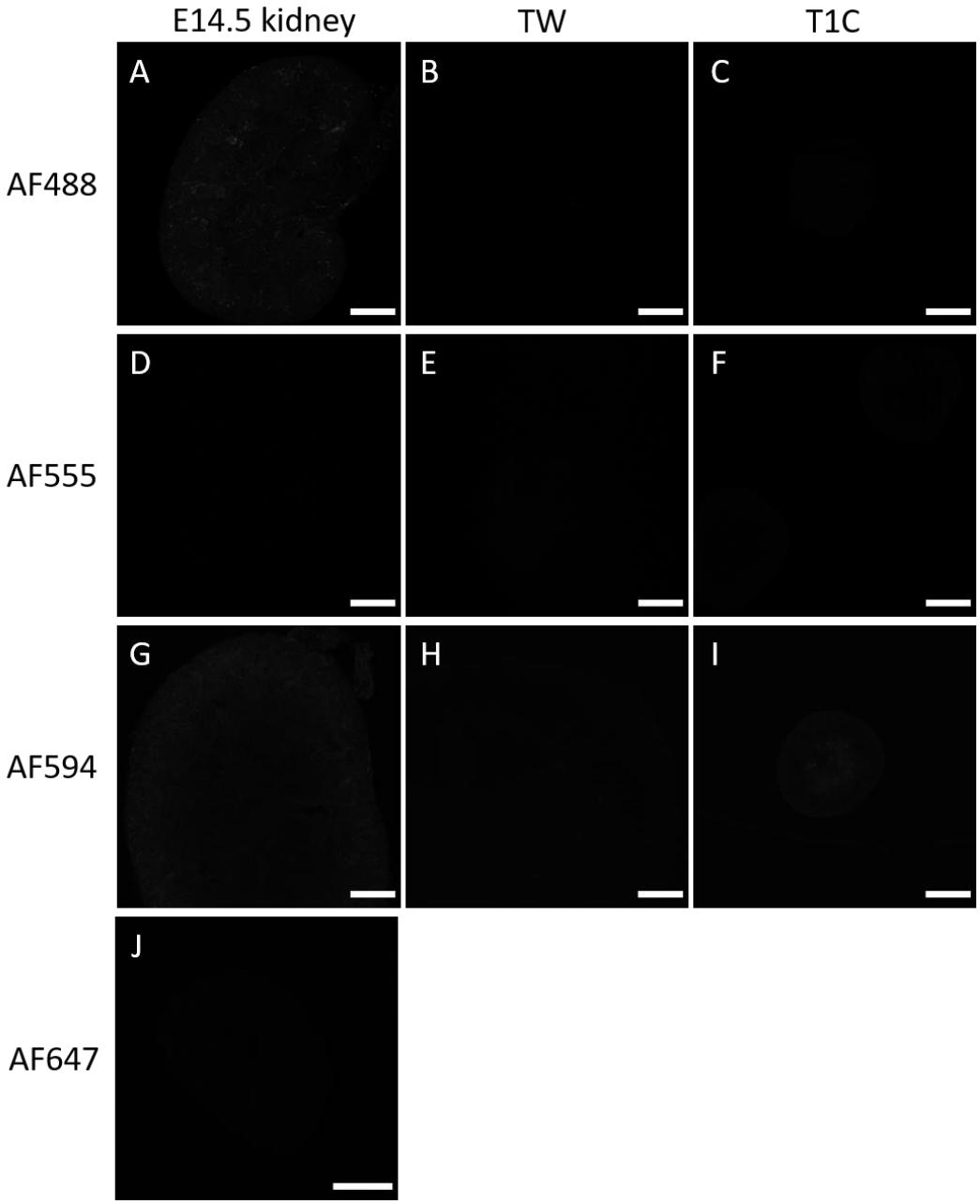

Figure A 4: Secondary-only control: Donkey-anti-rabbit secondary antibodies. The antibodies with the conjugates AlexaFluor488 (A-C), AlexaFluor555 (D-F), AlexaFluor594 (G-I) and AlexaFluor647 (J) were tested on an E13.5 kidney (A, D, G, J), Transwell-cultured kidneys (B, E, H) and kidneys cultured in type 1 collagen (C, F, I). Scale bars: 200 µm

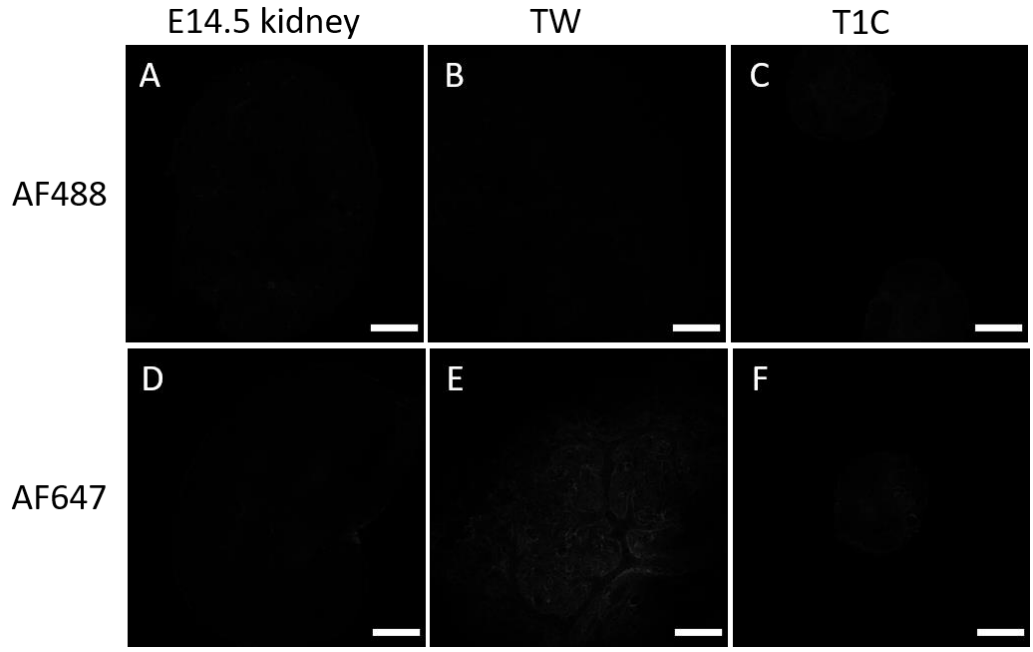

Figure A 5: Secondary-only control: Donkey-anti-goat secondary antibodies. The antibodies with the conjugates AlexaFluor488 (A-C) and AlexaFluor647 (D-F) were tested on an E13.5 kidney (A, D), Transwell-cultured kidneys (B, E) and kidneys cultured in type 1 collagen (C, F). Scale bars: 200 µm

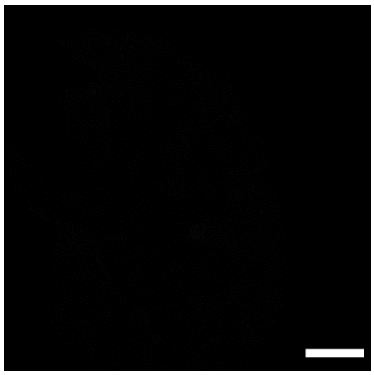

Figure A 6: Secondary-only control: Donkey-anti-sheep-AlexaFluor594 antibody. The antibody was tested on an E14.5 kidney. Scale bar: 200 µm

Supporting data for vascular perfusion experiments:

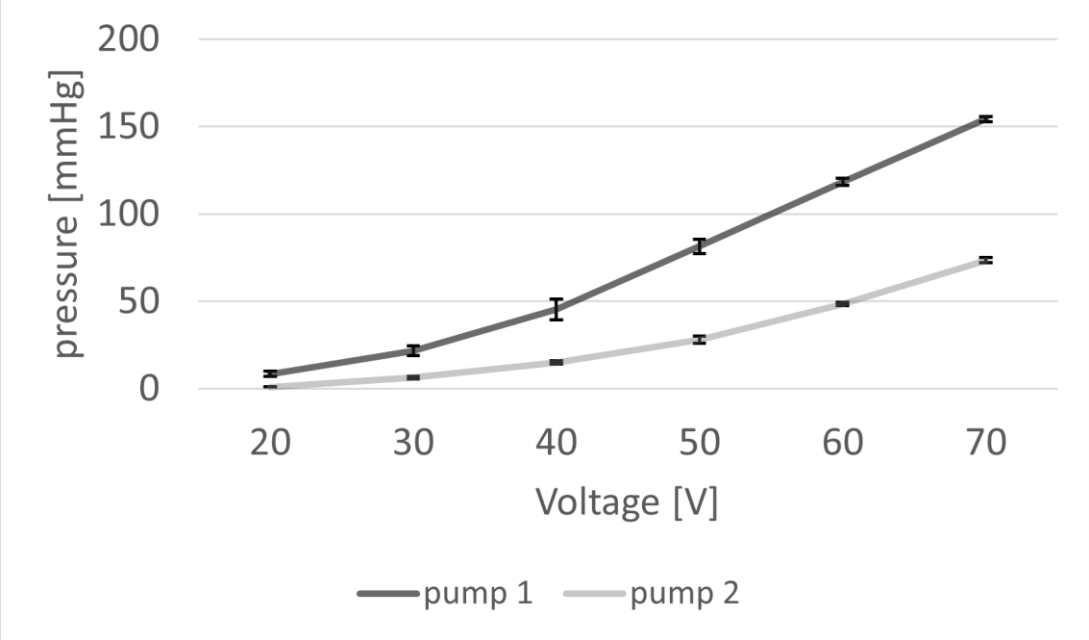

Figure A 7: differences of the output pressure between pumps of the same type at the same voltage. The output pressure of two pumps of the same type was measured and plotted against the voltage. All measurements were done in triplicates. The error bars display the standard deviation.

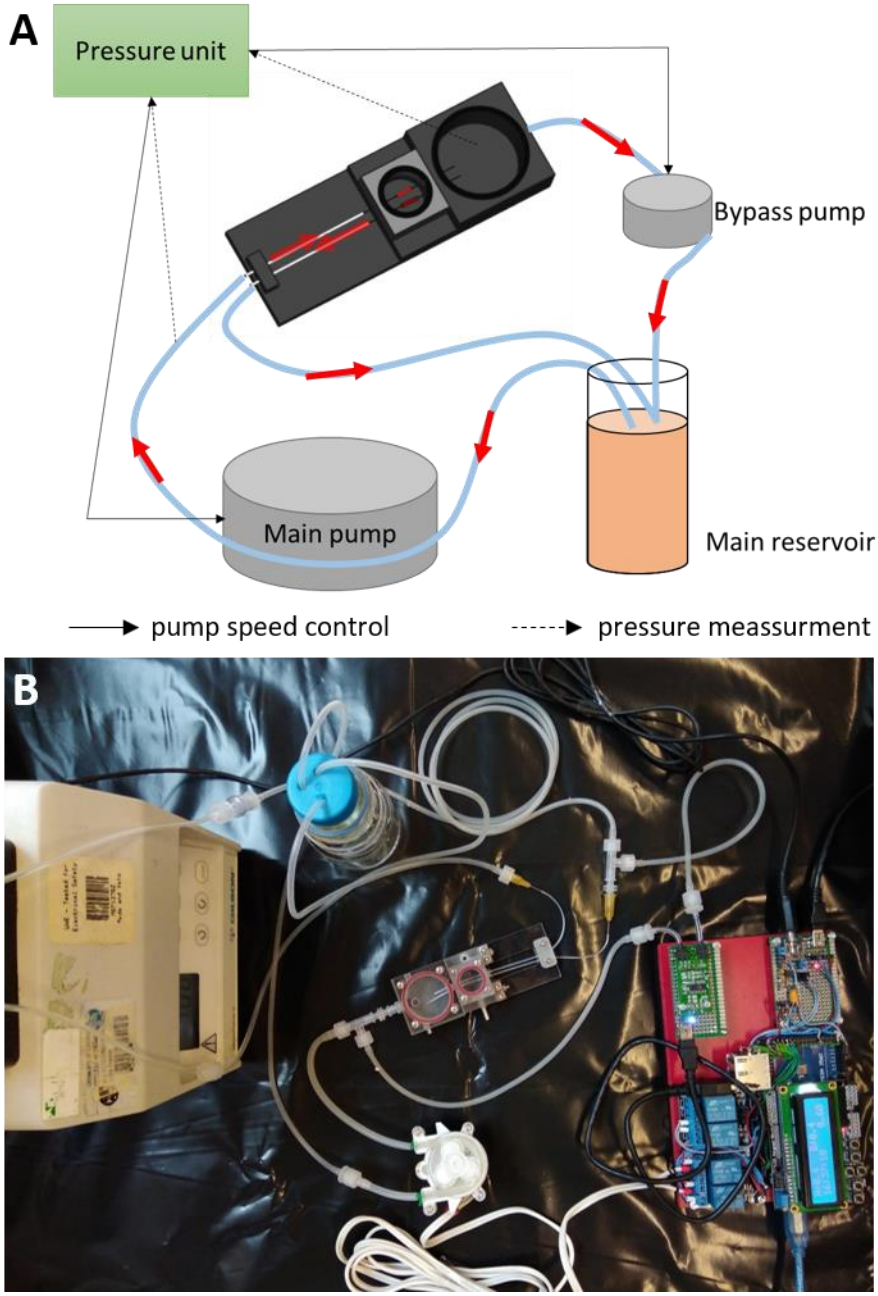

Figure A 8: experimental design to separate venous from arterial flow. A: schematic of the design. Medium is aspirated from the main reservoir and pumped through the artery into the secondary reservoir, leading to a pressure increase within the secondary reservoir. The increasing pressure drives the liquid through the vein back into the main reservoir. To lower the venous flow, a bypass pump, controlled by a pressure sensor, transfers part of the liquid from the secondary reservoir to the main reservoir. B: image of the experimental design.

Channel perfusion results

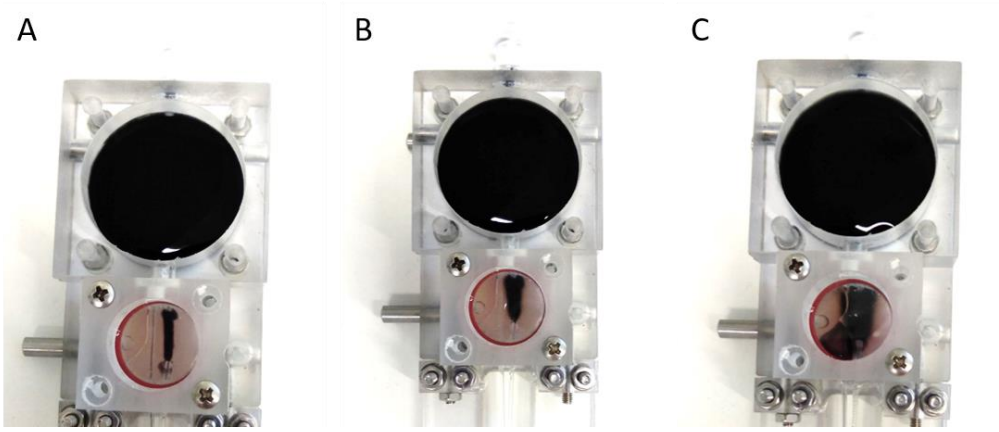

Figure A 9: perfusion of ink through channel in type 1 collagen. Images were taken after 0 min (A) 10 min (B) and 40 min (C)

List of conference presentations:

International Cell Culture Under Flow Meeting (February 18-19, 2020). *Dual chamber design for accessible, bidirectional perfusion of whole blood vessels*

Scottish Cardiovascular Forum (February 1, 2020). Development of a bi-directional perfusion bioreactor for accessible culture of primary blood vessels